CENTRE D'HYDROGÉOLOGIE

Université de Neuchâtel

Use of stable isotope analyses to assess natural attenuation of chlorinated ethenes in groundwater

PhD thesis presented to the faculty of Sciences of the University of Neuchâtel
to satisfy the requirements of the degree of Doctor of Philosophy in Science

by

Yumiko Abe

Thesis Jury defence date: 24th September 2007
Public presentation date: 12th October 2007

Jury members:
Daniel Hunkeler (director of the thesis), Associate professor, University of Neuchâtel
Jakob Zopfi, University of Neuchâtel
Poul L. Bjerg, Professor, Technical University of Denmark
Ramon Aravena, Professor, University of Waterloo, Canada

Université de Neuchâtel

FACULTE DES SCIENCES
Secrétariat-Décanat de la faculté
Rue Emile-Argand 11
CP 158
CH-2009 Neuchâtel

IMPRIMATUR POUR LA THESE

Use of stable isotope analysis to assess natural attenuation of chlorinated ethenes in groundwater

Yumiko ABE

UNIVERSITE DE NEUCHATEL

FACULTE DES SCIENCES

La Faculté des sciences de l'Université de Neuchâtel,
sur le rapport des membres du jury

MM. D. Hunkeler (directeur de thèse),
J. Zopfi, R. Aravena (Waterloo, Canada)
et P.L. Bjerg (Lyngby, Danemark)

autorise l'impression de la présente thèse.

Neuchâtel, le 8 novembre 2007

Le doyen :
T. Ward

UNIVERSITE DE NEUCHATEL
FACULTE DES SCIENCES
Secrétariat-décanat de la faculté
Rue Emile-Argand 11 - CP 158
CH-2009 Neuchâtel

Téléphone : +41 32 718 21 00 Fax : +41 32 718 21 03 E-mail : secretariat.sciences@unine.ch www.unine.ch/sciences

To my parents
Yoshiyuki & Kumiko Abe

who continue to learn, grow and develop
&
who have taught me, shown me and
let me explore the spirit of life

ACKNOWLEDGEMENTS

This project was funded by Swiss Science Foundation. In the framework of this thesis, I wish gratefully to acknowledge the following persons and institutions.

The studies presented in Chapters 2 and 3 were carried out as a joint project with the University of Waterloo. The field work at Angus, Ontario and the following microbiological analyses would not have been possible without the assistance and the support from the following persons:
Prof. Ramon Aravena from the University of Waterloo for his assistance with the organization of the field work at Angus and granting us with materials and space needed for the laboratory analyses carried out at the University of Waterloo, as well as his hospitability to host us at his home in Toronto,
Bob Ingleton and Paul Johnson from the University of Waterloo for the preparation of field equipment,
Wayne Noble from the University of Waterloo for carrying out the chlorinated ethenes, ethene, ethane, methane and dissolved organic carbon concentrations analyses,
Dr. Jakob Zopfi from the Laboratory of Microbiology at the University of Neuchâtel for his assistance in ordering the PCR primers, improving the PCR protocols, as well as the interpretation of the obtained results, and
Vanessa Di Marzo from the Laboratory of Microbiology at the University of Neuchâtel for her assistance in the molecular analyses including the extraction of DNA and RNA from sediment samples.

The field investigation at Rødekro, Denmark presented in Chapter 5 was carried out as collaboration with Orbicon (Roskilde, Denmark) and Technical University of Denmark (DTU). The study consists of many parts of which the following persons have dedicated their contributions:
Dr. Mette Broholm for organizing the field works, providing us with the previous data collected at Orbicon, and her hospitability in our stay at Copenhagen,
Staff at Orbicon for carrying out the sampling sessions in February 2006 and April 2007,
Staff at DTU for concentration analyses of chlorinated ethenes, ethene, ethane and methane,
Dr. Orafan Shouakar-Stash from the University of Waterloo for chlorine isotope analysis of *cis*-dichloroethene, and
Simon Jeannottat as a post-grad student at the Centre of Hydrogeology from the University of Neuchâtel for arranging and doing the sampling session in September 2006, the carbon isotope analysis of vinyl chloride, and iron and manganese concentration analysis.

The laboratory study presented in Chapter 4 also contains contributions from the following persons and institutions.
Prof. Jim Spain at the Georgia Institute of Technology for kindly providing us with the pure culture used,
Staff at the laboratory of SiREM (Ontario, Canada) for carrying out the cDCE and VC degradation experiments with the mixed culture KB-1,
Dr. Orafan Shouakar-Stash from the University of Waterloo for chlorine isotope analysis of *cis*-dichloroethene, and
Dr. Jakob Zopfi from the Laboratory of Microbiology at the University of Neuchâtel for his assistance with preparing anoxic growth media.

I wish to express my gratitude to the members of thesis committee, Prof. Paul Bjerg from DTU, Prof. Ramon Aravena from the University of Waterloo and Dr. Jakob Zopfi from the University of Neuchâtel for helping me improve the thesis after the defense.

I also would like to thank the Center of Hydrogeology (CHYN) and the Laboratory of Microbiology at the University of Neuchâtel for providing pleasant working environment. Members of the CHYN isotope laboratory (Daniel Bouchard and Barbara Morasch) with whom I spent many hours baby-sitting the capricious IRMS and shared the innovative new tricks, I enjoyed the isotope jokes with both of them despite the mysteriously large number of dead flies in the lab. Many of the hilarious moments in the traditional CHYN Friday night-out club (original principal members including Ray, Michaël, Alain, etc. at café du Cerf, then moved onto Bleu café and to Chauffage with renewed members including Alain, Daniel Bouchard, Michel, Rob, Fabien, Sandrine, etc.) which was later transformed into a Thursday hang-out club (members including Andrés, Rob, Jaouher, etc. at bar Gibraltar) are clearly remembered. Without us, the City of Neuchâtel would suffer from the surplus of beers.

There are a number of people without whom this thesis would not have been finished, and to whom I am greatly indebted.
First of all, I thank my family in Japan who seem so far away but remain so close to me. Without them, without a place to go back to, I would have just been a lost person. My friends from Japan have always reminded me of the stable time axis of friendship despite a series of hello-goodbyes during the past 11 years. My friends during my 7 years in the US, who are particularly energetic and trouble-magnetic, have always reminded me of the possibilities in professional and personal lives, how one should never give up and how efforts don't betray. Knowing such hyper-encouraged people around the world has always motivated me to go on. My friends in Neuchâtel have provided me with the first-hand moral support during the last four years. I have accumulated a lot of funny and bizarre stories with them which are to be continued. They also had to share my difficult and shaky moments, and for that, I thank them all.

My list of special thanks extends, of course, to the school life, and I would like to thank three persons who have suffered the most from my swinging moods. First off, I thank my office mate Barbara who never failed to show her kindness to me. Our office life continued to improve over time, and reached a point where her absence at work somehow creates a sense of loneliness. I am also grateful to Jakob for his understanding and lenience with me which very often was counter-intuitive for his professional achievements.

Last but absolutely not the least; I do not even know how to thank my thesis director Daniel Hunkeler. I have learnt so many things from him, not only about Hydrogeology but also about attitudes towards a professional life. His ability to make things happen, his enthusiasm and passion in his profession, his persistence with solving a problem, his patience, to name a few… I will never be able to return as much as he gave to me. International field trips and hours and hours of discussion with him, all of it piled up and were built up as this thesis. I am glad that I came to Switzerland to work with him. Thank you, Daniel.

Abstract

Chlorinated ethenes are among the most frequently detected groundwater contaminants in industrially developed countries. Although their degradation pathways have been understood, assessing the progress of natural attenuation of chlorinated ethenes still remains a challenge. Chlorinated ethenes undergo sequential reductive dechlorination under anoxic conditions; hence, the presence of less chlorinated transformation intermediates indicates the transformation of more chlorinated parent compound. However, the transformation intermediates can be degraded by other pathways such as aerobic and anaerobic oxidation and abiotic reduction which make it difficult to identify the fate of these intermediates. This thesis explored the possibilities and limits of the use of compound-specific stable isotope analysis as a field investigation tool to document and to quantify the progress of natural attenuation of chlorinated ethenes. The thesis focused particularly on the fate of reductive dechlorination intermediates such as *cis*-dichloroethene (cDCE) and vinyl chloride (VC) as the success of natural attenuation of chlorinated ethenes depends principally on the fate of these compounds. Two field investigations were carried out to demonstrate the use of stable isotope analysis to characterize the progress of natural attenuation of chlorinated ethenes. Laboratory studies evaluated the use of combined carbon and chlorine isotope analysis to distinguish different degradation pathways of cDCE and VC, and the approach was employed at a field site to determine the fate of cDCE. Numerical studies evaluated the field applicability of isotope-based quantification to estimate the extent of degradation and the first-order reaction rate based on the Rayleigh equation under various flow conditions. In addition, a scheme to quantify the reductive dechlorination rates of chlorinated ethenes based on field concentration and isotope data at one of the field sites was proposed and studied numerically.

Field investigations took place at a site where a tetrachloroethene- (PCE) plume discharged through the streambed accompanied by high levels of hydrological and geochemical variability (Angus site) and at another site characterized by a 2-km long plume of chlorinated ethenes (Rødekro site). At the Angus site, sampling was carried out at the discharging area in the streambed. Spatially detailed sampling allowed the identification of various redox and hydrological conditions. The progress of reductive dechlorination of chlorinated ethenes at each sampling location was determined by carbon isotope analysis. The approach is based on the principle that the carbon isotope ratio of an accumulating intermediate progressively approaches that of the parent compound because all carbons in the ethene backbone are preserved during the course of reductive dechlorination. The carbon isotope analysis suggested that the site consisted of locations with various degrees of reductive dechlorination ranging from insignificant to complete dechlorination. At locations where the accumulation of an intermediate was observed, the carbon isotope ratio of the accumulating intermediate remained stable at that of the parent compound; thus, the observed concentration decrease was caused solely by the effect of dispersion. At some locations, the carbon

isotope ratio of ethene, the final product of reductive dechlorination, became more enriched than that of the original PCE indicating further transformation of ethene likely to ethane. The conclusions drawn from carbon isotope analysis were compared to the information provided by other field indicators for complete reductive dechlorination (strong redox conditions and the presence of *Dehalococcoides*). Complete reductive dechlorination was observed under sulfate-reducing and methanogenic conditions. However under sulfate-reducing conditions cDCE accumulation also took place at different locations. Different progress of reductive dechlorination under sulfate-reducing conditions was caused primarily by the difference in sediment compositions. Relatively permeable streambed gives rise to a faster discharge rate, hence a shorter residence time of the water which resulted in incomplete reductive dechlorination to cDCE. On the other hand, complete reductive dechlorination was observed at a location with relatively impermeable streambed. Therefore, the progress of reductive dechlorination is not only driven by the local redox conditions, but also by the local hydrological conditions. The presence of *Dehalococcoides* based on taxon-specific PCR analysis was confirmed at locations under methanogenic conditions which carried out complete reductive dechlorination and the further reduction of ethene to ethane, but *Dehalococcoides* was not detected at a location under sulfate-reducing conditions with ethene as a final degradation product.

At the Rødekro site, sampling was carried out along the plume centerline at multiple depths. The concentration analysis of chlorinated ethenes suggested cDCE accumulation. However, under the observed redox conditions (manganese-reducing), both reductive dechlorination and anaerobic oxidation of cDCE could take place. The conservation of carbons in the ethene backbone during reductive dechlorination implies that the combined carbon isotope ratios of all chlorinated ethenes and ethene remain constant as long as reductive dechlorination is the only active transformation pathway. Therefore, carbon isotope analysis of chlorinated ethenes can provide valuable information to indicate whether reductive dechlorination is the only degradation pathway or the intermediates are degraded by other degradation pathways such as oxidative degradation which involves with the loss of carbons, hence enrichment in combined carbon isotope ratios. At the Rødekro site, the combined carbon isotope ratio remained constant at the majority of the plume, suggesting that reductive dechlorination was the only transformation pathway. However at the plume front, the combined ratio deviated from that of the source value indicating the possibilities of either anaerobic oxidation of intermediates (cDCE or VC) or further reductive dechlorination to ethene (even though it was not detected at the site). Based on the low concentrations of VC and the isotope mass balance calculations, anaerobic oxidation of VC could not possibly give rise to the observed deviation in the combined carbon ratio. Therefore, it was postulated that either anaerobic oxidation of cDCE or complete reductive dechlorination to a non-detected end product took place at the plume front.

Although carbon isotope analysis can indicate the progress of reductive dechlorination and the possibility of alternative degradation pathways, it can not identify the responsible degradation mechanism at field scales. Therefore, the use of combined carbon and chlorine isotope analysis was evaluated to distinguish different degradation pathways. Because different pathways involve with breaking of different bonds, it was expected that the ratio between carbon and chlorine isotope fractionation would be different for different pathways. Laboratory studies revealed that aerobic oxidation of VC was accompanied by significantly smaller chlorine isotope fractionation compared to that for reductive dechlorination of VC and cDCE. This difference is caused by the absence of the cleavage of a carbon-chlorine bond in the initial step of aerobic oxidation of VC. As a result, the ratio between the chlorine and carbon isotope fractionation is smaller for aerobic oxidation compared to reductive dechlorination. The dual isotope approach was tested at the Rødekro site to determine the fate of accumulating cDCE. A strong shift in chlorine isotope ratios (6‰) which were highly correlated with a shift in carbon isotope ratios (14‰) was observed, indicting that cDCE was transformed by reductive dechlorination. Therefore, at the Rødekro site, reductive dechlorination was the responsible degradation pathway.

Field isotope data are often used to estimate the extent of degradation and the first-order degradation rate based on the Rayleigh isotope fractionation equation. The premise of the Rayleigh-based quantification method is that groundwater travels at a constant velocity corresponding to a uniform residence time distribution much like plug-flow. However, groundwater residence time varies due to the effect of dispersion caused by the subsurface heterogeneity. In order to evaluate the field applicability of the Rayleigh-based quantification method, the effect of residence time variability was evaluated using an analytical 2D solution to the advection-dispersion equation. Residence time variability was represented by varying the dispersion coefficient. The studies revealed that the Rayleigh-based quantification methods generally underestimate the extent of degradation and the degradation rate. The magnitude of the underestimation increases with the increasing dominance of dispersion over advection in flow conditions. Therefore, the effect of dispersion needs to be considered for the Rayleigh-based quantification methods. If the flow and transport parameters such as groundwater velocity and dispersion coefficients can be estimated at a site of interest, the degree of underestimation can be corrected based on the systematic type-curves presented in the thesis.

Due to the simultaneous formation and transformation of intermediate compounds, the Rayleigh-based quantification methods do not apply to reductive dechlorination of chlorinated ethenes. Therefore, a scheme to quantify the dechlorination rate during reductive dechlorination of chlorinated ethenes using a series of 3D analytical solutions which accommodate consecutive reactions was developed. The conservation of carbons in the ethene backbone during reductive dechlorination has an important implication that the summed molar concentrations of all chlorinated ethenes and ethene can be considered

as a quasi-conservative tracer as long as reductive dechlorination is the only transformation pathway. Since isotope analyses confirmed that reductive dechlorination is the responsible pathway at the Rødekro site, the concentration and isotope data at the Rødekro site were used to quantify the dechlorination rate of each chlorinated ethene species. Flow and transport model was calibrated to the summed concentrations of chlorinated ethenes. Based on the calibrated transport model, the dechlorination rates were estimated based on the carbon isotope and the concentration data separately for comparison. The concentration-based quantification method tends to yield greater transformation rates than the isotope-based method especially when the contaminant concentrations are low. However, the difference between the two methods is relatively small by a factor of four, suggesting that once effective flow and transport parameters are obtained, relatively stable transformation rates can be estimated. Parameter sensitivity analyses revealed that the variation in groundwater velocity is directly reflected in the quantified transformation rate; thus, it plays a significant role in quantifying the rate.

In conclusion, the studies demonstrated that stable carbon analysis is a robust and sensitive tool to identify the progress of reductive dechlorination of chlorinated ethenes and the possibility of other degradation pathways of intermediate compounds even under geochemically and hydrologically complex conditions and even if only a small level of degradation occurs. Although carbon isotope analysis alone can not conclusively determine the fate of degradation intermediates such as cDCE and VC, the use of combined chlorine and carbon isotope analysis can assist in elucidating their fate at field scales. Furthermore, based on the field isotope data, it is possible to estimate the degradation rate even for a complex reaction series such as sequential reductive dechlorination of chlorinated ethenes. And the accuracy of the rate quantification increases with increased knowledge of local flow conditions.

Keywords:
Natural attenuation, chlorinated ethenes, reductive dechlorination, compound-specific isotope analysis, carbon and chlorine isotope analysis, Rayleigh equation, reaction rate.

Table of Contents

1. INTRODUCTION **1**

1.1 GENERAL BACKGROUND 1

1.2 NATURAL ATTENUATION AS A REMEDIATION STRATEGY 3

1.2.1 Surface water-groundwater interface 4

1.2.2 Constrains for the use of natural attenuation 4

1.3 DEGRADATION PATHWAYS OF CHLORINATED ETHENES 5

1.3.1 Sequential reductive dechlorination 5

1.3.2 Oxidative degradation 7

1.4 DEMONSTRATING THE OCCURRENCE OF NATURAL ATTENUATION 8

1.5 COMPOUND-SPECIFIC STABLE ISOTOPE ANALYSIS 10

1.5.1 Rayleigh equation 10

1.5.2 Dual isotope approach 11

1.5.3 Isotope fractionation during chlorinated ethene degradation 12

1.5.4 Isotope behaviors during reductive dechlorination 13

1.6 OBJECTIVES OF THE RESEARCH 14

2. COMBINING GEOCHEMICAL AND ISOTOPE DATA TO EVALUATE THE FATE OF CHLORINATED ETHENES DISCHARGING THROUGH THE STREAMBED SEDIMENTS **16**

2.1 INTRODUCTION 17

2.2 STUDY SITE DESCRIPTION 18

2.3 STUDY METHODS 20

2.3.1 Streambed temperature measurements 20

2.3.2 Streambed water sampling 20

2.3.3 Sediment-core sampling 21

2.3.4 Analyses 21

2.4 RESULTS AND DISCUSSION 22

2.4.1 Determination of sampling locations 22

2.4.2 Spatial variability of chlorinated ethenes 23

2.4.4 Physical and geochemical characterization of selected locations 26

2.4.4 Concentrations and carbon isotope ratios of chlorinated ethenes 28

2.5 SUMMARY AND IMPLICATIONS 32

3. COMPARISON OF GEOCHEMICAL, ISOTOPE, AND MICROBIAL INVESTIGATION METHODS TO CHARACTERIZE THE FATE OF VC 33

3.1 INTRODUCTION 34
3.2 MATERIALS AND METHODS 36
3.2.1 Site Description 36
3.2.2 Sediment samples 37
3.2.3 Microcosm study 37
3.2.4 Molecular biology methods 38
3.2.5 Chemical analyses 39
3.3 RESULTS AND DISCUSSION 39
3.3.1 Assessment of complete in situ reductive dechlorination potential 39
3.3.2 Assessment of cDCE and VC oxidation potential 41
3.3.3 Possible effect of streambed consolidation 43
3.4 SUMMARY AND IMPLICATIONS 43

4. MAGNITUDE OF CARBON AND CHLORINE ISOTOPE EFFECTS DURING AEROBIC OXIDATION OF VC AND REDUCTIVE DECHLORINATION OF VC AND CDCE 45

4.1 INTRODUCTION 46
4.2 RATIONALE AND CALCULATION METHOD 48
4.2.1 Comparison of isotope enrichment factors 48
4.2.2 Apparent Kinetic Isotope Effect 48
4.2.3 Dual isotope approach based on AKIE 50
4.3 MATERIALS AND METHODS 51
4.3.1 VC aerobic oxidation experiment 51
4.3.2 VC and cDCE anaerobic reductive dechlorination experiments 51
4.3.3 Isotope ratio analysis 52
4.4 RESULTS AND DISCUSSION 52
4.4.1 Bulk isotope fractionation 52
4.4.2 Dual isotope approach based on the experimental data 54
4.4.3 Apparent kinetic isotope effects 55
4.4.4 Dual isotope approach based on AKIE 56
4.5 SUMMARY AND IMPLICATIONS 57

5. USE OF GEOCHEMICAL AND ISOTOPE DATA TO EVALUATE THE FATE OF CHLORINATED ETHENES IN A 2-KM CHLORINATED ETHENE PLUME 58

5.1 INTRODUCTION 59
5.2 STUDY SITE. 60
5.3 STUDY METHODS 63
5.3.1 Groundwater sampling 63
5.3.2 Analyses 63
5.3.3 Sampling sessions 64
5.4 RESULTS AND DISCUSSION 65
5.4.1 Identification of redox zones 65
5.4.2 Pyrite oxidation 67
5.4.3 Plume concentration evolution along the plume centerline 68
5.4.4 Isotope behaviors of chlorinated ethenes along the plume centerline 71
5.4.5 Fate of chlorinated ethenes in the lower zone 73
5.4.6 Fate of cDCE 74
5.4.7 Fate of VC 75
5.4.8 Quantification of reaction rates along the plume core 75
5.5 SUMMARY AND IMPLICATIONS 77

6. DOES THE RAYLEIGH EQUATION APPLY TO EVALUATE FIELD ISOTOPE DATA IN CONTAMINANT HYDROGEOLOGY? 78

6.1 INTRODUCTION 79
6.2 THEORY AND MODELING 81
6.2.1 Simulation of concentrations and isotope data 81
6.2.2 Evaluation of simulated data and quantification of uncertainty 84
6.2.2.1 Estimation of isotope enrichment factors 85
6.2.2.2 Estimation of the fraction remaining or the extent of biodegradation 85
6.2.2.3 Estimation of first-order rate constants 86
6.3 RESULTS AND DISCUSSION 87
6.3.1 Estimation of isotope enrichment factors 87
6.3.2 Estimation of the extent of biodegradation 89
6.3.3 Estimation of first-order reaction rate constants 91
6.3.4 Effect of chemical heterogeneity 93
6.4 SUMMARY AND IMPLICATIONS 94

7. QUANTIFICATION OF REDUCTIVE DECHLORINATION RATES USING THE FIELD CONCENTRATION AND CARBON ISOTOPE DATA 96

7.1 INTRODUCTION 97
7.2 SITE DESCRIPTION 99
7.3 VALIDATION OF ASSUMPTIONS 100
7.4 MODELING APPROACH 103
7.4.1 Transport model 103
7.4.2 Reactive transport model 104
7.4.3 Isotope model 104
7.5 MODEL IMPLEMENTATION 105
7.5.1 Model domains 105
7.5.2 Flow and transport model calibration 105
7.5.3 Quantification of transformation rates 106
7.5.4 Parameter sensitivity analyses 107
7.6 RESULTS AND DISCUSSION 107
7.6.1 Transport model 107
7.6.2 Reactive and isotope models 108
7.6.3 Parameter sensitivity analyses 112
7.6.4 Comparison of different methods to estimate a reaction rate 113
7.7 SUMMARY AND IMPLICATIONS 116

8. CONCLUSIONS, IMPLICATIONS AND OUTLOOK 117

8.1 CONCLUSIONS 117
8.1.1 Assessment of natural attenuation of chlorinated ethenes 117
8.1.2 Quantification of natural attenuation 119
8.1.3 Limiting step during reductive dechlorination 120
8.1.4 Factors influencing the progress of reductive dechlorination 120
8.2 PRACTICAL IMPLICATIONS 121
8.3 OUTLOOK 122

REFERENCES 124

APPENDIX A: EFFECT OF MOLECULE SIZE ON CARBON ISOTOPE FRACTIONATION DURING BIODEGRADATION OF CHLORINATED ALKANES BY *XANTHOBACTER AUTOTROPHICUS* GJ10 **137**

A.1 INTRODUCTION 138

A.2 MATERIALS AND METHODS 139

A.2.1 Bacterial growth conditions 139

A.2.2 Culture experiments 140

A.2.3 Preparation of cell-free extracts 140

A.2.4 Cell-free extract experiments 140

A.2.6 Calculations 141

A.3. RESULTS AND DISCUSSION 142

A.3.1 Pure culture studies 142

A.3.2 Cell-free extract studies 144

A.4 References 145

APPENDIX B: SUPPORTING INFORMATION FOR CHAPTER 6. 'DOES THE RAYLEIGH EQUATION APPLY TO EVALUATE FIELD ISOTOPE DATA IN CONTAMINANT HYDROGEOLOGY?' **148**

B.1 Text 149

B.2 References 151

Chapter 1

Introduction

1.1 General Background

Industrial development coincides with the increased production and use of synthetic organic chemicals. Decades of negligent disposals and accidental spills of these organic chemicals became apparent in the late 1970s. With the discovery of such hazardous waste sites in industrial countries, it became clear at many locations that these organic chemicals seeped into the subsurface environment, contaminating the aquifer materials and groundwater. Since then, much effort has been devoted to identify the impacted water bodies. According to a survey, an estimated 7% of the ambient groundwater resources of the United States currently contain at least one of the 60 volatile organic chemicals tested in the study (Squillace *et al.* 1999). Many of the identified organic contamination sources originate from leaking underground storage and septic tanks (Wiedemeier *et al.* 1997; Squillace *et al.* 1999). In industrially developed countries, the most frequently observed organic contaminants in shallow groundwater are, by far, tetrachloroethene (PCE) and trichloroethene (TCE) which are used regularly as degreasing and dry-cleaning agents (Wiedemeier *et al.* 1997; Squillace *et al.* 1999; Bundesamt für Umwelt 2004; Moran *et al.* 2007). From 1998 to 2001, total releases of PCE and TCE to the environment in the US are estimated to amount to 33 and 11 million kilograms, respectively (USEPA 2003).

Since the 1980s, considerable efforts have been made to investigate the contaminated sites by locating the contaminant sources and delineating the contaminant plumes with a network of monitoring wells. Cleanup activities were attempted to restore the contaminated soils and groundwater by physical procedures such as pump-and-treat, but it became clear in the early 1990s that such cleanup attempts were often ineffective and failed to meet the cleanup goals (Mackay and Cherry 1989; Wiedemeier *et al.* 1997). The ineffectiveness of the pump-and-treat approach was due to tailing and rebound phenomena of contaminant concentrations. It was mainly attributed to the fact that the sources of organic contaminants exist as liquids immiscible with water (nonaqueous-phase liquids, NAPLs) which become trapped in aquifer materials and slowly dissolve into the groundwater, creating a continuous contaminant source (Mackay and Cherry 1989). Therefore, the rehabilitation of contaminated sites by pump-and-treat approach alone is seen as remediation in perpetuity. It is particularly cumbersome when the NAPL is denser than water (DNAPL); such is the case for chlorinated solvents. DNAPLs can sink and accumulate deep in the aquifer, complicating the identification of NAPL locations. In addition, the presence of impermeable lenses can provide additional contaminant sinks by entrapping NAPLs as isolated pools. Such isolated pools can be unknowingly drilled through during the site investigation process, resulting in

the accidental expansion of the contamination into deeper parts of the aquifer or into a different aquifer (Mackay and Cherry 1989). The identification of NAPLs as a continuous contaminant source led to a shift in the remedial framework where the dissolved contaminants in a plume and a source zone need to be treated in different ways (Bedient *et al.* 1999).

In terms of source treatment methods, a number of innovative technologies emerged in the 1990s using physical, chemical and biological processes. Physical treatments include processes such as excavation, extraction, destruction, and containment as *in situ* source treatment methods. Extraction of volatile organic compounds from the source zone includes the use of soil vapor extraction (Hutzler *et al.* 1991; Hadim *et al.* 1993; Heron *et al.* 2005) and air-sparging (Johnson *et al.* 1993; Bass *et al.* 2000; McCray 2000). Destruction of contaminants by pyrolysis at 1600 to 2000°C is termed vitrification (Hamby 1996; Bedient *et al.* 1999; Khan *et al.* 2004). Containment of contaminants at the source zone requires the use of impermeable barriers to prevent the spreading of the contaminants into surrounding aquifer as well as the injection of chemical grouts (such as sodium silicate or polyacrylamide) or slurry grouts such as cement-based or lime fly ash to solidify the interstitial pore space (Hamby 1996). Soil flushing systems by injecting surfactants such as sodium sulfosuccinate (Pennell *et al.* 1994) and/or cosolvents such as alcohol (Jawitz *et al.* 2000) enhance the mobilization of NAPLs, and mobilized NAPLs can be collected from a extraction well (Bedient *et al.* 1999; Zhou and Rhue 2000; Soga *et al.* 2004). Alternatively, chemical and biological treatments such as chemical oxidation by potassium permanganate (Schnarr *et al.* 1998; McGuire *et al.* 2006), bioventing, biostimulation and bioaugmentation to enhance the contaminant degradation have been utilized (Hopkins and McCarty 1995; Harkness *et al.* 1999; Salanitro *et al.* 2000; Song *et al.* 2002; Gentry *et al.* 2004; McGuire *et al.* 2006). Biostimulation refers to a remediation approach which directly injects specific carbon sources such as acetate or lactose to manipulate the subsurface system so as to enhance the biological activity suitable for the degradation of a contaminant of interest. On the other hand, bioaugmentation supplements the subsurface system with specific microorganisms capable of degrading a contaminant of interest. Concerning the remediation of contaminant plumes, the use of funnel and gate systems to direct the plume to reactive barriers by which contaminants can be transformed into benign products has been practiced (Richardson and Nicklow 2002). In addition, chemical oxidation, biostimulation and bioaugmentation can also be used for plume remediation (Hopkins and McCarty 1995; Harkness *et al.* 1999; Salanitro *et al.* 2000; Song *et al.* 2002; Gentry *et al.* 2004). On the other hand, at some contaminated site it may be possible to leave the contaminated aquifer materials and groundwater intact to allow nature to restore the affected environment. The process is termed natural attenuation, and the decision to accept natural attenuation as a remedial strategy varies among countries and generally depends on the level of contamination, the local land and

groundwater use and the influence of contamination on the surrounding environments and human health as described in detail in section 1.4 (Wiedemeier *et al.* 1997; Rügner *et al.* 2006).

1.2 NATURAL ATTENUATION AS A REMEDIATION STRATEGY

The recent improvement in the understanding of subsurface properties and contaminant transport processes enabled detailed documentation of the evolution of contaminant plumes. Many of the organic contaminant plumes were found either stable or shrinking in size without intervention (Wiedemeier *et al.* 1997; Bedient *et al.* 1999). Based on these observations, the use of natural attenuation as a passive remedial approach became increasingly accepted particularly for well-studied fuel hydrocarbons. Natural attenuation is a remediation approach which utilizes naturally occurring processes such as dispersion, sorption, and degradation to control the spreading of groundwater contamination (Wiedemeier *et al.* 1997; Rügner *et al.* 2006). Although dispersion and sorption result in decreasing contaminant concentrations along the plume, they do not contribute to the contaminant mass reduction. In addition, the effect of sorption does not contribute to the decreasing contaminant concentrations if the contaminant source is continuous and the plume is at a steady state. Therefore, contaminant degradation (chemical and biological) is often the key factor to the successful application of natural attenuation. In general, difficulties with plume remediation arise from the facts that it involves a large volume of affected groundwater and that subsurface hydrology is complex (Squillace *et al.* 1999). Natural attenuation makes use of indigenous subsurface processes; thus, it is potentially capable of ‘treating’ a large volume of affected groundwater regardless of complex plume geometries caused by the subsurface heterogeneity. In addition to the use of natural attenuation as a plume remediation strategy, it is also applied in the final step of the source zone remediation since the remediation of the source is often incomplete (Soga *et al.* 2004; Friis *et al.* 2006), causing a less significant but sparse presence of contaminants, which may be best treated by natural attenuation.

In terms of natural attenuation mediated by biodegradation, numerous studies proved that organic contaminants once thought to be recalcitrant to biological transformation could be utilized and degraded by indigenous microbial communities. During the process of biodegradation, organic compounds serve either as electron donors or as electron acceptors. When serving as an electron donor, the organic compound is oxidized, and the microbially mediated reaction is coupled to the reduction of one of the common electron acceptors such as oxygen, nitrate, ferric iron, sulfate, and carbon dioxide. On the other hand, some highly chlorinated solvents can serve as electron acceptors themselves when coupled to the oxidation of an electron donor (Vogel *et al.* 1987). The process is termed reductive dechlorination as chlorinated solvents are reduced, and a chlorine substituent is replaced by a hydrogen atom. Therefore,

regardless of organic compounds serving as electron donors or acceptors, groundwater geochemical conditions play a significant role in determining the occurrence of biodegradation.

1.2.1 Surface water-groundwater interface

Groundwater and surface water are not isolated components of the hydrologic system, but are instead linked closely and interact with each other. Consequently, the contamination of one can affect the other. According to a study, 51% of 1218 contaminated sites are estimated to impact surface water bodies (USEPA 1991); however, only a few studies (Schwarzenbach *et al.* 1983; Vroblesky *et al.* 1996; Lorah and Olsen 1999; Conant 2004) have been carried out to understand the fate of contaminants in the surface water-groundwater interface. It is mainly because of the difficulty associated with tracing the groundwater contaminants along its transport path to the surface water. However, the importance of surface water-groundwater interface has been increasingly recognized as a zone which can attenuate significant amounts of contaminants.

River-water not only flows through the open river channel, but also through interstitial pores of the riverbed sediments, creating a mixing zone with subsurface water. The alluvial plain sediments also are frequently higher in hydraulic conductivity than the adjacent uplands (Woessner 2000; Fleckenstein *et al.* 2006), providing elevated water connectivity between the river and the underlying groundwater in which water is exchanged and mixed laterally from beneath the stream channel with saturated sediments (Morrice *et al.* 1997). Hence, the mixing zone in the surface water-groundwater interface is hydrologically dynamic. The mixing zone is not only dynamic in terms of hydrological aspects, but also in terms of biogeochemical aspects. It supports high biogeochemical activities due to the presence of organic-matter rich sediments, and is referred to as the hyporheic zone which lies within the upper layer of sediments beneath surface water bodies. At the hyporheic zone, a variety of important nutrients is cycled by different redox-driven reactions such as aerobic respiration, nitrification, denitrification, metal oxidation, metal reduction, sulphur oxidation, sulphate reduction, methanogenesis, methane oxidation, acetogenesis, and fermentation (Allan 1995). Therefore, when groundwater interacts with surface water systems, it is expected to experience various geochemical conditions in the hyporheic zone (Bourg and Bertin 1993). Since natural attenuation of organic compounds mediated by biological degradation depends on the geochemical conditions, the wide variety of geochemical conditions supported in the hyporheic zone is expected to play a significant role in reducing the organic contaminant mass.

1.2.2 Constrains for the use of natural attenuation

Concepts for the use of monitored natural attenuation in contaminated groundwater and land management vary among countries. It originates from the difference in the recognition of ‘receptors’ of the contamination among countries. In some countries such as Germany and Denmark, the soil and groundwater itself is regarded as the principal receptor of the contamination for the precautionary

protection of soil and groundwater. Hence, if compliance criteria for groundwater are exceeded, remediation measures must be undertaken (Rügner *et al.* 2006). On the other hand, countries such as the United States, The Netherlands and the United Kingdoms, the receptors of the contamination are the ecosystem and human health. Therefore, risk-based contaminated groundwater and land management is practiced by defining the possible exposure pathways to quantify the daily exposure levels (Rügner *et al.* 2006). Under such legislative concepts, remediation measures are required when the exposure level exceeds the acceptable level; hence, remediation targets are defined which does not exceed the acceptable daily intake and exposure of the contaminants of concern at the receptor. Therefore, whether natural attenuation can be an acceptable remediation approach depends on the defined remediation goals which vary among countries.

In addition to the legislative considerations which may or may not support the use of natural attenuation as a remediation approach, there are several practical considerations which may limit the use of natural attenuation. The limitations of implementing natural attenuation include the fact that the complete remediation may require a long time which necessitate the long-term monitoring program for a site undergoing natural attenuation and more importantly that transformation intermediates can be more toxic than their precursor compounds as is the case for chlorinated ethenes. PCE and TCE produce vinyl chloride (VC) via *cis*-dichloroethene (cDCE) by sequential reductive dechlorination, and VC is a confirmed carcinogen. In such a case, negligent acceptance of natural attenuation as a remediation approach at a site could result in transforming the site into a more severely contaminated site.

1.3 Degradation Pathways of Chlorinated Ethenes

Although reductive dechlorination of PCE and TCE (frequently detected contaminants in groundwater) can give rise to carcinogenic VC, chlorinated ethenes can also be microbially oxidized under different geochemical conditions. In addition to microbial processes, reductive transformation of chlorinated ethenes can also occur abiotically caused by reductants such as Fe(II) or S(-II) (Butler and Hayes 1999; Lee and Batchelor 2002; Lee and Batchelor 2004).

1.3.1 Sequential reductive dechlorination

Chlorinated ethenes are relatively oxidized compounds due to the presence of electronegative substituents; therefore, they often serve as an electron acceptor coupled to an electron donor, generally H_2 produced mainly by the fermentative processes. Under anaerobic conditions, the chlorine substituent of chlorinated ethenes can be replaced by hydrogen (reductive dechlorination) to form ethene as the final degradation product. In general, the tendency to undergo reductive dechlorination decreases with the decreasing number of chlorines as their ability to serve as an electron acceptor decreases in the same order due to the loss of electronegative substituents (Vogel *et al.* 1987; Wiedemeier *et al.* 1997; Bradley 2000). Their

ability to serve as electron acceptors is confirmed from a thermodynamic perspective (Table 1). Reductive dechlorination of PCE to TCE is ubiquitous in anoxic aquifers and can readily take place under nitrate-reducing conditions; hence, PCE can be a stronger electron acceptor than Fe(III). Transformation of TCE to cDCE requires more reducing conditions, such as iron-reducing. Transformation of cDCE to VC can proceed under sulfate-reducing conditions (Vogel *et al.* 1987; Bradley 2003) although the accumulation of cDCE under sulfate-reducing conditions are reported from microcosm and enrichment culture studies (Bagley and Gossett 1990; Pavlostathis and Zhuang 1993; Boopathy and Peters 2001). The dechlorination of VC to ethene is generally associated with methanogenic conditions (Wiedemeier *et al.* 1997; Bradley 2000; Witt *et al.* 2002); however, contradictory results are reported from studies which demonstrated VC reductive dechlorination to ethene by enrichment cultures without the involvement of methanogenic activities (Flynn *et al.* 2000) and in the presence of high sulfate concentrations (Hoelen and Reinhard 2004). These contradictory results suggest that different microbial communities may be involved with reductive dechlorination of cDCE and VC under sulfate-reducing and methanogenic conditions.

Incomplete reductive dechlorination can occur when chlorinated ethenes can not serve as electron acceptors due to the abundance of other naturally present electron acceptors which compete with chlorinated ethenes (Table 1). Since reductive dechlorination of cDCE and VC requires strongly reducing conditions (Bradley 2000), field studies report the frequent accumulation of cDCE (Wiedemeier *et al.* 1997; Witt *et al.* 2002). The comparison of thermodynamic properties of chlorinated ethenes (Table 1) suggests that cDCE has the lowest reduction potential, agreeing with the field observation of cDCE accumulation. On the other hand, some laboratory studies suggest that the rate of VC dechlorination to ethene is approximately two orders of magnitude slower than the preceding series of dechlorination steps, giving rise to the accumulation of VC (Magnuson *et al.* 1998). In contrast, some field observations report that the estimated reaction rates during reductive dechlorination increase with the decreasing number of chlorine substituents, which contradicts the laboratory observations (Wiedemeier *et al.* 1997). Therefore, the laboratory and field observations do not always agree with the theoretical prediction based on thermodynamic properties of chlorinated ethenes.

In addition to the limitation imposed by the presence of other electron acceptors, incomplete reductive dechlorination can also result from the lack of electron donor species (such as H_2), which can be produced by the means of fermentation. Natural organic matters in subsurface environments can be utilized by fermentative microorganisms (Appelo and Postma 2005); however, to date there is no study which report the importance of the natural organic matters with the progress of reductive dechlorination. Field studies agree that a mixed contaminant source of chlorinated ethenes and fuel components triggers higher rates of reductive dechlorination than a source consisting only of chlorinated ethenes (Wiedemeier *et al.* 1997). The biodegradation of fuel components can take place readily, and it depletes the naturally present

electron acceptors, creating a condition where reductive dechlorination can serve as alternative electron acceptors. In addition, reductive dechlorination can proceed strongly particularly when fuel components start to be fermented to produce H_2, the electron donor for reductive dechlorination (Wiedemeier *et al.* 1997).

Table 1 Standard reduction potentials at pH 7.0 (Wiedemeier *et al.* 1997)

Oxidants	Reductants	E_h^0 (V)
$O_2 + 4H^+ + 4e^-$	$2H_2O$	+0.81
$NO_3^- + 6H^+ + 6e^-$	$1/2N_2 + 3H_2O$	+0.75
$MnO_2 + 4H^+ + 2e^-$	$Mn^{2+} + 2H_2O$	+0.57
$PCE + H^+ + e^-$	$TCE + Cl^-$	+0.58
$TCE + H^+ + e^-$	$cDCE + Cl^-$	+0.55
$VC + H^+ + e^-$	$Ethene + Cl^-$	+0.49
$cDCE + H^+ + e^-$	$VC + Cl^-$	+0.36
$Fe(OH)_3 + 3H^+ + 3e^-$	$Fe^{2+} + 3H_2O$	+0.06
$SO_4^{2-} + 9H^+ + 8e^-$	$HS^- + 4H_2O$	-0.22
$CO_2 + 8H^+ + 8e^-$	$CH_4 + 2H_2O$	-0.24
$H^+ + e^-$	½ H_2	-0.41

The accumulation of cDCE and VC may also occur because of the absence of suitable microbial community at the site. A few number of organisms are isolated and shown to respire on chlorinated ethenes (Holliger *et al.* 1993; Holliger *et al.* 1999; Maymo-Gatell *et al.* 1999; Bradley 2003). Complete anaerobic dechlorination of PCE to ethene have been observed in mixed and enriched culture studies (Vogel and McCarty 1985; Freedman and Gossett 1989; DiStefano *et al.* 1991; de Bruin *et al.* 1992; Loffler *et al.* 1997), but to date the genus *Dehalococcoides* which utilizes H_2 as the electron donor is the only known group of microorganisms which can cometabolically (strains 195 and FL2) or metabolically (strains Y51 and VS) dechlorinate VC to ethene (Maymo-Gatell *et al.* 1999; Bradley 2000; Loffler *et al.* 2000; Cupples *et al.* 2003; He *et al.* 2003). A comprehensive survey of 24 chlorinated ethene contaminated sites report that the presence of *Dehalococcoides*, detected by DNA-based molecular probe targeted to *Dehalococcoides*, had a high correlation to complete *in situ* reductive dechlorination (Hendrickson *et al.* 2002).

1.3.2 Oxidative degradation

While the rate of reductive transformation tends to decrease with a decreasing number of chlorine atoms, the possibility for oxidative transformation increases. Consequently, VC tends to be oxidized most readily

while the oxidation of PCE does not take place (Bradley and Chapelle 2000). It has been demonstrated that TCE, cDCE, and VC can be cometabolically oxidized under aerobic conditions (Nelson *et al.* 1987; Little *et al.* 1988; Wackett and Gibson 1988; Oldenhuis *et al.* 1989; Tsien *et al.* 1989), and cDCE and VC can be metabolically oxidized under aerobic conditions (Hartmans *et al.* 1985; Hartmans and de Bont 1992; Bradley and Chapelle 1998; Klier *et al.* 1999; Bradley and Chapelle 2000; Coleman *et al.* 2002). The responsible microorganisms possess non-specific oxygenases, which can fortuitously oxidize chlorinated ethenes. cDCE and VC can also be metabolically oxidized under anaerobic conditions to produce CO_2 (Bradley *et al.* 1998; Bradley and Chapelle 1998). Microcosm studies revealed that the rate of anaerobic VC mineralization as recovered $^{14}CO_2$ decreased in the order of aerobic, Fe(III)-reducing, SO_4^{2-}-reducing, and methanogenic conditions (Bradley and Chapelle 1998). Direct anaerobic mineralization of cDCE requires stronger oxidants, and it can take place under Mn(IV)-reducing conditions (Bradley *et al.* 1998). The anaerobic mineralization of cDCE under Fe(III)- and SO_4^{2-}-reducing conditions proceeds via an initial rate-limiting reduction to VC, which in return is anaerobically oxidized to CO_2 (Bradley and Chapelle 1998). In addition, cDCE and VC can also be oxidized under humic-acid-reducing condition to produce CO_2 and CH_4 (Bradley *et al.* 1998).

While the mechanism for anaerobic oxidation of cDCE and VC is not yet understood, the aerobic oxidation of chlorinated ethenes involves a universal catalytic reaction, epoxidation by mono- or di-oxygenases, as an initial step (Fox *et al.* 1990; Hartmans and de Bont 1992; van Hylckama Vlieg *et al.* 1996; van Hylckama Vlieg *et al.* 1998; Coleman and Spain 2003). Currently, it is generally accepted that VC can be readily degraded under aerobic conditions although only a few bacteria, strains of *Mycobacterium* (Hartmans and de Bont 1992; Coleman *et al.* 2002), *Nocardioides* (Coleman *et al.* 2002) and *Pseudomonas* (Verce *et al.* 2000), have so far been identified. However, a survey based on the construction of microcosms from 37 chlorinated ethene contaminated sites demonstrated that aerobic VC oxidation took place readily in 23 microcosms, suggesting the wide spread of microbial communities capable of aerobic VC oxidation (Coleman *et al.* 2002).

1.4 Demonstrating the Occurrence of Natural Attenuation

Before using monitored natural attenuation as a remedial option, it must be clearly demonstrated that natural attenuation processes efficiently and persistently protect the environment from harmful impacts (Rügner *et al.* 2006). Typical ways to determine whether biodegradation is occurring to remediate a contaminated aquifer are to evaluate 1) historical site data to demonstrate the plume stability and the loss of contaminant mass over time, 2) the chemical and geochemical data such as the consumption of electron acceptors and donors as well as the presence of metabolic byproducts (Beller 2000; Elshahed *et al.* 2001; Griebler *et al.* 2004) and the changes in enantiomeric fraction of chiral compounds (Zipper *et al.* 1998;

Williams *et al.* 2003; Reitzel 2005) and 3) microbiological data such as the use laboratory microcosms constructed from local aquifer materials to demonstrate the ability of indigenous microbial communities to degrade the contaminant (Wiedemeier *et al.* 1997; Bedient *et al.* 1999). The first type of data is valuable to show that the plume is attenuated over time, but it does not necessarily indicate that the contaminants are being destroyed. The second type, on the other hand, provides characteristic chemical and geochemical signatures resulting from the biological destruction of contaminants when compared to the unaffected part of the aquifer. The third type of data can provide information for estimating a degradation rate, if the contaminant can be degraded at all.

Despite several available approaches to demonstrate the occurrence of natural attenuation, the demonstration of the actual progress of natural attenuation can be difficult. Typically, decreasing field concentration data along the plume centerline are interpolated to quantify the extent of biodegradation. However, decreases in contaminant concentrations over distance can result from contaminant attenuation due to sorption and dilution caused by dispersion, implying that field concentration data alone can not provide a conclusive evidence for the occurrence of natural attenuation. Laboratory microcosm studies are not commonly used for site-specific natural attenuation assessment because it is time-consuming. It is also affected by culture biases due to the preferential enrichment of the target microbial community; thus, derived degradation rates often overestimate the *in situ* degradation rate (Wiedemeier *et al.* 1997).

In addition to the above-mentioned drawbacks with demonstrating the occurrence of natural attenuation, for the case of chlorinated ethenes, there are some constrains with chemical and geochemical data to support the occurrence of natural attenuation. Chlorinated ethenes undergo sequential reductive dechlorination under anoxic conditions; hence, the presence of less chlorinated transformation intermediates indicates the transformation of more chlorinated parent compounds. However, the transformation intermediates can be degraded by other pathways such as aerobic and anaerobic oxidation and abiotic reduction in which the detection of metabolites would not be feasible due to their ubiquitous presence. In addition, PCE used at the industrial grade may contain less chlorinated ethenes as impurities. In such a case, the presence of less chlorinated ethenes does not indicate the occurrence of reductive dechlorination. Nevertheless, it is important to identify the fate of reductive dechlorination intermediates in order to demonstrate the feasibility and the efficacy of natural attenuation of chlorinated ethenes. Thus, despite the fact that chlorinated ethenes are among the most frequently detected groundwater contaminates and the natural attenuation of chlorinated ethenes can be considered as a remediation approach, the monitoring of the progress of natural attenuation of chlorinated ethenes is encountered by the lack of appropriate tools to document and quantify the progress of such processes at field scales. In the last decade, the compound-specific stable isotope approach has been recognized as a potential tool to investigate the chlorinated-ethene contaminated sites.

1.5 COMPOUND-SPECIFIC STABLE ISOTOPE ANALYSIS

In recent years, compound-specific stable isotope analysis has developed into a new and innovative investigation tool to document the progress of natural attenuation in contaminant hydrology. Early works from laboratory studies demonstrated that the biodegradation of organic compounds are accompanied by isotope fractionation due to the difference in reaction rates between the compounds with light isotopes and those with heavy isotopes (Heraty *et al.* 1999; Hunkeler *et al.* 1999; Meckenstock *et al.* 1999; Sherwood Lollar *et al.* 1999; Hunkeler and Aravena 2000). The heavy isotopes progressively become enriched as the biodegradation proceeds over time. This isotope enrichment phenomenon is described by an empirical expression, the Rayleigh equation, which relates the difference in heavy to light isotope ratios to the changes in concentrations over time. Isotope fractionation originates only from the chemically and biologically mediated transformation of a compound, and not from other physical processes such as sorption and dispersion (Harrington *et al.* 1999; Slater *et al.* 2000; Schüth *et al.* 2003). In other words, the isotope approach enables the quantification of contaminant concentration decreases due only to biodegradation, which could not be achieved by conventional investigation methods. The isotope approach has been applied increasingly to demonstrate the occurrence of *in situ* biodegradation at contaminated sites (Sturchio *et al.* 1998; Hunkeler *et al.* 1999; Meckenstock *et al.* 1999; Sherwood Lollar *et al.* 1999; Kolhatkar *et al.* 2002; Richnow *et al.* 2003; Richnow *et al.* 2003; Griebler *et al.* 2004).

1.5.1 Rayleigh isotope fractionation model

The Rayleigh isotope fractionation model was originally developed for alcohol distillation processes in a batch system and was later adapted to the isotope fractionation phenomenon (Clark and Fritz 1997). The model relates the changes in isotope ratios to the changes in concentrations by:

$$1000 \cdot \ln(\frac{R}{R_0}) = \varepsilon \cdot \ln\left[\frac{C}{C_0}\right] \qquad (1)$$

where R is the observed isotope ratio, R_0 the initial isotope ratio, ε the enrichment factor [‰], C the observed concentration, and C_0 the initial concentration. Equation 1 is often termed the Rayleigh equation and it can be approximated by:

$$\partial^{13}C = \partial^{13}C_0 + \varepsilon \cdot \ln\frac{C}{C_0} \qquad (2)$$

where $\delta^{13}C=(R_C/R_{C\_std}-1)*1000‰$ where R_C and R_{C_std} are the carbon isotope ratio of the sample and the standard, respectively. Enrichment factors are related to the relative reaction rates of the compound with light and heavy isotopes:

$$\varepsilon = (1-\frac{^{H}k}{^{L}k}) \cdot 1000 = (1-\alpha) \cdot 1000 \qquad (3)$$

where ${}^{L}k$ is the reaction rate of the light isotope, ${}^{H}k$ is that of the heavy isotope and α is termed as fractionation factor. The ratio between ${}^{L}k$ and ${}^{H}k$ approximates the reaction ratio of the compound with light and heavy isotopes. Enrichment factors are generally derived from laboratory studies in a closed system to maintain the mass balance. As the degradation proceeds, the compound becomes progressively enriched in heavy isotopes, resulting from isotope fractionation. The values of enrichment factors are compound specific and depends on an enzymatic degradation pathway (Morasch *et al.* 2002; Hirschorn *et al.* 2004; Chartrand *et al.* 2005) although the laboratory-derived enrichment factor slightly varies for the same compound degraded by the same mechanism depending on the type of experiment (i.e. pure culture vs. mixed culture) and on the bacterium used for pure-culture experiments (Meckenstock *et al.* 2004).

It is widely accepted that the estimation of enrichment factors from field isotope data is smaller than the laboratory-derived value since C/C_0 measured in the field is not only caused by the biodegradation, but also by groundwater dilution due to dispersion. Therefore, laboratory-derived enrichment factors instead of the field-derived counterparts are generally used for the data interpretation. Based on the field isotope data and the literature value of an enrichment factor, the relative concentration term (C/C_0) in Equation 1 can be estimated by assuming the isotope ratio at the source to be R_0. The calculated C/C_0 represents the non-degraded fraction or the remaining fraction of the compound at the measured location, and it does not resemble the measured C/C_0 obtained from the concentration data which are affected by sorption and dilution effect. Several studies report the extent of biodegradation based on such interpolation of field isotope data (Stehmeiner *et al.* 1999; Sherwood Lollar *et al.* 2001; Mancini *et al.* 2002; Meckenstock *et al.* 2002; Richnow *et al.* 2003; Griebler *et al.* 2004; Peter *et al.* 2004). In addition, by assuming a first-order reaction kinetics, the intrinsic reaction rate can be estimated (Hunkeler *et al.* 2002; Morrill *et al.* 2005). The derivation of a first-order rate constant based on the isotope data is expressed as:

$$k = -\frac{\frac{1000}{\varepsilon}\cdot \ln(\frac{R}{R_0})}{\tau} \qquad (4)$$

where k is the reaction rate and τ is the mean water residence time calculated from estimated hydrological parameters (generally the distance traveled divided by the estimated groundwater velocity).

1.5.2 Dual isotope approach

The premise of the use of the Rayleigh-type interpretation of field isotope data is that the responsible degradation pathway which causes the observed isotope fractionation is known *a priori*. However, a number of organic compounds can be biodegraded by different reaction mechanisms under different or same redox conditions, complicating the identification of the responsible degradation pathway. Laboratory studies reveal that the isotope approach can distinguish the responsible degradation mechanism if different degradation pathways involve breaking of different bonds which are accompanied by different isotope

enrichment factors (Hirschorn *et al.* 2004). Nonetheless, field-derived isotope enrichment factors as mentioned above, because they are affected by the effect of dilution, can not be used to determine the responsible degradation pathway. Therefore, the Rayleigh interpolation of field isotope data under a condition in which more than one possible reaction pathways can concomitantly take place would limit the use of isotope approach as it could result in misleading conclusions by selecting an inappropriate enrichment factor.

The use of paired isotope analyses, or dual isotope analyses in which isotope ratios of two elements are quantified, has been recognized as a more promising approach to trace the responsible degradation pathway at the field scale. Two sets of isotope ratio measurements are plotted against each other, and the correlation between the two resembles the ratio between the enrichment factors of two elements as derived by the division of Equation 2 by an analogous expression with respect to another isotope element, for example chlorine, yields:

$$\frac{\Delta\delta^{37}Cl}{\Delta\delta^{13}C} = \frac{\varepsilon_{Cl}}{\varepsilon_{C}} \qquad (5)$$

where $\Delta\delta^{37}$Cl and $\Delta\delta^{13}$C are the differences between the initial and the final isotope ratios of chlorine and carbon isotopes, respectively. Equation 5 is independent of contaminant concentrations; thus, it is expected to assist in determining the degradation mechanism from field investigation. Laboratory studies on carbon and hydrogen isotope effects during biodegradation of benzene clearly distinguished the aerobic and anaerobic degradation pathways since hydrogen isotope effects vary significantly between the two reactions (Hunkeler *et al.* 2001; Morasch *et al.* 2002; Mancini *et al.* 2003). The dual isotope approach was employed at a methyl *tert*-butyl ether contaminated site to successfully identify the zones undergoing aerobic and anaerobic degradation (Zwank *et al.* 2005).

1.5.3 Isotope fractionation during chlorinated ethene degradation

Laboratory studies have reported the carbon isotope enrichment factors associated with the reductive dechlorination of PCE, TCE, cDCE and VC (Bloom *et al.* 2000; Slater *et al.* 2001; Hunkeler *et al.* 2002), cometabolic oxidation of TCE, cDCE and VC under aerobic conditions (Barth *et al.* 2002; Chu *et al.* 2004) and metabolic and aerobic VC oxidation (Chartrand *et al.* 2005) as summarized in Table 2. Reported carbon enrichment factors for reductive dechlorination of TCE, cDCE and VC were obtained from experiments where the compound of interest was directly used as a substrate (Bloom *et al.* 2000; Slater *et al.* 2001). Reductive dechlorination is accompanied by significant isotope fractionation, and the magnitude increases in the order of decreasing number of chlorine substituents. On the other hand, aerobic oxidation in general gives rise to a relatively small carbon isotope effect. The cause for the large isotope enrichment factor determined for TCE cometabolic oxidation is not yet clarified (Barth *et al.* 2002).

Table 2 Experimentally derived enrichment factors for chlorinated ethene degradation

		Enrichment factor (‰)	Culture type used
PCE	Reductive dechlorination	-5.5 (Slater *et al.* 2001)	Consortium
TCE	Reductive dechlorination	-6.6 and -2.5 (Bloom *et al.* 2000)	Consortium
		-13.8 (Slater *et al.* 2001)	Consortium
	Aerobic/Cometabolic oxidation	-1.1 (Chu *et al.* 2004)	Pure culture
		-18.2 (Barth *et al.* 2002)	Pure culture
cDCE	Reductive dechlorination	-20.4 (Slater *et al.* 2001)	Consortium
		-14.1 and -16.1 (Bloom *et al.* 2000)	Consortium
		-19.9 (Hunkeler *et al.* 2002)	Microcosm
	Aerobic/Cometabolic oxidation	-0.4 (Chu *et al.* 2004)	Pure culture
VC	Reductive dechlorination	-22.4 (Slater *et al.* 2001)	Consortium
		-21.5 (Bloom *et al.* 2000)	Consortium
		-31.1 (Hunkeler *et al.* 2002)	Microcosm
	Aerobic oxidation	-5.7 (Chu *et al.* 2004)	Pure culture
		-7.0 to -8.2 (Chartrand *et al.* 2005)	Pure culture
	Aerobic/Cometabolic oxidation	-3.2 to -4.8 (Chu *et al.* 2004)	Pure culture

1.5.4 Isotope behaviors during reductive dechlorination

Due to the simultaneous transformation and formation of reaction intermediates during reductive dechlorination, the interpretation of the observed isotope ratios of chlorinated ethenes is complicated. The parent compound (PCE) follows a typical Rayleigh relation where decreasing concentrations are accompanied by increasing isotope ratios. Therefore, for the parent compound of reductive dechlorination, Rayleigh-based isotope data interpretations apply. However, intermediate compounds do not follow the Rayleigh-type behavior because they are simultaneously formed and transformed. The initial isotope ratio of a reaction intermediate at the time of formation is significantly lighter than the precursor depending on the isotope enrichment factor for the transformation step. As the reaction proceeds, the isotope ratios of intermediates also increase linearly.

The trend is depicted in Figure 1 where consecutive formations of less chlorinated ethenes result in lighter carbon isotope ratio. Simultaneous presence of a heavier product and a lighter precursor can occur especially between TCE and cDCE because the isotope enrichment factor of cDCE is greater than that of TCE. The presence of more enriched product compared to its precursor can also result from a situation in which the transformation rate of a product is faster than that of the precursor (van Breukelen *et al.* 2005). Laboratory and field studies reported similar patterns in the evolution of isotope ratios of reaction intermediates (Hunkeler *et al.* 1999; Bloom *et al.* 2000; Song *et al.* 2002). The distinctive isotope trend during reductive dechlorination is that the carbon isotope ratio of the final product or the accumulating species resembles that of the original compound since carbons in the ethene backbone are conserved during sequential reductive dechlorination of chlorinated ethenes (Hunkeler *et al.* 1999). Therefore, the

carbon isotope approach assists in the identification of an accumulating species. However, the effect of sorption under non-steady conditions in terms of plume development can possibly have adverse effects in which the isotope ratio of an accumulating species does not reach that of the parent compound (van Breukelen *et al.* 2005). There have been few field investigations using the carbon isotope approach to demonstrate the reductive dechlorination of chlorinated ethenes. Early studies demonstrated that carbon isotope fractionation was accompanied by decreasing concentrations over distance (Hunkeler *et al.* 1999; Sherwood Lollar *et al.* 2001; Song *et al.* 2002; Vieth *et al.* 2003). Studies tracing the complete reductive dechlorination of PCE to ethene demonstrated the complex isotope evolution of reaction intermediates during the process as shown in Figure 1 (Hunkeler *et al.* 1999; Song *et al.* 2002).

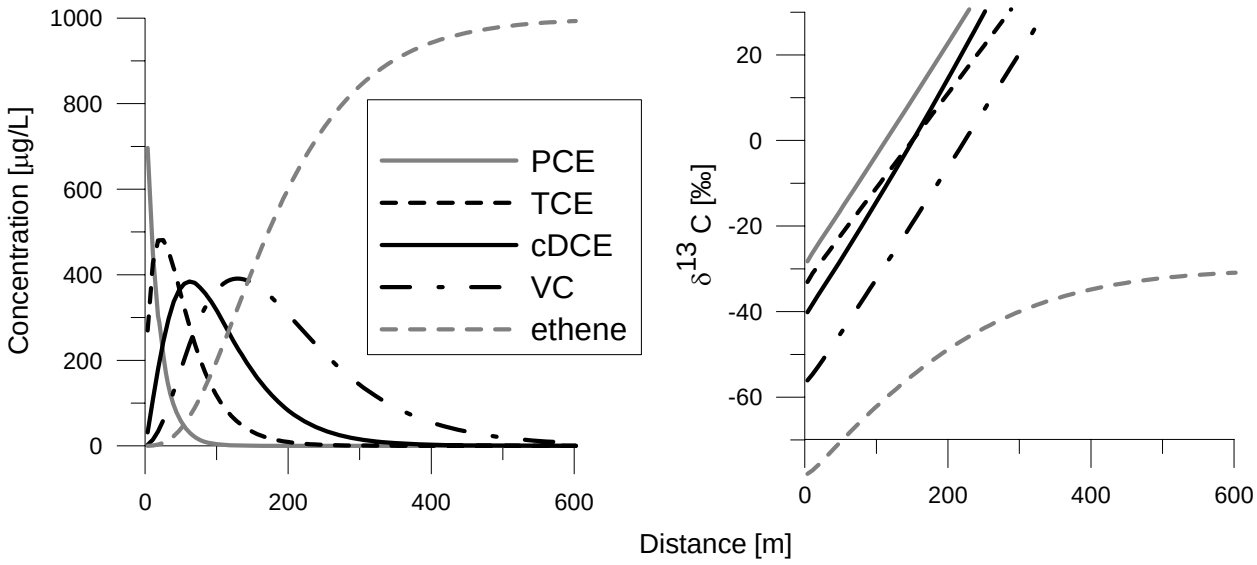

Figure 1 Concentration and isotope behaviors during reductive dechlorination of PCE based on numerical 1D transport simulation (reproduction from van Breukelen *et al.* 2005)

1.6 OBJECTIVES OF THE RESEARCH

The main objective of the thesis was to evaluate the possibilities and limits of the compound-specific stable isotope approach to assess and quantify the natural attenuation of chlorinated ethenes at field scales. The research focused particularly on the fate of the transformation intermediates, cDCE and VC, because the further degradation of these compounds usually determines the feasibility of natural attenuation as a remediation approach and also because the assessment of the fate of these compounds is particularly difficult due to the possibility of different degradation pathways. The research included laboratory- and field-scale investigations as well as numerical studies to qualitatively and quantitatively assess the natural attenuation of chlorinated ethenes. Specifically, the applicability of isotope approach at field scales to determine the progress of reductive dechlorination, to deduce the possibility of alternative degradation pathways and to identify the responsible on-going degradation pathway was investigated. The isotope

approach was examined at a surface water-groundwater interface in the PCE-discharging streambed where hydrologically and geochemically dynamic conditions were identified (Angus site) and at a site where a low level of degradation was expected as characterized by a 2-km long chlorinated-ethene plume (Rødekro site). Specific objectives and study methods of individual chapters are summarized below.

Chapter 2: A field study on the use of carbon isotope analysis to determine the progress of reductive dechlorination was carried out at a site consisting of the PCE-discharging streambed where hydrological and geochemical conditions varied significantly.

Chapter 3: The field isotope observations presented in Chapter 2 were compared with the results from geochemical and microbial investigation methods to evaluate the compatibility of different field parameters to assess the progress of reductive dechlorination.

Chapter 4: The combined carbon and chlorine isotope approach to distinguish between reductive dechlorination and aerobic oxidation of cDCE and VC was examined with laboratory experiments.

Chapter 5: A field investigation of the use of carbon isotope approach to deduce the possibility of alternative degradation pathways of intermediates from reductive dechlorination as well as the use of combined carbon and chlorine isotope approach to determine the fate of cDCE was carried out for a 2-km long chlorinated-ethene plume where very low level of transformation was expected.

Chapter 6: The degree of uncertainties with the Rayleigh-based quantification of the extent of biodegradation and the degradation rate was systematically quantified under various field conditions using a two-dimensional analytical solution.

Chapter 7: A scheme to estimate the transformation rates during reductive dechlorination based on the field carbon isotope data was proposed and demonstrated for the field investigation presented in Chapter 5 using a three-dimensional analytical solution.

Chapter 8: Conclusions from the thesis as well as applications of the findings and outlook are presented.

Chapter 2

Combining geochemical and isotope data to evaluate the fate of chlorinated ethenes discharging through streambed sediments

Abstract

A detailed field investigation was carried out to evaluate the use of stable carbon isotope analysis at field scales under geochemically and hydrologically complex conditions and to determine the fate of chlorinated ethenes in the streambed where a tetrachloroethene (PCE) plume discharged. Sediment and water samples from the streambed were taken at different depths to characterize the lithology, concentrations of redox-sensitive species as well as concentrations and carbon isotope ratios of PCE and its transformation products. Hydrochemical analysis was effectively employed to characterize the complex hydraulic interactions as well as the variation in local redox conditions in the streambed, and the carbon isotope analysis was crucial to identify the final degradation product at each location and to distinguish the chlorinated-ethene concentration decreases caused by reductive dechlorination and by other physical processes. The results demonstrated that even for a relatively small studied area (25 m x 15 m), there was a significant spatial variability of discharge rates, redox conditions and extents of PCE transformation, and these factors were closely related to one another. In a high discharge zone under nitrate-reducing conditions, no significant biodegradation of PCE was observed. At a location with an intermediate discharge rate under predominantly iron-reducing conditions, *cis*-dichloroethene (cDCE) was the main compound with constant isotope ratios indicating no further degradation. At a location with a very low discharge rate under predominantly sulphate-reducing conditions, cDCE and vinyl chloride (VC) became strongly enriched in ^{13}C and ethene was present, suggesting complete reductive dechlorination. In contrast, another location in a relatively high discharge zone and also under sulphate-reducing conditions was accompanied by the accumulation of cDCE. The difference in local discharge rates probably gave rise to the difference in the fate of cDCE under sulphate-reducing conditions. Finally, at a location under methanogenic conditions with a low discharge rate and a high sedimentary organic matter content, ethene became enriched in ^{13}C suggesting its further transformation, to ethane which was present throughout the location.

Abe, Y., Aravena, R., Parker, B.L., Cherry, J.A., Zopfi, J. and Hunkeler, D.
To be partially submitted to the Journal of Contaminant Hydrology

2.1 INTRODUCTION

Chlorinated ethenes are among the most frequently detected groundwater contaminants in developed countries (Wiedemeier *et al.* 1997; Squillace *et al.* 1999; Bundesamt für Umwelt 2004). The occurrence of chlorinated ethenes in groundwater is of concern because of their high toxicity. Due to their high density and viscosity (Pankow and Cherry 1996), chlorinated solvents can migrate to a substantial depth in aquifers. Their relatively low hydrophobicity results in a low tendency toward sorption, which facilitates the formation of long contaminant plumes (Schwarzenbach *et al.* 1983; Wiedemeier *et al.* 1997). Sites contaminated with chlorinated ethenes are difficult to remediate since they often show complex contaminant distribution patterns and involve a large volume of affected groundwater and aquifer materials. Thus, the use of natural attenuation as an alternative site remediation method is of great interest (Lu *et al.* 1999).

Chlorinated ethenes are relatively oxidized compounds due to the presence of electronegative subsistent; therefore, they often serve as electron acceptors with the organic material as the electron donor species. Generally, tetrachloroethene (PCE) can be reductively dechlorinated under at least nitrate-reducing conditions and trichloroethene (TCE) under at least iron-reducing conditions whereas reductive dechlorination of *cis*-dichloroethene (cDCE) and vinyl chloride (VC) generally requires sulfate-reducing or better methanogenic conditions (Vogel and McCarty 1985; Vogel *et al.* 1987; Freedman and Gossett 1989; DiStefano *et al.* 1991; Maymo-Gatell *et al.* 1995; Rügge *et al.* 1999; Bradley 2000). Apart from reductive dechlorination, TCE, cDCE and VC can be oxidized metabolically and co-metabolically under aerobic and/or anaerobic conditions (Nelson *et al.* 1987; Little *et al.* 1988; Wackett and Gibson 1988; Oldenhuis *et al.* 1989; Tsien *et al.* 1989; Davis and Carpenter 1990; Fox *et al.* 1990; Rasche *et al.* 1990; Rasche *et al.* 1990; Vannelli *et al.* 1990; Bradley and Chapelle 1998; Verce *et al.* 2001). VC (as well as cDCE to a much less extent) can also be transformed to CH_4 under methanogenic conditions (Bradley and Chapelle 1999). In addition, abiotic reduction of PCE, TCE and cDCE to acetylene and VC to ethene by iron-bearing minerals has been reported (Lee and Batchelor 2002; Lee and Batchelor 2004).

According to a survey carried out by the US EPA, approximately 50% of contaminated groundwater sites are estimated to impact a surface water body (USEPA 1991); thus, understanding the fate of contaminants at the groundwater-surface water mixing zone is important to assess the impact of the groundwater contamination to surface waters. When groundwater interacts with a surface water system, it can experience various levels of strongly reducing conditions over a relatively short distance due to the frequent presence of organic-matter-rich sediments in streambed deposits (Bourg and Bertin 1993). As mentioned, reductive dechlorination of chlorinated ethenes is sensitive to redox conditions, and complete reductive dechlorination often requires methanogenic conditions which are not ubiquitous in aquifers, the strongly-reducing hyporheic zone in the streambed is expected to serve as an important zone for

enhancing the progress of reductive dechlorination and reducing the contaminant mass (Lorah and Olsen 1999; Conant *et al.* 2004; Chapman *et al.* 2007). In addition to reductive dechlorination, as the chlorinated ethene plume discharges into a surface water body, the aerobic oxidation of recalcitrant cDCE and VC can be expected.

Despite the fact that chlorinated ethenes are among the most frequently detected groundwater contaminants and that their various degradation pathways have been understood, assessing the progress of natural attenuation of chlorinated ethenes still remains a challenge. In terms of sequential reductive dechlorination, the presence of less chlorinated transformation intermediates indicates the transformation of more chlorinated parent compounds. However, the transformation intermediates can be degraded by other pathways whose metabolites are ubiquitous in groundwater; thus, metabolite analyses are generally not feasible. Although natural attenuation of chlorinated ethenes can be considered as a passive remediation approach, it is encountered by the lack of appropriate tools to document and quantify the progress of natural attenuation of chlorinated ethenes at field scales. The compound-specific stable isotope analysis has been proposed as a new and innovative tool to investigate the progress of natural attenuation of organic contaminants (Meckenstock *et al.* 2004). Although the carbon isotope analysis has been used at a few chlorinated-ethene contaminated sites (Hunkeler *et al.* 1999; Sherwood Lollar *et al.* 1999), the applicability of the approach under different field conditions remained unclear.

The objective of this study is to evaluate the use of carbon isotope analysis under geochemically and hydrologically complex conditions and to investigate the degradation patterns of chlorinated ethenes in the streambed where a PCE plume discharges. Due to the complex water exchange processes inherent in groundwater-surface water interface, mixing and dilution effects can influence the concentrations of precursors and products. Therefore, the site was ideal for comparing the traditional concentration-based and the isotope-based approaches to assess the progress of natural attenuation. The study focuses particularly on the fate of cDCE and VC because the success of natural attenuation of chlorinated ethenes critically depends on whether these relatively recalcitrant intermediates are removed (Bradley 2000). Stable carbon isotope analysis is particularly suitable for tracing the fate of cDCE and VC because the reductive dechlorination of these compounds is accompanied by a strong carbon isotope effect (Bloom *et al.* 2000). In order to sample a large variation of hydrological conditions, streambed temperatures were measured thoroughly to identify different groundwater discharge patterns at the study site (Conant 2004; Anderson 2005). The streambed was sampled at multiple depths to evaluate the spatial variability of redox conditions and their effect on contaminant degradation.

During reductive dechlorination of chlorinated ethenes, each step is accompanied by a characteristic carbon isotope fractionation. However, due to the simultaneous transformation and production of reaction intermediates, reaction intermediates are depleted in ^{13}C at first, compared to the isotope ratio of a

precursor compound, then they become progressively enriched (Bloom *et al.* 2000; Slater *et al.* 2001). Therefore, the interpretation of carbon isotope data during reductive dechlorination is complicated. Despite the complex carbon isotope behaviors, carbon isotope approach assists in identifying the accumulating species during incomplete reductive dechlorination. Due to the conservation of carbons in the ethene backbone during reductive dechlorination, the final product (complete or incomplete) is accompanied by the carbon isotope ratio which resembles that of the original compound (PCE in this case) (Bloom *et al.* 2000; Slater *et al.* 2001).

2.2 STUDY SITE DESCRIPTION

The study site is located 80 km northwest of Toronto and 5 km northeast of the Borden hydrogeological research site of the University of Waterloo. The aquifer was contaminated with PCE by dry-cleaning operations which started in early 1970s until 1994. PCE DNAPL dissolution causes a contaminant plume which travels in a confined aquifer for approximately 195 m until it discharges into the Pine River (Figures 1 and 2). The riverbank opposite from the contaminated side does not have a detectable level of PCE and its transformation products, indicating that all of the contaminated groundwater discharges into the river (Conant *et al.* 2004).

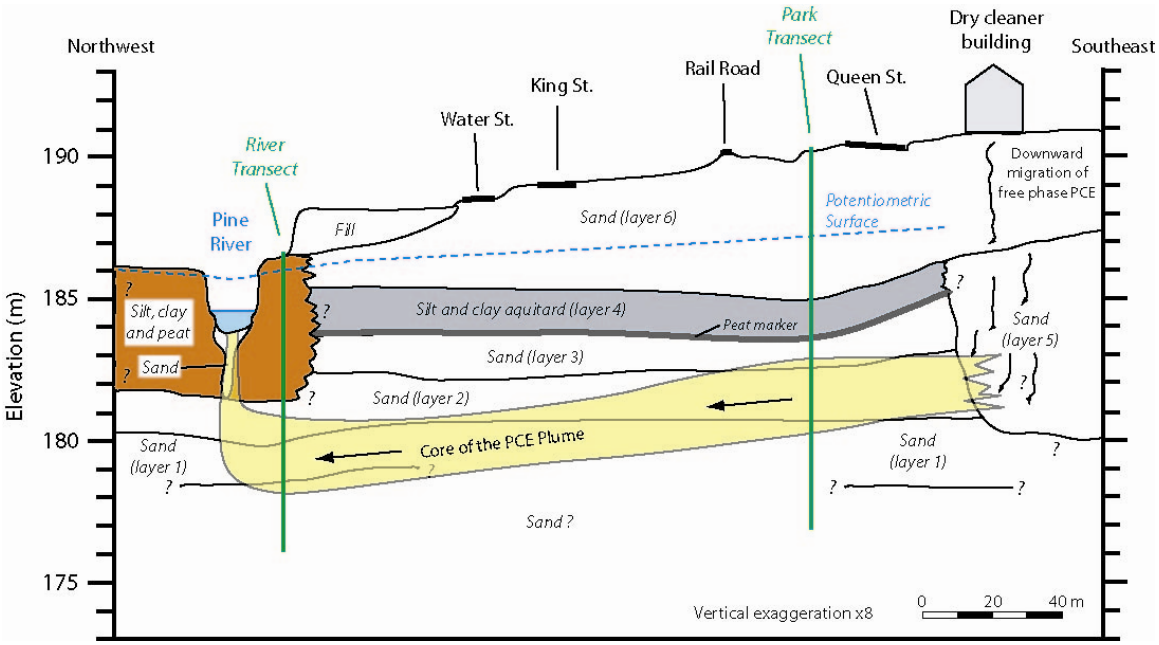

Figure 1 Stratigraphic description of the site and the PCE plume migration pathway (Pittet 2001).

A 30-m-wide transect of vertical profiles at the source zone depicted four distinct concentration maxima (Guilbeault *et al.* 2005), and isotope data from another study suggested that the plume consists of different sources of PCE (Hunkeler *et al.* 2004). The isotope study also showed that the contaminant plume

experiences very little biodegradation during its migration to the river as indicated by low concentrations of PCE transformation products and relatively stable carbon isotope ratios throughout the migration (Hunkeler *et al.* 2004). Hydraulic and contaminant transport processes in the streambed were investigated previously in the PCE plume discharge zone (Conant *et al.* 2004). The study demonstrated that the low hydraulic conductivity deposits and the geological heterogeneity of the streambed controlled groundwater discharge and contaminant distribution patterns. The PCE degradation products, TCE, cDCE and VC, were present at elevated concentrations in the streambed; however, it is not clear from the previous studies whether these compounds were further transformed, neither were the processes responsible for such transformations identified.

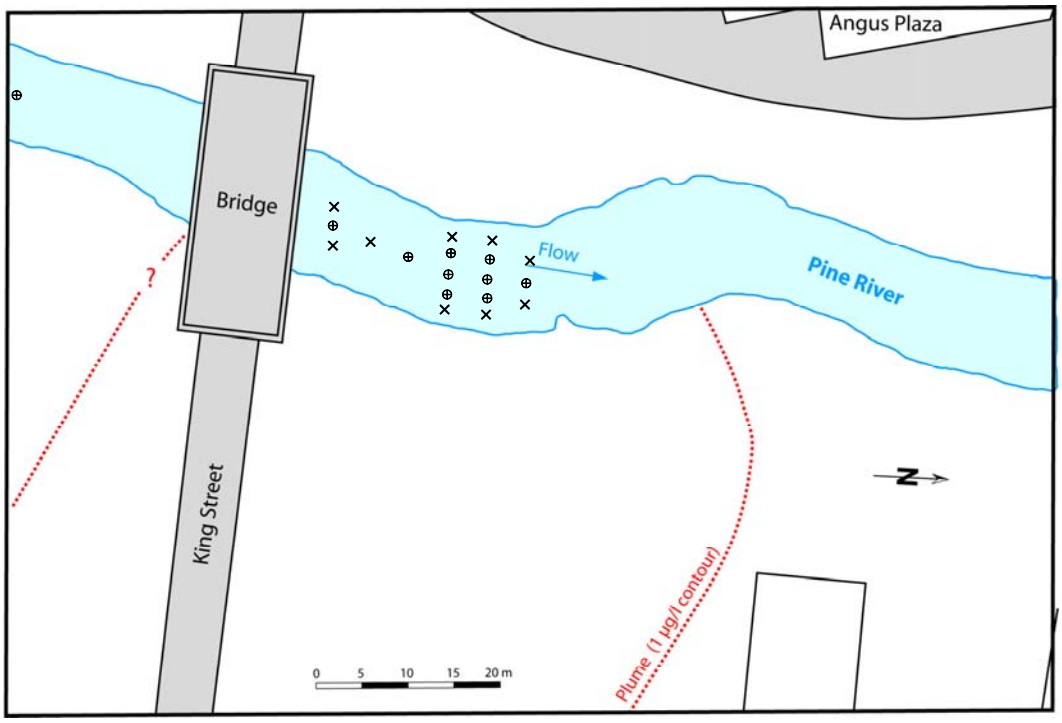

Figure 2 Plan view of the studied area (Pittet 2001). Depth profiles of water and sediment samples were collected from locations indicated as a circle and a plus mark while locations where water samples were collected only at the depth of 30 cm are indicated as an x.

2.3 STUDY METHODS

2.3.1 Streambed temperature measurements

In order to identify the zones of groundwater discharge, streambed temperature was measured at a depth of 30 cm from the streambed surface throughout a 20 m x 15 m study area. Temperature was measured with a StowAway® TidbiT® temperature logger (Onset Computer Corporation, Pocasset, Massachusetts) which was directly pushed into the streambed. A total of 93 measurements were collected and compared

with a previous study (Conant 2004). The middle section of the study area was not accessible because a tree had fallen into the river.

2.3.2 Streambed water sampling

The sampling locations were selected based on the streambed temperature map and the information from a previous study on the contaminant distribution (Conant *et al.* 2004). In particular, zones with elevated cDCE and VC concentrations were targeted as well as a zone with high PCE discharge for comparison. At the selected 19 locations, water samples were taken at a depth of 30 cm to evaluate the spatial distribution of the contaminants (Figure 2). At 9 of the 19 locations, samples were taken at the depth of 10, 30, 50, 70 and 90 cm to obtain vertical profiles (Figure 2). Water samples from the streambed were taken by manually pushing in a drive-point sampler (Conant *et al.* 2004) which had an inner dead volume of 1.5 mL. Water was collected in a connected syringe, and before each sampling, approximately 20 mL of water was discarded to rinse the inner tube of the sampler. When taking samples for a vertical profile, the sampler was hammered deeper upon completion of sampling at a shallower depth. A total volume of 200 mL was taken from each location for analyzing alkalinity, dissolved iron, major cations and anions, as well as the concentrations of chlorinated ethenes and ethene/ethane/methane and carbon isotope ratios of chlorinated ethenes and ethene. The withdrawn volume represented an approximate radius of influence of 5 cm assuming a porosity of 0.35; hence, it did not affect adjacent sampling depths. Water samples for anion and cation analyses were filtered with a sterile filter (0.45 μm), and those for cation analysis were immediately acidified with 1 M nitric acid. Triplicate of 20-mL samples for the concentration and carbon isotope analyses of chlorinated ethenes and ethene/ethane/methane were treated with NaOH to pH 10 for the inactivation of microbial activities. Temperature, pH, conductivity and dissolved oxygen concentrations were measured on-site. For dissolved oxygen concentrations, a colorimetric method was used (Hach DR/850 Colorimeter, USA).

2.3.3 Sediment-core sampling

For each of the 9 locations where vertical profiling was carried out, an approximately 90 cm sediment core was sampled. A 2” diameter aluminum pipe was used with a piston consisting of two double-rubber disks. For core sampling, the piston was always kept at the streambed surface while driving down the aluminum pipe by hammering. After the pipe was driven to the depth of 90 cm, the pipe was pulled out. The piston prevented the sand from sliding out of the tube. Immediately after sampling, the aluminum tube was cut by a tube cutter at different intervals, and the sediment core was sampled at approximately 3, 10, 30 and 70 cm from the top of the core. Each sediment sample was taken in quadruple, preserved in screw-capped plastic tubes, and immediately immersed in liquid nitrogen for sedimentary organic matter (SOM) content analysis. The left-over sediment samples were kept in zip-lock bags for grain-size analysis.

2.3.4 Analyses

Major anion and cation concentrations were determined with an ion chromatograph (Dionex DX-120). Detection limits for anions and cations were 0.1 mg/L. Dissolved iron concentrations were measured colorimetrically using the phenanthroline method with a detection limit of 0.05 mg/L. Chlorinated ethene concentrations were analyzed with a HP-6890 gas chromatograph 6890 equipped with a HP-7694 head space autosampler (Agilent, Palo Alto, USA) and an electron capture detector and a flame ionization detector. After headspace equilibration, a Shimadzu MNZ-1 gas chromatograph (Shimadzu, Japan) was used for ethene, ethane and methane concentration analyses. Detection limits were 0.9, 0.6, 1.9, 1.0, 0.5, 0.5, 0.4 μg/L for PCE, TCE, cDEC, VC, ethene, ethane and methane concentrations, respectively. In order to compare contamination levels at different locations, PCE equivalent concentrations were calculated by multiplying the total molar concentration of chlorinated ethenes and ethene by the molecular weight of PCE. Carbon isotope ratios of chlorinated ethenes were analyzed by a gas chromatograph coupled to an isotope-ratio mass spectrometer with a combustion interface (Thermo Finnigan, Germany). The system was equipped with a purge-and-trap concentrator (Velocity XPT, USA) connected to a cryogenic trap. For ethene isotope analysis, 20 mL of an aqueous sample in 40 mL glass vial was shaken for 1 h and 5 mL of headspace was subtracted with a syringe. The headspace sample was injected to a 2.5 mL loop injector which was connected directly to a cryogenic trap at -160°C. Minimum concentrations for PCE, TCE, cDEC, VC and ethene isotope analysis were approximately 5, 10, 10, 5 and 10 μg/L, respectively. All isotope ratios are reported relative to VPDB using the delta notation as $\delta^{13}C=(R/R_{std}-1)*1000$ (‰) where R and R_{std} are the isotope ratio of the sample and the VPDB standard, respectively.

The SOM content of sediment samples was analyzed for an approximately 100 mg of dried and ground sample using a Rock-Eval 6 pyrolysis instrument with standard cycles (Epspitalié *et al.* 1985; Behar *et al.* 2001). The grain size distribution of sediment samples were analyzed using a standard sand shaker with sieve sizes 18 to 120 ASTM. The uniformity coefficient (UC) was determined which corresponds to the ratio of grain size that has 60 percent of the material finer than itself, to the grain size that has 10 percent finer than itself.

2.4 Results and Discussion

2.4.1 Determination of sampling locations

The measured streambed temperatures varied from 12.0 to 17.0°C at the depth of 30 cm. At the time of sampling, the river water temperature ranged between 15.8 and 20.4°C, and the local groundwater temperature on average was reported to be relatively stable at 9.8°C (Hunkeler *et al.* 2004). Therefore, a colder streambed temperature represents the zone of faster groundwater discharge whereas a warmer streambed temperature indicates the slow discharge or stagnant zone (Conant 2004). In the studied area,

two zones with relatively high discharge were observed (Figure 3). These discharge zones as well as the measured temperature range corresponded well with the previous study (Conant 2004), implying the stable flow condition at the site over time.

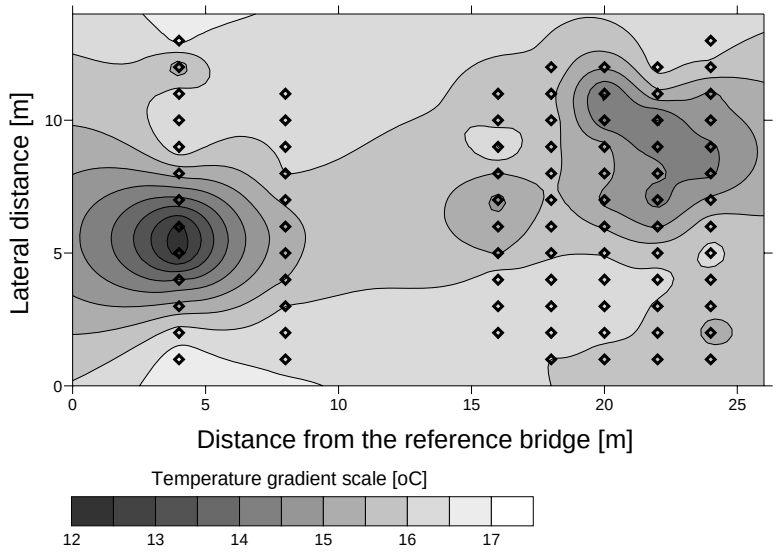

Figure 3 Streambed temperature map of the studied area at the depth of 30 cm. Open points indicate the locations with temperature measurements.

2.4.2 Spatial variability of chlorinated ethenes

A total of 53 samples were analyzed from 19 locations (Figure 2), covering different discharge zones and targeting particularly zones with elevated cDCE and VC concentrations, based on the previous study (Conant *et al.* 2004), to investigate their fate. Sampling locations will be denoted as the distance from the reference bridge and the lateral distance across the river from the western shore hereafter (e.g., 4-6 for 4 m away from the bridge and 6 m from the western shore). The concentrations of chlorinated ethenes, ethene and ethane are summarized in Table 1. Figure 4 shows the PCE equivalent concentrations and contaminant composition at 30 cm below the streambed surface. At the high discharge zone, 4 m away from the bridge, mainly PCE was detected. Further downgradient, there was a significant variation in contaminant concentrations and compositions. The highest contaminant concentration was found at 16-6 where PCE equivalent concentration reached a value of 1369.5 μg/L. However, just 2 m away from this point, the concentration dropped to 9.8 μg/L. The rapid change in the concentrations was most likely caused by the variability in local flow conditions created by the physical heterogeneity in streambed deposits and the geometry of the discharging plume.

In terms of vertical profiles of chlorinated ethene concentrations, not all the profiles contained detectable levels of chlorinated ethenes. In general, locations with relatively low streambed temperature indicating high discharge zones (4-6 and 12-6) tend to have decreasing concentrations in the discharging

direction except at location 24-6. However, locations with slow discharge characterized by elevated streambed temperatures did not demonstrate a depth-dependent distribution of chlorinated ethenes. At five of the nine locations, concentrations were sufficient at all depths for carbon isotope analysis. Therefore, the following discussions focus on the results from these five vertical profiles (namely 4-6, 16-4, 16-6, 20-6 and 24-6).

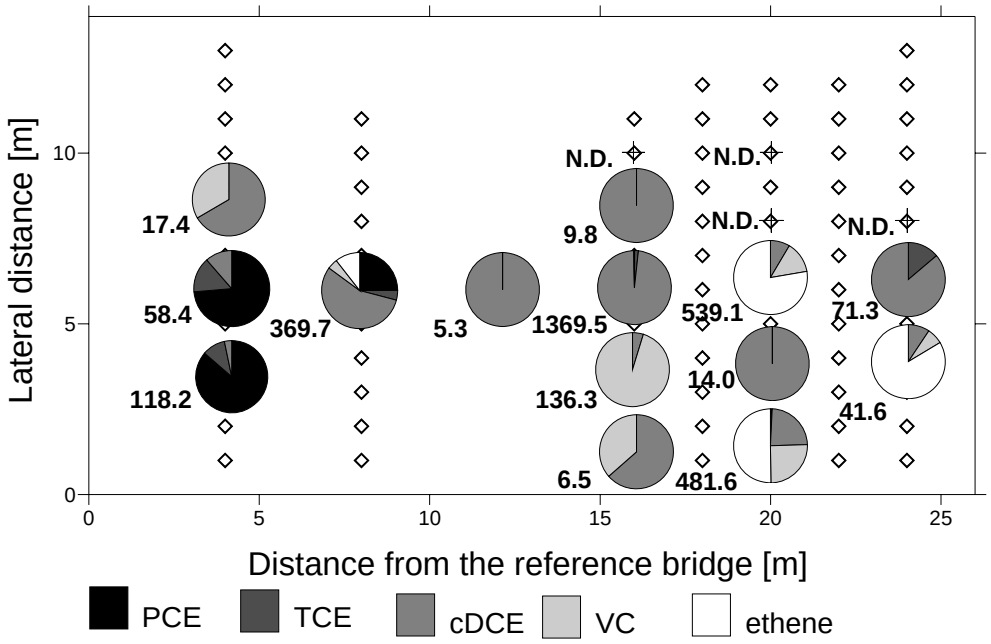

Figure 4 Spatial variability of PCE and its transformation products at 30 cm below the streambed surface. Concentrations are expressed in μg-PCE/L. N.D. stands for not detected.

Table 1 Geochemical data and concentrations and isotope ratios of chlorinated ethenes, ethene and ethane (- indicates samples not analyzed)

		T	cond	O_2	NO_3^-	Fe^{2+}	SO_4^{2-}	CH_4	PCE		TCE		cDCE		VC		ethene		ethane
Loc.	z(cm)	°C	µS/cm	mg/l	mg/l	mg/l	mg/l	mg/l	µg/l	‰	µg/l	‰	µg/l	‰	µg/l	‰	µg/l	‰	µg/l
	10	14.8	730	0.37	8.39	-	15.00	0.01	44.6	-30.85	6.7		<1.9		<1.0		<0.5		<0.5
	30	13.8	722	0.31	8.71	0.05	14.78	0.00	43.0	-31.14	6.9		<1.9		<1.0		<0.5		<0.5
4-6	50	13.3	727	0.39	9.26	<0.05	15.62	0.00	56.5	-30.66	6.8		<1.9		<1.0		<0.5		<0.5
	70	13.0	770	0.30	10.19	0.43	18.47	0.01	120	-29.42	7.8		2.1		<1.0		<0.5		<0.5
	90	14.7	871	0.00	7.24	-	31.32	0.01	338	-27.26	17.4	-32.21	31.5	-28.11	<1.0		<0.5		<0.5
	10	17.0	471	0.24	0.47	-	18.84	0.07	<0.9		<0.6		<1.9		<1.0		<0.5		<0.5
12-6	30	15.9	466	0.53	1.43	-	18.79	0.02	<0.9		<0.6		<1.9		<1.0		<0.5		<0.5
	50	15.8	749	0.10	<0.1	-	18.50	0.03	31.3	-29.47	9.0	-30.71	23.4	-29.44	<1.0		<0.5		1.2
	70	16.2	756	0.20	0.22	-	20.33	0.01	54.3	-28.79	8.1	-28.65	10.7	-28.85	<1.0		<0.5		<0.5
	10	19.9	1045	0.30	-	2.68	<0.1	15.55	<0.9		<0.6		<1.9		<1.0		15	-12.79	40
	30	19.5	1075	0.26	1.45	3.19	0.62	18.75	<0.9		<0.6		<1.9		<1.0		22	-10.58	58
16-4	50	17.7	1036	0.18	0.39	-	1.08	16.73	<0.9		<0.6		<1.9		<1.0		1.4		64
	70	17.0	884	0.16	0.33	1.75	12.32	4.52	0.9		7.6		421	-14.92	102	-28.45	65	-32.70	64
	90	17.3	872	<0.10	1.95	2.05	7.18	2.03	<0.9		3.3		837	-15.50	207	-26.16	479	-26.27	75
	10	17.9	818	0.28	0.39	1.84	35.27	0.31	1.3		23.2	-14.74	1130	-25.46	1.2		1.5		1.7
	30	16.8	804	0.21	0.31	-	34.93	0.14	1.1		17.3	-12.74	778	-26.13	<1.0		0.9		<0.5
16-6	50	15.5	789	0.24	0.56	-	34.44	0.14	1.1		15.4	-11.07	983	-26.36	<1.0		1.3		<0.5
	70	15.7	804	<0.10	<0.1	-	33.31	0.12	1.5		16.6	-12.87	1067	-26.21	<1.0		<0.5		<0.5
	90	16.5	814	<0.10	0.43	-	32.85	0.09	1.8		15.7	-12.48	914	-26.31	1.1		<0.5		<0.5
	10	18.2	735	0.34	<0.1	-	1.59	10.85	<0.9		<0.6		25	-25.97	<1.0		0.4		<0.5
	30	16.8	754	0.19	0.34	-	2.76	2.30	<0.9		<0.6		5.7		<1.0		<0.5		<0.5
16-8	50	15.7	747	0.29	0.23	-	6.33	2.70	<0.9		<0.6		3.4		<1.0		<0.5		<0.5
	70	16.6	774	0.23	0.26	-	5.66	0.06	<0.9		<0.6		<1.9		<1.0		<0.5		<0.5
	90	16.7	795	<0.10	<0.1	0.09	19.85	1.46	<0.9		<0.6		3.1		<1.0		<0.5		<0.5
	10	19.9	1264	0.50	<0.1	0.05	0.31	18.76	<0.9		<0.6		<1.9		<1.0		1.8		130
	30	19.0	568	0.90	<0.1	0.09	0.17	18.91	<0.9		<0.6		<1.9		<1.0		<0.5		386
20-4	50	19.2	447	0.90	0.14	-	0.33	4.01	<0.9		<0.6		<1.9		<1.0		1.8		528
	70	18.6	423	1.00	0.18	0.05	0.74	6.25	<0.9		<0.6		<1.9		<1.0		<0.5		654
	90	-	-	1.10	1.00	<0.05	5.03	1.93	<0.9		<0.6		<1.9		<1.0		2.1		218
	10	-	789	1.80	<0.1	-	17.23	0.26	<0.9		<0.6		15.3	27.64	16.1	5.77	78	-31.35	1.1
	30	-	760	1.30	<0.1	-	19.34	0.17	<0.9		<0.6		27.0	25.17	27.9	2.38	71	-32.60	0.5
20-6	50	-	767	1.10	0.31	-	23.75	0.08	<0.9		<0.6		34.2	20.59	30.1	-4.14	51.4	-35.72	<0.5
	70	18.3	725	0.60	0.78	-	24.79	0.07	<0.9		<0.6		35.5	18.84	32.4	-6.49	45.6	-40.02	<0.5
	90	19.3	727	0.40	<0.1	-	<0.1	0.07	<0.9		<0.6		11.2	40.26	25.1	6.79	46	-41.26	<0.5
	10	19.5	832	0.70	6.62	-	0.71	13.44	<0.9		<0.6		<1.9		<1.0		<0.5		5.7
	30	19.7	804	1.30	<0.1	-	0.46	9.15	<0.9		<0.6		<1.9		<1.0		<0.5		4.2
20-8	50	18.2	782	0.78	<0.1	-	0.56	8.85	<0.9		<0.6		<1.9		<1.0		<0.5		<0.5
	70	17.4	775	0.46	<0.1	-	0.97	4.73	<0.9		<0.6		<1.9		<1.0		0.5		2.4
	90	16.9	761	0.62	0.19	-	<0.1	6.53	<0.9		<0.6		<1.9		<1.0		0.9		5.4
	10	15.6	816	0.21	<0.1	-	1.06	0.05	<0.9		<0.6		36.6	-26.75	<1.0		<0.5		<0.5
	30	15.1	813	0.19	<0.1	-	<0.1	0.01	<0.9		7.8		35.9	-28.75	<1.0		<0.5		<0.5
24-6	50	14.5	814	0.20	<0.1	-	<0.1	0.01	<0.9		10.9		30.5	-29.29	<1.0		<0.5		<0.5
	70	13.9	846	<0.10	<0.1	-	<0.1	0.01	2.1		10.6		16.3	-29.49	<1.0		<0.5		<0.5
	90	14.1	960	<0.10	<0.1	-	0.66	0.01	1.7		9.6		6.4		<1.0		<0.5		<0.5

2.4.3 Physical and geochemical characterization of selected locations

Previously estimated discharge velocities had a high correlation with measured streambed temperatures as shown in Table 2, implying the validity of employing these velocity estimates to the selected locations.

Table 2 Sediment characteristics, water temperature and estimated discharge velocity

Location	Depth (cm)	Sediment type	Uniformity coefficient	SOM (%)	DOC (mg C/L)	Temp* (°C)	Velocity (m/d)
4-6	0-10	Sand	1.47	0.06	3.7	13.8	1
	10-30	Sand	2.20	0.11	7.3		
	30-50	Sand	2.56	0.06	4.0		
	50-70	Sand	2.57	0.88	3.9		
16-4	0-30	Sand	2.61	0.09	12.0	19.5	0.058-0.086
	30-50	Sand/silt	3.06	0.13	11.2		
	50-70	Sand/silt	3.41	11.25	7.7		
16-6	0-10	Sand	2.51	0.07	6.5	16.8	0.27
	10-30	Sand	1.96	0.15	6.9		
	30-50	Sand	1.82	0.01	10.6		
	50-70	Sand	1.78	0.02	7.3		
20-6	0-10	Sand/silt	2.06	0.10	6.2	>18.3**	0.0035
	10-30	silt/clay	1.74	0.03	5.1		
	30-50	silt/clay	2.16	0.03	3.7		
	50-70	Gravel/silt	1.77	0.09	4.3		
24-6	0-10	Sand/silt	1.68	-	-	15.1	0.74
	10-30	Sand/silt	2.23	0.15	-		
	30-50	Sand	1.98	-	-		
	50-70	Sand	1.94	0.08	-		

* Streambed temperature value represent the measurement at the depth of 30 cm

** Exact temperature measurement was not recorded, but assumed to be greater than the value from a deeper zone

In terms of sediment composition, sand was the main component of the streambed in general. However, at locations 16-4, 20-6 and 24-6, clay, silt and gravel were detected at some depths. Uniformity coefficients generally did not correlate with the sediment composition. The SOM content was in general quite low except for the deepest point in 16-4. In addition, the DOC content was relatively stable at the studied area, and slightly elevated DOC levels were determined at the location 16-4 with a high SOM content. However, the same level of elevated DOC was observed at location 16-6 without the presence of SOM-rich sediments. At the sampling locations which consisted solely of sand (4-6 and 16-6), the temperature at the depth of 30cm was significantly lower than the average river water temperature indicating relatively fast groundwater discharge, which is consistent with previous discharge velocity measurements (Table 2). In contrast, at 16-4 and 20-6 where finer sediment materials were present, the water temperature was more elevated, suggesting a slower discharge. The exception to the correlation between the sediment composition and the discharge velocity was observed at location 24-6 where a high discharge velocity was

accompanied by relatively fine sediment materials near the streambed surface. As previously reported (Conant 2004), discharge velocity estimation was based on the results from slug tests performed in a mini-piezometer. The center of the 10-cm screened intervals was placed at the depth of 0.49 to 0.70 cm below the streambed surface. Therefore, the presence of fine sediment in the top 30 cm at location 24-6 probably did not affect the obtained velocity.

In terms of geochemical composition of the water samples from the selected locations (refer to Table 1), the dissolved oxygen concentrations remained low at all depths for all sampling locations, revealing that this part of the river was under anoxic conditions. Substantial variations in redox conditions occurred among locations, and each location was characterized for the prevailing redox conditions. General redox characterization criteria have been proposed (Christensen *et al.* 2000) and were used as a reference although sulfide concentrations were not analyzed in this study.

At location 4-6 in a high discharge zone, the highest NO_3^- concentrations were detected with values of up to 10.2 mg/L indicating relatively oxidizing conditions (Table 1). Although SO_4^{2-} concentration decreased at this location, SO_4^{2-} reduction is unlikely given the presence of NO_3^-. At the high discharge zone, groundwater flow lines likely converged and if the chemistry varied between different flow lines in the aquifer, steep lateral concentration gradients would occur in the discharge zone. Correspondingly, if the concentration profile was not exactly aligned along a flow line, concentration changes with depth would be observed that were not due to reactive processes. This phenomenon also explains why the electrical conductivity decreased towards the river and some anomalous isotope trends occurred as discussed later.

At location 16-6, NO_3^- concentrations were low, Fe^{2+} was detected and SO_4^{2-} concentrations remained stable, indicating iron-reducing conditions (Table 1). In contrast, at 20-6, in the top four depths, the SO_4^{2-} decreased and Fe^{2+} was nearly absent due probably to sulfate reduction leading to the precipitation of Fe^{2+}. Surprisingly, in the lowest point, SO_4^{2-} was absent although it was present further upward, which might be due to stagnant conditions caused by the presence of impermeable sediments at the deepest sampling point. At location 24-6, sulfate-reducing conditions prevailed based on the absence of nitrate and sulfate. At 16-4, redox conditions seem to change from predominantly sulfate-reducing to methanogenic as indicated by the higher SO_4^{2-} concentration in the lower two sampling points and the higher methane concentrations in the upper three points. The shift in redox conditions occurred probably due to the presence of a SOM-rich layer at 50-70 cm in depth.

In summary, there are substantial variations in redox conditions among mentioned locations, with the most oxidizing conditions in the zone with the lowest streambed temperature (high discharge, 4-6) and the most reducing conditions at 16-4 with the highest streambed temperature. These observations indicate that redox conditions are controlled by the residence time of the interstitial water in the streambed and to a

certain extent by variations in the sediment SOM content. However, the exception to the general correlation between the streambed temperature and local redox conditions occurred at location 24-6 where relatively low streambed temperatures and sulfate-reducing conditions were observed.

2.4.4 Concentrations and carbon isotope ratios of chlorinated ethenes

The concentrations and isotope ratios at selected locations are plotted in Figure 5 to facilitate the comparison of depth-dependent behaviors at these locations. At location 4-6, in the high discharge zone, the PCE concentration decreased without the occurrence of degradation products except at the lowest depth (Figure 5). In addition, the isotope ratios of PCE decreased in upward direction contrary to what would be expected from the occurrence of biodegradation. The observed isotope trend was likely due to the mixing of two converging flow lines in which two separate flow lines carrying the different sources of PCE merged at the depths between 70 and 90 cm. Indeed, a previous study showed that the isotope ratios of PCE plume just upgradient from this location varied between -27.7‰ and -30.4‰ due to the presence of multiple PCE sources (Hunkeler *et al.* 2004). Hence at location 4-6, the variation in isotope ratios did not originate from reductive dechlorination of PCE but from the variation in the PCE sources. Reductive dechlorination of PCE could not occur at this location because the reducing potential was not sufficiently high and the residence time in the streambed was not sufficiently long.

Location 16-6 had the highest concentrations of chlorinated ethenes, mainly in the form of cDCE (Figure 5). The isotope ratios of cDCE were substantially more negative compared to that of TCE, typical for reductive dechlorination of TCE (Bloom *et al.* 2000). The isotope ratios of cDCE remained quite stable in upward direction despite substantial concentration variations, indicating that no further transformation of cDCE occurred at this location. The isotope ratios of cDCE were similar to those of PCE in the upgradient plume (Hunkeler *et al.* 2004), which would be typical if complete transformation of PCE to a single intermediate compound occurred. At this location under iron-reducing conditions, the reductive dechlorination of chlorinated ethenes could proceed to cDCE but the further transformation of cDCE could not take place. Transformation of PCE and TCE under iron-reducing conditions have been demonstrated by a long-term injection test at a landfill leachate site as well (Albrechtsen *et al.* 1999).

At location 20-6 under sulphate-reducing condition, relatively low concentrations of cDCE, and higher concentrations of VC and ethene were detected (Figure 5). In the upper four sampling points, the isotope ratios of cDCE showed highly enriched values and steadily increased from 18.8‰ to 27.6‰ and those of VC from -6.5‰ to 5.8‰, demonstrating reductive dechlorination of cDCE and VC. Ethene isotope ratios were more negative than those of VC, but approaching the isotope ratios of the PCE source. Thus, ethene was the final degradation product at this location. Carbon isotope ratios of cDCE, VC and ethene became progressively enriched upward except at the deepest point, demonstrating that complete reductive dechlorination to ethene is active at the location despite the short migration distance

investigated. In the deepest sampling point, the isotope ratios of cDCE and VC were strongly enriched due probably to a stagnant and more reducing condition at this depth as already indicated by the absence of SO_4^{2-}. The total concentration of chlorinated ethene and ethene increased in a upward direction despite active reductive dechlorination at the site. The increasing concentrations could suggest decreasing contaminant concentrations at the source that was effectively recorded by the profile because of the extremely slow discharge rate which could cause a long residence time at this location.

At location 24-6 which also was under sulfate-reducing condition, the dominant contaminant was cDCE. As shown in Figure 4, the concentrations and isotope ratios of cDCE increases with distance, suggesting the complete reductive dechlorination of TCE. However, the isotope ratio of cDCE does not increase beyond that of the source value indicating accumulation of cDCE without further transformation which is consistent with the absence of VC and ethene.

Thus, although both 20-6 and 24-6 seem to be under sulphate-reducing conditions, reductive dechlorination proceeds to ethene in 20-6 and to cDCE in 24-6. The accumulation of cDCE at location 24-6 might be caused by the relatively high discharge rate, which would result in a shorter residence time of the water. Furthermore, comparison of a number of laboratory studies indicates that under sulphate-reducing conditions complete reductive dechlorination does not always occur. Most studies report the accumulation of cDCE under sulfate-reducing conditions (Bagley and Gossett 1990; Pavlostathis and Zhuang 1993; Boopathy and Peters 2001) while others report that complete reductive dechlorination to ethene by enrichment cultures without the involvement of methanogenic activities (Flynn *et al.* 2000) and with the presence of high sulfate concentrations (Hoelen and Reinhard 2004) were observed. Hence, the microbial community and environmental conditions may have varied between the two locations leading to a different degree of reductive dechlorination. It is possible that insufficient electron donors were available in the sampled zone of 24-6 as indicated by no significant increase in the methane concentration. The alternative hypothesis that detected chlorinated ethenes and ethene at location 20-6 were transported from a deeper depth, thereby complete dechlorination did not take place at the sampled location is unlikely because of the observed depth-dependent enrichment in ^{13}C. If the transformed compounds were transported, the isotope ratios should not vary with depth.

At location 16-4, cDCE, VC and ethene were present in the deepest two sampling points. While the isotope ratios of VC were substantially more negative than those of cDCE as in the location 20-6, the isotope ratios of ethene were similar to those of VC, which contradicted the assumption that ethene was the final degradation product. In addition, the isotope ratios of ethene were strongly enriched in two uppermost sampling points. The observed pattern clearly demonstrate that ethene was further degraded throughout the location. Strong isotope enrichment due to further degradation of ethene was previously observed in laboratory study but has not been observed at the field scale yet (Bloom *et al.* 2000). Ethane

was the likely degradation product of ethene as it was present throughout the profile. Most laboratory studies on enrichment cultures, microcosms as well as mixed cultures produce ethene as the end product of reductive dechlorination (DiStefano *et al.* 1991; Maymo-Gatell *et al.* 1995; Maymo-Gatell *et al.* 1999; Bloom *et al.* 2000; Flynn *et al.* 2000; Cupples *et al.* 2003; He *et al.* 2003). However, the formation of ethane as the final product of complete reductive dechlorination has been observed with chlorinated ethene degradation studies with a flow-through column packed with anaerobic river sediments and anaerobic sludge (de Bruin *et al.* 1992) and with an enrichment culture (Komatsu *et al.* 1994). In addition, microbial reduction of ethene to ethane is reported under methanogenic conditions (Koene-Cottaar and Schraa 1998). Therefore, under strongly reducing conditions, ethane can be the final product of reductive dechlorination even though the process may involve different microorganisms from the dechlorinating communities. The complete degradation of chlorinated ethenes to ethane and possibly other products at location 16-4 took place because of the strongly reducing conditions caused by the presence a SOM-rich layer and the prolonged residence time of the water in the streambed. Elevated ethane concentrations (130 to 654 μg/L) were also detected at another location (20-4), where no chlorinated ethenes were and the streambed temperature was close to that of the river indicating a slow discharge (Table1).

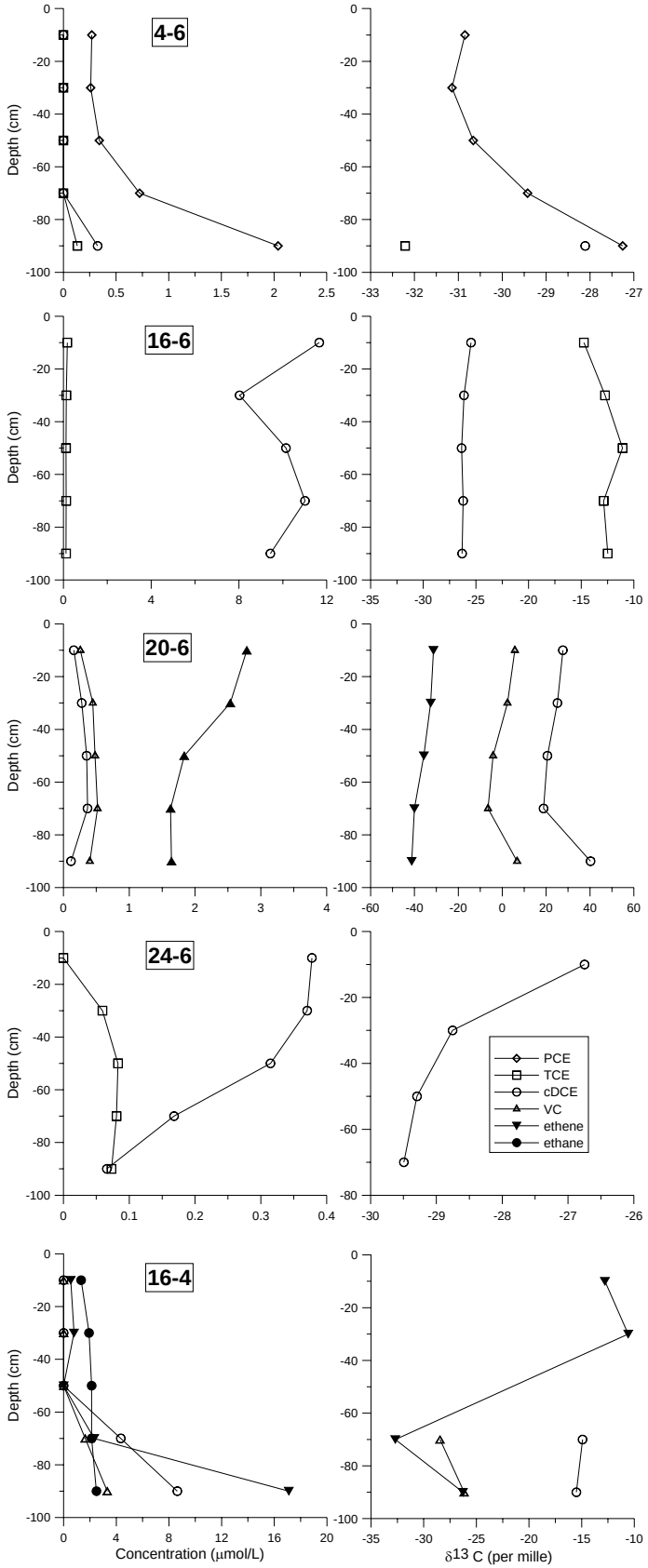

Figure 5 Depth-variant concentrations and isotope ratios at selected locations

2.5 SUMMARY AND IMPLICATIONS

The study demonstrated that the carbon isotope analysis provides further information on the fate of contaminants that cannot be inferred by the concentration and redox data alone. Carbon isotope analysis was effective for identifying the final transformation product of reductive dechlorination under various redox and hydrological conditions. The progress of reductive dechlorination was clearly demonstrated by the carbon isotope analysis. Geochemical analysis suggests that local redox conditions significantly influenced the progress of reductive dechlorination as widely known (Bradley 2000). However, under sulfate-reducing conditions, both cDCE accumulation and complete reductive dechlorination to ethene were observed, indicating that sulfate-reducing conditions are not always sufficient for the dechlorination of cDCE. Results indicate that the progress of reductive dechlorination is controlled not only by redox conditions, but also by local flow conditions and the SOM levels in sediments which may be regarded as an indicator for the abundance of electron donor. Under methanogenic conditions, based on the carbon isotope data ethane was identified as the final product of complete reductive dechlorination at location 16-4. This study also demonstrated that the limiting step during complete reductive dechlorination is rather the dechlorination of cDCE, and cDCE and VC reductive dechlorination probably requires similar conditions and could take place concurrently as reported from the laboratory studies (Haston and McCarty 1999; Flynn *et al.* 2000). Such observations could be explained by the similar thermodynamic properties of cDCE and VC dechlorination reactions (Heimann and Jakobsen 2006). Therefore, dechlorination of VC to ethene and further to ethane is probably not as recalcitrant as generally assumed at field scales.

Acknowledgements

Concentrations of chlorinated ethenes, ethene, ethane and methane and the SOM content were analyzed by Wayne Noble at the University of Waterloo.

Chapter 3

Comparison of geochemical, isotope, and microbial investigation methods to characterize the fate of VC

Abstract

Geochemical and microbiological methods were employed and compared to determine the fate of VC in the streambed where a PCE plume discharges and various degree of reductive dechlorination was observed based on the previous field concentration and isotope results. The *in situ* potentials of complete reductive dechlorination were assessed based on the three factors: strongly reducing conditions, the presence of sedimentary organic matters (SOM) and the presence of *Dehalococcoides*. The SOM content was considered as available carbon source for fermentative activities which produce H_2, a recognized electron donor for reductive dechlorination of chlorinated ethenes. The presence of *Dehalococcoides* was evaluated with 16S rDNA based PCR primers specific to the organism. For assessing aerobic VC and cDCE oxidation potentials, microcosms were constructed with local sediments from different locations and different depths. In addition, PCR primers specific to a gene encoding a key enzyme for aerobic VC oxidation were used to screen the study site for the presence of microbial communities capable of carrying out aerobic VC oxidation. For the occurrence of complete reductive dechlorination, geochemical data (redox-sensitive anions, methane and SOM analyses) and the specific PCR primers for *Dehalococcoides* distinguished locations with ethene and ethane as the end product of reductive dechlorination. Locations under methanogenic conditions with a high SOM content and the presence of *Dehalococcoides* demonstrated the presence of ethane as a final product while a location under sulfate-reducing conditions with a low SOM content and the apparent absence of the organism was accompanied by ethene as a final product. The result suggests the three investigated parameters do not always indicate the possibility of complete reductive dechlorination. Based on the microcosm study, aerobic cDCE oxidation is not expected at the site. For aerobic VC oxidation, both microcosm and PCR results demonstrated that the site possesses microbial communities capable of aerobically oxidizing VC.

Abe, Y., Aravena, R., Parker, B.L., Cherry, J.A., Zopfi, J. and Hunkeler, D.
To be partially submitted to the Journal of Contaminant Hydrology

3.1 INTRODUCTION

Tetrachloroethene (PCE) and trichloroethene (TCE) are among the most frequently detected contaminants in groundwater (Squillace *et al.* 1999; Moran *et al.* 2007). Reductive dechlorination of PCE and TCE can readily take place to produce mainly *cis*-dichloroethene (cDCE) under anoxic conditions (Wiedemeier *et al.* 1997; Bradley 2000), but the further dechlorination of cDCE to vinyl chloride (VC) and to a benign end product ethene and ethane generally requires strongly-reducing and fermentative conditions (Vogel *et al.* 1987; Bagley and Gossett 1990; de Bruin *et al.* 1992; Komatsu *et al.* 1994; Holliger *et al.* 1999; Bradley 2000; Boopathy and Peters 2001; Bradley 2003; He *et al.* 2003). Complete anaerobic dechlorination of PCE to ethene have been observed in mixed and enriched culture studies (Vogel and McCarty 1985; Freedman and Gossett 1989; DiStefano *et al.* 1991; de Bruin *et al.* 1992; Loffler *et al.* 1997), but to date the genus *Dehalococcoides* which utilized H_2 as the electron donor is the only isolated and identified group of microorganisms which can cometabolically (strains 195 and FL2) or metabolically (strains Y51 and VS) dechlorinate VC to ethene (Maymo-Gatell *et al.* 1999; Bradley 2000; Loffler *et al.* 2000; Cupples *et al.* 2003; He *et al.* 2003). A few studies demonstrated the further reduction of ethene to ethane during the course of reductive dechlorination (de Bruin *et al.* 1992; Komatsu *et al.* 1994). In general, it is considered that determinant factors for the complete *in situ* dechlorination of chlorinated ethenes are strongly-reducing conditions which allow chlorinated ethenes to serve as electron acceptors, the availability of H_2 as the electron donor, and the presence of appropriate microorganisms such as *Dehalococcoides* (Wiedemeier *et al.* 1997; Bradley 2000; Hendrickson *et al.* 2002; Bradley 2003; Duhamel and Edwards 2006).

In order to assess the occurrence of complete reductive dechlorination of chlorinated ethenes to ethene, several investigation methods have been proposed and tested. Since each step of reductive dechlorination is a redox-sensitive process, geochemical approaches rely on the identification of local redox conditions based on concentrations of redox-sensitive species (Bradley *et al.* 1998; Witt *et al.* 2002). In addition, the availability of electron donors can be evaluated by the direct measurement of H_2 concentrations at a site (Yang and McCarty 1998; Witt *et al.* 2002) although a recent laboratory study demonstrated the reductive dechlorination of cDCE and VC by a mixed culture containing *Dehalococcoides ethenogenes* 195 is not controlled by H_2 levels (Heimann and Jakobsen 2006). In terms of the presence of appropriate microorganisms, recent advances in molecular diagnostics enable the assessment of the presence or the absence of target DNA sequences. Direct extraction of nucleic acids from environmental samples such as sediment and groundwater eliminates the cultural biases, which often is the case for laboratory enrichment studies. The 16S rDNA-based primers targeting a characteristic sequence for *Dehalococcoides* are available (Fennell *et al.* 2001; Hendrickson *et al.* 2002; Müller *et al.* 2004).

Incomplete reductive dechlorination results in the accumulation of intermediate compounds such as cDCE and VC. The presence of VC in groundwater is of concern due to its toxicity. However, VC can be degraded by various other degradation pathways. It can be microbially oxidized under oxic (Davis and Carpenter 1990; Hartmans and de Bont 1992; Bradley and Chapelle 1998; Verce *et al.* 2001) and anoxic (Bradley and Chapelle 1996; Bradley and Chapelle 1998; Bradley *et al.* 1998; Bradley and Chapelle 2000) conditions, and the abiotic reduction by iron-bearing minerals has been reported (Lee and Batchelor 2002; Lee and Batchelor 2004). Aerobic oxidation of VC to CO_2 utilizes a ubiquitous nonspecific monooxygenase (Hartmans *et al.* 1992; van Hylckama Vlieg *et al.* 1996; van Hylckama Vlieg *et al.* 1998; Coleman and Spain 2003; Coleman and Spain 2003), which may contribute to the field observations of disappearing VC concentrations at the fringes of a plume where oxic conditions are reestablished (Witt *et al.* 2002). A study based on the construction of microcosms from 37 chlorinated ethene contaminated sites demonstrated that aerobic VC oxidation took place readily in 23 microcosms, suggesting the wide spread of microbial communities capable of aerobic VC oxidation (Coleman *et al.* 2002). Aerobic oxidation of VC can be demonstrated by some microbial methods such as the use of microcosms constructed from local materials (Bradley and Chapelle 1998; Klier *et al.* 1999). PCR primers targeting the DNA sequence of an enzyme epoxyalkane:coenzyme M transferase (EaCoMT), which is an important enzyme to channel the initial intermediates into the central metabolic pathway during aerobic VC oxidation are available (Coleman and Spain 2003; Coleman and Spain 2003).

The objectives of the study are to evaluate the use of above-mentioned investigation methods (geochemical and microbial parameters) for the occurrence of complete reductive dechlorination and to assess the potential of aerobic VC oxidation in the streambed. The site consists of a PCE plume discharging into a river where the progress of reductive dechlorination varied significantly in the streambed as documented by the carbon isotope analysis (Chapter 2). The site was particularly suitable for comparing different investigation methods due to the observed variation in the progress of reductive dechlorination. In order to evaluate three factors (strongly reducing conditions, the sufficient supply of electron donors and the presence of *Dehalococcoides*) associated with the occurrence of complete reductive dechlorination, geochemical data (redox-sensitive anion and sedimentary organic matter (SOM) content analyses) and the 16S rDNA based specific PCR primers targeting *Dehalococcoides* (Hendrickson *et al.* 2002) were employed. The availability of H_2 in subsurface environments is closely linked to the fermentative processes of organic matters (Appelo and Postma 2005). Although H_2 concentrations were not measured, the SOM content in the streambed was considered as the carbon source to support the fermentative processes which produced H_2. In addition, the occurrence of aerobic VC oxidation at the site was not confirmed by the carbon isotope analysis (Chapter 2), but the presence of oxic conditions near the streambed surface could allow aerobic VC oxidation to take place. Hence, microcosms were constructed

with the sediment samples from different locations at different depths to evaluate the potential aerobic oxidation of VC and cDCE. In addition, PCR primers specific to the EaCoMT gene were used to screen the study site for the presence of microbial communities capable of carrying out aerobic VC oxidation.

3.2 MATERIALS AND METHODS

3.2.1 Site Description

The study site is located in Angus, Ontario, Canada. A PCE plume caused by a former dry-cleaning facility travels 195 m in a confined aquifer until it discharges into the Pine River. The detailed description of the site appears in Chapter 4. In brief, PCE and its dechlorination intermediates at the source travels without further transformation until the plume discharges into the river (Conant *et al.* 2004; Hunkeler *et al.* 2004). However, in the streambed of the discharge zone, significant variations in the progress of reductive dechlorination were observed. The previous study based on the geochemical and carbon isotope data demonstrated that local redox conditions and the local discharge condition, which affects the residence time of the water, determined the progress of reductive dechlorination. The observed variations in local redox conditions were caused primarily by the local discharge rates and TOC contents. The variation in discharge rates arose from differences in sediment compositions. In general, the streambed consisted of sand and gravel, but the middle part of the river contained clay and silt at the depth of approximately 50 to 90 cm. Figure 1 shows the contaminant distribution pattern in the streambed based on the previous study (Chapter 4).

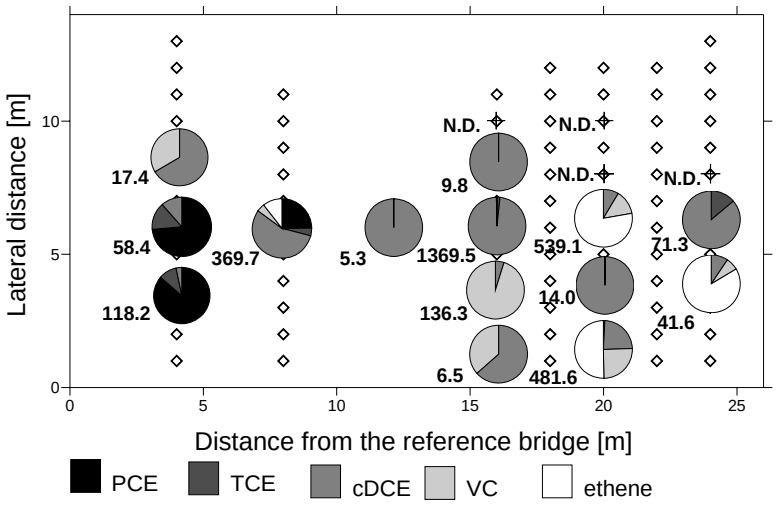

Figure 1 PCE-normalized concentrations (μg-PCE/L) and proportions of chlorinated ethenes and ethene in the streambed at the depth of 30 cm. N.D. stands for not detected.

3.2.2 Sediment samples

Sediment cores were collected from 10 locations (Figure 2) and the sampling method is described in Chapter 4. Sediment cores were disassembled on site. Sediment samples were collected at approximately 3, 10, 30 and 70 cm from the top of the core to correspond to the depths of water samples except for the depth of 3cm for which it was not possible to collect a water sample without interference from river water n. Each sediment sample was collected in quadruple, preserved in 1.5-mL screw-capped plastic tubes, and immediately frozen in liquid nitrogen for TOC analysis and DNA and RNA extractions. Sampled locations are denoted as the lateral distance from the bridge and the distance from the western shore hereafter (e.g., 4-6 for 4 m away from the bridge and 6 m from the western shore).

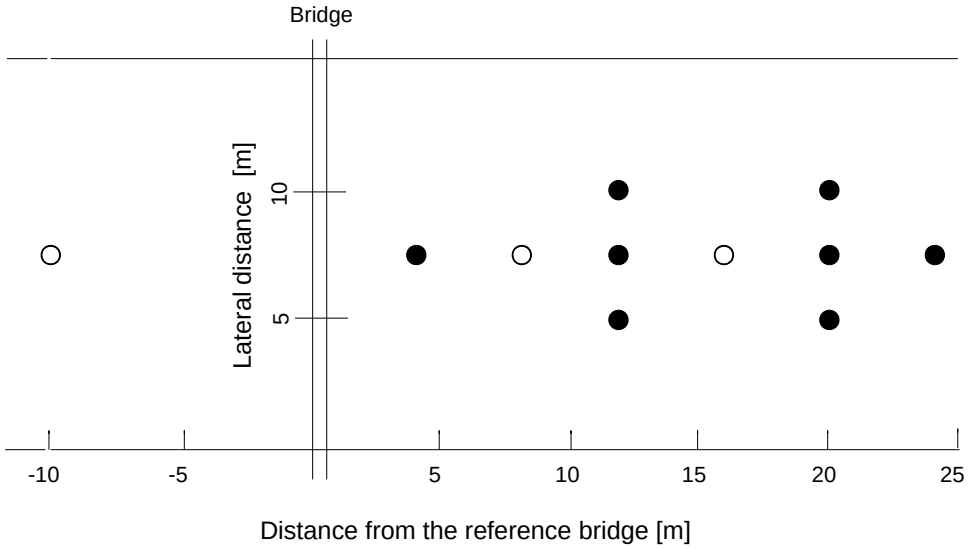

Figure 2 Sampling locations for the microcosm study (open circles) and the vertical profile study (filled circles). A control for the vertical profile study was taken from -24 m and not shown in the figure.

3.2.3 Aerobic microcosm study

Sediment cores of 30 cm were collected from three locations shown in Figure 2 for microcosms. Microcosm sediment cores were sealed completely from both ends and kept cool until microcosm construction. Microcosm sediments were collected from 1) 18 m downgradient with a high level of contaminant discharge, 2) 10 m downgradient with a moderate level of contaminant discharge, and 3) -10 m upgradient without any previous contaminant exposure. Each sediment core of 30 cm was further divided into sections of 10 cm. Two series of nine microcosms (VC and cDCE series) were constructed from three sediment cores with three depths. Microcosms consisted of approximately 10 g wet sediment and 10 mL minimum salt medium (Hunkeler and Aravena 2000) in a 60 mL serum bottle capped with a Viton® stopper. Control microcosms (one per core) were autoclaved three times and treated with NaN_3 to a final concentration of 1 % (wt/wt) in order to inactivate microbial activities. VC (>99.5 % purity, Fluka,

Switzerland) and cDCE (>99.5 % purity, Fluka, Switzerland) were added to each series at the initial air-phase concentration of 0.5mM.

Microcosm degradation experiments with VC were carried out four times during one and a half years of incubation period. Before starting an experiment, all microcosms were left uncapped under the fume hood for three hours to release any traces of VC and to equilibrate dissolved oxygen concentrations. During the course of incubation, microcosms were kept on a rotary shaker at 21 °C. The GC analysis did not detect any reductive dechlorination product (ethene and ethane) during the experiments, and the O_2 level was kept above 2 mg/L to maintain the oxic conditions by weekly monitoring of O_2 concentrations.

3.2.4 Molecular biology methods

Sediment samples from the streambed and microcosms were preserved at -80 °C until further processing. DNA was extracted with the FastDNA SPIN kit (Bio101) and a FastPrep bead-beating machin (Bio101). RNA was extracted with lysing matrix tubes (FastRNA Green Kit, Qbiogene) and solutions from the RNeasy mini Kit for plants (Qiagen). The RNA extracts were then treated with Rnase-free Dnase RQ1 (Promega) to eliminate co-extracted DNA. RT-PCR was carried out with the ImProm-II Reverse Transcription System (Promega) in a PTC-200 thermocycler (MJ Research Inc.). PCR reactions were carried out targeting the V3 hypervariable region on the 16S rDNA gene (≈200 bp) by using primers Eub338f and Eub518r (Ovreas *et al.* 1997) to test whether the extracted DNA and reversely transcribed RNA were amplifiable. The DNA and cDNA samples were subjected to PCR with specific primers to the EaCoMT gene (CoM-F1L and CoM-R2E) for aerobic VC oxidation (Coleman and Spain 2003) and to the *Dehalococcoides*-specific sequence (Fp DGC 774 and Rp DHC 1212) for anaerobic VC dechlorination (Hendrickson *et al.* 2002). The same PCR conditions as the original works were used (Hendrickson *et al.* 2002; Coleman and Spain 2003). Positive controls were prepared from extracting the DNA from *Nocardioides* sp JS 614 (Coleman *et al.* 2002) for aerobic VC oxidation and the community DNA from KB-1 mixed culture (SiREM, Guelph, ON, Canada). In order to increase the sensitivity of molecular detection, a repeated PCR approach was employed for both sets of primers. The PCR amplification process was repeated twice for DNA samples and three times for cDNA samples whereby ten-fold dilution of the previous PCR product was used as a template for the following PCR. PCR products were analyzed on 1.3% agarose gels (Eurobio, France) after ethidium bromide staining. The relative intensity of PCR products on an electrophoresis gel was qualitatively indicated as weak (+) to strong (+++) as shown in a electrophoresis gel picture (Figure 3).

3.2.5 Chemical analyses

For cDCE and VC concentration measurements for the microcosm study, 0.2 mL headspace samples were analyzed by a gas chromatograph (GC) equipped with a flame ion detector (Model 4130, Carlo Erba Strumentazione, Italy). The GC was equipped with a glass column packed with 1 % AT-1000 (Alltech,

USA). The oven temperature was kept isothermal at 130 °C. The detection limits were 1.0 and 1.5 ug/L for cDCE and VC, respectively. For O_2 concentration measurements, 0.1 mL headspace samples from microcosms were analyzed by a GC equipped with a thermal conductivity detector (SRI 310C, SRI Instruments, Torrance, CA, USA). The oven temperature was kept isothermal at 60 °C. The detection limit was 0.3 mg/L. For stable carbon isotope ratio measurements for the microcosm study, a Thermo Finnigan Trace gas chromatograph (GC) equipped with a Poraplot Qcolumn (25m x 0.32 mm) and coupled to a Thermo Finnigan Delta Plus XP isotope-ratio mass spectrometer (IRMS) to a combustion interface set to 940ºC (Thermo Finnigan, Bremen, Germany) was used. Samples were loop-injected based on the concentrations measured from the GC. TOC content of sediment samples from the site were analyzed for an approximately 100 mg of dried and ground sample using a Rock-Eval 6 pyrolysis instrument with standard cycles (Epspitalié *et al.* 1985; Behar *et al.* 2001).

3.3 RESULTS AND DISCUSSION

3.3.1 Assessment of complete *in situ* reductive dechlorination potentials

Three investigation parameters (redox conditions, SOM content, and the presence of *Dehalococcoides*) to assess the potential for complete reductive dechlorination were evaluated based on the results from the concentration and carbon isotope ratio data (Chapter 2) as a reference for the progress of reductive dechlorination (Table 1). Redox conditions were characterized based on the concentration data of redox-sensitive species (Christensen *et al.* 2000). Locations which demonstrated complete reductive dechlorination were accompanied by sulfate-reducing (20-6) to methanogenic (16-4 and 20-4) conditions. The SOM analysis revealed generally very low levels of SOM at the site except for two locations (16-4 and 20-4). These two locations are under methanogenic conditions and carry out complete reductive dechlorination to ethane. However, other methanogenic locations have a low SOM content (16-8 and 20-8); thus, a high SOM content is not a direct indicator of strongly reducing conditions. Alternatively, it is possible that high concentrations of methane observed at locations 16-8 and 20-8 might be caused by the transport of methane from a deeper zone as methane is relatively mobile in subsurface systems (Wiedemeier *et al.* 1997; Bedient *et al.* 1999). The taxon-specific PCR primers targeting *Dehalococcoides* were used to identify the presence of the organism in the streambed sediment. PCR products from DNA samples did not contain a detectable level of *Dehalococcoides* for most locations, but positive PCR responses were obtained from locations 16-4 and 20-4 with various expression levels (Figure 3) where complete *in situ* reductive dechlorination to ethane was observed. Although PCR-amplifiable cDNA from RNA extraction were obtained, all samples did not contain a detectable level of *Dehalococcoides*; therefore, the activity level of *Dehalococcoides* at 16-4 and 20-4 at the time of sampling is not known.

Table 1 Parameters used for investigating the potentials of complete reductive dechlorination and aerobic VC oxidation

Loc.	Depth (cm)	temp **(oC)**	Sediment composition	Final product	Redox condition	SOM (%)	*Dehalo.* DNA	DO (mg/L)	EaCoMT DNA
	0-10		sand			0.11	-		+
-24-6	10-30	16.8	sand	N.D.*	SO_4^{2-} to	0.18	-	0.19	-
	30-50	16.6	silt/clay	N.D.	methano.	N.A.**	-	0.27	-
	50-70	16.0	sand	N.D.		0.16	-	0.00	-
	0-10		sand			0.06	-		+++
4-6	10-30	14.8	sand	N.D.	NO_3 to	0.11	-	0.37	+++
	30-50	13.8	sand	N.D.	Fe(III)	0.06	-	0.31	-
	50-70	13.0	sand	N.D.		0.88	-	0.30	++
	0-10		sand	N.D.		0.05	-		++
12-6	10-30	17.0	sand	N.D.	Fe(III) to	0.02	-	0.24	++
	30-50	15.9	sand	N.D.	SO_4^{2-}	0.08	-	0.53	++
	50-70	16.2	sand	cDCE		0.07	-	0.20	-
	0-10		sand			0.09	-		+++
16-4	30-50	19.5	sand/silt	ethane	methano.	0.13	-	0.26	-
	50-70	17.0	sand/silt	ethane		11.25	+++	0.16	-
	0-10		sand			0.07	-		+++
16-6	10-30	17.9	sand	cDCE	Fe(III)	0.15	-	0.28	-
	30-50	16.8	sand	cDCE		0.01	-	0.21	+
	50-70	15.7	sand	cDCE		0.02	-	0.00	-
	10-30		sand	N.D.		0.04	-		++
16-8	30-50	16.8	sand/silt	N.D.	methano.	0.06	-	0.19	-
	50-70	16.6	sand/silt	N.D.		0.04	-	0.23	+
	0-10		sand			0.04	-		++
20-4	10-30	19.9	sand	ethane		0.70	+	0.50	-
	30-50	19.0	sand/silt	ethane	methano.	2.35	++	0.90	-
	50-70	18.6	sand/silt	ethane		1.81	+++	1.00	-
	0-10		sand/silt			0.10	-		++
20-6	10-30	16.2	silt/clay	ethene	SO_4^{2-}	0.03	-	n.a	-
	30-50	15.5	silt/clay	ethene		0.03	-	n.a	+
	50-70	18.3	gravel/silt	ethene		0.09	-	0.60	+
	0-10		sand			0.13	-		+
20-8	10-30	19.5	sand	N.D.	methano.	0.15	-	0.70	++
	30-50	19.7	sand	N.D.		0.15	-	1.30	++
	50-70	17.4	sand/silt	N.D.		0.11	-	0.46	-
	10-30	15.6	sand/silt	cDCE		0.15	-	0.21	++
24-6	30-50	15.1	sand/silt	cDCE	SO_4^{2-} to	N.A.	-	0.19	-
	50-70	13.9	sand	cDCE	methano.	0.08	-	0.00	+

*N.D. stands for chlorinated ethenes, ethene, or ethane were not detected. At the depth of 0-10 cm, water samples were not taken for concentration and carbon isotope ratios of chlorinated ethenes.
**N.A. stands for not analyzed.

The three investigated parameters distinguished between locations with ethene and ethane as the final product of complete reductive dechlorination. The locations with ethane as a final product (16-4 and 20-4) were identified to be under methanogenic conditions with elevated SOM content and the presence of

Dehalococcoides. On the other hand, at location 20-6, reductive dechlorination to ethene occurred although redox conditions remained at sulfate-reducing and *Dehalococcoides* could not be detected. The results suggest that the absence of apparent methanogenic and fermentable organic matters at a site should not be considered as the *a priori* limiting factor for the occurrence of complete *in situ* reductive dechlorination to ethene or to ethane. In general, the presence of *Dehalococcoides* is considered to play an important role in complete reductive dechlorination as suggested by a study which distinguished the complete and incomplete reductive dechlorination at 24 chlorinated ethene contaminated sites based on the concurrent presence of *Dehalococcoides* and ethene (Hendrickson *et al.* 2002). In contrast, another study reported the absence of *Dehalococcoides* in one of the groundwater samples from locations which carried out complete reductive dechlorination to ethene although authors suspected the cause to be the PCR detection limit (Lu *et al.* 2006). Since *Dehalococcoides* utilizes H_2 as the electron donor, the apparent absence of the organism agrees with the low SOM content which could lead to a low level of H_2-producing fermentative activity at location 20-6. Although the apparent absence of *Dehalococcoides* at location 20-6 could also be attributed to the PCR detection limit, the possibility still remains that other microorganisms or as consortia of indigenous microbial communities without *Dehalococcoides* could carry out the complete reductive dechlorination of chlorinated ethenes to ethene.

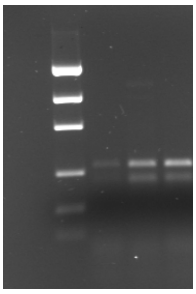

Figure 3 PCR results with the primers specific to *Dehalococcoides*. From left: ladder, samples 20-4 at 10 cm, 30 cm, and 70 cm. The relative intensities of the three locations were considered to determine the semi-quantitative measures ranging weak (+) to strong (+++).

3.3.2 Assessment of cDCE and VC oxidation potentials

Aerobic oxidation potentials of cDCE and VC were investigated by the use of microcosms and the PCR primers specific to the EaCoMT gene which is the key enzyme for aerobic VC oxidation (Coleman and Spain 2003; Coleman and Spain 2003). Microcosms were monitored for one and a half years, and control microcosms did not demonstrate significant concentration decreases. During the course of microcosm monitoring, VC was continuously degraded but cDCE did not. Thus the potential of aerobic VC oxidation was supported but not that of cDCE. Four degradation experiments were carried out to determine the first-order reaction rates (Table 2). The representative growth curves from the first set of experiments are

presented in Figure 4. The first experiment which took place right after the sediment-core sampling clearly demonstrated that all microcosms were capable of degrading VC under oxic conditions. Although the location 1 does not have the previous history of VC exposure, three microcosms from different depths aerobically degraded VC at the same level as the other locations where chlorinated-ethene contamination has been confirmed. The independence of the previous history of exposure for cDCE and VC aerobic oxidation has been reported elsewhere (Bradley and Chapelle 1998).

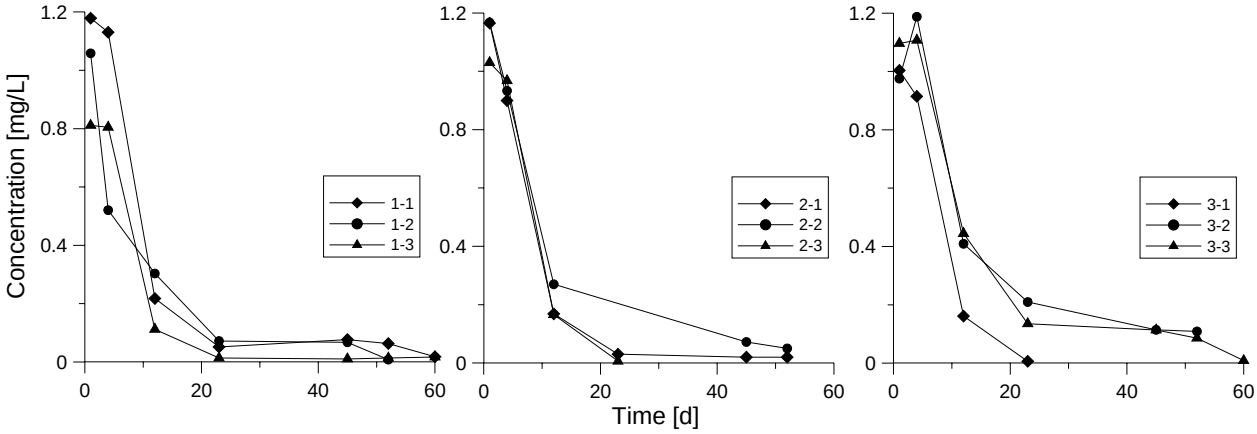

Figure 4 Growth curves from the experiments in August 2004

The initial reaction rates were faster than those measured approximately two months after the first experiment probably due to the high level of microbial activity with organic matters as suggested by the observed rapid consumption of O_2. In general, the reaction rates increased over incubation period, implying that microcosms became enriched in the microbial community which was capable of utilizing VC as the only carbon and energy source. Along with the degradation experiment, isotope enrichment factors for each microcosm were measured from the last experiment. The isotope results (Table 2) reveal that the carbon enrichment factors obtained from microcosms lie in the range of reported values for aerobic VC oxidation between -5.7 ‰ (Chu *et al.* 2004) and -8.2 ‰ (Chartrand *et al.* 2005) for pure cultures. In addition, extracted DNA samples from all microcosms at the end of the last experiment resulted in positive responses to PCR primers specific to the EaCoMT gene. Therefore, the isotope and PCR-based results confirmed that the microcosms carried out the aerobic VC oxidation.

The result from PCR primers specific to the EaCoMT gene from sediment samples is summarized in Table 1. In general, the EaCoMT gene was detected mainly in the top layer (the top 3 cm from the streambed surface) for all sampled locations, suggesting that microbial communities which can carry out aerobic VC oxidation are ubiquitously present at the site. Some locations also resulted in a positive PCR response at deeper depths even at 70 cm where dissolved O_2 was not detected. Although PCR amplifiable cDNA products obtained from RNA extraction, all samples did not contain a detectable level of EaCoMT

gene; therefore, the activity level of aerobic VC-oxidizing microbial communities is not known. But these communities at deeper depths are probably dormant due to the lack of O_2. Although aerobic VC oxidation could not be documented by the contaminant concentration and isotope ratio analyses, the two methods to investigate the aerobic oxidation potentials of VC and partly of cDCE agree that the site has a potential of aerobic VC oxidation, regardless of the location.

Table 2 Reaction rates (expressed in half-lives [d]) and enrichment factors derived from VC microcosms

	August 2004	October 2004	February 2005	January 2006	ε (‰) Jan.2006
1-1	9.5	31.3	4.9	1.5	-5.6
1-2	10.1	62.7	4.9	4.9	-5.6
1-3	10.9	21.3	9.2	2.0	-6.3
2-1	12.8	28.8	4.9	2.8	-3.9
2-2	8.5	34.5	5.0	2.2	-4.6
2-3	8.8	41.7	4.9	1.5	-6.7
3-1	9.1	58.2	4.9	2.1	-4.1
3-2	13.5	24.2	4.9	2.0	-7.0
3-3	11.7	53.3	NA	2.0	-4.1

3.3.3 Possible effect of streambed consolidation

The streambed sediment of the study site consists mainly of loosely consolidated sand but several locations consisted also of a silt and clay layer (Table 1). Although the sediment composition data do not reveal the level of streambed consolidation, the presence of the EaCoMT gene at deeper depths suggests the possibility of the sediment mixing caused by high flow seasons, hence, an indication of the loose streambed. In addition, the locations with the presence of the EaCoMT gene at deeper depths generally had a relatively low streambed temperature, indicative of relatively fast groundwater discharge and permeable streambed. On the other hand, two locations where the EaCoMT gene was detected only at the depth of 0 to 10 cm (16-4 and 20-4) consistently had a relatively elevated streambed temperature, indicating a greater influence from the stream water and rather stagnant flow conditions. These two locations also contain silt layer at the depth of 30 to 70 cm; hence, it is possible that the silt layer at these locations enhanced the streambed consolidation and prevented from the sediment mixing. Furthermore, these locations also correspond to the locations where *Dehalococcoides* was detected. Enhanced streambed consolidation might have contributed to the enrichment of a local microbial community while other locations impacted by the sediment mixing would have been flushed seasonally. The absence of Dehalococcoides at location 20-6 where complete reductive dechlorination took place might originate from the fact that the dechlorinating community was not sufficiently enriched to be detected by the PCR analysis.

3.4 SUMMARY AND IMPLICATIONS

The study demonstrated that the investigated site had the potentials for complete reductive dechlorination of chlorinated ethenes and aerobic VC oxidation. In terms of complete reductive dechlorination, parameters such as the redox conditions, the SOM content and the presence of *Dehalococcoides* gave rise to comparable results and distinguished between locations with ethene and ethane as the final product of reductive dechlorination. The results demonstrate that the presence of *Dehalococcoides*, methanogenic conditions and a high SOM content yielded ethane as a final product. On the other hand, a location with ethene as the final product of reductive dechlorination was accompanied by the apparent absence of *Dehalococcoides,* sulfate-reducing conditions and a low SOM content. The presence of a silt layer accompanied by high SOM contents probably contributed to the development of stable and enriched microbial community by consolidating the streambed, which perhaps allowed the detection of *Dehalococcoides*. Microcosm studies suggest that aerobic cDCE oxidation is not likely at the site, but that of VC is. The results from the PCR analysis also support the potential of aerobic VC oxidation at the site. Carbon isotope analysis indicated the removal of VC via reductive dechlorination; however, it did not indicate the possibility of aerobic VC oxidation at the site. Carbon isotope analysis could not detect the aerobic VC oxidation at the site because of the difficulties with obtaining water samples at the oxic part of the streambed (due to the river water intrusion) and because of the difficulties with distinguishing the two degradation pathways of VC when both pathways are simultaneously present.

Acknowledgement

The RNA extractions of sediment samples as well as some of the PCR series were performed by Vanessa Di Marzo at the University of Neuchâtel.

Chapter 4

Magnitude of carbon and chlorine isotope effects during aerobic oxidation of VC and reductive dechlorination of VC and cDCE

Abstract

Laboratory experiments were carried out to evaluate if combined carbon and chlorine isotope analyses can be used to distinguish between aerobic oxidation and reductive dechlorination of chlorinated ethenes. Experimental data followed a Rayleigh-relation, and carbon and chlorine isotope enrichment factors were determined (-7.2, -0.3, -12.6, -1.4, -18.5 and -1.5‰ for carbon and chlorine isotope enrichment factors of aerobic VC oxidation, reductive dechlorination of VC, and reductive dechlorination of cDCE, respectively). Carbon and chlorine isotope enrichment factors as well as the ratio between the two were significantly different between aerobic oxidation and reductive dechlorination. In order to compare observed isotope fractionation factors and the ratio between carbon and chlorine fractionation factors to the theoretically estimated kinetic isotope effect (KIE) values, apparent KIE (AKIE) values were calculated from the observed isotope data by correcting the isotopic dilution effects (1.0073, 1.0003, 1.0259, 1.0014, 1.0384 and 1.003 in the respective order as enrichment factors above). In addition, experimental data from published studies for three other reactions involving in a C-Cl bond cleavage were evaluated in terms of AKIE. Smaller AKIE values than theoretical KIE estimates (1.057 and 1.013 for carbon and chlorine isotope effects, respectively) were obtained. It could result from the effect of commitment to catalysis, substrate transport across the cell membrane, or incomplete bond breaking during the transition state. The effects of commitment to catalysis and substrate transport across the cell membrane cancels out when two isotope elements are compared. The results reveal that the ratio between carbon and chlorine AKIE values had a narrow range of 0.15 to 0.18, which is close to the theoretical estimate of 0.23. The study demonstrated that the use of dual isotope approach is independent of the substrate concentrations; thus, it has a potential in determining the responsible reaction pathway at the field scale where contaminant dilution and sorption affect the concentrations. The results suggest that the dual isotope approach can distinguish between aerobic oxidation and reductive dechlorination of chlorinated ethenes at the field scale. In addition, it is possible to estimate the ratio between AKIE values of two isotope effects, and the estimated ratio can assist in elucidating the responsible reaction mechanism.

Abe, Y., Shouakar-Stash, O., Aravena, R., Zopfi, J., and Hunkeler, D.

To be submitted to Environmental Science and Technology

4.1 INTRODUCTION

The use of stable isotope analysis has increasingly become an important tool to assess the progress of natural attenuation of organic contaminants at the field scale. The isotope approach has the advantage that it is not influenced by dilution due to dispersion and by sorption, which are inherent in subsurface systems (Harrington *et al.* 1999; Slater *et al.* 2000; Schüth *et al.* 2003). The approach relies on isotope fractionation which results from the microbial tendency to degrade the molecules with light isotopes slightly faster than the molecules with heavy isotopes. As a result, the remaining contaminant becomes progressively enriched in the heavy isotope. The decreasing contaminant concentrations and the increasing contaminant isotope ratios are mathematically related by the Rayleigh equation with a reaction- and compound-specific isotope enrichment factor as key parameter. The Rayleigh-type interpretation of field isotope data can be used to estimate the extent of biodegradation (Sherwood Lollar *et al.* 2001; Richnow *et al.* 2003) and the first-order degradation rate (Morrill *et al.* 2005).

Although the isotope approach based on the Rayleigh-type interpretation has been applied at numerous field sites, such an interpretation depends strongly on the underlying assumption that the active degradation pathway is known *a priori*. Laboratory studies showed that the magnitude of observed isotope effects depends on the enzymatic reaction mechanism, and a certain compound can have different characteristic isotope enrichment factors for different degradation pathways (Morasch *et al.* 2002; Chu *et al.* 2004; Hirschorn *et al.* 2004). However, the identification of the degradation pathway of a compound based on the field isotope data is complicated since field-derived isotope enrichment factors are generally underestimated and unreliable. It is because the field concentration data which enter the Rayleigh equation are affected not only by the degradation, but also by contaminant dilution and sorption, leading to the overestimation of the observed concentration decrease due exclusively to the degradation (Kopinke *et al.* 2005; Abe and Hunkeler 2006). In addition, if a site simultaneously undergoes different degradation pathways of a compound, the observed isotope fractionation is a mixture of individual isotope fractionations of different pathways, and the observation can lead to a misinterpretation. Therefore, the reliable use of isotope approach at the field scale is limited to contaminated sites where only a single degradation pathway is responsible and identified.

In order to overcome the limitation imposed by the possibility of different degradation pathways, the two-dimensional isotope approach, which involves isotope ratio measurements of two elements of the compound, has been proposed (Heraty *et al.* 1999; Hunkeler *et al.* 2001; Morasch *et al.* 2002; Mancini *et al.* 2003; Zwank *et al.* 2005; Sturchio *et al.* 2007) and employed for evaluating the methyl *tert*-butyl ether contaminated sites (Kuder *et al.* 2005; Zwank *et al.* 2005). The premise of the dual approach is that by measuring the isotope ratios of two elements of a compound (such as $^{13}C/^{12}C$ and $^{2}H/^{1}H$ or $^{13}C/^{12}C$ and $^{37}Cl/^{35}Cl$), a characteristic correlation between the two isotope effects can be obtained. The characteristic

correlation is independent of contaminant concentrations unlike the field estimation of enrichment factors as explained later. Hence, it can indicate the responsible degradation pathway. If the dual approach is used to distinguish two simultaneously occurring degradation pathways, the two degradation pathways must involve cleavage of different bonds. Once the active degradation pathway at a contaminated site is confirmed, typical Rayleigh-type analyses can be carried out to estimate the extent of degradation and the first-order reaction rate.

The present study aims at evaluating the feasibility of dual isotope approach for determining the fate of vinyl chloride (VC) and *cis*-dichloroethene (cDCE) as they can be degraded or transformed by different pathways. VC and cDCE can be reductively dechlorinated under strongly reducing conditions (Maymo-Gatell *et al.* 1997; Holliger *et al.* 1999; Maymo-Gatell *et al.* 1999; Bradley 2000). In addition, they can be oxidized under aerobic (Hartmans and de Bont 1992; Klier *et al.* 1999; Bradley and Chapelle 2000) and anaerobic conditions (Bradley and Chapelle 1996; Bradley and Chapelle 1997; Bradley and Chapelle 1998; Bradley *et al.* 1998; Bradley and Chapelle 2000). Furthermore, abiotic reduction of cDCE and VC by iron-bearing minerals has been reported (Butler and Hayas 1999; Dayan *et al.* 1999; Lee and Batchelor 2002). The present study reports the laboratory experiments on carbon and chlorine isotope effects of aerobic VC oxidation and reductive dechlorination of VC and cDCE.

Aerobic VC oxidation involves the formation of an epoxide at the carbon double bond as an initial rate-limiting step (Fox *et al.* 1990; Hartmans and de Bont 1992; van Hylckama Vlieg *et al.* 1996; van Hylckama Vlieg *et al.* 1998). Due to the lack of breaking of a C-Cl bond, the observed carbon isotope effect is small and ranges between -3.2 to -8.2‰ (Chu *et al.* 2004; Chartrand *et al.* 2005), consequently only a small chlorine isotope effect is expected. A strong carbon isotope effect is observed during the reductive dechlorination of cDCE and VC which ranges between -14.1 and -20.4‰ and -22.4 to -31.1‰, respectively (Bloom *et al.* 2000; Slater *et al.* 2001; Hunkeler *et al.* 2002) although the precise mechanism of reductive dechlorination of VC and cDCE is not yet understood. So far, a concerted mechanism which involves the simultaneous nucleophilic addition of cob(I)alamin to one of the carbons in the ethene and the protonation of the other carbon has been postulated (Glod *et al.* 1997). In this study, isotope enrichment factors for carbon and chlorine were determined for each compound and pathways. They were compared to evaluate if different ratios are obtained for different pathways, the premises for using the dual isotope approach at the field scale. To gain additional insight into the factors that control the magnitude of isotope fractionation, position-specific isotope effects were calculated, denoted as apparent kinetic isotope effect (AKIE) and both the actual values and ratios for different isotopes compared to theoretical values.

4.2 RATIONALE AND CALCULATION METHOD

4.2.1 Comparison of isotope enrichment factors

The characteristic isotope fractionation of a given compound during the reaction process can be quantified base on measured isotope date. The difference between the isotope ratios before and after the reaction is related to the isotope enrichment factor according to the Rayleigh equation. Using carbon as an example, the equation states as follows:

$$\ln\frac{(1000+\partial^{13}C)}{(1000+\partial^{13}C_0)}=\frac{\varepsilon}{1000}\ln\frac{C}{C_0} \qquad (1)$$

where $\delta^{13}C$ is the measured isotope ratio at time *t*, $\delta^{13}C_0$ is the initial isotope ratio, ε is the isotope enrichment factor, C is the substrate concentration at time *t*, and C_0 is the initial concentration. The equation can be approximated by:

$$\partial^{13}C=\partial^{13}C_0+\varepsilon\cdot\ln\frac{C}{C_0} \qquad (2)$$

The division of Equation 2 by an analogous expression with respect to chlorine isotope yields:

$$\frac{\Delta\delta^{37}Cl}{\Delta\delta^{13}C}=\frac{\varepsilon_{Cl}}{\varepsilon_C} \qquad (3)$$

where $\Delta\delta^{37}$Cl and $\Delta\delta^{13}$C are the differences between the initial and the final isotope ratios of chlorine and carbon isotopes, respectively. Equation 3 is independent of contaminant concentrations; thus, it is expected to assist in determining the degradation mechanism from field investigation.

4.2.2 Apparent Kinetic Isotope Effect

Kinetic isotope effect (KIE) results from the difference in the reaction rates between a bond with light and heavy isotopes as shown in Equation 4:

$$KIE=\left(\frac{^{L}k}{^{H}k}\right) \qquad (4)$$

where ^{L}k and ^{H}k are the reaction rates of molecules with a light and a heavy isotopes, respectively. Assuming that a single bond is completely broken when passing from the ground state to the transition state and taking into account only differences in zero-point vibrational energies between bonds with different isotopes, the KIE is expected to correspond to:

$$KIE=\exp\left[\frac{h\cdot c\cdot{}^{L}\nu_R}{2\cdot\kappa\cdot T}\cdot\left(1-\sqrt{\frac{^{L}m_{red}}{^{H}m_{red}}}\right)\right] \qquad (5)$$

where h is the Planck constant, c is the speed of light, $^{L}\nu_R$ is the wave number (cm^{-1}), κ is the Boltzmann constant, T is the absolute temperature, and $^{L}m_{red}$ and $^{H}m_{red}$ are the reduced mass between two atoms in the

bond of interest (m_{red}=(m_1*m_2/(m_1+m_2)) where *m1* and *m2* are different masses of the atoms in a bond). KIE values calculated using this simplified equation are frequently denoted as Streitwieser semiclassical limits.

However, for compound-specific isotope analysis, isotope ratios of a given compound are measured as a bulk molecule; thus, the obtained ratio includes not only the abundance of heavy isotope at a reactive position, but also at non-reactive positions. As a result, the actual KIE is partially "diluted" by the presence of non-reactive positions whose isotope ratios remain constant during the reaction and by the presence of multiple identical reactive sites within a molecule. These factors need to be corrected for, in order to estimate the position-specific isotope effect, termed apparent kinetic isotope effect (AKIE). Since AKIE values are reactive position-specific, they are comparable among different compounds with different structures and with the Streitwieser KIE estimates. AKIE is the ratio of the reaction rates with heavy or light isotope in the reacting bond, and it is calculated after considering for the two isotopic dilution effects. Bulk isotope fractionation needs to be corrected for isotopic dilutions caused by the presence of non-reactive positions as follows (Morasch *et al.* 2004; Elsner *et al.* 2005):

$$\alpha_{rp} - 1 \approx \frac{n}{x} \cdot (\alpha_{bulk} - 1) \qquad (6)$$

where α_{rp} is the reactive-position-specific fractionation factor, *n* is the number of the atoms of the element considered in a molecule, *x* is the number of the considered atoms which are located at the reactive site, α_{bulk} is the measured isotope fractionation factor. In addition, the simultaneous presence of multiple and identical reacting positions (intramolecular competition) also contribute to the observed isotopic dilution. The effect of intramolecular competition can be corrected by:

$$AKIE = \frac{1}{1 + z \cdot \varepsilon_{rp} / 1000} \qquad (7)$$

where *z* is the number of atoms in identical reactive positions, ε_{rp} is the reactive-position-specific isotope enrichment factor (α =1+ε /1000). AKIE values obtained from experiments or field investigations can be compared with the estimated KIE values to elucidate an unknown reaction mechanism. The theoretical KIE estimates for the C-Cl bond cleavage at vibration frequency of 750 cm^{-1} are 1.057 and 1.013 for carbon and chlorine stable isotopes, respectively. However, corrected AKIE values can still be lower than the theoretical KIE value 1) if the bond is not completely broken in the transition state, 2) if the transport of a substrate across the cell membrane to an enzyme is the rate-determining step as shown previously for the case of PCE reductive dechlorination (Nijenhuis *et al.* 2005), and/or 3) if the catalytic step is fast compared to the preceding binding steps (Northrop 1977). The relative velocity of reactive to binding steps is often expressed as the *commitment to catalysis* which corresponds to the ratio between the rate of catalytic step to the rate of the substrate-enzyme dissociation step (Northrop 1977). The larger the

commitment to catalysis, the smaller is the observed isotope fractionation. The effect of commitment to catalysis on KIE is expressed as:

$$AKIE = \frac{\chi + KIE}{\chi + 1} \qquad (8)$$

where χ is the level of commitment to catalysis. AKIE is smaller than the intrinsic KIE if the commitment to catalysis is high. Although some studies assume the level of commitment to catalysis to be negligible (Hunkeler and Aravena 2000), different bacteria can have different levels of commitment to catalysis for a given enzymatic reaction, possibly giving rise to the reported variation in the fractionation factors.

4.2.3 Dual isotope approach based on AKIE

While already the ratio of enrichment factors for different isotopes can differentiate degradation pathways, this ratio cannot directly be compared to theoretically expected ratios because the ε values do not only depend on the reaction mechanisms, but also on the molecule size. Therefore, the ratio between the two AKIE values was evaluated because ratios between AKIE values can be compared to theoretical ratios. The advantage of using dual isotope approach is that the effect of commitment to catalysis as well as the substrate transport across the cell membrane on isotope effects disappears by comparing two isotope elements when AKIE values of two isotope elements are compared (Elsner *et al.* 2005; Zwank *et al.* 2005). As discussed in detail in the review article (Elsner *et al.* 2005), the masking of intrinsic KIE due to commitment to catalysis can be termed out by dividing Equation 8 by an analogous expression for another isotope element. The resultant expression is as follows for the case of carbon and chlorine isotopes:

$$\frac{(\alpha_{rpCl}^{\subset})^{-1} - 1}{(\alpha_{rpC}^{\subset})^{-1} - 1} = \frac{KIE_{Cl} - 1}{KIE_C - 1} \cdot \frac{1 + KIE_C \cdot (z_C - 1)}{1 + KIE_{Cl} \cdot (z_{Cl} - 1)} \approx \frac{KIE_{Cl} - 1}{KIE_C - 1} \qquad (9)$$

where $\alpha_{\mathrm{rp}}^{\subset}$ is the obtained fractionation factor at a reactive position affected by commitment to catalysis, KIE_{CL} and KIE_C are the theoretical values of KIE based on Streitwieser semiclassical limits for chlorine and carbon isotopes, respectively. Equation 9 can then be simplified by assuming that α_{rp} is close to unity and ε is very small (which generally is valid for carbon and chlorine isotope effects) as:

$$\frac{KIE_{Cl} - 1}{KIE_C - 1} = \frac{\varepsilon_{Cl} \cdot \frac{n_{Cl}}{x_{Cl}} \cdot z_{Cl}}{\varepsilon_C \cdot \frac{n_C}{x_C} \cdot z_C} \qquad (10)$$

The left hand side (LHS) term is based on Streitwieser semiclassical limits whereas the right hand side (RHS) is based on the experimentally derived values. Equation 10 depicts the relative isotope effects between carbon and chlorine isotopes, and it is independent of the effect of commitment to catalysis and

the substrate transport across the membrane since these two effects influence both carbon and chlorine isotope effects to the same extent.

4.3 MATERIALS AND METHODS

4.3.1 VC aerobic oxidation experiment

Nocardioides strain JS614 was kindly provided by Dr. Spain's laboratory (Georgia Institute of Technology, Atlanta, GA,USA) and used for the aerobic VC oxidation experiments due to its relatively fast growth compared to other available aerobic VC oxidizers (Coleman *et al.* 2002). The culture medium was prepared as described elsewhere (Coleman *et al.* 2002). The stock culture was kept in a 250 mL glass bottle with a Mininert-Valves (Vici Precision Sampling, Baton Rouge, LA) with 100 mL headspace equilibrated with air, and it was fed with the initial air-phase concentration of 0.5 mM VC after phase equilibration (>99% Fluka, Switzerland). The air-phase VC concentration was monitored with a gas chromatograph regularly. As the VC concentration decreased below detection limit, gas-phase VC was added with a syringe at a final air-phase concentration of 0.5 mM. After the addition of VC for three times, 50 mL portion of the culture was transferred into three bottles containing 100 mL of fresh medium and received the same treatment. For the experiment, a 20 mL portion of the transferred stock culture was added to a 60 mL serum bottle capped with a Viton stopper. In total, 20 replicas of 60 mL bottles containing 20 mL of the culture were prepared. Each bottle received a final air-phase VC concentration of 0.5 mM and was placed on a rotary shaker to enhance the equilibration in the air and aqueous phases. After two hours of shaking, bottles were removed from the shaker and placed still for 30 minutes to stabilize the air-phase concentration, and initial VC concentrations of each bottle was measured. For a negative control, one of the 20 bottles was inactivated with sodium azide to a final w/w concentration of 1% before adding VC. During the course of the experiment, VC concentrations were monitored, and each time a multiple of a half-log decrease in VC concentrations with respect to the initial concentrations was observed, two bottles were inactivated by adding sodium azide and kept at 4 $^{\circ}$C.

4.3.2 VC and cDCE anaerobic reductive dechlorination experiments

The experiments for VC and cDCE reductive dechlorination were carried out at the laboratory of SiREM, Ontario, Canada. Commercially available KB-1 mixed culture from the laboratory was used for both experiments. The culture was kept in 160 mL vial with a Teflon stopper and an aluminum cap. The starting VC and cDCE concentrations in liquid phase were adjusted at 50 and 90 mg/L (or 0.8 and 0.9 mM) for VC and cDCE respectively. Due to the presence of iron sulfide solids in the medium to maintain anoxic conditions, the experiments were carried out statically to avoid rupturing of bacterial aggregates, which caused a drawback as mentioned later. During the course of experiments, a small volume (2 to 4 mL depending on the estimated concentrations) of aqueous samples was withdrawn with a syringe.

Aqueous samples were alkalized immediately with NaOH to pH 10 to inactivate the microbial activity. Samples were kept at 4 °C until analyses.

It must be mentioned that due to the lack of adequate agitation and stirring during the experiment, the air-aqueous phase transfer of VC was probably not equilibrated. The phase transfer of VC was achieved only by the effect of slow molecular diffusion. Since VC degradation took place in the aqueous phase, the aqueous VC concentration decreased, and ^{13}C and ^{37}Cl became enriched over time. However, due to the presence of headspace which contained non-degraded VC with the original isotopic signatures, the aqueous phase continuously received less enriched VC from the headspace via molecular diffusion. Furthermore, as the experiment progressed, the volume of headspace increased, creating a bigger pool of isotopically less-enriched VC. Therefore, the observed isotope effect for VC was smaller than expected. VC and cDCE experiments were carried out similarly, but the absence of agitation during the experiment and sampling did not cause the same effect for cDCE due to its lower Henry constant, dimensionless values of 1.14 and 0.17 for VC and cDCE, respectively (Yaws 1999).

4.3.3 Isotope ratio analysis

Carbon isotope ratios of VC and cDCE were analyzed by a gas chromatograph coupled to an isotope-ratio mass spectrometer with a combustion interface (Thermo Finnigan, Germany). The system was equipped with a purge-and-trap concentrator (Velocity XPT, USA) connected to a cryogenic trap. Minimum concentrations for VC and cDCE carbon isotope analysis were approximately 10 and 5 μg/L, respectively. All isotope ratios are reported relative to VPDB using the delta notation as $\delta=(R/R_{std}-1)*1000‰$ where R and R_{std} are the isotope ratio of the sample and the standard, respectively. Chlorine isotope ratios of VC and cDCE were analyzed by a continuous flow-isotope ratio mass spectrometer (Iso Prime, Micromass, currently GV Instruments) equipped with a gas chromatograph (Agilent 6890) and a CTC analytics CombiPAL SPME autosampler as described elsewhere in detail (Shouakar-Stash *et al.* 2006).

4.4 Results and Discussion

4.4.1 Bulk isotope fractionation

In Figures 1, the obtained isotope data are plotted according to the Rayleigh equation. A linear trend can be observed indicating that isotope fractionation was constant throughout the experiments. The obtained bulk enrichment factors (ε_{bulk}) were summarized in Table 1. The bulk enrichment factors for carbon isotopes were similar to the values reported previously (-14.1 to -20.4‰ and -3.2 to -8.2‰ for cDCE reductive dechlorination and aerobic VC oxidation, respectively) except for the VC anaerobic dechlorination (Bloom *et al.* 2000; Slater *et al.* 2001; Hunkeler *et al.* 2002; Chu *et al.* 2004; Chartrand *et al.* 2005). Previous studies report that VC reductive dechlorination involves a significant carbon isotope effect with the enrichment factor in the range of -22.4 to -31.1‰ (Bloom *et al.* 2000; Hunkeler *et al.*

2002). However, the values obtained from this study was approximately half as much as expected likely due to the lack of agitation as explained in Material and Methods section. Consequently, chlorine isotope fractionation would also be expected to be influenced at the same level.

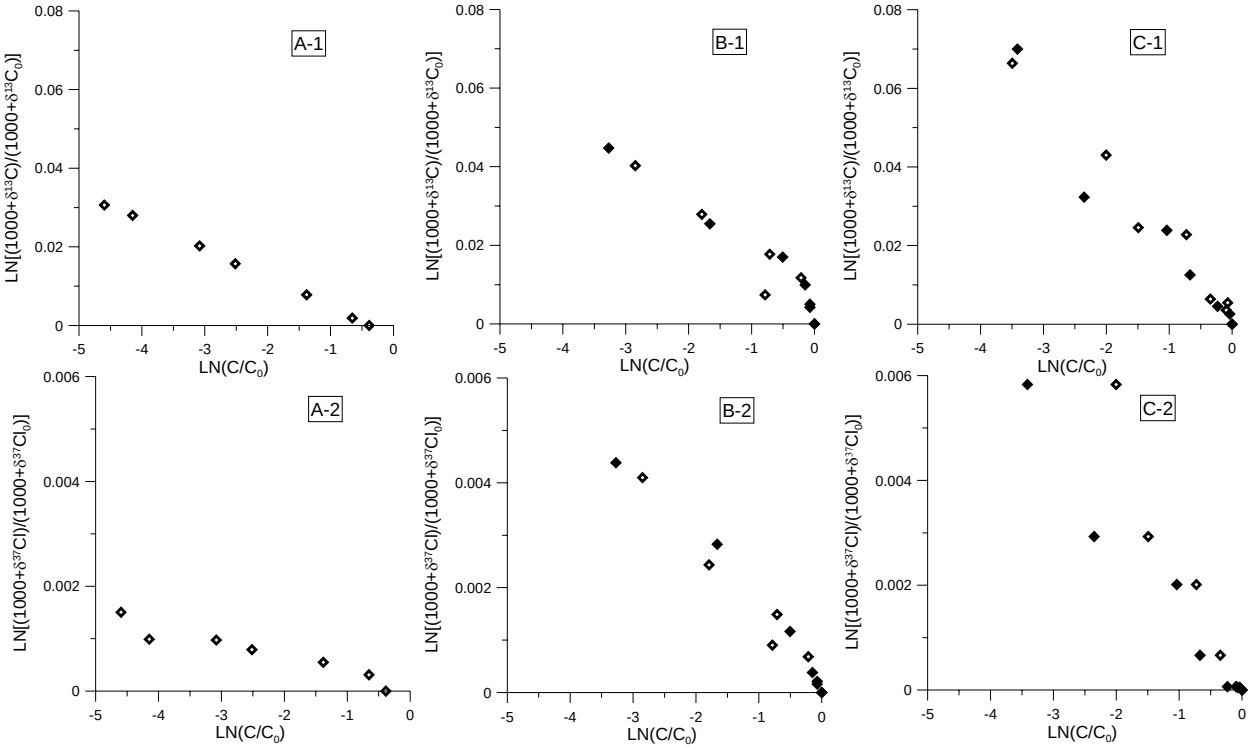

Figure 1 Rayleigh plots for each experiment for carbon and chlorine isotopes. Series 1 is for carbon and series 2 is for chlorine isotope. A: aerobic VC oxidation, B: VC reductive dechlorination (duplicate), and C: cDCE reductive dechlorination (duplicate).

In general, observed chlorine isotope fractionation was smaller than the carbon isotope fractionation regardless of the substrate and the reaction mechanisms involved (Table 1). A particularly small chlorine isotope enrichment factor was observed for the aerobic VC oxidation which is related to the reaction mechanism. The reaction is mediated by the formation of an epoxide as the rate-determining step which does not involve in the cleavage of a C-Cl bond (van Hylckama Vlieg *et al.* 1996). For comparison, carbon and chlorine isotope fractionation factors from the literature for three reactive processes which involve a cleavage of C-Cl bond were included in Table1. TCE reductive dechlorination was accompanied by a small chlorine isotope fractionation with an enrichment factor of -0.5‰ as estimated from a field study of a TCE contaminated site (Sturchio *et al.* 1998), while the field-derived carbon isotope enrichment factor from another TCE contaminated site was –7.1‰ (Sherwood Lollar *et al.* 1999). Chlorine and carbon enrichment factors of –3.8 and –43.4‰ were measured from a laboratory experiment during the aerobic degradation of dichloromethane (DCM) via S_N2 reaction to yield inorganic chloride and formaldehyde (Heraty *et al.* 1999). Similarly, S_N2 reaction of 1,2-dichloroethane (DCA) carried out by

Xanthobacter autotrophicus GJ10 gave rise to the chlorine and carbon enrichment factors of –4.5‰ (Lewandowicz *et al.* 2001) and –27 to -32‰ (Hunkeler and Aravena 2000), respectively. The chlorine and carbon enrichment factors from VC and cDCE reductive dechlorination from this study are in the same range as those values previously reported.

4.4.2 Dual isotope approach based on the experimental data

For all experiments, a linear correlation between observed $\delta^{13}C$ and $\delta^{37}Cl$ values was obtained as shown in Figure 2. The slope of a $\delta^{13}C$ and $\delta^{37}Cl$ plot approximates to $\varepsilon_{bulk\_Cl}/\varepsilon_{bulk\_C}$ ratio (Equation 3). The regression results show that the slope of aerobic VC oxidation was significantly smaller than that of VC and cDCE reductive dechlorination results, which were both in the similar range to other studies ($\varepsilon_{bulk\_Cl}/\varepsilon_{bulk\_C}$ ratios of 0.07, 0.09, and 0.14-0.17 for TCE, DCM, and DCA). Since the dual isotope approach plotted in this manner omits the concentration term from the Rayleigh equation, it has the advantage that laboratory and field data can be compared directly because the calculation is not influenced by the effect of contaminant dilution or sorption. By measuring the isotope ratios of two elements and plot them against each other, the characteristic slope for a given reaction mechanism can be obtained without *a priori* knowledge of the enrichment factor of neither element. The different slope for aerobic oxidation of VC and reductive dechlorination of VC indicates that different pathways of VC degradation can be distinguished using the dual isotope approach.

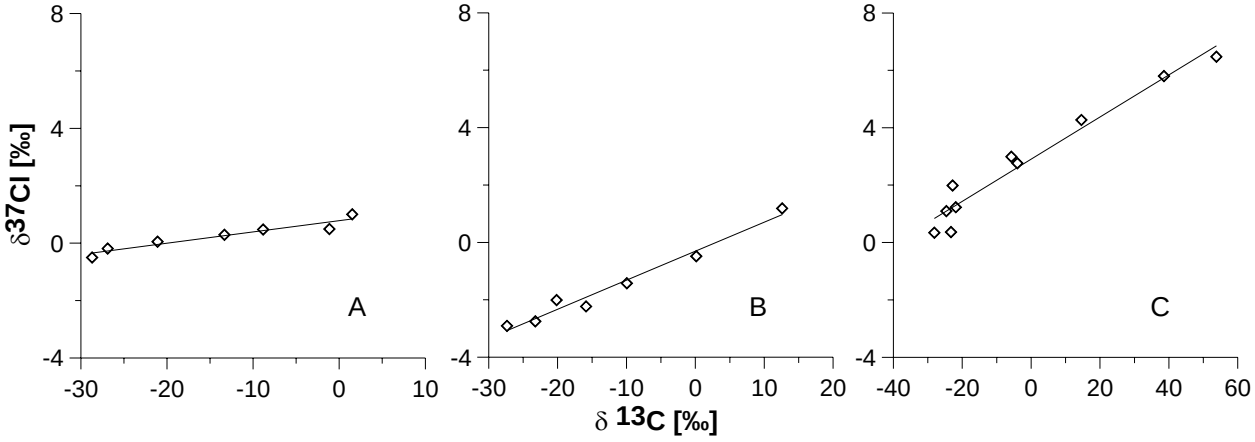

Figure 2 Comparison of $\delta^{13}C$ and $\delta^{37}Cl$ plots. A: VC aerobic oxidation (slope=0.04), B: VC reductive dechlorination (slope=0.11), C: cDCE reductive dechlorination (slope=0.08).

4.4.3 Apparent kinetic isotope effects

In order to facilitate the comparison of isotope effects from the studied reactions and to compare them to theoretical values, AKIE values were calculated from the experimental data as well as from other studies as shown in Table 1. For reductive dechlorination of VC and cDCE, a concerted mechanism which would

involve two carbon atoms during the C-Cl bond cleavage has been proposed although the precise mechanism is not yet understood (Glod *et al.* 1997). Therefore, AKIE values were calculated for two scenarios (one carbon vs. two carbon involvement) (Table 1). Depending on the reaction scenario, the number of carbon atoms at the reactive site (*x*) varies for VC reductive dechlorination and the number of identical reactive positions (*z*) for cDCE reductive dechlorination.

Table 1 AKIE values for carbon and chlorine isotopes (n, x, z are defined according to Eq.10)

		measured	One carbon involved				Two carbon involved			
		ε_{bulk}	n	x	z	AKIE	n	x	z	AKIE
VC	C	-7.2	2	2	1	1.0073				
oxidation	Cl	-0.3	1	1	1	1.0003				
VC	C	-12.6	2	**1**	1	1.0259	2	**2**	1	1.0128
dechlorination	Cl	-1.4	1	1	1	1.0014	1	1	1	1.0014
cDCE	C	-18.5	2	2	**2**	1.0384	2	2	**1**	1.0188
dechlorination	Cl	-1.5	2	2	2	1.0030	2	2	2	1.0030
TCE	C	-7.1	2	1	1	1.0144	(Sherwood Lollar *et al.* 1999)			
dechlorination	Cl	-0.5	3	1	1	1.0015	(Sturchio *et al.* 1998)			
DCM	C	-42.4	1	1	1	1.0443	(Heraty *et al.* 1999)			
	Cl	-3.8	2	2	2	1.0038				
DCA	C	-29.5	2	2	2	1.0304	(Hunkeler and Aravena 2000)			
	Cl	-4.5	2	2	2	1.0045	(Lewandowicz *et al.* 2001)			

* ε_{bulk} for TCE, DCM and DCA studies are reported in the references given in the table

** Bold-face numbers for VC and cDCE dechlorination indicates the difference brought by assuming different reaction mechanisms

The AKIE values for aerobic VC oxidation were significantly smaller than the values for other reactions as expected. A particularly small chlorine AKIE value supports the postulation that the secondary isotope effect gives rise to the chlorine isotope fractionation for aerobic oxidation of VC. Secondary isotope effects result from heavy isotopes present in positions adjacent to the bonds involved in the reactions and are approximately one order of magnitude smaller than the primary isotope effect. For the reductive dechlorination of VC and cDCE, the carbon AKIE values based on the reaction mechanism with one carbon involvement were closer to the values from other studies and the theoretical estimates (1.057 and 1.013 for carbon and chlorine isotopes, respectively). However, results from the two carbon involvement scenario demonstrate that calculated AKIE values were lower than the theoretical KIE estimates for both carbon and chlorine isotope effects. Such deviation from the theoretical estimates can be caused by the effects of commitment to catalysis, substrate transport across the cell membrane or incomplete bond breaking during the transition state. The effects of commitment to catalysis and substrate transport across the cell membrane are expected to affect the carbon and chlorine isotope effects to the same extent. Therefore, the relative magnitude of carbon and chlorine isotope effects is evaluated in the following section.

4.4.4 Dual isotope approach based on AKIE

AKIE-based dual isotope interpretation can provide useful information regarding the type of bond cleavage by comparing with the theoretical estimates. Such a comparison can assist in elucidating the reaction mechanism from isotope data of two elements as demonstrated for a anaerobic degradation of methyl *tert*-butyl ether (Zwank *et al.* 2005). In order to facilitate the comparison of observed isotope data with the theoretical estimate under the framework of AKIE, observed isotope effects were corrected based on Equation 10. The left hand side (LSH) term of Equation 10 estimates the ratio between the two isotopes effects based on theoretical Streitwieser semiclassical limits while the right hand side (RHS) term corresponds to the ratio between the two isotope effects based on the experimental values. Although aerobic VC oxidation does not involve the cleavage of C-Cl bond as a rate-determining step, it was included for the comparison. All other reactions utilized for the comparison involve with the C-Cl bond cleavage; therefore, the experimentally derived ratios (denoted as calculated AKIE ratio based on the RHS term of Eq.10) should correspond to each other and to the theoretically derived ratio (denoted as expected AKIE ratio based on the LHS term of Eq.10).

For the reductive dechlorination of VC and cDCE, concerted mechanism resulted in similar values to other studies as well as to the theoretical value. The experimentally derived ratios are in general in the narrow range of 0.11 to 0.18 for the cleavage of C-Cl bond while the ratio from aerobic VC oxidation is much smaller at 0.04. If less reliable values for VC (no shaking during experiment) and TCE (field data) are neglected a range of 0.15 to 0.18 is obtained.

Table 2 Comparison between calculated and expected AKIE ratios

		One carbon involved				Concerted mechanism				
		n	x	z	Calculated AKIE ratio	n	x	z	Calculated AKIE ratio	Expected AKIE ratio
VC	C	2	**1**	1	0.06	2	**2**	1	0.11	0.23
	Cl	1	1	1		1	1	1		
cDCE	C	2	2	**2**	0.08	2	2	**1**	0.16	0.23
	Cl	2	2	2		2	2	2		
TCE					0.11					
DCM					0.18					
DCA					0.15					
VC oxidation					0.04					

4.5 SUMMARY AND IMPLICATIONS

The carbon and chlorine isotope enrichment factors from aerobic VC oxidation and VC and cDCE reductive dechlorination reactions were experimentally determined according to the Rayleigh equation. Aerobic VC oxidation and VC reductive dechlorination resulted in significantly different enrichment

factors for both carbon and chlorine isotopes and the ratio between the two. This allows distinguishing the two processes based on the comparison of carbon and chlorine bulk isotope enrichment factors. Carbon and chlorine AKIE values were calculated from VC and cDCE reductive dechlorination and compared with the theoretical KIE estimates for C-Cl bond cleavage. In addition, experimental data from three other reactions involving a C-Cl bond cleavage were evaluated in terms of their AKIE values. Calculated carbon and chlorine AKIE values were smaller than the theoretical KIE estimates based on Streitwieser semiclassical limits. Smaller AKIE values than KIE estimates could result from the effects of commitment to catalysis, substrate transport across the cell membrane, or incomplete bond breaking during the transition state. As the effects of commitment to catalysis and substrate transport across the cell membrane cancel out when two isotope elements are compared, a characteristic ratio ranging between 0.15 and 0.18 is obtained for the C-Cl bond cleavage, and the ratio is similar to the theoretical estimates of 0.23. The result indicates that the ratio between AKIE-based carbon and chlorine enrichment factors can be theoretically predicted. Therefore, the dual isotope approach based on AKIE can assist in elucidating the responsible reaction mechanism by estimating the theoretical ratio between enrichment factors of two elements based on Streitwieser semicalssical limits.

Acknowledgement

Chlorine isotope analysis was performed by Orfan Shouakar-Stash at the University of Waterloo.

Chapter 5

Use of geochemical and isotope data to evaluate the fate of chlorinated ethenes in a 2-km chlorinated-ethene plume

Abstract

A field investigation was carried out in a tetrachloroethene (PCE) contaminated site equipped with a large number of multilevel monitoring wells. The study was based on the geochemical and isotope data obtained along the plume centerline in order to better characterize the site and to determine the fate of *cis*-dichloroethene (cDCE). Geochemical data revealed that the site consisted of distinctively different redox conditions as a function of depth due to the presence of pyrite in the deeper part of the aquifer. In the zone near to the surface where pyrite was absent, relatively oxidizing conditions prevailed. On the other hand, due to the pyrite oxidation coupled to oxygen and nitrate reductions, the deeper zone where pyrite was present underwent reducing conditions such as iron-, manganese- and sulfate-reduction. Consequently, the progress of reductive dechlorination of chlorinated ethenes in the two zones was different. In the oxidizing zone, reductive dechlorination stopped at trichloroethene (TCE). In contrast, in the reducing zone, the accumulation of cDCE was identified by the carbon isotope ratio of cDCE which resembled that of the source PCE. The combined carbon isotope ratios of all chlorinated ethene species indicated that reductive dechlorination was the only active degradation pathway along the plume except at the plume front. At the plume front, the combined carbon isotope ratios were higher than the rest of the plume suggesting that carbons in the ethene backbone of chlorinated ethenes had been lost. In order to investigate the possibility of cDCE anaerobic oxidation under prevailing manganese-reducing conditions at the site, several samples were analyzed for cDCE chlorine isotope ratios. The results revealed that cDCE chlorine isotope ratios were strongly fractionated continuously throughout the plume including the plume front, suggesting the involvement of a C-Cl bond cleavage; thus, reductive dechlorination was the likely pathway for the observed carbon and chlorine isotope fractionation. Although only a low level of vinyl chlorine (VC) was present at the site, it was speculated that VC reductive dechlorination took place at redox micro niches mediated by the presence of clay. However, given the low concentrations of VC (less than 1% of cDCE), VC dechlorination did not play a significant role in reducing the contaminant mass in the lower zone.

5.1 INTRODUCTION

Industrial development coincided with the increased use of chlorinated ethenes such as tetrachloroethene (PCE) and trichloroethene (TCE) for the past 50 years. These solvents have been used for fabric dry-cleaning, metal and plastic degreasing, and the production of electric components. As a result of heavy use of PCE and TCE, many aquifers in the industrially developed world are contaminated by them (Wiedemeier *et al.* 1997; Squillace *et al.* 1999; Moran *et al.* 2007). Since the groundwater contamination by chlorinated ethenes is ubiquitous yet the active remediation of the contaminated groundwater such as pump-and-treat is difficult due to the presence of DNAPL source and the large volume of affected groundwater, natural attenuation of these contaminated aquifers has gained a significant interest as passive but effective remedial strategies (Wiedemeier *et al.* 1997).

Degradation pathways of chlorinated ethenes are complex. Sequential reductive dechlorination of PCE yields TCE, *cis*-dichloroethene (cDCE), vinyl chloride (VC), and eventually ethene and ethane under the specific ranges of redox potential (Vogel *et al.* 1987; Bradley 2000). During reductive dechlorination, chlorinated ethenes serve as electron acceptors. As the number of chlorine substituents decreases, the tendency to become dechlorinated decreases, and it consequently requires stronger reducing conditions (Vogel *et al.* 1987). Frequently, cDCE and VC accumulates as a result of incomplete reductive dechlorination caused by an inadequate redox potential and the lack of available electron donor (Wiedemeier *et al.* 1997). In addition to reductive dechlorination, microbial oxidation of cDCE and VC to CO_2 has been observed under aerobic (Bradley and Chapelle 1998; Bradley 2000; Bradley and Chapelle 2000) and iron-reducing and manganese-reducing (Bradley and Chapelle 1997; Bradley *et al.* 1998) conditions. The fermentative degradation of VC to methane and to CO_2 via acetate under methanogenic conditions has also been reported (Bradley and Chapelle 2000). Apart from the microbial degradation pathways, iron-bearing minerals such as pyrite and magnetite are known to abiotically reduce PCE, TCE and cDCE to acetylene via dichloro-elimination and VC to ethene by reductive dechlorination (Lee and Batchelor 2002).

Although much is known about the degradation pathways of chlorinated ethenes, the field demonstration of their degradation remains a challenge. Recent developments of compound-specific stable isotope analysis methods make it possible to differentiate concentration changes due to dilution by dispersion or sorption from those due to biodegradation. It was shown that sorption to aquifer materials does not significantly change isotope ratios (Harrington *et al.* 1999; Slater *et al.* 2000; Schüth *et al.* 2003). Moreover, the isotope approach can distinguish between different enzymatic degradation pathways as different pathways give rise to different magnitudes of isotope fractionations (Hirschorn *et al.* 2004). Therefore, the isotope approach potentially can be a useful tool to assess the *in situ* degradation of chlorinated ethenes. However, due to the spontaneous transformation and production of chlorinated

ethenes in reductive dechlorination as well as the possibility of different degradation pathways under a specific redox condition, the interpretation of the field isotope data is complex (Hunkeler *et al.* 1999; Bloom *et al.* 2000; van Breukelen *et al.* 2005).

The present study investigated a PCE contaminated site where cDCE accumulation occurs. The objective was to identify the fate of cDCE and VC using the isotope approach. Due to the possibility of either reductive dechlorination or anaerobic oxidation of cDCE under characteristic redox conditions at the site, the combined carbon and chlorine isotope approach was employed to clarify the responsible degradation mechanism. Redox conditions were characterized based on concentrations of redox-sensitive species and sulfur isotopes in SO_4^{2-} to identify the potential for different degradation pathways of chlorinated ethenes. In order to clarify the contaminant transformation throughout the plume, carbon isotope approach was used to document the progress of reductive dechlorination and to evaluate the possible occurrence of other degradation pathways. Despite the apparent accumulation of cDCE at the site, the possibility of direct anaerobic oxidation of cDCE could not be excluded under the observed redox condition. Therefore, combined carbon and chlorine isotope approach was employed to elucidate the responsible cDCE degradation pathways. The carbon isotope data was also interpreted to estimate the *in situ* transformation rates of PCE and cDCE.

5.2 STUDY SITE.

The study site is located in the city of Rødekro in southern Jütland, Denmark. The PCE contamination was caused by a regional dry-cleaning facility which operated from 1967 to 1980. The PCE source zone was delineated by the field observation and it was isolated at one location as it resulted from leakage from the underground storage tanks. At the source zone, mono-aromatic hydrocarbons were reported to be present previously, but at the time of investigation, they had been almost depleted. Based on the intensive network of 55 multilevel monitoring wells with 150 screens, the contaminant plume was delineated and the plume migration patterns in longitudinal and vertical directions were characterized. The plume migrates towards south for approximately 1.2 km, and it alters the migration direction to southeast for approximately 1 km (Figure 1). The center of the plume, estimated based on the contaminant concentration analysis, is indicated in Figure 1. The unconfined aquifer of Quaternary age at the site consists mainly of relatively homogeneous fluvio-glacial sand with occasional presence of gravel, silt and clay lenses (Figure 2). This part of Jütland aquifers generally contain a very low level of organic matter and significant amounts of iron mainly in the amphibole/pyroxene fraction (Postma and Brockenhuus-Schack 1987; Postma *et al.* 1991). The local hydraulic gradient was estimated to be 0.0013 m/m throughout the study area. Based on the pumping test, the local hydraulic conductivity was estimated to be $6.5 \cdot 10^{-4}$ m/s (55 m/d), and the groundwater velocity was estimated to be approximately 0.24 m/d assuming a porosity of 0.3.

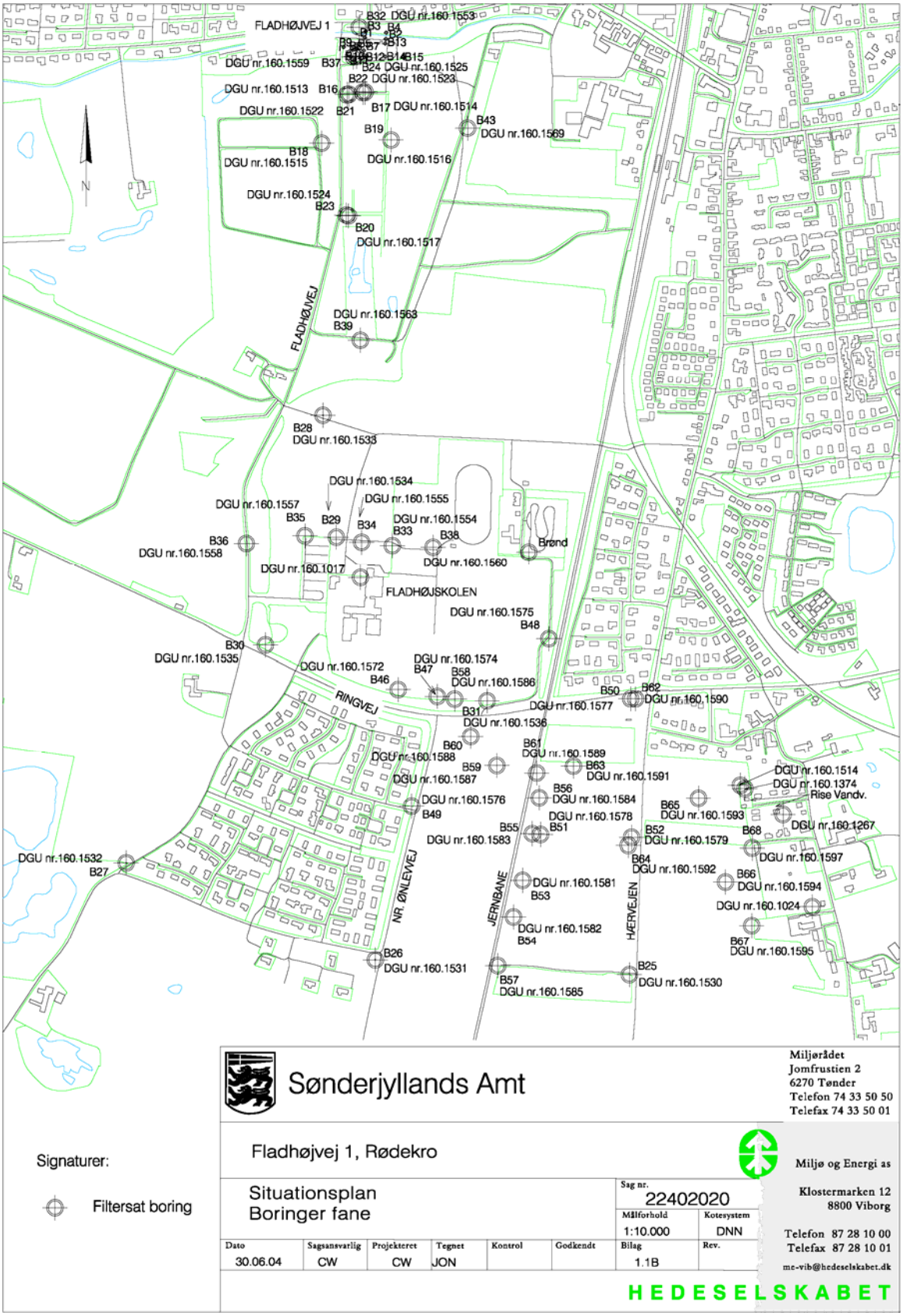

Figure 1 Monitoring well location at the site (Scale in 1:10,000) (Hedeselskabet 2005)

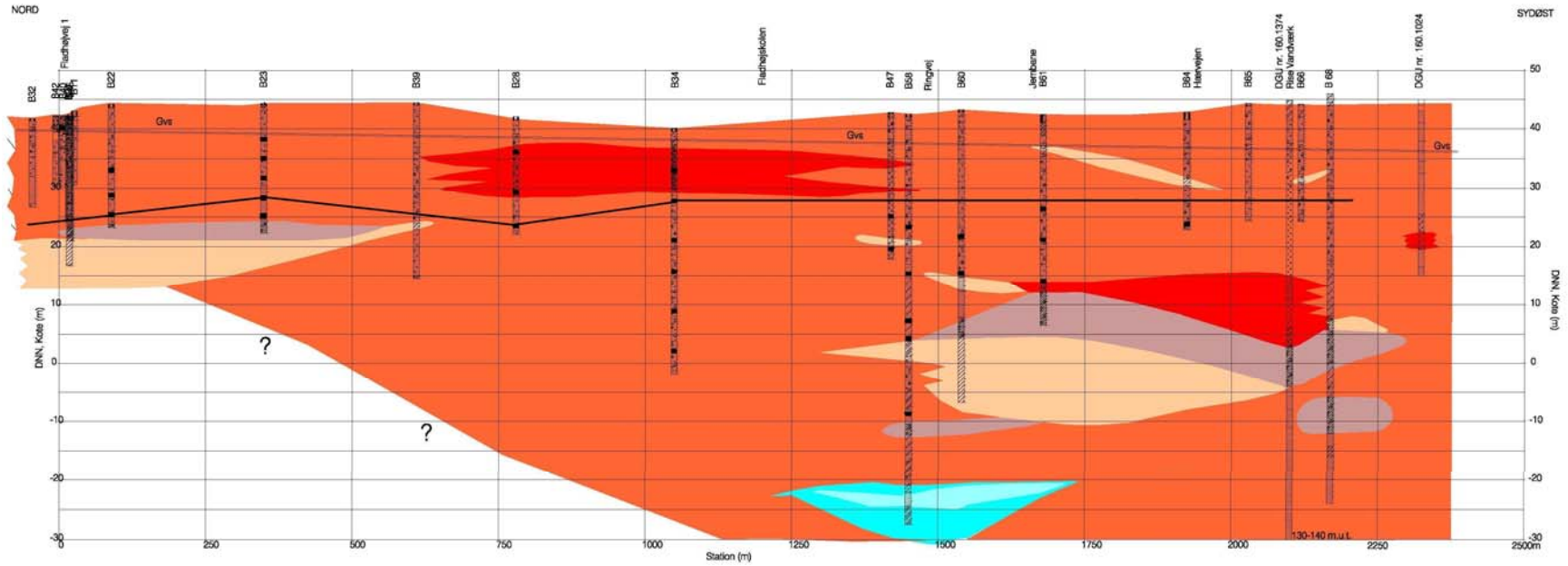

Smeltevandssand	Fluvio-glacial sand
Smeltevandsgrus	Fluvio-glacial gravel
Smeltevandsler	Fluvio-glacial fine sediments
Moræneler	Clayey sediments
Glimmersand	Micaceous sand
Glimmerler	Micas

Figure 2 Geological cross section along the center of the plume. Solid line indicates the approximate location of redox transition zone

5.3 STUDY METHODS

5.3.1 Groundwater sampling

Each monitoring location consists of a bundle of 1 to 7 PVC pipes of 2" diameter installed to different depths to allow multilevel sampling at each location. Each PVC pipe has a screen interval ranging from 1 to 4 m. In general, smaller screened intervals (1 m) were installed in the source and near-source zones and larger screened intervals further downgradient. Groundwater was sampled after abstracting at least three well volumes of water using a submersible pump at 12 m below the ground level. Samples for anion and cation analyses were filtered with a sterile filter (0.45 μm) and collected in 100 mL polystyrene bottles, and those for cation analysis were immediately acidified with 1 M nitric acid to pH 2. For the stable carbon and chlorine isotope analyses of chlorinated ethenes, samples were collected in quadruplet in 40 mL standard VOC glass vials without headspace, except for the VC samples that were collected in 1-L Schott bottles without headspace. For sulfur isotope analysis, duplicate samples of 500 mL were collected in Schott bottles without headspace. Contaminant concentration and carbon and chlorine isotope samples were collected without headspace, and treated immediately with concentrated NaOH to pH 10 to inactivate microbial activity.

5.3.2 Analyses

Temperature, pH, dissolved oxygen and electric conductivity of samples were measured on site using a flow-through cell until stable measurements could be obtained. Major anion and cation concentrations were determined with an ion chromatograph (Dionex DX-120, USA) except for dissolved manganese and iron which were measured colorimetrically (Hach DR/850 Colorimeter, USA). Detection limits for anions and cations were 0.5 mg/L. Chlorinated ethene concentration were analyzed with a HP-6890 gas chromatograph 6890 equipped with a HP-7694 head space autosampler (Agilent, Palo, Alto, USA) and an electron capture detector and a flame ionization detector. After headspace equilibration, a Shimadzu MNZ-1 gas chromatograph (Shimadzu, Japan) was used for ethene, ethane, methane, and acetylene concentration analyses. Detection limits were 0.9, 0.6, 1.9, 1.0, 0.5, 0.5, 10, 5.0 μg/L for PCE, TCE, cDEC, VC, ethene, ethane, methane and acetylene concentrations, respectively. Carbon isotope ratios of chlorinated ethenes were analyzed by a gas chromatograph coupled to an isotope-ratio mass spectrometer with a combustion interface (Thermo Finnigan, Germany). The system was equipped with a purge-and-trap concentrator (Velocity XPT, USA) connected to a cryogenic trap. 20-mL sample was purged for 10 minutes at the purging rate of 40 mL/min and cooled at a cryogenic trap at -140 ^{0}C. Minimum concentrations for PCE, TCE, cDEC and VC isotope analysis were approximately 5, 10, 10, and 5 μg/L, respectively. In order to achieve a better detection limit of 0.2 μg/L for VC, a 1-L sample was purged for 20 minutes at the purging rate of 80 mL/min, followed by the same procedure as described above. For VC analysis, a small portion of sample was discarded to create headspace, and the glass purging tube was

directly submerged into a 1-L sample bottle and stabilized at the bottle cap with a thick Teflon disk. The sample bottle was continuously stirred on a magnetic stirrer. Chlorine isotope analysis was performed as described previously (Shouakar-Stash *et al.* 2006). All isotope ratios are reported relative to a standard using the delta notation $\delta=(R/R_{std}-1)*1000(‰)$ where R and R_{std} are the isotope ratio of the sample and the standard, respectively.

5.3.3 Sampling sessions

Preliminary investigations took place during the years 2001 to 2005 concurrently as monitoring wells were being installed. A total of 55 multilevel wells with 150 screens were sampled some days after the completion of well instillation at each location. Before sampling, the groundwater flow conditions were reestablished and wells were purged. Based on the preliminary investigations, 37 screens from 14 wells were selected for more detailed investigation in February 2006 where samples for contaminant concentrations and stable carbon isotope ratios were collected. Several screens were analyzed also for anions and cations to assure the stability of local redox conditions at the site by comparing with the results from previous analysis. The contaminant concentrations and stable carbon isotope ratios shown in this study are based on this sampling campaign unless otherwise indicated.

Since VC concentrations were not sufficiently high to measure its stable carbon isotope ratios, 1-L samples were collected from wells exceeding the minimum VC concentrations (0.2 μg/L) for VC carbon isotope measurements in July 2006 to test the analytical method for 1-L samples. Having demonstrated the feasibility of the method, additional 1-L samples for VC carbon isotope analysis as well as samples for geochemical parameters and stable chlorine isotope analysis of cDCE were collected in September 2006. Finally, in order to better evaluate the fate of cDCE and VC, samples for possible biological and abiotic transformation products (ethene, ethane and acetylene) were collected from several wells in April 2007. The samples were analyzed also for major anion and cation concentrations, chlorinated ethene concentrations, carbon isotope ratios of VC, carbon and chlorine isotope ratios of cDCE, and sulfur isotope ratios of sulfates.

Redox conditions at the site appeared rather stable over time as shown in Figure 3 based on the comparison between the first and the last sampling campaigns. The x-y plots generally demonstrate a slope of unity, indicating that the analyzed redox-sensitive species were fairly constant in concentrations over time. Dissolved iron concentrations were also stable between the two campaigns (data not shown). For the sake of consistency, the values from the first preliminary sampling campaign are used hereafter unless otherwise indicated.

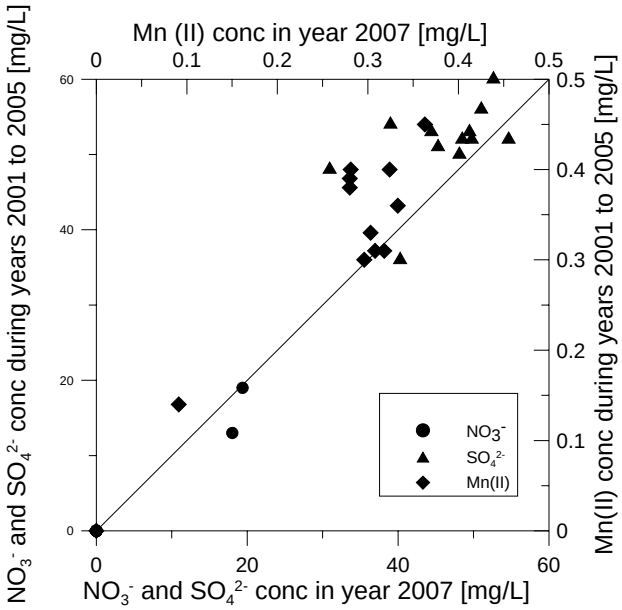

Figure 3 Cross validation of redox-sensitive parameters over time

5.4 RESULTS AND DISCUSSION

5.4.1 Identification of redox zones

Table 1 summarizes the concentrations of all redox-sensitive species analyzed in this study. In general, the samples collected from less than 12 to 15 m below the surface contain relatively elevated O_2 and NO_3^- concentrations, suggesting oxidizing conditions. On the other hand, samples below these depths are deprived of O_2 and NO_3^- and contain Mn^{2+}, Fe^{2+}, and elevated SO_4^{2-} concentrations. Furthermore, slightly elevated methane concentrations are observed from samples taken from the downgradient area (1330m onwards) where a large clay lens is present. Near the clay lens, redox micro-niches are expected to develop due to the elevated level of electron donor availability in the clay lens. The presence of a low level of methane, despite the high sulfate levels, may originate from these redox micro-niches which are under methanogenic conditions. Thus, the site apparently exhibits different redox zones as a function of depth and the presence of clay lens. The depth-dependent evolution of redox conditions is shown in Figures 4. Near to the surface, the presence of abundant O_2 and NO_3^- indicates an oxidizing zone although the oxidants are progressively consumed with depth. The disappearance of oxidants is accompanied by the appearance and rapid increase of reduced species (namely Mn(II), Fe(II)) and SO_4^{2-}. Therefore, the redox condition progresses to Mn(IV)- and Fe(III)-reducing conditions from approximately 10 to 15 m below the surface. This zone is denoted as 'redox transition zone' hereafter where as the aerobic zone above is denotes as upper zone, and the zone below as lower zone.

Table 1 Concentrations of redox parameters in the sampled wells

Well number	Distance [m]	Depth [m]	O_2 [mg/L]	NO_3^- [mg/L]	Mn^{+2} [mg/L]	Fe^{+2} [mg/L]	SO_4^{2-} [mg/L]	CH_4 [mg/L]
*B5-3	0	-2.75	NA	2.1	NA	0.24	NA	<0.01
B5-2	0	-5.5	4.97	15.0	0.14	0.70	35	0.023
B5-1	0	-8.5	5.21	16.0	<0.001	<0.005	38	<0.01
B11-3	18	-4.5	2.17	13.0	0.47	0.03	43	<0.01
B11-2	18	-7.5	4.45	28.0	0.01	<0.005	25	<0.01
B16	105	-8	0.30	3.7	0.84	0.15	36	0.014
*B22-3	100	-11	5.93	25.2	NA	NA	27	NA
*B22-2	100	-15	0.10	7.4	NA	NA	52	NA
*B22-1	100	-19	0.10	<0.5	NA	NA	52	NA
B20	355	-6.5	8.56	18.0	<0.005	<0.005	31	<0.01
B23-4	350	-9.5	1.77	19.0	<0.005	<0.005	36	<0.01
B23-3	350	-12.5	0.19	13.0	0.14	<0.005	48	<0.01
B23-2	350	-15.75	0.08	<0.5	0.33	<0.005	57	<0.01
B23-1	350	-18.75	0.09	<0.5	0.36	<0.005	52	<0.01
*B28-3	750	-5.5	NA	7.9	NA	NA	19	NA
*B28-2	750	-12.5	3.58	7.9	NA	NA	45	NA
*B28-1	750	-18.5	0.19	<0.5	0.41	0.18	53	<0.01
B34-6	1000	-6.5	0.56	12.0	0.23	<0.005	39	<0.01
B34-5	1000	-12.5	0.09	<0.5	0.49	0.20	51	<0.01
B34-4	1000	-18.5	0.07	<0.5	0.28	0.35	51	<0.01
B34-3	1000	-24.5	0.07	<0.5	0.31	0.32	49	<0.01
B34-2	1000	-31.5	0.07	<0.5	0.33	0.28	51	0.014
B34-1	1000	-38.5	0.09	<0.5	0.35	0.39	47	<0.01
*B47-2	1330	-17.5	0.11	<0.5	NA	0.40	54	0.034
*B47-1	1330	-23.5	0.07	<0.5	NA	0.46	54	0.028
*B58-10	1340	-19	0.13	<0.5	0.37	0.82	49	0.034
B58-8	1340	-27	0.12	<0.5	0.30	0.45	53	0.019
*B58-7	1340	-35.5	0.09	<0.5	NA	0.89	50	0.058
B58-6	1340	-38.5	0.10	<0.5	0.31	0.96	54	0.028
*B58-4	1340	-51	0.05	<0.5	0.41	0.67	52	0.038
*B60-3	1430	-21.5	0.12	<0.5	0.40	0.43	50	0.048
*B60-2	1430	-27.5	0.16	<0.5	0.38	0.99	53	0.025
***B60-1	1430	-33.5	0.18	<0.5	0.31	0.81	50	NA
*B61-3	1580	-16	0.16	<0.5	0.45	NA	60	NA
*B61-2	1580	-21.5	0.15	<0.5	0.40	0.60	52	0.037
*B61-1	1580	-28.5	0.14	<0.5	0.39	0.60	56	0.032
**B64	1810	-19	0.28	<0.5	0.48	0.40	NA	NA
*B67	2020	-19	0.22	<0.5	NA	0.15	57	<0.01

* samples collected in February 2006, NA stands for Not Analyzed.
** samples collected in July 2006
*** samples collected in April 2007

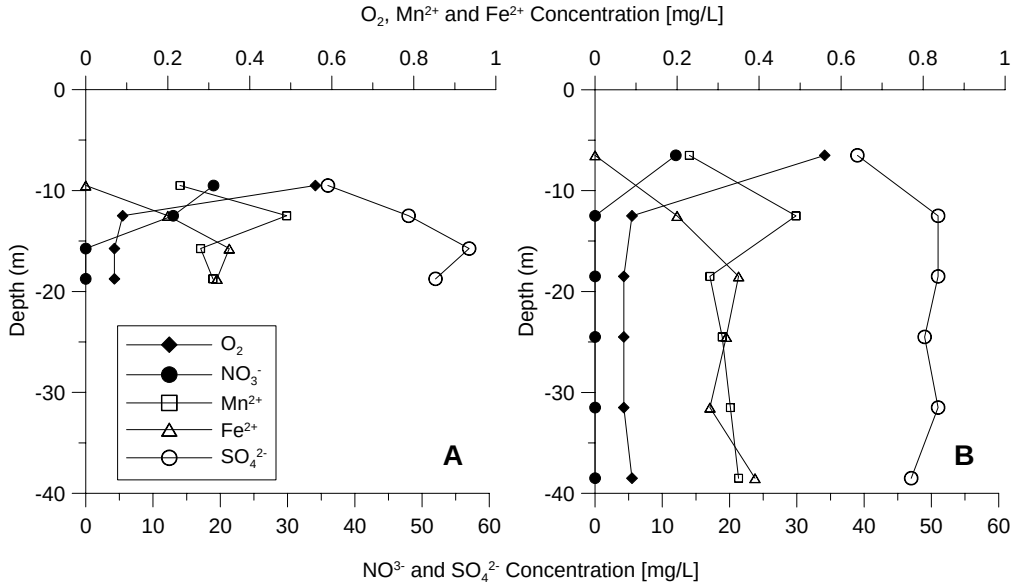

Figure 4 Vertical profiles of redox-sensitive concentrations. A: Well B23, B: Well B34

5.4.2 Pyrite oxidation

The increase of SO_4^{2-} and Fe(II) concentrations which coincides with the disappearance of O_2 and NO_3^- suggest that pyrite oxidation takes place in the redox transition zone. Pyrite oxidation with O_2 and NO_3^- has been observed at field scales (Postma *et al.* 1991), but the direct pyrite oxidation with NO_3^- has not been experimentally demonstrated (Schippers and Jørgensen 2001; Schippers and Jørgensen 2002). Pyrite oxidation processes with O_2 and NO_3^- are summarized by the overall equations as follow:

$$2FeS_2 + 7O_2 + 2\ H_2O \Rightarrow 2Fe^{2+} + 4SO_4^{2-} + 4H^+$$

$$5FeS_2 + 14NO_3^- + 4H^+ \Rightarrow 7N_2 + 5Fe^{2+} + 10SO_4^{2-} + 2H_2O$$

Indeed, the presence of pyrite in the sandy aquifers in Jütland is well known (Postma *et al.* 1991). An electron balance was calculated for the responsible redox couples based on the observed concentrations assuming that pyrite oxidation took place in the redox transition zone. For B23 between –12.5 and –15.75 m, the decreases in O_2 and NO_3^- concentrations correspond to 1.06 mol/L of electron loss while the increase in SO_4^{2-} concentration requires 1.12 mol/L of electron gain. Similarly, for B34 between –12.5 and –18.5 m, the balance is 1.03 and 1.50 mol/L of electron loss and gain, respectively. Within the limit of uncertainty, the electron transfer in the redox transition zone could be explained fairly well by the occurrence of pyrite oxidation coupled to O_2 and NO_3^- reduction. Furthermore, the measured sulfur isotope ratios of SO_4^{2-} from several wells (B23s, B34-2, and B58-2 and 4) varied in the range of -2.6 to -5.0 ‰. Hence the sulfur is strongly depleted in ^{34}S compared to marine sulfate (e.g. from gypsum) consistent with the addition of ^{34}S depleted sulfur by pyrite, which is typically in the range of-20 to 0‰ (Clark and Fritz 1997). Therefore, due to the lack of pyrite in the upper zone, the redox condition remains

oxic to denitrifying in the upper zone, and the rapid consumption of O_2 and NO_3^- in the redox transition zone due to pyrite oxidation creates more reducing conditions in the lower zone.

5.4.3 Plume concentration evolution along the plume centerline

Figure 5 shows the progress of the plume for individual chlorinated ethene species in terms of concentrations along the plume centerline, and the measured concentrations are reported in Table 2. In general, the plume is quite shallow for the first 500 m due to the presence of a clayey zone underneath. It then plunges and widens progressively due to the diverging groundwater flow under the clay lens. Near to the surface (up to approximately 10 m in depth), the plume consists predominantly of PCE whereas the lower zone consists mainly of cDCE. Interestingly, the redox transition zone corresponds to where the plume starts to sink and become predominant in cDCE (compare Figure 2 and Figure 5).

The presence of distinct redox zones as a function of depth affects the plume evolution and the dominant chlorinated ethenes species within each redox zone. In the upper zone where oxidizing conditions prevail, a small amount of PCE could still be transformed to TCE under denitrifying conditions (Vogel *et al.* 1987; Bradley 2000). However, in the redox transition zone, O_2 and NO_3^- are quickly deprived due to the occurrence of pyrite oxidation (Postma *et al.* 1991). Because of the lack of better electron acceptors such as O_2 and NO_3^-, PCE and TCE start to serve as electron acceptors of preference in the redox transition and lower zones (Vogel *et al.* 1987; Bradley 2000). Under Mn(II)- and Fe(II)-reducing conditions found in the lower zone, accumulation of cDCE occurs because the reduction of cDCE to VC and further requires stronger reducing conditions (Vogel *et al.* 1987; Bradley 2000). However, the presence of VC at low concentrations suggests that such transformation still takes place in the lower zone despite the unfavorable redox conditions, or it may simply be transported from the source. Further dechlorination of VC does not seem to occur since end products of dechlorination (ethene and ethane) were not detected at the site; thus, the concentration data suggests that cDCE accumulation is predominant and partial reductive dechlorination is incomplete at VC. Based on the redox conditions and contaminant concentration analysis, the general trend of *in situ* reductive dechlorination was captured. However, the progress of reductive dechlorination especially regarding the possibility of reductive dechlorination beyond cDCE as well as the origin and the fate of VC remain unclear. Therefore, compound-specific isotope analysis was employed for the further investigation of the site.

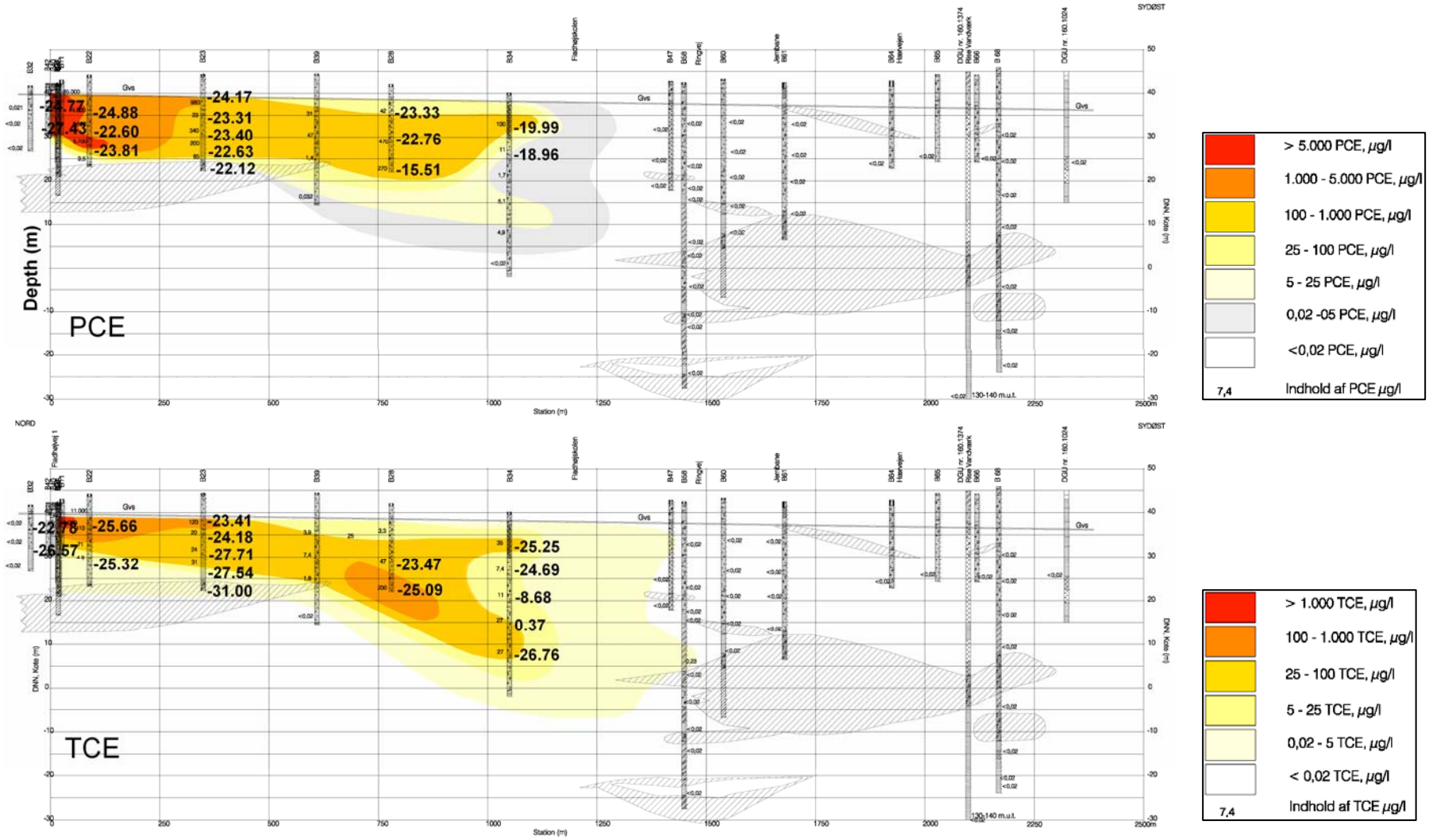
PCE
Depth (m)
-24.77
-27.43
-24.88
-22.60
-23.81
-24.17
-23.31
-23.40
-22.63
-22.12
-23.33
-22.76
-15.51
-19.99
-18.96
130-140 m.u.t.
Station (m)
> 5.000 PCE, µg/l
1.000 - 5.000 PCE, µg/l
100 - 1.000 PCE, µg/l
25 - 100 PCE, µg/l
5 - 25 PCE, µg/l
0,02 -05 PCE, µg/l
<0,02 PCE, µg/l
7,4
Indhold af PCE µg/l
TCE
-22.78
-26.57
-25.66
-25.32
-23.41
-24.18
-27.71
-27.54
-31.00
-23.47
-25.09
-25.25
-24.69
-8.68
0.37
-26.76
> 1.000 TCE, µg/l
100 - 1.000 TCE, µg/l
25 - 100 TCE, µg/l
5 - 25 TCE, µg/l
0,02 - 5 TCE, µg/l
< 0,02 TCE, µg/l
7,4
Indhold af TCE µg/l

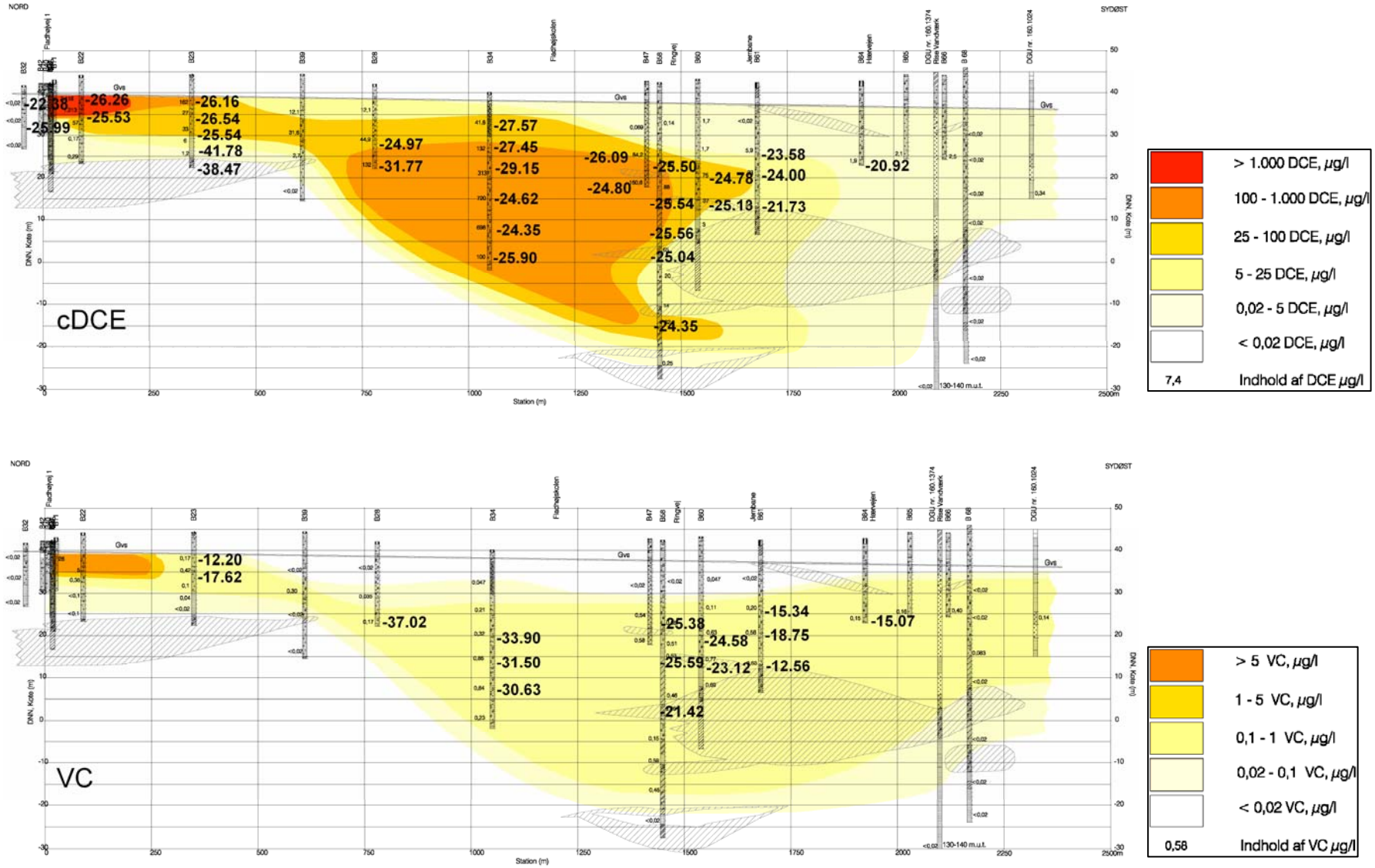

Figure 5 Contaminant distribution and isotope ratios along the center of the plume (Hedeselskabet 2005)

Table 2 Concentrations and $\delta^{13}C$ values of chlorinated ethenes

Well number	Distance [m]	Depth below surface [m]	PCE conc. [μmol/L]	PCE $\delta^{13}C$ [‰]	TCE conc. [μmol/L]	TCE $\delta^{13}C$ [‰]	cDCE conc. [μmol/L]	cDCE $\delta^{13}C$ [‰]	VC conc. [μmol/L]	VC $\delta^{13}C$ [‰]	Combined $\delta^{13}C$ [‰]
B5-3	0	-2.75	578.906	-24.92	44.904	-26.18	10.494	-26.35	0.035		-25.03
B5-2	0	-5.5	9.045	-25.14	1.827	-26.57	1.663	-25.49	0.010		-25.39
B5-1	0	-8.5	1.568	-25.61	0.002		BD		BD		-25.60
B11-3	18	-4.5	192.969	-24.77	15.222	-22.78	5.846	-22.38	0.048		-24.56
B11-2	18	-7.5	15.076	-27.43	1.294	-28.19	2.904	-25.99	0.011		-27.26
B16	105	-8	21.106	-24.88	6.698	-24.10	0.434	-26.26	BD		-24.72
B22-3	100	-11	1.628	-22.60	2.207	-25.66	4.047	-25.53	0.002		-24.96
B22-2	100	-15	2.352	-23.81	0.373		0.405		0.001		-23.81
B22-1	100	-19	0.011		0.007	-25.32	0.002		BD		-25.32
B20	355	-6.5	3.317	-24.17	1.294	-23.41	2.685	-26.16	0.029	-12.20	-24.72
B23-4	350	-9.5	0.096	-23.31	0.003	-24.18	0.002	-26.54	BD	-17.62	-23.40
B23-3	350	-12.5	2.774	-23.40	0.297	-27.71	6.538	-25.54	0.002		-24.99
B23-2	350	-15.75	1.568	-22.63	0.434	-27.54	0.188	-41.78	BD		-25.25
B23-1	350	-18.75	1.688	-22.12	0.065	-31.00	0.020	-38.47	BD		-22.63
B28-3	750	-5.5	0.157	-23.33	0.027		0.084		BD		-23.33
B28-2	750	-12.5	6.030	-22.76	1.142	-23.47	2.183	-24.97	0.001		-23.36
B28-1	750	-18.5	1.930	-15.51	3.425	-25.09	3.743	-31.77	0.003	-37.02	-25.81
B34-6	1000	-6.5	0.320	-19.99	0.183	-25.25	0.306	-27.57	BD		-24.04
B34-5	1000	-12.5	0.090	-18.96	0.114	-24.69	1.364	-27.45	0.004		-26.76
B34-4	1000	-18.5	0.022		0.320	-8.68	2.822	-29.15	0.006	-33.93	-27.08
B34-3	1000	-24.5	0.003		0.056	0.37	4.702	-24.62	0.011	-31.50	-24.35
B34-2	1000	-31.5	0.013		0.152	-26.76	5.874	-24.35	0.016	-30.63	-24.43
B34-1	1000	-38.5	BD		0.011		1.037	-25.9	0.004		-25.90
B47-2	1330	-17.5	BD		BD		1.004	-26.09	0.014		-26.09
B47-1	1330	-23.5	0.001		BD		2.176	-24.80	0.013		-24.80
B58-10	1340	-19	BD		BD		1.036	-25.50	0.010	-25.38	-25.50
B58-8	1340	-27	BD		BD		0.994	-25.54	0.011	-25.59	-25.54
B58-7	1340	-35.5	BD		0.003		1.139	-25.56	0.009	-23.02	-25.54
B58-6	1340	-38.5	BD		BD		0.714	-25.04	0.010	-21.42	-24.99
B58-4	1340	-51	BD		BD		0.383	-24.35	0.012	-17.98	-24.17
B60-3	1430	-21.5	BD		BD		1.344	-24.78	0.014	-24.58	-24.78
B60-2	1430	-27.5	0.001		BD		2.378	-25.13	0.012	-23.12	-25.12
B60-1	1430	-33.5	-		-		0.126		0.012	-16.82	-16.82
B61-3	1580	-16	BD		BD		0.186	-23.58	0.004	-15.34	-23.41
B61-2	1580	-21.5	BD		BD		0.724	-24.00	0.010	-18.75	-23.92
B61-1	1580	-28.5	BD		BD		0.135	-21.73	0.012	-12.56	-21.01
B64	1810	-19	BD		BD		0.058	-20.92	0.004	-15.07	-20.51
B67	2020	-19	BD		BD		0.001		0.001		

* BD stands for below detection limits

5.4.4 Isotope behaviors of chlorinated ethenes along the plume centerline

At the source B5-3, carbon isotope ratios of PCE, TCE and cDCE slightly decrease in the respective order (-24.92, -26.18 and –26.35 ‰), which is the typical isotope evolution during sequential reductive

dechlorination (Bloom *et al.* 2000; Slater *et al.* 2001). However, their isotope ratios are quite similar to each other. The transformation of PCE to TCE and to cDCE and the dissolution of PCE from its DNAPL source take place simultaneously, causing the isotope ratio of PCE to remain stable due to the continuous addition of the fresh PCE source with its original isotope ratio. Therefore, despite PCE reductive dechlorination is expected to occur at the source based on the presence of TCE, cDCE and VC, the isotope ratio of PCE remains similar to its original DNAPL value. PCE becomes slightly enriched in ^{13}C in the upper zone over a distance of 1000m suggesting limited transformation to TCE. On the other hand, the isotope ratios of TCE and cDCE do not exhibit a stable fractionation pattern, and they remain largely unchanged throughout the first 1000 m of plume migration in the upper zone, suggesting that they are not being transformed. The general isotope trend is depicted in Figure 6 in which the sampled depths with the highest total chlorinated ethenes concentrations are plotted over distance to represent the 'core' of the plume. The slight variations in TCE and cDCE isotope ratios observed in the first 1000 m probably reflect the source variability in their isotopic compositions. The isotopic compositions of TCE and cDCE near the source zone are expected to vary depending on the seasonal climatic changes. For example, a low flow season would contribute to a longer residence time of the groundwater, which would result in a longer reaction time; hence, it would give rise to more enriched 'source' TCE and cDCE isotope ratios. Therefore, isotopic variations of TCE and cDCE at the source could be reflected to their isotope ratios over distance in the upper zone since the local groundwater velocity is relatively slow at 0.24 m/d. Small amount of VC is present from the source and throughout the upper zone. Although isotope data for VC in the upper zone is scarce, the values at B20.and B23 are enriched (-12.20 and -17.62‰), suggesting the degradation of VC. Since VC can be readily degraded by aerobic oxidation (Hartmans and de Bont 1992; Bradley 2000), this degradation pathway might contribute to the enriched VC isotope ratios.

At or just below the redox transition zone where NO_3^- becomes below detection limit, typical isotopic patterns of reductive dechlorination are observed (B23 at –15.75 and –18.75 m, B28 at –18.5 m, and B34 at –12.5 m, Table 2) where isotope ratios of PCE, TCE, cDCE, and VC (if present) become progressively lighter (Bloom *et al.* 2000; Slater *et al.* 2001). This trend is indicative of the sequential reductive dechlorination of PCE to cDCE or to VC. In addition, the dominant chlorinated ethene species in the transition zone evolves with distance from PCE at B23, TCE and cDCE at B28, then finally to cDCE at B34, suggesting the influence of groundwater residence time, or the reaction time, on the progress of reductive dechlorination in the transition zone.

In the lower zone starting at 1000 m away from the source, cDCE becomes the dominant species. The isotope ratios of cDCE progressively increases toward that of the original PCE values (approximately -25.0‰), suggesting the accumulation of cDCE in the majority of the lower zone. Small levels of VC are present although the reductive dechlorination of cDCE to VC generally requires a strongly reducing

condition which is not observed in the lower zone given the presence of high SO_4^{2-} concentration. Observed VC concentrations are in general less than 1% of its precursor cDCE concentrations, suggesting that cDCE dechlorination takes place only at redox micro niches near the large clay lens where favorable redox conditions (such as methanogenic as evidenced by low levels of methane) are established. Figure 6 shows the general isotope trend observed in the lower zone along the 'core' of the plume. Both cDCE and VC isotope ratios reach that of the source PCE at approximately 1350 m from the source. The accumulation of cDCE in the majority of the plume and the further dechlorination of cDCE to VC at redox micro niches could explain the observed phenomenon. At further downgradient, the carbon isotope ratios of cDCE and VC both increase beyond that of the source PCE, and VC becomes more enriched than cDCE. The observation that the VC becomes heavier than cDCE is reported previously (Bloom *et al.* 2000), and it is expected to occur when the transformation rate of VC is greater than that of cDCE (van Breukelen *et al.* 2005). It implies that at redox micro niches, reductive dechlorination proceeds at a faster rate than in the majority of the plume.

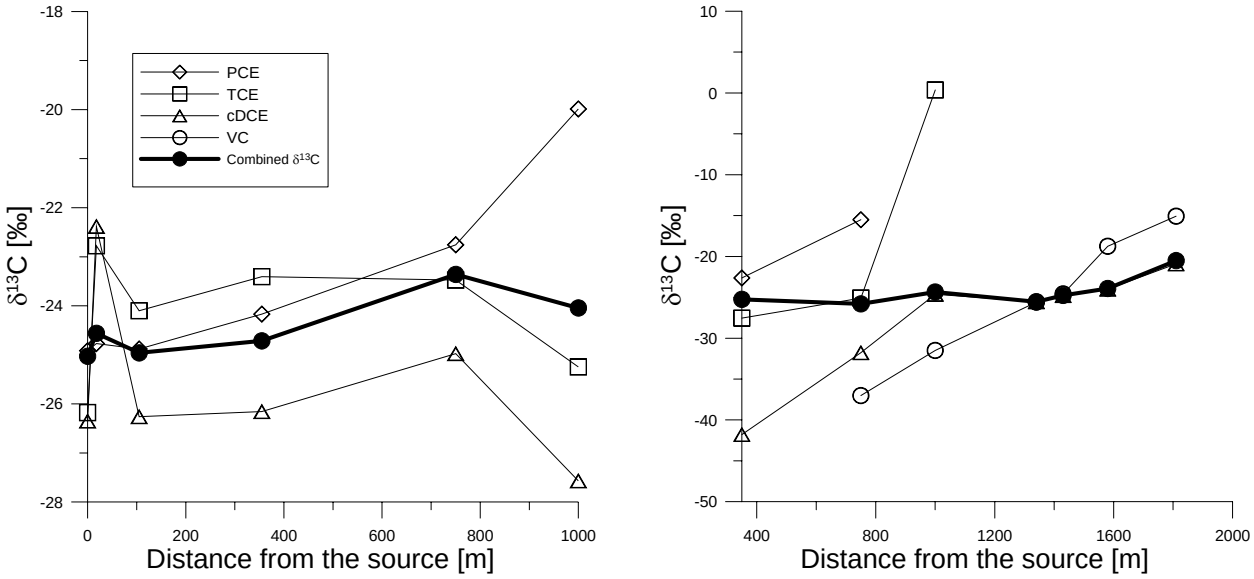

Figure 6 Isotope evolutions along the core of the plume determined by the highest observed concentrations of total chlorinated ethenes.

5.4.5 Fate of chlorinated ethenes in the lower zone

Chlorinated ethenes can be degraded by different pathways such as anaerobic oxidation and reduction mediated by iron-bearing minerals; thus, the carbon isotope data was further interpreted to deduce the possibility of such pathways at the site. During the sequential reductive dechlorination, the combined carbon isotope ratios should remain constant because the sequential dechlorination of chlorinated ethenes

does not involve with a removal of carbons from the chlorinated-ethene pool; hence, carbons in the ethene backbone are conserved. Alternative degradation pathways such as anaerobic oxidation to CO_2 and abiotic reduction to acetylene involve a loss of carbons from the pool of chlorinated ethenes. The carbon isotope balance shown in Table 2 reveals that except for wells at the plume front, the combined carbon isotope ratios remain relatively stable within the limit of analytical precision, suggesting that reductive dechlorination is the only active transformation pathway in the majority of the plume. The values at the plume front wells B61 and B64 are enriched in ^{13}C compared to the source values, which indicates either that VC is further degraded to ^{13}C depleted ethene and ethane that does not accumulate or that cDCE or VC at the plume front are degraded by other pathways. At the plume front where the combined carbon isotope ratios increase, the possibility remains that cDCE is anaerobically oxidized as it is reported to occur under Mn(IV) reducing conditions (Bradley and Chapelle 1998). In order to evaluate the fate of cDCE at the plume front, the relative isotope effect between carbon and chlorine was characterized.

5.4.6 Fate of cDCE

Reductive dechlorination of cDCE involves with a rate-determining C-Cl bond cleavage which results in a strong carbon and chlorine isotope effects (Chapter 4). To date, isotope studies on anaerobic oxidation of any of chlorinated ethenes have not been reported, but similar to aerobic oxidation of VC the electron rich double bond may be attacked in an initial step which does not involve with a C-Cl cleavage. Hence, the chlorine isotope effect from anaerobic oxidation is expected to be small compared to the carbon isotope effect, as demonstrated for aerobic VC oxidation in Chapter 4. Therefore, different isotopic patterns are expected for the reduction and oxidation of cDCE when carbon and chlorine isotope effects are compared. Several samples (B23-1, 3 4, B28-1, B34-2, B58-4 and 7, B60s, B61s and B64) were analyzed for carbon and chlorine isotope ratios of cDCE. The measured chlorine isotope values were plotted against corresponding carbon isotope values in Figure 7.

A strong and linear correlation between carbon and chlorine isotope ratios indicates that both elements are involved in the initial transformation step. The observed slope between the carbon and chlorine isotope ratios is 0.49, much higher than the slope obtained from the laboratory experiment presented in Chapter 4, which was 0.11. The difference between the obtained slope from this study and that from the laboratory study may originate from the fact that the cDCE in this study results from sequential reductive dechlorination of PCE whereas the laboratory experiment utilized manufactured cDCE. As sequential reductive dechlorination proceeds, the chlorine isotope ratio of cDCE has already become enriched, which may affect the observed chlorine isotope effect. Despite the different level of correlation between carbon and chlorine isotope effects from the laboratory study, the strong chlorine fractionation observed at the site indicates that reductive dechlorination of cDCE to VC is the likely transformation pathway of cDCE instead of the direct anaerobic oxidation of cDCE.

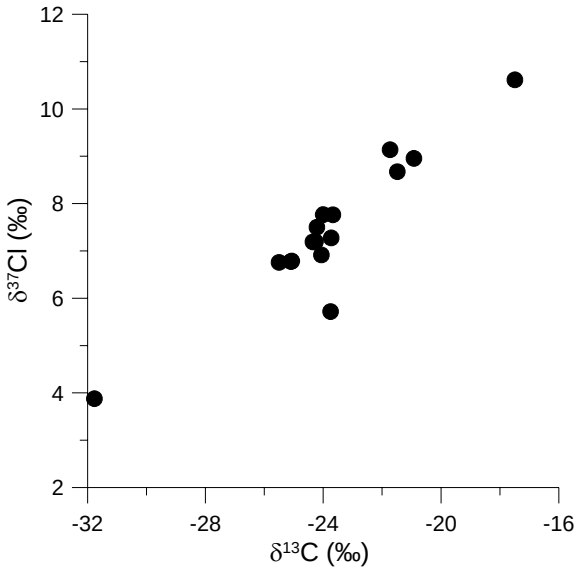

Figure 7 Correlation of chlorine and carbon isotope effect of cDCE

5.4.7 Fate of VC

Even though Figure 6 illustrates an increasing trend of VC carbon isotope ratios, the reductive dechlorination of VC in the majority of the plume is unlikely except at redox micro niches created by the presence of clay lens in the deeper part of the aquifer. The first half of increasing trend of VC isotope ratios in Figure 6, up to 1350 m where VC isotope ratio reaches –25.0‰, is probably caused by the slow transformation of cDCE over distance. As reductive dechlorination of TCE to cDCE progresses with distance, the cDCE becomes increasingly enriched in ^{13}C as observed. Increasingly enriched cDCE gives rise to the increasing carbon isotope ratios of the produced VC. On the other hand, the second half of increasing VC isotope ratios is probably due to the further reductive dechlorination of VC at redox micro niches. The VC dechlorination is indicated by the strong carbon isotope enrichment at the deep and downgradient part of the plume (B58-4, B60-1, B61s and B64). The absence of ethene and ethane might be caused by the difficulties with preserving these volatile compounds in liquid samples, or they may be quickly consumed by indigenous microorganisms. However, given the low concentrations of VC (less than 1% of cDCE), VC dechlorination does not play a significant role in reducing the contaminant mass in the lower zone.

5.4.8 Quantification of reaction rates along the plume centerline

Quantification of reaction rates from isotope data is previously reported by combining the Rayleigh equation and a first-order reaction kinetics as follows (Hunkeler *et al.* 2002; Morrill *et al.* 2005):

$$k = \frac{\frac{1000}{\varepsilon} \cdot \ln\left(\frac{R}{R_0}\right)}{t}$$

where k is the first-order reaction rate, ε is the isotope enrichment factor, R and R_0 are the isotope ratio at a location of interest and at a source respectively, t is the mean travel time defined generally by the distance traveled divided by the average groundwater flow velocity. Due to the simultaneous transformation and production of intermediate products during sequential reductive dechlorination, only the parent compound can be used to estimate the transformation rate. For this study, the transformation rate of PCE to TCE in the upper zone, and the transformation rate of cDCE to VC in the lower zone can be calculated based on the carbon isotope data. In the lower zone, cDCE precursor compounds (PCE and TCE) are completely consumed at most locations; therefore, cDCE can be considered as the parent compound to VC. The data from the 'core' of the plume (namely wells B5-3, B11-3, B16, B20 and B34-6 for the upper zone and B58-7, B60-2, B61-2, and B64 for the lower zone) were used for the rate estimation. Calculated reaction rates are presented in Table 3 assuming that the PCE source at B5-3 and the cDCE isotope values at the well B47-2 as the initial PCE and cDCE value respectively, and enrichment factors of –5.2 and –17.8‰ for PCE and cDCE, respectively (van Breukelen *et al.* 2005). The travel time t was calculated based on the distance from the respective source to a well and the estimated groundwater velocity of 0.24 m/d. The reaction rates were estimated for each well at different distance with respect to its corresponding source.

PCE transformation rate in the upper zone is the highest near to the source, but the estimated rates vary significantly with distance. The estimated cDCE transformation rates in the lower zone are in a relatively narrow range. Reductive dechlorination of both PCE and cDCE in the upper and lower zones are quite slow at the site. Other field studies report the PCE half-life ranging 0.57 to 10.00 years and cDCE half-life range of 0.76 to 11.87 years depending on sites (Wiedemeier *et al.* 1997). A newer study reported the field cDCE transformation rate of 0.1 to 1 $year^{-1}$ (Lu *et al.* 2006). The reaction rates estimated from this study based on the carbon isotope ratios are in the same order of magnitude as the reported values, but in the lower limits of reported ranges. However, all reported field estimated transformation rates are based on the chlorinated-ethene concentration decrease over distance or time and are affected by the effect of dispersion; hence, the reported values may overestimate the true transformation rates.

Table 3 Estimated first-order transformation rates for PCE and cDCE

well ID	$\delta^{13}C$	k_{PCE} *(year^{-1})*	$t_{1/2}$ *(year)*	well ID	$\delta^{13}C$	k_{cDCE} *(year^{-1})*	$t_{1/2}$ *(year)*
B5	-24.92	-		B58	-25.54	-	
B11	-24.77	0.142	4.88	B60	-24.78	0.044	16.238
B16	-24.88	0.007	117.02	B61	-24.00	0.033	21.392
B20	-24.17	0.037	19.05	B64	-20.92	0.051	13.989
B28	-22.76	0.051	13.94				
B34	-19.99	0.084	8.16				

5.5 SUMMARY AND IMPLICATIONS

The study demonstrated the effectiveness of stable carbon isotope analysis for documenting the progress of reductive dechlorination of chlorinated ethenes in a large-scale PCE contaminated site. Combined carbon isotope ratios of chlorinated ethenes were particularly valuable to indicate the possibility of alternative degradation pathways to reductive dechlorination. Combined ratios at the plume front suggested the possibility of an alternative transformation pathway of cDCE or the occurrence of complete reductive dechlorination despite the absence of final degradation product. In order to determine the fate of cDCE at the plume front, particularly the possibility of cDCE anaerobic oxidation under manganese-reducing conditions, several samples were analyzed for cDCE chlorine isotope ratios. The results revealed that cDCE became progressively enriched in ^{37}Cl at the plume front, indicating that reductive dechlorination was the likely pathway for the observed isotope fractionations. Furthermore, dechlorination rates of a parent compound (PCE) and cDCE (when precursor compounds PCE and TCE are not present simultaneously) can be estimated based on the Rayleigh-type interpretation of the carbon isotope data.

Multilevel sampling was indispensable to properly characterize the redox conditions at the site in order to identify the depth-dependent redox variations caused by the presence of pyrite in the deeper part of the aquifer. The presence of pyrite played an important role in determining the progress of reductive dechlorination of chlorinated ethenes as the occurrence of pyrite oxidation depleted the competitive electron acceptors (oxygen and nitrate) from the subsurface environment, creating conditions more favorable for reductive dechlorination. In the zone without pyrite in the upper part of the plume, reductive dechlorination stopped at TCE, and slow PCE dechlorination rates were estimated based on the PCE carbon isotope fractionation. While the presence of pyrite increased the potential for reductive dechlorination, it only proceeded to cDCE. The accumulation of cDCE was caused by insufficient electron donor availability to create more reducing conditions which would allow further reductive dechlorination as well as the possible absence of microbial community which could carry out complete reductive dechlorination. Further, reductive dechlorination to VC only occurred further downgradient close to the clay lens where electron donors were likely more abundant.

Acknowledgements

Dr. Mette Broholm provided us with the access to the site and the data from previous investigations performed at Orbicon. Concentrations of chlorinated ethenes, ethene and methane were analyzed at Danish Technical University. Simon Jeannottat sampled and analyzed the 1-L VC samples for carbon isotope ratios and the anion analysis from the sampling session which took place in September 2007. Orfan Shauakar-Stash analyzed the chlorine isotope ratios of cDCE at the University of Waterloo.

Chapter 6

Does the Rayleigh equation apply to evaluate field isotope data in contaminant hydrogeology?

Yumiko Abe and Daniel Hunkeler
Environmental Science and Technology, 40, 1588-1596, 2006

Abstract

Stable isotope data have been increasingly used to assess in-situ biodegradation of organic contaminants in groundwater. The data are usually evaluated using the Rayleigh equation to evaluate whether field data follow a Rayleigh trend, to calculate the extent of contaminant biodegradation and to estimate first order rate constants. However, the Rayleigh equation was developed for homogeneous systems while in the subsurface, contaminants can migrate at different velocities due to physical heterogeneity. This paper presents a method to quantify the systematic effect that is introduced by applying the Rayleigh equation to a field isotope data. For this purpose, the travel time distribution inherent in groundwater samples is characterized by an analytical solution to the advection-dispersion equation. The systematic effect was evaluated as a function of the magnitude of physical heterogeneity, geometry of the contaminant plume, and degree of biodegradation. Results revealed that the systematic effect always led to an underestimation of the actual values of isotope enrichment factors, the extent of biodegradation, and first-order degradation rate constants, especially in the dispersion-dominant region representing a higher degree of physical heterogeneity. A substantial systematic effect occurs especially for the quantification of first-order degradation rate constants (up to 50% underestimation of actual rate) while it is relatively small for quantification of the extent of biodegradation (<5% underestimation of actual degree of biodegradation). The magnitude of the systematic effect is in the same range as the uncertainty due to uncertainty of the analytical data, of the isotope enrichment factor and the average travel time.

6.1 INTRODUCTION

Compound-specific isotope analysis has been increasingly used to assess natural attenuation of organic compounds at contaminated sites. Isotope analysis has been used to investigate sites contaminated with BTEX compounds (Stehmeier et al. 1999; Mancini et al. 2002; Meckenstock et al. 2002; Richnow et al. 2003; Richnow et al. 2003; Griebler et al. 2004; Peter et al. 2004; Steinbach et al. 2004), methyl *tert*-butyl ether (MTBE) (Kolhatkar *et al.* 2002; Zwank *et al.* 2005), and chlorinated hydrocarbons (Sturchio *et al.* 1998; Hunkeler *et al.* 1999; Sherwood Lollar *et al.* 2001; Song *et al.* 2002; Morrill *et al.* 2005). These studies demonstrated a trend of increasing carbon (or hydrogen) isotope ratios of contaminants accompanied by decreasing concentrations because responsible microbial communities preferably consume the molecules with lighter isotopes. Physical factors such as dispersion, sorption, and evaporation are generally assumed to have an insignificant influence on the extent of isotope ratios (Meckenstock *et al.* 2004) although a recent study suggests sorption-induced isotope fractionation (Kopinke *et al.* 2005). Under certain conditions, sorption may lead to isotopic enrichment at the fringe of expanding plumes although the effect has not yet been demonstrated at the field scale (Kopinke *et al.* 2005). Isotope fractionation is usually quantified by the Rayleigh equation which relates the normalized isotope ratio and the normalized residual concentration by an isotope fractionation factor. For a number of field studies, the Rayleigh equation has been used to evaluate whether field data follow a Rayleigh trend (Kolhatkar *et al.* 2002; Griebler *et al.* 2004; Steinbach *et al.* 2004), to calculate the extent of contaminant biodegradation (Sherwood Lollar *et al.* 2001; Kolhatkar *et al.* 2002; Mancini *et al.* 2002; Meckenstock *et al.* 2002; Richnow *et al.* 2003; Richnow *et al.* 2003; Griebler *et al.* 2004; Peter *et al.* 2004; Morrill *et al.* 2005) and to estimate first order rate constants by combining the Rayleigh equation with the first order rate law (Morrill *et al.* 2005). In the first case, the goal is usually to substantiate the importance of reactive processes and not to derive field-based isotope enrichment factors for further use. Field-based isotope enrichment factors can provide some indications on the relative importance of reactive and non-reactive processes on the concentration decrease.

Although the Rayleigh equation was originally developed for homogeneous batch systems (Clark and Fritz 1997), it is increasingly applied for flow-through systems such as column and field studies (Sturchio *et al.* 1998; Hunkeler *et al.* 1999; Stehmeier *et al.* 1999; Sherwood Lollar *et al.* 2001; Kolhatkar *et al.* 2002; Mancini *et al.* 2002; Meckenstock *et al.* 2002; Song *et al.* 2002; Richnow *et al.* 2003; Richnow *et al.* 2003; Griebler *et al.* 2004; Peter *et al.* 2004; Steinbach *et al.* 2004; Morrill *et al.* 2005). In a flow through system, physical and chemical heterogeneity influences the interpretation of isotope data and is expected to lead to an underestimation of the amount of biodegradation when the Rayleigh equation is applied, as recently shown by Kopinke *et al*. 2005 (Kopinke *et al.* 2005). Due to physical heterogeneity, the travel time of contaminants between the source and a monitoring point varies depending on the flow path. In

addition, reaction rates can vary between and within different flow paths due to changes in geochemical conditions and microbial populations (hereafter referred to as chemical heterogeneity). Finally, the observed shift in isotope ratios in the bulk aqueous phase may not adequately reflect isotope fractionation at the microscale due to mass transfer limitations (Kopinke *et al.* 2005). The main aim of this study is to quantify the expected uncertainty introduced by physical heterogeneity on the estimation of isotope enrichment factors, the extent of biodegradation, and first order degradation rates from the Rayleigh-type isotope data analysis. In addition, some calculations were carried out to evaluate the effect of chemical heterogeneity.

At field sites, groundwater flow velocity varies as a function of physical heterogeneity. As a result, groundwater samples contain a mixture of contaminant molecules that have traveled at a variety of velocities between the source and a sampling point. The contaminants were thus subject to a variety of residence times and consequently underwent various degrees of biodegradation. When the resultant average concentrations and isotope ratios are used to quantify isotope enrichment factors, the extent of biodegradation and biodegradation rates, a systematic effect may be introduced because the Rayleigh equation relies on the assumption that the system is homogeneous. In this study, the following approaches were chosen to quantify this effect: (1) Contaminant concentrations and isotope ratios were simulated, taking into account travel time variations between the source and an observation point. (2) The obtained data were evaluated to estimate isotope enrichment factors, the extent of biodegradation and degradation rates using the Rayleigh equation. (3) The systematic effect was evaluated by comparing the obtained parameters with the "true" parameters used as input parameters in the calculations or with the "true" decrease in concentration derived from the calculations. An analytical approach was used to simulate concentrations and isotope ratios rather than a numerical approach because it allowed a rapid evaluation of a large number of field scenarios. The evaluated scenarios included various dispersive conditions, various degrees of biodegradation, as well as various plume geometries. The effect of chemical heterogeneity was evaluated by varying the degradation rate as a function of travel time although this approach does not cover all possible effects of chemical heterogeneity. In addition to the systematic effect, the calculated entities are also affected by uncertainty in the analytical data and uncertainty in the parameters used to calculate them. For comparison, the uncertainty due to these factors was also quantified and is denoted as random uncertainty. Finally, the systematic effect and random uncertainty associated with the application of the Rayleigh equation was estimated for a number of published field studies.

6.2 THEORY AND MODELING

6.2.1 Simulation of concentrations and isotope data

Concentrations and isotope ratios were simulated for field scenarios with various levels of physical heterogeneity using a Lagrangian approach. According to this approach, the travel time distribution is conceptualized by tagged fluid particles traveling at different velocities along separate flow paths (streamlines) of various tortuosity (Cvetkovic and Dagan 1994). Exchange of mass between streamlines and pore-scale dispersion are not considered. Thus, the spreading of a plume occurs mainly from differences in velocity at the macroscopic scale rather than at the microscopic scale (Dagan 1988). This representation of physical heterogeneity corresponds to the concept of segregated flow for non-ideal reactors in chemical engineering (Weber and DiGiano 1996; Kopinke *et al.* 2005). The Lagrangian approach has the advantage that transport and reaction can be treated separately (Cvetkovic and Dagan 1994; Finkel *et al.* 1998). Solute transport between the source and a control plain located at a distance x can be characterized by a probability density function (PDF) $g(\tau, x)$ for the travel time τ of a conservative solute, while reactions are described by a reaction function. The reaction function $\Gamma(\tau, t)$ describes the progress of a reaction with respect to the travel time τ of a tagged particle and the time t, which corresponds to the elapsed time since emplacement of the source. The normalized breakthrough curve of a reacting compound is obtained by combining the travel time PDF with the reaction function according to:

$$c(t,x) = C(t,x)/C_0 = \int_{\tau} g(\tau,x)\cdot\Gamma(\tau,t)\cdot d\tau \qquad (1)$$

In this study, an analogous approach is used to characterize transport and degradation of a compound between the source area and a monitoring well. The monitoring well is considered to sample a number of streamlines representing different travel times. In order to reproduce breakthrough curves at monitoring wells, the travel time PDF and the reaction function need to be defined. The travel time PDF can be obtained in different ways: by simulating the response of an instantaneous tracer injection using analytical (Lenda and Zuber 1970; Wexler 1992) or numerical models (Cornaton 2004) or by deriving it from stochastic properties of the hydraulic conductivity (Dagan 1989). In this study, the travel time PDF was characterized by an analytical solution to the advection-dispersion equation. This approach has the advantage that deviations from the Rayleigh-type behavior can be rapidly assessed for a wide range of various parameters. The proposed method can also be incorporated with any other travel time PDF. The 2D solution was selected for the travel time PDF because field sites are frequently equipped with fully-screened monitoring wells, which sample the average concentrations over a certain depth interval. Furthermore, tracer experiments are frequently carried out with such monitoring wells; thus, the derived dispersion coefficients represent travel time variations within a certain depth interval of the aquifer.

Finally, transverse dispersion in the vertical direction is usually considered to be relatively insignificant in comparison to dispersion in other directions (Charbeneau 2000).

The travel time PDF is given as follows (Lenda and Zuber 1970; Wexler 1992):

$$g(\tau, x, y) = \frac{x}{4\sqrt{\pi D_x \tau^3}} \cdot \exp\left[-\frac{(x - vt)^2}{4D_x \tau}\right] \cdot \left\{ erfc\left[\frac{y - w/2}{2\sqrt{D_y \tau}}\right] - erfc\left[\frac{y + w/2}{2\sqrt{D_y \tau}}\right]\right\} \quad (2)$$

where x is the longitudinal distance of a monitoring point from the source, y is the lateral distance from the center of the plume, D_x is the longitudinal dispersion coefficient, v is the average groundwater flow velocity, w is the width of the source, and D_y is the transverse dispersion coefficient. This equation is obtained by the integration of the solution for a point injection with a Dirac pulse as initial condition along the y-axes (Lenda and Zuber 1970). Biodegradation of the organic compounds is described by first-order degradation kinetics, and the reaction function is given by:

$$\Gamma(\tau, t) = e^{-k \cdot \tau} \cdot H(t - \tau) \quad (3)$$

where k is the first-order rate constant, and H is the heaviside function. In the following sections, it is assumed that t is much larger than τ, the travel time between the source and a monitoring well. In other words, the plumes are considered to be stationary. Therefore, $H(t-\tau)$ corresponds to 1, and the concentration observed at x is independent of t. It is noteworthy to point out that the integral of Equation 2 with respect to τ is smaller than 1 because of the transverse dispersion.

Substitution of Equations 2 and 3 into Equation 1 and application of the dimensionless parameters given below yields:

$$\frac{C(X_D, Y_D)}{C_0} = c(X_D, Y_D) = \int_T \frac{\sqrt{Pe \cdot X_D}}{4\sqrt{\pi \cdot T^3}} \exp\left[-\frac{Pe(X_D - T)^2}{4 \cdot T \cdot X_D} - Da \cdot T\right] \cdot \left[erfc\left(\frac{Y_D - 1}{2\sqrt{\frac{X_D \cdot T \cdot G^2}{F \cdot Pe}}}\right) - erfc\left(\frac{Y_D + 1}{2\sqrt{\frac{X_D \cdot T \cdot G^2}{F \cdot Pe}}}\right)\right] dT \quad (4)$$

with:

$$c = \frac{C}{C_0} \qquad Pe = \frac{x \cdot v}{D_x} = \frac{x}{\alpha_x} \qquad T = \frac{v \cdot \tau}{x_R} = \frac{\tau}{\bar{\tau}}$$

$$X_D = \frac{x}{x_R} \qquad Y_D = \frac{y}{w/2} \qquad G = \frac{x_R}{w/2}$$

$$Da = \frac{k \cdot x_R}{v} = k \cdot \bar{\tau} \qquad F = \frac{\alpha_x}{\alpha_y}$$

where c is the dimensionless concentration; C_0 the initial concentration; X_D the dimensionless distance from the source; Y_D the lateral dimensionless distance from the center of the plume; Pe the Peclet number; α_x the longitudinal dispersivity; α_y the transverse dispersivity; F the ratio between longitudinal and transverse dispersivities often considered to be 10 (Gelhar *et al.* 1992; Charbeneau 2000); x_R the distance of a sampling point from the source; $\overline{\tau}$ the mean travel time between the source and the sampling point at x_R ($\overline{\tau} = x_R / v$); G the location of the sampling point along the flow direction relative to the half source width; and Da is the Damköhler number. There are different definitions of the Damköhler number (Weber and DiGiano 1996; Schwarzenbach *et al.* 2003). The chosen Damköhler number relates the rate of advective transport to the rate of degradation. A large Da indictes that degradation is fast compared to transport and vice-versa. The Peclet number represents the dominance of advection over dispersion; thus, higher Pe suggests an advection-dominant flow condition and vice versa. According to the definition of Pe above, the dispersivity increases with travel distance as often observed at field sites (Domenico and Robbins 1984; Gelhar *et al.* 1992; Hess *et al.* 1992; Rajaram and Gelhar 1995) by holding Pe constant. G can be roughly seen as the plume geometry with respect to the source width, and it varies considerably (Wiedemeier *et al.* 1997; Cozzarelli *et al.* 2001; Thornton *et al.* 2001; Steinbach *et al.* 2004).

Equation 4 was numerically integrated with respect to T although an approximate solution exists (Domenico 1987). The approximate solution has been used widely in common analytical models such as BIOCHLOR (Aziz *et al.* 2000) and BIOSCREEN (Newell *et al.* 1996). The approximate solution was used to estimate the velocity of groundwater (Borden *et al.* 1997), the contaminant plume length (Tong and Rong 2002), and the first-order rate constant (Stenback *et al.* 2004). However, this solution is prone to an increased level of errors especially outside of the plume centerline in comparison to the numerically integrated solution (Guyonnet and Neville 2004). Therefore, numerical integration is used in this study. Numerical integration was carried out with Matlab using the adaptive Lobatto quadrature function. Using the integrand of Equation 4, breakthrough curves (BTC) were generated to visualize the travel time distribution of molecules arriving at the sampling point (Fig. 1). As the flow becomes dispersion dominated (smaller Pe values), the peak of the BTC shifts to earlier travel times. This trend is further enhanced as the degree of biodegradation increases (larger Da values).

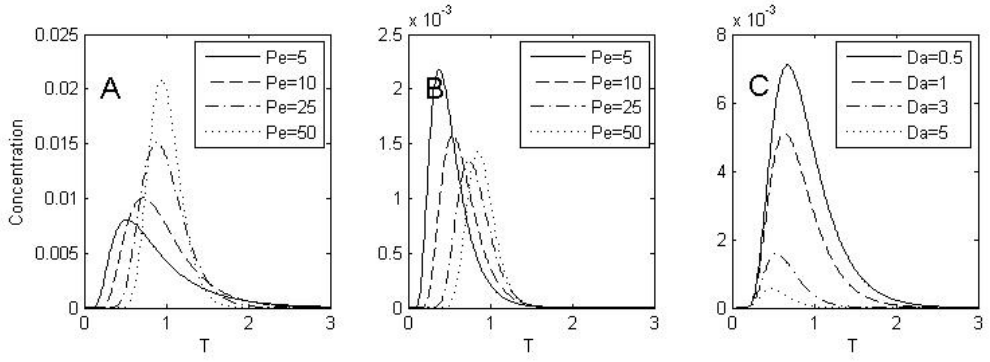

Figure 1. Simulated breakthrough curves: (A) without degradation; (B) with degradation at *Da* = 3; and (C) with various degradation rates at *Pe* = 10.

Equation 4 was used to calculate the concentration decrease between the source and a monitoring point. To obtain the isotope ratio at the monitoring point, using carbon as an example, Equation 4 was computed separately for ^{13}C and ^{12}C under identical conditions except for the Damköhler number. The Damköhler numbers for ^{13}C and ^{12}C are related by the isotope fractionation factor, α, as follows:

$$\alpha = \frac{^{13}Da}{^{12}Da} \tag{5}$$

The expected isotope ratio at a given location divided by the initial isotope ratio is given by:

$$\frac{R(X_D,Y_D)}{R_0} = \frac{C_{13}(X_D,Y_D)/C_{13,0}}{C_{12}(X_D,Y_D)/C_{12,0}} = \frac{c_{13}(X_D,Y_D)}{c_{12}(X_D,Y_D)} \tag{6}$$

This approach can be considered to represent the behavior of organic compounds that are degraded throughout the contaminant plume and not only at the fringes of the plume.

6.2.2 Evaluation of simulated data and quantification of uncertainty

Equations 4 and 6 were used to simulate changes in concentrations and isotope ratios, respectively, between the source and a monitoring point for various field scenarios. The resulting data were evaluated to derive isotope fractionation factors, the extent of biodegradation, and first-order degradation rate constants using the Rayleigh equation as described below. The obtained values were compared with the "true" values to estimate the systematic effect associated with the application of the Rayleigh equation. The deviation from the true values was evaluated as a function of variable dispersion, which reflects variable degrees of physical heterogeneity (Pe), different ratios between plume length and plume width (G), and different degrees of biodegradation (Da). The dimensionless parameters were varied as follows: (1) Pe was varied between 1-50, (2) G between 1-20 based on typical values observed at field site (see Table S1 in the Supporting Information in Appendix B), and (3) Da between 1-10. For comparison, the random

uncertainty due to uncertainties of the analytical method and the chosen isotope enrichment factor was also calculated for the extent of biodegradation B and first-order rate constant k.

6.2.2.1 Estimation of isotope enrichment factors

Although it is generally accepted that isotope enrichment factors should be determined by laboratory experiments, it can be of interest to estimate field-based isotope enrichment factors and to compare them with laboratory based values. Such a comparison can provide some insight into the overall contribution of biodegradation to the observed concentration decrease. Therefore, we evaluate the relationship between field-estimated and laboratory-derived isotope enrichment factors. To simulate the estimation of isotope enrichment factors from field data, concentrations and isotope ratios were calculated using Equations 4 and 6 for a set of 10 dimensionless distances, X_D, between 0.1 and 1 at intervals of 0.1. Unless otherwise specified, *Da* was set to 3, corresponding to 95% biodegradation between the source and the most downgradient sampling point (x_R). Based on the 10 data points, the isotope enrichment factor was estimated using the Rayleigh equation and the least square linear regression:

$$1000 \cdot \ln(\frac{R}{R_0}) = \varepsilon_{Rayleigh} \cdot \ln[f] \tag{7}$$

where $f = C/C_0$. Here f is given by $c(X_D, Y_D)$ calculated from Equation 4. The obtained isotope enrichment factor $\varepsilon_{Rayleigh}$ was compared to the "true" isotope enrichment factor ε_{true} ($\varepsilon_{true} = (\alpha\text{-}1)*1000$) where α is the original isotope fractionation factor used in Equation 5 for the simulation of isotope ratios.

6.2.2.2 Estimation of the fraction remaining or the extent of biodegradation

The fraction remaining, f, is given by:

$$f_{Rayleigh} = \left(\frac{R}{R_0}\right)^{\frac{1000}{\varepsilon_{true}}} \tag{8}$$

Instead of the fraction remaining, the result is often presented as a fraction biodegraded in percentages (Richnow *et al.* 2003):

$$B_{Rayleigh}[\%] = (1\text{-}f_{Rayleigh}) \cdot 100 \tag{9}$$

In this study, f and B were calculated based on Equations 8 and 9 with the ratio R/R_0 obtained from Equation 6, and they are denoted as $f_{Rayleigh}$ and $B_{Rayleigh}$, respectively. According to the Rayleigh equation (Eq.7), $f_{Rayleigh}$ should correspond to C/C_0. However, the concentration also decreases due to hydrodynamic dispersion; therefore, $f_{Rayleigh}$ was compared to the fraction remaining relative to the contaminant concentration that would be expected if no degradation occurs (for comparison, see Figure S1 in the Supporting Information in Appendix B):

$$f_{true} = \frac{C}{C_{dispersion}} \tag{10}$$

where C is the concentration remaining due to the effect of dispersion and degradation; and $C_{dispersion}$ is the concentration remaining in the absence of biodegradation. In this study, f_{true} was calculated by dividing Equation 4 by an analogous equation with $Da = 0$ to simulate a non-degrading conservative tracer, and B_{true} was obtained by $B_{true}=(1-f_{true})\cdot 100$. Again, the calculated $f_{Rayleigh}$ and $B_{Rayleigh}$ values are compared to their reference values, f_{true} and B_{true} to characterize the systematic effect.

The random uncertainty of B due to the uncertainties associated with R, R_0 and ε was evaluated based on Equation 8 and 9 whereby R and R_0 were assumed to have the same uncertainty linked to the analytical methods. Differentiating Equation 9 with respect to ε and R and applying the law of the propagation of uncertainty, the following expressions are obtained for the random uncertainty of B estimations:

$$\left(\frac{\partial B_{Rayleigh}}{B_{Rayleigh}}\right)^2 = \left(\frac{\exp(-Da)}{1-\exp(-Da)}\right)^2 \cdot \left[Da^2 \cdot \left(\frac{\partial \varepsilon_{true}}{\varepsilon_{true}}\right)^2 + 2 \cdot \left(\frac{1000}{\varepsilon_{true}}\right)^2 \cdot \left(\frac{\partial R}{R}\right)^2\right] \quad (11)$$

where ∂f, ∂R and $\partial\varepsilon$ are the standard deviations of the corresponding parameters. For this study, the relative uncertainty of R ($\partial R/R$) caused by measurement uncertainty was assumed to correspond to the typical analytical uncertainty of 0.03%. The $\partial\varepsilon/\varepsilon$ were assumed to vary between 10 to 50% corresponding to the typical range of the standard deviations for a compound if all published values for isotope enrichment factors are taken into account.

6.2.2.3 Estimation of first-order rate constants

First-order rate constants can be estimated from calculated isotope ratios by combining the Rayleigh equation with the first-order rate law to substitute f as $f = \exp(-k \cdot \bar{\tau})$ (Hunkeler *et al.* 1999; Morrill *et al.* 2005):

$$\ln\left(\frac{R}{R_0}\right) = -\frac{\varepsilon_{true}}{1000} \cdot k_{Rayleigh} \cdot \bar{\tau} \quad (12)$$

Accordingly, the estimated rate constant is given by:

$$k_{Rayleigh} = -\frac{\frac{1000}{\varepsilon_{true}} \cdot \ln\left(\frac{R}{R_0}\right)}{\bar{\tau}} = \frac{\ln(f)}{\bar{\tau}} \quad (13)$$

The "true" rate constant can be obtained by manipulating the definition of the Damköhler number since the Damköhler number is a function of k:

$$k_{true} = -\frac{Da}{\bar{\tau}} \quad (14)$$

The systematic effect, the ratio between estimated and true rate constant, therefore, corresponds to:

$$\frac{k_{Rayleigh}}{k_{true}} = \frac{\frac{1000}{\varepsilon_{true}} \cdot \ln\left(\frac{R}{R_0}\right)}{Da} = \frac{\ln(f)}{Da} \tag{15}$$

where R/R_0 was calculated using Equation 6.

As in the estimation of random uncertainties of f and B, the random uncertainty of k due to the uncertainties of ε, $\overline{\tau}$ and R is derived from differentiating Equation 13 and is given by:

$$\left(\frac{\partial k_{Rayleigh}}{k_{Rayleigh}}\right)^2 = \left(\frac{\partial \varepsilon_{true}}{\varepsilon_{true}}\right)^2 + \left(\frac{\partial \overline{\tau}}{\overline{\tau}}\right)^2 + 2 \cdot \left(\frac{1000}{Da \cdot \varepsilon_{true}}\right)^2 \cdot \left(\frac{\partial R}{R}\right)^2 \tag{16}$$

Similarly as for B, the relative uncertainty of R ($\partial R/R$) was assumed to correspond to 0.03% and $\partial\varepsilon/\varepsilon$ was varied between 10 and 50%. In addition, $\partial\overline{\tau} / \overline{\tau}$ was assumed to correspond to 20%.

6.3 Results and Discussion

6.3.1 Estimation of isotope enrichment factors

In Figure 2, the relationship between the isotope enrichment factor derived from the simulated data set ($\varepsilon_{Rayleigh}$) and the isotope enrichment factor used to generate the data set (ε_{true}) is illustrated in the form of type curves for various *Pe, Da* and *G*. The estimated $\varepsilon_{Rayleigh}$ always underestimates ε_{true}. As *Pe* becomes larger, or the flow becomes advection-dominant, the effect becomes smaller due to a narrower travel time PDF (Fig. 1A). Therefore, when *Pe* is large as in the column studies, the error is minimized, whereas when *Pe* is smaller as in the field studies, the effect varies significantly with the chosen dimensionless parameters. Figure 2A demonstrates that for large *Da* values, corresponding to the relatively fast degradation compared to migration, greater deviation from ε_{true} values is expected. For a large *Da*, the measured isotope ratio is dominated by molecules with a short residence time (Fig. 1C) corresponding to a relatively small shift in $\delta^{13}C$. Accordingly, the calculated $\varepsilon_{Rayleigh}$ is smaller than ε_{true}. The $\varepsilon_{Rayleigh}/\varepsilon_{true}$ ratio is also sensitive to *G* (Fig. 2B). Larger *G* corresponds to a longer plume relative to the source width. The longer the plume, the more the concentrations are diminished due to transverse dispersion in addition to biodegradation; therefore, the underestimation of ε is enhanced with increasing *G*. For a typical *Pe* of 10 and typical ratios of plumes lengths to source widths of up to 20, $\varepsilon_{Rayleigh}$ is expected to be as much as 50% smaller than ε_{true}

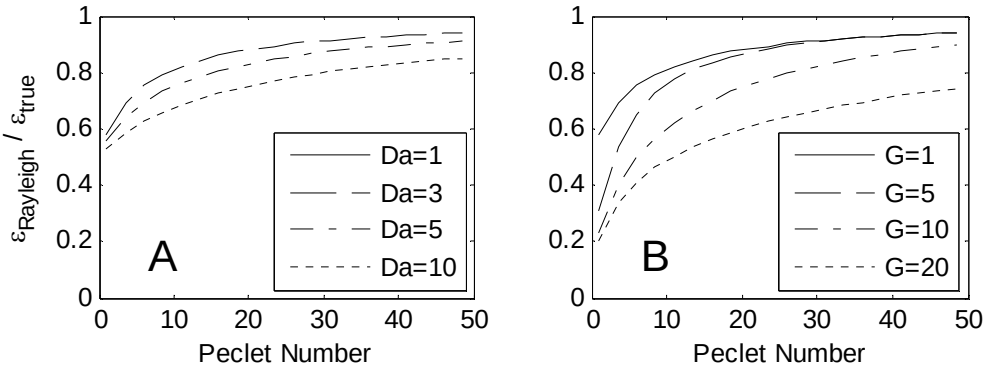

Figure 2 Type curves for the systematic effect (expressed as $\varepsilon_{Rayleigh}/\varepsilon_{true}$) associated with estimating isotope enrichment factors: (A) assuming *G* = 1 and 4 different *Da* values ; and (B) assuming *Da* = 3 and 4 different *G* values.

The magnitude of the systematic effect associated with the ε calculation was estimated for a published MTBE field study (Kolhatkar *et al.* 2002; Kuder *et al.* 2005). Because the study reported laboratory ε value derived from microcosms with site material, the model-predicted underestimation of ε can be compared to the actual underestimation of ε. To calculate the systematic effect, dimensionless parameters, *Pe*, *G* and *Da*, were estimated based on site specific data. *Pe* was assumed to correspond to a typical value of 10. G was estimated based on the location of the most downgradient well for two source widths of 10 and 20 m because the actual source width was unknown. *Da* was estimated to be 2.4 based on the $\delta^{13}C$ of the most downgradient well and the corresponding isotope enrichment factors from the laboratory. The ratio $\varepsilon_{Rayleigh}/\varepsilon_{true}$ was calculated as described in the method section except that X_D values were selected according to the locations of the sampling wells. According to these calculations, the ratio $\varepsilon_{Rayleigh}/\varepsilon_{true}$ corresponds to 0.55-0.59 (Table 1). This corresponds well to the ratio between field- and laboratory-based isotope enrichment factors, $\varepsilon_{field}/\varepsilon_{lab}$, which was 0.62. The good agreement between estimated and actually observed ratios suggests that the factors incorporated into our approach (travel time distribution and hydrodynamic dispersion) are responsible for the underestimation of ε based on field isotope data.

Table 1. Systematic effect of isotope enrichment factor derived from field data expressed as $\varepsilon_{Rayleigh}/\varepsilon_{true}$ and comparison with $\varepsilon_{field}/\varepsilon_{lab}$

	MTBE
ε_{field} [‰]	-8.1
ε_{lab} [‰]	-13±1.1
	(Kuder et al. 2005)
$\varepsilon_{field}/\varepsilon_{lab}$	0.62
$\varepsilon_{Rayleigh}/\varepsilon_{true}$	0.55 (w=10m)
	0.59 (w=20m)

6.3.2 Estimation of the extent of biodegradation

The expected systematic effect associated with assessing the extent of biodegradation, B, from field isotope data is illustrated in Figure 3. As in the estimation of ε, isotope data lead to the underestimation of the actual *B*, particularly under dispersion-dominant flow conditions (low *Pe* region). The systematic effect for estimating *B* is smaller than the *ε* estimation, and it is independent of *G* values (Figure 3B). These observations can be explained by the fact that dilution due to transverse dispersion hardly affects isotope ratios, but strongly affects concentrations.

For groundwater risk assessment, the fraction of contamination remaining after a certain distance is often of key interest, which corresponds to *f* (Einarson and Mackay 2001). The calculated $f_{Rayleigh}$ can be up to 5 times larger than the actual f_{true} for *Pe*=10 and *G* up to 20 (see Figure 2S in the Supporting Information in Appendix B). However, a systematic effect of *f* by a factor of up to 5 remains quite small compared to the decrease in concentrations which is often several orders of magnitude. The different behavior of systematic effect of *f* , compared to B, is expected because *f* approaches 0 as the degree of degradation increases while *B* approaches 1. As a result, the systematic effect on *f* increases with increasing *Da*, while the systematic effect on *B* becomes small.

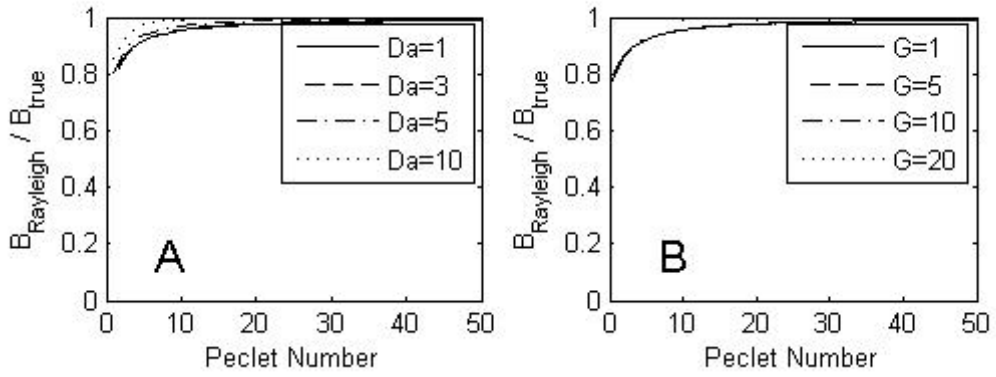

Figure 3. Type curves for the systematic effect (expressed as $B_{Rayleigh}/B_{true}$) associated with estimating the extent of biodegradation: (A) assuming *G* = 1 with 4 different *Da* values and (B) assuming *Da* = 3 with 4 different *G* values.

The degree of random uncertainty associated with estimating *B* is plotted in Figure 4 as a function of *Da* for two different isotope enrichment factors. Similar to the systematic effect discussed above, the random uncertainty of *B* decreases as a function of *Da*, as previously observed (Morasch *et al.* 2004). For *Da*<5, the uncertainty of *B* is slightly smaller for the smaller isotope enrichment factor and increases with increasing uncertainty of *ε*. For small *Da* corresponding to small shifts in isotope ratios, the random uncertainty is dominated by the uncertainty on the isotope analysis (*∂R/R*), while for larger *Da*, the contribution of the uncertainty associated with the isotope enrichment factor dominates (Fig. 4C).

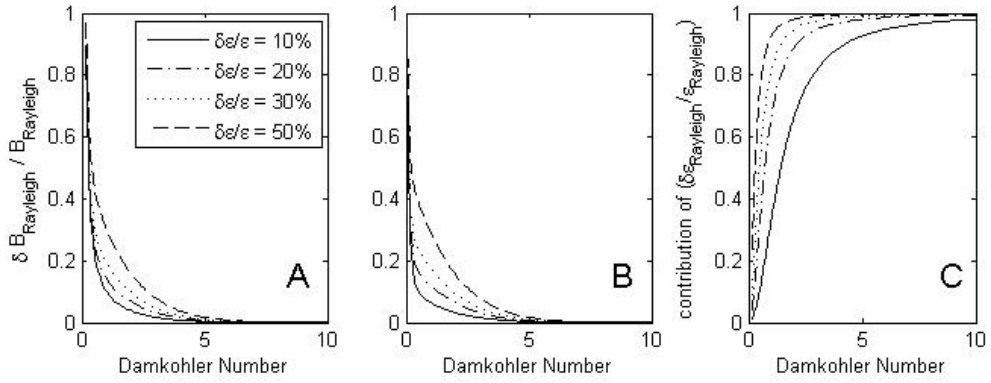

Figure 4. Random uncertainty of extent of biodegradation ($\delta B/B$) for ε_{true} = 3‰ (A) and ε_{true} = 10‰ (B) and contribution of the uncertainty of ε ($\delta\ \varepsilon_{true} / \varepsilon_{true}$) to the overall random uncertainty (C). $\delta R/R$ held constant at 0.03%,

For several published field sites, $B_{Rayleigh}$ values as well as the expected systematic effect and random uncertainty associated with them were calculated (Kolhatkar *et al.* 2002; Richnow *et al.* 2003; Griebler *et al.* 2004). The first example is the MTBE site which was mentioned in the previous section, the second example a BTEX/PAH contaminated site (Böckelmann *et al.* 2001; Herfort and Ptak 2002; Böckelmann *et al.* 2003; Griebler *et al.* 2004), and the third a landfill site where mixed contamination was observed (Kjeldsen 1993; Richnow *et al.* 2003). The estimation of $B_{Rayleigh}/B_{true}$ ratio was performed for the monitoring well furthest from the source area based on the dimensionless parameters *Pe, Da* and *G* (Table 2). The random uncertainties of $B_{Rayleigh}$ were quantified as described in the method section (Equations 11 and 12) using the parameters given in Table 2. It was assumed that $\partial R/R$ corresponds to 0.03% and the uncertainty of ε was estimated for each compound separately based on laboratory ε values (Table 2). *m/p*-Xylene was not included because of the lack of sufficient ε values to calculate the standard deviation ($\partial\varepsilon$). Calculated $B_{Rayleigh}/B_{true}$ ratios and $\partial B/B$ are listed in Table 2.

The calculated $B_{Rayleigh}/B_{true}$ ratios indicate that the extent of biodegradation was underestimated by 2 to 10% for the considered sites and compounds (Table 2). The smallest systematic effect was observed for *o*-xylene, which showed the highest level of biodegradation. The random uncertainty ($\partial B/B$) was in the same range as the systematic effect except for benzene, which had a relative random uncertainty of 35%. The smallest random uncertainties (MTBE and *o*-xylene) occurred when either the uncertainty of the isotope enrichment factor, $\partial\varepsilon/\varepsilon$, was very small (MTBE) or *Da* was large (o-xylene), resulting in a very small fraction of contaminant remaining. The large random uncertainty of benzene was due to the small *Da* and the relatively large uncertainty of ε. In summary, the calculations for the field sites and the general evaluations (Fig. 3 and 4) indicate that for $Da<3$, the random uncertainty may frequently be more

important than the systematic effect for a typical *Pe* of 10, unless the uncertainty of ε is very small. For larger *Da*, both the systematic effect and random uncertainty are expected to be small.

Table 2. Estimations of the systematic effect and random uncertainty associated with the Rayleigh-type evaluation of field isotope data

	MTBE site[1) 4)]	BTEX/PAH site [5)]				Landfill site [6)]
	MTBE	Benzene	Toluene	*o*-Xylene	*m/p*-Xylene	*m/p*-Xylene
v [m/d]	0.26	2	2	2	2	0.5
w [m]	10 & 20	120	120	120	120	270
x_R [m]	23.5	105	105	105	105	47
G	4.7 & 2.4	1.8	1.8	1.8	1.8	0.35
Pe at x_R	10	8.3[2)]	8.3[2)]	8.3[2)]	8.3[2)]	10
$\partial\delta\varepsilon/\varepsilon$ [3)]	0.085	0.29	0.41	0.62		
Da at x_R	2.40	0.50	2.34	5.31	2.18	3.12
$\boldsymbol{B_{Rayleigh}}$ **[%]**	**91.1**	**39.5**	**90.4**	**99.5**	**88.7**	**95.6**
$\boldsymbol{B_{Rayleigh}/B_{true}}$	**0.9**	**0.97**	**0.94**	**0.98**	**0.94**	**0.95**
$\boldsymbol{\partial B_{Rayleigh}/B_{Rayleigh}}$	**0.02**	**0.35**	**0.11**	**0.02**		
$\boldsymbol{k_{Rayleigh}}$ **[d^{-1}]**	**0.0027**	**0.0099**	**0.046**	**0.104**	**0.029**	**0.023**
$\boldsymbol{k_{Rayleigh}/k_{true}}$	**0.71**	**0.88**	**0.68**	**0.53**	**0.70**	**0.67**
$\boldsymbol{\partial k_{Rayleigh}/k_{Rayleigh}}$	**0.22**	**0.50**	**0.47**	**0.66**		

Values in bold are the simulation results.
1) The calculation was carried out for two source widths. However, only one average result is reported because the calculation is not sensitive to the source width (Fig. 3B and 5B)
2) Calculated based on results of tracer tests reported in reference 49. For other sites a typical Pe of 10 was used.
3) Standard deviation calculated based on all values given in quoted references (MTBE: Kuder *et al.* 2005, Benzene: Mancini *et al.* 2003, Toluene: Meckenstock *et al.* 1999 and Morasch *et al*. 2001, and o-xylene: Richnow *et al.* 2003 and Morasch *et al.* 2004)
4) Kolhatkar *et al.* 2002
5) Gribler *et at.* 2004
6) Richnow *et al.* 2003

6.3.3 Estimation of first-order reaction rate constants

The systematic effect associated with the calculation of field-derived first-order rate constants is illustrated in Figure 5. The systematic effect on $k_{Rayleigh}$ depends significantly on *Da*, and is rather independent of *G* as in the case for the $B_{Rayleigh}$ estimation. As *Pe* increases, the effect decreases, but at the typical flow condition of *Pe* = 10, a significant amount of systematic effect is involved (Figure 5A). The systematic effect on $k_{Rayleigh}$ is much larger than that on $B_{Rayleigh}$ and increases with increasing *Da*. The different behaviors in terms of expected systematic effect on $B_{Rayleigh}$ and $k_{Rayleigh}$ estimations arise from the fact that the $k_{Rayleigh}$ calculation is based on $f_{Rayleigh}$ (see Equation 13). As discussed above, the systematic effect on $f_{Rayleigh}$ is larger than on $B_{Rayleigh}$. Furthermore, as *Da* increases, the systematic effect on $B_{Rayleigh}$ is diminished (Fig. 3) because $B_{Rayleigh}$ approaches 1 while it increases for $f_{Rayleigh}$ because $f_{Rayleigh}$ approaches 0 (Supporting information Figure S2 in Appendix B).

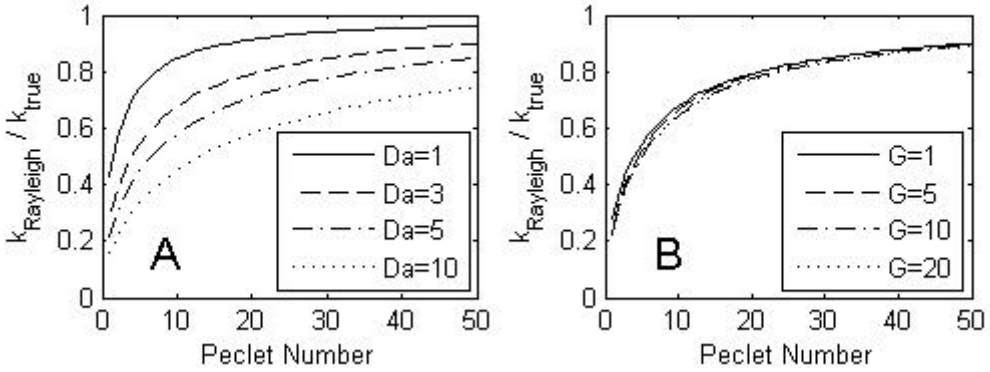

Figure 5. Type curves for the systematic effect (expressed as $k_{Rayleigh}/k_{true}$) associated with estimating the first-order reaction rate constant: (A) assuming G = 1 and 4 different Da values and (B) assuming Da = 3 and four different G values.

The random uncertainty associated with estimating $k_{Rayleigh}$ is depicted in Figure 6 in terms of a series of $\partial\varepsilon/\varepsilon$ values for two different ε values as well as the expected contribution of $\partial\varepsilon/\varepsilon$ to the random uncertainty, $\partial k/k$. For a small Da, the systematic effect is large and is dominated by the $\partial R/R$. For a larger Da, $\partial k/k$ stabilizes to a certain value depending on $\partial\varepsilon/\varepsilon$ and $\partial\overline{\tau}/\overline{\tau}$, which contribute equally to $\partial k/k$ (Equation 16).

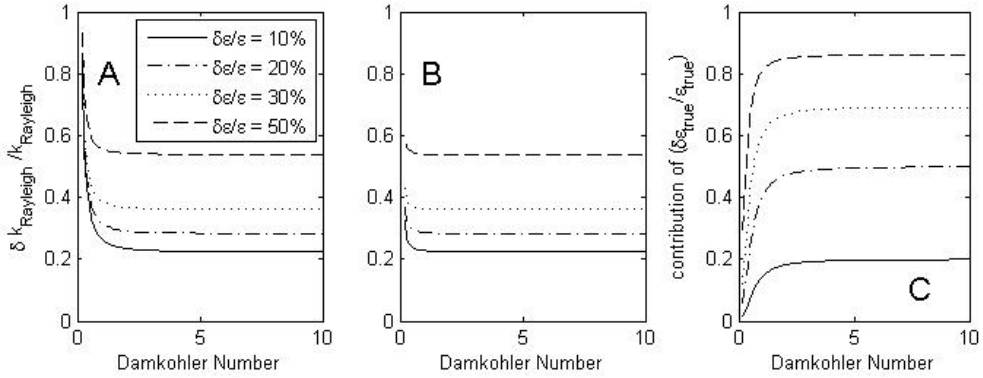

Figure 6. Random uncertainty of the estimation of first-order rate constants ($\partial k/k$) for ε_{true} = 3‰ (A) and ε_{true} = 10‰ (B) and contribution of the uncertainty of ε_{true} ($\partial\varepsilon_{true}/\varepsilon_{true}$) to the overall random uncertainty (C). $\partial R/R$ held constant at 0.03%, *and* $\delta\overline{\tau}/\overline{\tau}$ at 20%.

For the previously mentioned field studies (Kolhatkar *et al.* 2002; Richnow *et al.* 2003; Griebler *et al.* 2004), the systematic effect and random uncertainty of $k_{Rayleigh}$ were quantified for the most downgradient wells (Table 2). In addition, the $k_{Rayleigh}$ values were calculated using Equation 13 where R and R_0 were calculated from the measured isotope ratios. The systematic effect was estimated using Equation 15, and the random uncertainty using Equation 16. The random uncertainty depends on $\delta\overline{\tau}/\overline{\tau}$ as much as it does

on $\delta\varepsilon$ /ε, but $\delta\overline{\tau}$ / $\overline{\tau}$ is difficult to estimate. In the calculation, an uncertainty of 20% was assumed for $\delta\overline{\tau}$ / $\overline{\tau}$. The $k_{Rayleigh}/k_{true}$ ratio suggests an underestimation of $k_{Rayleigh}$ of up to 47%. The random uncertainty on the *k* estimation is rather large, particularly for the BTEX/PAH site and reaches up to 66%. In contrast to $B_{Rayleigh}$, the random uncertainty is the largest for the compound with the largest *Da*. For larger uncertainty in average travel time ($\overline{\tau}$), the uncertainty will be even larger.

6.3.4 Effect of chemical heterogeneity

In addition to the effect of physical heterogeneity, the Rayleigh-type data interpretation is expected to be affected by variations of degradation rates between and along flow paths that are sampled. While there are a number of detailed studies about spatial variations of redox conditions within a plume (Borden *et al.* 1997; Christensen *et al.* 2000; Christensen *et al.* 2001; Cozzarelli *et al.* 2001), less is known about the spatial variation of degradation rates of organic compounds. Some studies have indicated that degradation rates are lower in low permeability zones (Aelion 1996; Cozzarelli *et al.* 2001). In this case, degradation rates would be related to travel time with faster flow paths showing higher rates. To simulate the effect of such a relationship on the systematic effect of *B*, the Damköhler number was linearly varied as a function of travel time with decreasing *Da* for increasing *T*. The total amount of biodegradation between the source and a sampling point was kept constant and corresponded to *Da*=3 (see Figure S3 in the Supporting Information in Appendix B). The slope of the Da curve *s* was varied between -0.3 and -1.2. The different scenarios correspond to a decrease of 10, 20 or 40% of the degradation rate if the travel time is doubled from one T to two T. The systematic effect decreases with increasing slope *s* (Table 3). As discussed above, the systematic effect for *B* is due to the fact that molecules with a short travel time, thus a small shift in $\delta^{13}C$, are overrepresented in the sample. If the degradation rate is higher for faster flow paths, this overrepresentation is diminished, consequently the systematic effect is smaller. If the relationship between degradation rate and travel time is inverse, the systematic effect increases (data not shown). In this case, the sample is dominated by molecules from fast flow paths with hardly any degradation and hardly any shift in $\delta^{13}C$. If the representative parameters for chemical heterogeneity, such as a degradation rate are not correlated with travel time, the error could lead to an increase or decrease depending on the scenario considered, and the exact effect from such chemical heterogeneity is difficult to quantify.

Table 3. Effect of simulated chemical heterogeneity on $B_{Rayleigh}/B_{true}$ [a].

s	$B_{Rayleigh}/B_{true}$
0	0.954
-0.3	0.954
-0.6	0.958
-1.2	0.979

[a] *s* corresponds to the rate at which *Da* decreases with increasing dimensionless travel time T

6.4 SUMMARY AND IMPLICATIONS

Presented type curves (Figures 2, 3, and 5) for systematic effects represent a large range of possible field scenarios; thus, they can serve as a reference to quickly estimate the degree of systematic effect associated with a site of interest. As expected, the Rayleigh-based approach to estimate the extent of biodegradation or first-order rate constants leads to a systematic underestimation of the actual value due to the fact that it does not accommodate the subsurface physical heterogeneity. As the degree of physical heterogeneity decreases (represented by advection dominant flow regime, or high Peclet numbers), the systematic effect decreases significantly. For a typical *Pe* of 10 and typical values for plume lengths (G<20) and degree of degradation (Da<10), the systematic effect on the extent of biodegradation is < 5%. This indicates that the isotope method for quantification of biodegradation is quite robust. This conclusion is consistent with several field studies that indicated that the predicted degree of biodegradation corresponds well to the concentration decrease (Richnow *et al.* 2003; Griebler *et al.* 2004). A larger systematic effect is expected for first order biodegradation rates (up to 50%). However, other methods for estimation of field degradation rates that are based on concentration data likely yield much larger errors. For example Stenback *et al.* (2004) (Stenback *et al.* 2004) demonstrated that rates calculated based on concentration data can vary by a factor of 3, depending on the chosen dispersion coefficients. The estimated systematic effect may be larger for certain scenarios of chemical heterogeneity (e.g., increasing degradation rates for increasing residence time). In addition, it has to be kept in mind that the evaluation relies on Fickian dispersion which may not be exactly met at field sites. Often, the tailing of breakthrough curves is more pronounced than expected based on Fickian dispersion (Dagan 1988; Garabedian *et al.* 1991; LeBlanc *et al.* 1991; Gelhar *et al.* 1992; Hess *et al.* 1992), accordingly the systematic effect would be somewhat larger than expected. However, the proposed method to estimate systematic effect associated with the application of the Rayleigh equation to heterogeneous field sites can be applied for any kind of travel time PDF as long as the corresponding breakthrough curve are given.

LIST OF SYMBOLS

α	[-]	Isotope fractionation factor
α_x	[L]	Longitudinal dispersivity
α_y	[L]	Transverse dispersivity
B	[%]	Fraction of biodegradation
B_{true}	[%]	"True" fraction of biodegradation
$B_{Rayleigh}$		Fraction of biodegradation estimated based on isotope data using laboratory derived "true" isotope enrichment factor
C	[M/L^3]	Concentration
C_0	[M/L^3]	Initial concentration
c	[-]	Dimensionless concentration
Da	[-]	Damköhler number
D_x	[L^2/T]	Longitudinal dispersion coefficient
D_y	[L^2/T]	Transverse dispersion coefficient
ε	[‰]	Isotope enrichment factor
ε_{true}	[‰]	"True" isotope enrichment factor derived from laboratory experiment
$\varepsilon_{Rayleigh}$	[‰]	Isotope enrichment factor estimated from field data
f	[%]	Fraction remaining
F	[-]	Ratio of longitudinal to transverse dispersivities
g	[-]	Travel time PDF
Γ	[-]	Reaction function
G	[-]	Distance of sampling point relative to source half-width
k	[T^{-1}]	First-order rate constant
k_{true}	[T^{-1}]	"true" first order rate constant (used to simulate data)
$k_{Rayleigh}$	[T^{-1}]	First order rate constant estimated based on isotope data using laboratory derived "true" isotope enrichment factor
Pe	[-]	Peclet number
R	[-]	Isotope ratio
R_0	[-]	Initial isotope ratio
t	[T]	Elapsed time since the source emplacement
τ	[T]	Travel time
$\overline{\tau}$	[T]	Mean travel time
T	[-]	Dimensionless travel time
v	[L/T]	groundwater flow velocity
w	[L]	Width of the source
x	[L]	Distance from source in flow direction
X_D	[-]	Dimensionless distance from source
x_R	[L]	Distance of sampling point from source
y	[L]	Lateral distance from center of plume
Y_D	[-]	Dimensionless lateral distance

Chapter 7

Quantification of reductive dechlorination rates using the field concentration and carbon isotope data

Abstract

The study aims at the quantification of transformation rates of chlorinated ethenes based on the field carbon isotope ratio and concentration data from a PCE contaminated site. The quantification approach was based on the analytical solutions for consecutive reactions. Summed molar concentrations of chlorinated ethenes were considered as a quasi-conservative tracer to improve the reliability of the analytical flow and transport models. Carbon isotope ratios of chlorinated ethenes were not only used to quantify transformation rates, but also to justify the use of the summed concentrations of chlorinated ethenes as intrinsic tracer concentrations. The combined carbon isotope ratios of chlorinated ethenes at the site did not change significantly for 1.5 km of plume migration, implying that the carbons in the ethene backbone of chlorinated ethenes were preserved during the migration. Thus, reductive dechlorination was the only transformation pathway for chlorinated ethenes. A 3D analytical transport model was used to calibrate the transport parameters (dispersivities and the size of the source zone) to the tracer data. Based on the calibrated transport model, the reactive-isotope model was simulated to quantify the transformation rates of all chlorinated ethenes. The rate quantification based on the field isotope and concentration observations were carried out separately and compared. The results suggest that concentration-based quantification method tends to yield greater transformation rates than the isotope-based method especially when the contaminant concentrations are low. However, the difference between the two methods is relatively small by the factor of four, suggesting that once effective flow and transport parameters are derived from simulating a tracer, relatively stable transformation rates can be obtained regardless of the method employed. Parameter sensitivity analyses revealed that the variation in groundwater velocity is directly reflected to the quantified transformation rate; thus, it plays a significant role in quantifying the rate. The source dimension does not affect the isotope-based rate quantification method as long as the observation points are along the plume core aligned to the plume centerline.

Abe, Y. and Hunkeler, D.

To be submitted to Ground Water

7.1 INTRODUCTION

At some contaminated sites it may be possible to let natural processes restore the affected soil and groundwater. The process is termed natural attenuation. The decision to accept natural attenuation as a remedial strategy depends on the local land and groundwater use and the influence of contamination on the surrounding environment and human health (Rügner *et al.* 2006). When considering natural attenuation as a remediation strategy, the feasibility and efficiency of the remedial process at a contaminated site need to be investigated. Such investigations often utilize groundwater models to draw a general conclusion on the contaminant plume behavior over distance and time (Lu *et al.* 1999; Clement *et al.* 2000; Brauner and Widdowson 2001; Schafer 2001). Predictive models to estimate the contaminant mass reduction over time due to natural attenuation and the restoration time period require *in situ* contaminant degradation rates. Therefore, reliable estimation of *in situ* degradation rates becomes critical for investigating the current and future progress of natural attenuation (Buscheck and Alcantar 1995; Borden *et al.* 1997).

In general, the rate of natural attenuation is quantified by a first-order reaction kinetics as more complex reaction kinetics models require the simultaneous estimation of multiple kinetic parameters from the limited field measurements, which increases the parameter uncertainties. Several concentration-based methods are used to estimate *in situ* degradation rates such as mass balance calculations between plume transects (Borden *et al.* 1997; Kao and Wang 2001), plume-centerline methods (Chapelle *et al.* 1996; Wiedemeier *et al.* 1997), single-well push-pull tests (Istok *et al.* 1997) and a field injection test (Rügge *et al.* 1999). Plume-centerline methods are most frequently used due to their easy implementation with the available field concentration data, and they often rely on analytical solutions for the advection-dispersion-reaction equation and incorporate longitudinal dispersion (Buscheck and Alcantar 1995; Chapelle *et al.* 1996) as well as transversal (Stenback *et al.* 2004) and vertical dispersions (Zhang and Heathcote 2003). Detailed numerical investigation to study the reliability of degradation rates estimated from these analytical methods reveals that they all tend to overestimate the true rates (Beyer *et al.* 2007). In addition to the concentration-based methods, compound-specific isotope analysis of a contaminant can also estimate the *in situ* degradation rate based on the Rayleigh isotope fractionation model (Hunkeler *et al.* 2002; Morrill *et al.* 2005). The effect of dispersion and sorption does not give rise to the observed isotope fractionation when the plume is at a steady state; thus, the reaction rate estimated based on the isotope approach is considered to be independent of these physical dilution and retardation effects. However, the interpretation of field isotope data based on the Rayleigh isotope fractionation model tend to underestimate the degradation rates because the Rayleigh model assumes a homogeneous and well-mixed system with a uniform contaminant residence time distribution (Kopinke *et al.* 2005; Abe and Hunkeler

2006). However, with the appropriate knowledge of field flow conditions, the degree of overestimation can be corrected (Abe and Hunkeler 2006).

Above-mentioned methods to estimate degradation rates are applicable for bimolecular reactions and not directly applicable for consecutive reactions such as reductive dechlorination of chlorinated ethenes. With the typical estimation methods, only the degradation rate of a parent compound can be estimated due to the simultaneous transformation and production of reaction intermediates, which result in a complex concentration evolution during the course of consecutive reactions. Therefore, the estimation of *in situ* degradation rates for reaction intermediates during sequential reductive dechlorination is cumbersome and often performed with a 1D, 2D and 3D analytical solution (van Genuchten 1985; Lunn *et al.* 1996; Sun *et al.* 1999) as implemented in BIOCHLOR (Aziz *et al.* 2000) or with numerical reactive transport models (Clement *et al.* 2000; van Breukelen *et al.* 2005; Ling and Rifai 2007). Furthermore, regardless of the nature of degradation reaction, these rate-estimation methods are based on transport parameters (particularly the dispersion coefficients) which ideally should be derived based on the concentration data of a non-reactive tracer released from the contaminant source zone. The lack of such tracer data greatly increases the uncertainties associated with flow and transport model parameter estimations.

Chlorinated ethenes such as tetrachloroethene (PCE) and trichloroethene (TCE) are among the most frequently detected groundwater contaminants (Squillace *et al.* 1999; Moran *et al.* 2007), but studies on estimating their *in situ* degradation rates based on analytical or numerical simulations are relatively scarce (Clement *et al.* 2000; Ling and Rifai 2007). It is partly because of the mathematical complexity mentioned above, but also because the produced intermediates can be degraded by various pathways under different redox conditions; thus, the identification of the active *in situ* degradation pathway itself is difficult (Wiedemeier *et al.* 1997; Bradley 2000). Under anaerobic conditions, reductive dechlorination can take place. PCE and TCE are readily transformed to dichloroethenes (DCE); however, further transformation to vinyl chloride (VC), and to ethene requires the site to be strongly reducing such as sulfate-reducing and methanogenic conditions (Vogel and McCarty 1985; Wiedemeier *et al.* 1997). In addition to reductive dechlorination, TCE, DCE and VC can be metabolically or cometabolically degraded to CO_2 by oxidative reactions under anaerobic and aerobic conditions (Hartmans *et al.* 1985; Nelson *et al.* 1987; Bradley 2000). Under methanogenic conditions, VC can be degraded to CH_4 and CO_2 (Bradley and Chapelle 2000). Moreover, abiotic reduction coupled to the oxidation of iron-bearing minerals such as pyrite leads to the formation of acetylene for PCE, TCE, and cDCE and ethene for VC (Lee and Batchelor 2002).

Objectives of the present study were to investigate the use of carbon isotope analysis of chlorinated ethenes quantify *in situ* transformation rates and to justify the use of the summed concentrations of chlorinated ethenes as quasi-conservative tracer concentrations to calibrate the transport model. In addition, based on the calibrated transport model, transformation rates of chlorinated ethenes were

quantified using the field isotope and concentration data for comparison. Obtained transformation rates were compared with the rates estimated by the plume-centerline method (Buscheck and Alcantar 1995), the Rayleigh-based isotope method for the parent compounds (Morrill *et al.* 2005), as well as a 1D numerical method to simulate the carbon isotope fractionation of chlorinated ethenes (van Breukelen *et al.* 2005). The premise for the use of summed concentrations of chlorinated ethenes as a quasi-conservative tracer is that during the course of reductive dechlorination of chlorinated ethenes, none of the carbon atoms in the ethene backbone are lost from the pool of chlorinated ethenes and ethene. Therefore, the combined carbon isotope ratios of chlorinated ethenes and ethene remain constant over distance if reductive dechlorination is the only transformation process. The variation in total carbon isotope ratios over distance indicates that carbon is lost from the pool; thus, other processes such as oxidative degradation is involved in the observed isotope fractionation and concentration decreases. Hence, as long as the total carbon isotope ratios remain constant, the summed molar concentrations of chlorinated ethenes (and ethene if present) can be treated as a 'tracer' to calibrate transport models. The study is based on the field observation at a PCE contaminated site where multi-level sampling wells were installed along the plume centerline. The approach is based on a three-dimensional analytical solution with numerical integration (Sager 1982; Wexler 1992), and the solution is modified to accommodate sequential reductive dechlorination (Sun *et al.* 1999).

7.2 SITE DESCRIPTION

The study site is located in the city of Rødekro in the southern Jütland, Denmark. The PCE contamination originates from a regional dry-cleaning facility which operated from 1967 to 1980. The PCE source is localized as it resulted from leakage from underground storage tanks. The plume extends approximately 2 km, suggesting a relatively low level of degradation activities. Based on the intensive network of 150 multilevel monitoring wells in 55 locations, the contaminant plume is delineated and the migration pattern of the plume is well characterized. The unconfined aquifer consists mainly of relatively homogeneous fluvio-glacial sand with occasional presence of gravel, silt and clay lenses (Figure 1). The local hydraulic gradient was estimated to be 0.0013 m/m throughout the study area. According to a pumping test, the local hydraulic conductivity was estimated to be 6.5×10^{-4} m/s (55 m/d), and the groundwater velocity was estimated to be approximately 0.24 m/d assuming a porosity of 0.3.

The plume can be roughly divided into two distinctive redox zones as a function of depth depending the presence (upper) and the absence (lower) of nitrate in the groundwater (Figure 1). The depth dependency of nitrate concentrations arises from the suspected presence of pyrite in the aquifer sediment (Postma *et al.* 1991). Pyrite oxidation coupled to the nitrate reduction in the lower zone deprives nitrate, which is a better electron acceptor than chlorinated ethenes. In the upper zone PCE can partially undergo

reductive dechlorination even with the presence of nitrate although the reductive dechlorination of PCE seems to occur slowly as suggested by relatively small PCE isotope fractionation (Table 1 and Figure 2-A). In contrast, in the lower zone the absence of nitrate creates a condition which enhances the progress of reductive dechlorination as indicated by strong isotope fractionation of chlorinated ethenes. Consequently, the progress of reductive dechlorination was significantly different between the upper and the lower zones (Chapter 6).

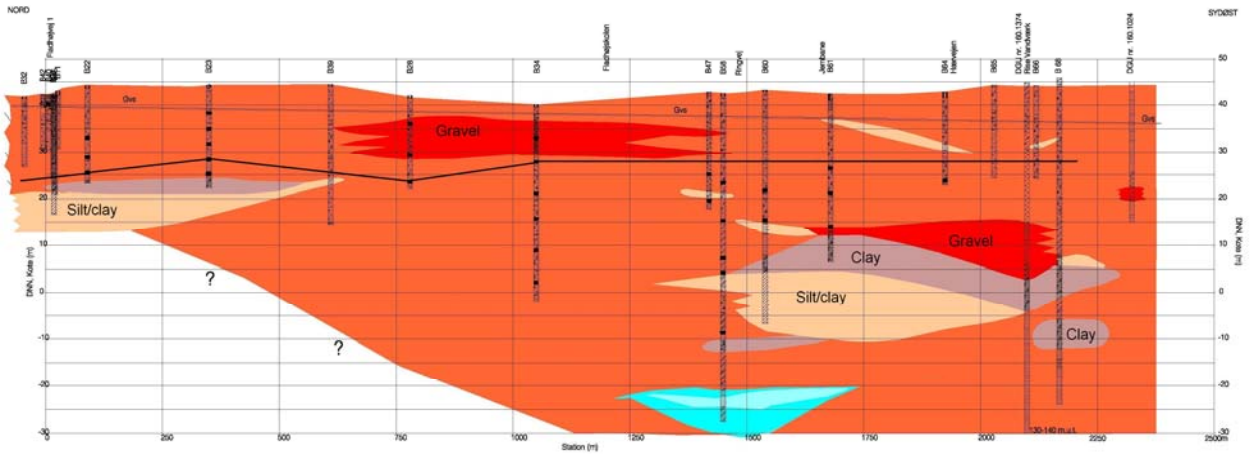

Figure 1 Geological cross section along the plume center: solid line separates the upper and lower zones.

7.3 VALIDATION OF ASSUMPTIONS

In order to use the summed concentrations of chlorinated ethenes as a quasi-conservative tracer to reliably calibrate flow and transport parameters, reductive dechlorination of chlorinated ethenes must be the only degradation pathway responsible for the observed concentration decreases over distance. Hence, the combined carbon isotope ratios based on all chlorinated ethene species need to remain constant as the source value (-25.0‰). Detailed field investigation of the contaminant plume is reported elsewhere (Chapter 5), and Tables 1-A and 1-B summarize the measured concentrations and carbon isotope ratios of chlorinated ethenes for the upper and the lower zones, respectively. The combined isotope ratios remain relatively stable within the analytical precision at -25.0‰ except at the plume front starting from 1500 m away from the source, suggesting that the sequential reductive dechlorination of PCE is likely the only active transformation process in the majority of the plume. Therefore, the use of the summed concentrations of chlorinated ethenes as a tracer is valid as long as the combined carbon isotope ratios remain at -25.0‰. Consequently, the data from the plume front at B61s and B64 need to be excluded from tracer simulations to characterize flow and transport parameters used in the model. However, they are included for the estimation of degradation rates. The chlorine isotope study (Chapter 5) revealed that the observed carbon isotope deviation at the plume front was caused by the fact that reductive dechlorination

proceeds beyond VC to ethene or to ethane even though the presence ethene and ethane could not be confirmed at the site. Due to the fact that the combined carbon isotope ratios do not include those of ethene, the combined ratios at the plume front are greater than the source value.

Table 1-A Concentrations and carbon isotope ratios for the upper zone

Well	Distance [m]	Depth [m]	NO_3^-	PCE		TCE		cDCE		VC		Total	Total
			mg/l	conc. µmol/L	$\delta^{13}C$ ‰	conc. µmol/L	$\delta^{13}C$ ‰	conc. µmol/L	$\delta^{13}C$ ‰	conc. µmol/L	$\delta^{13}C$ ‰	Conc. µmol/L	$\delta^{13}C$ ‰
B5-3	**0**	**-2.75**	**2.1**	**578.9**	**-24.92**	**44.90**	**-26.18**	**10.49**	**-26.35**	**0.035**		**634.3**	**-25.03**
B5-2	0	-5.5	15	9.045	-25.14	1.827	-26.57	1.663	-25.49	0.010		12.55	-25.39
B5-1	0	-8.5	16	1.568	-25.61	0.002		0.000		0.000		1.570	-25.60
B11-3	**18**	**-4.5**	**13**	**193.0**	**-24.77**	**15.22**	**-22.78**	**5.846**	**-22.38**	**0.048**		**214.1**	**-24.56**
B11-2	18	-7.5	28	15.08	-27.43	1.294	-28.19	2.904	-25.99	0.011		19.28	-27.26
B16	**105**	**-8**	**3.7**	**21.11**	**-24.88**	**6.698**	**-24.10**	**0.434**	**-26.26**	**0.000**		**28.24**	**-24.72**
B22-3	100	-11	25.15	1.628	-22.60	2.207	-25.66	4.047	-25.53	0.002		7.884	-24.96
B22-2	100	-15	7.36	2.352	-23.81	0.373		0.405		0.001		3.131	-23.81
B20	355	-6.5	18	3.317	-24.17	1.294	-23.41	2.685	-26.16	0.029	-12.20	7.324	-24.72
B23-3	**350**	**-12.5**	**13**	**2.774**	**-23.40**	**0.297**	**-27.71**	**6.538**	**-25.54**	**0.002**		**9.611**	**-24.99**

* Values in bold letters represent the 'core' of the plume in the upper zone

Table 1-B Concentrations and carbon isotope ratios for the lower zone

Well	Distance [m]	Depth [m]	NO_3^-	PCE		TCE		cDCE		VC		Total	Total
			mg/l	conc. µmol/L	$\delta^{13}C$ ‰	conc. µmol/L	$\delta^{13}C$ ‰	conc. µmol/L	$\delta^{13}C$ ‰	conc. µmol/L	$\delta^{13}C$ ‰	conc µmol/L	$\delta^{13}C$ ‰
B28-1	**750**	**-18.5**	**<0.5**	**1.930**	**-15.51**	**3.425**	**-25.09**	**3.743**	**-31.77**	**0.003**	**-37.02**	**9.100**	**-25.81**
B34-4	1000	-18.5	<0.5	0.022		0.320	-8.68	2.822	-29.15	0.006	-33.93	3.169	-27.08
B34-3	**1000**	**-24.5**	**<0.5**	**0.003**		**0.056**	**0.37**	**4.702**	**-24.62**	**0.011**	**-31.50**	**4.771**	**-24.35**
B34-2	1000	-31.5	<0.5	0.013		0.152	-26.76	5.874	-24.35	0.016	-30.63	6.055	-24.43
B34-1	1000	-38.5	<0.5	0.000		0.011		1.037	-25.90	0.004		1.053	-25.89
B47-2	1330	-17.5	<0.5	0.000		0.000		1.004	-26.09	0.014		1.018	-26.09
B47-1	**1330**	**-23.5**	**<0.5**	**0.001**		**0.000**		**2.176**	**-24.80**	**0.013**		**2.190**	**-24.80**
B58-10	1340	-19	<0.5	0.000		0.000		1.036	-25.50	0.010	-25.38	1.046	-25.50
B58-8	1340	-27	<0.5	0.000		0.000		0.994	-25.54	0.011	-25.59	1.005	-25.54
B58-7	1340	-35.5	<0.5	0.000		0.003		1.139	-25.56	0.009	-23.02	1.152	-25.54
B58-6	1340	-38.5	<0.5	0.000		0.000		0.714	-25.04	0.010	-21.42	0.723	-24.99
B58-4	1340	-51	<0.5	0.000		0.000		0.383	-24.35	0.012	-17.98	0.395	-24.17
B60-3	1430	-21.5	<0.5	0.000		0.000		1.344	-24.78	0.014	-24.58	1.359	-24.77
B60-2	1430	-27.5	<0.5	0.001		0.000		2.378	-25.13	0.012	-23.12	2.391	-25.12
B61-3	1580	-16	<0.5	0.000		0.000		0.186	-23.58	0.004	-15.34	0.190	-23.41
B61-2	**1580**	**-21.5**	**<0,5**	**0.000**		**0.000**		**0.724**	**-24.00**	**0.010**	**-18.75**	**0.734**	**-23.92**
B61-1	1580	-28.5	<0.5	0.000		0.000		0.135	-21.73	0.012	-12.56	0.146	-21.01
B64	1810	-19	<0.5	0.000		0.000		0.058	-20.92	0.004	-15.07	0.063	-20.51

* Values in bold letters represent the 'core' of the plume in the lower zone

The second assumption is that the level of biodegradation is sufficient enough to give rise to detectable shifts in the isotope ratios so as for the carbon isotope ratios to serve as an indicator to quantify the transformation rates. Due to the presence of two distinctive redox zones as a function of depth, the

upper and the lower zones demonstrate different isotopic behaviors of chlorinated ethenes as shown in Figures 2. Figures 2-A and 2-B illustrate the isotope behaviors of individual chlorinated ethene species along the 'core' of the plume for the two zones. At each location the depth which corresponds to the highest summed contaminant concentration is assumed to represent the 'core' of the plume (Tables 1). In the lower zone at the well B34, the depth of 31.5 m (B34-2) has the highest summed concentration; however, based on the $\delta^{13}C$ of TCE (0.37‰), B34-3 was considered to better represent the general plume evolution. The isotope ratio of TCE at B34-2 (-26.76‰) may indicate that this depth was aligned to a flow path which experiences a less level of the reductive dechlorination.

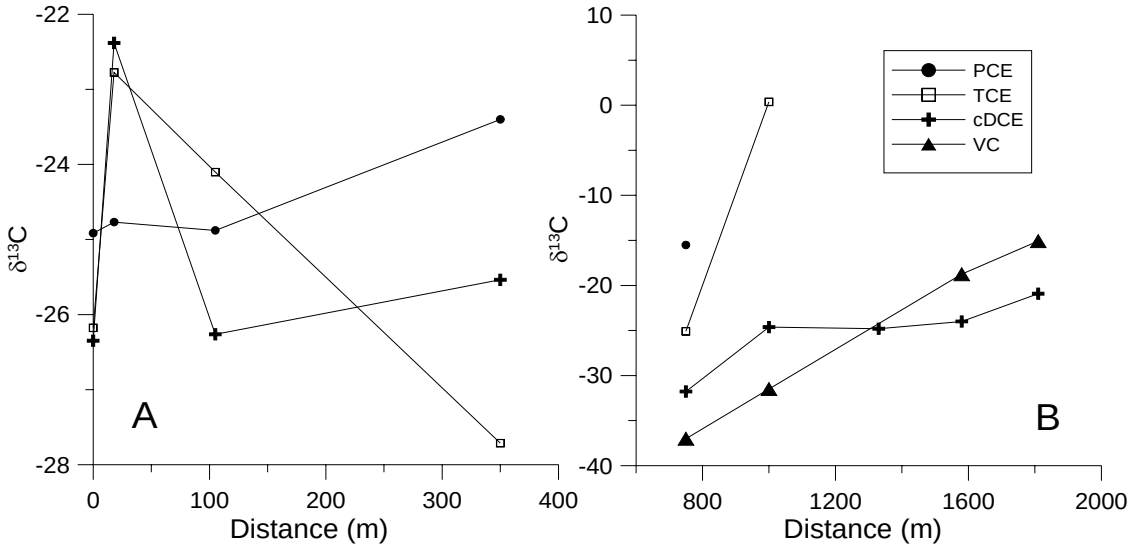

Figure 2 Isotope behavior of chlorinated ethene along the plume core: A: Upper zone and B: Lower zone

Figure 2A demonstrates that in the upper zone, the carbon isotope ratios of PCE slightly but steadily increase over distance. However, the isotope ratios of TCE and cDCE fluctuate in a relatively narrow range of -23.0 to -28.0‰, suggesting that their isotopic variations do not result from the isotope fractionation during reductive dechlorination, but it is rather caused by the source variation in TCE and cDCE isotope ratios over time as described in Chapter 5. Therefore, only PCE can be subjected to the quantification of the transformation rate in the upper zone. The lower zone starts from 750 m away from the source where the contaminant concentrations are the highest in the absence of nitrate (refer to Chapter 5 for the complete data set). All chlorinated ethene species become enriched in ^{13}C over distance in the lower zone as shown in Figure 2B. There is only one isotope data point for PCE due to its low concentrations, but PCE is expected

to follow reductive dechlorination as well; therefore, all species including PCE in the lower zone can be subjected to the quantification of transformation rates.

7.4 MODELING APPROACH

In this study, analytical solutions were employed to quantify the transformation rates of chlorinated ethenes during reductive dechlorination. Flow and transport parameters were first calibrated with the tracer concentration data. Calibrated parameters were then used in the reactive-isotope models to simulate sequential reductive dechlorination of PCE. In order to simulate the isotope ratios of chlorinated ethenes, light and heavy isotopomers of each chlorinated ethene species were calculated separately. Due to the presence of distinctive upper and lower zones, models were developed separately.

7.4.1 Transport model

In order to model the transport behavior, a 3D analytical solution with numerical integration was employed to include the effect dispersion in all directions and to accommodate the multi-level observation wells along the center of the plume. An approximate solution exists (Domenico 1987), but the numerical integration greatly decreases the errors especially when dispersivity, simulation time, and dimensionality (from 2D to 3D) are increased and when a reactive species is simulated (Guyonnet and Neville 2004; Srinivasan *et al.* 2007; West *et al.* 2007). Analytical models were preferred over numerical models due to the lack of geological information in lateral directions and beneath the source zone and because of the presence of two distinctive zones. In addition, this study is intended to evaluate the use of field carbon isotope data to estimate the transformation rates during the course of chlorinated ethenes, and the use of analytical models facilitates a general but quick characterizing the flow and transport parameter sensitivities with respect to the estimated rates. The effect of sorption and retardation was not incorporated as the plume is at a steady state in terms of contaminant concentrations as confirmed by stable concentration measurements over four years. The analytical transport solution used in this study is presented elsewhere (Sager 1982; Wexler 1992) and corresponds to:

$$c(x,y,z,t) = \frac{c_0 x \exp\left[\frac{vx}{2D_x}\right]}{8\sqrt{\pi D_x}} \int_0^t \frac{1}{\tau^{3/2}} \exp\left[-\left(k + \frac{v^2}{4D_x}\right)\tau - \frac{x^2}{4D_x\tau}\right] \cdot \left(erfc\left[\frac{y - W/2}{2\sqrt{D_y\tau}}\right] - erfc\left[\frac{y + W/2}{2\sqrt{D_y\tau}}\right]\right) \cdot \left(erfc\left[\frac{z - H/2}{2\sqrt{D_z\tau}}\right] - erfc\left[\frac{z + H/2}{2\sqrt{D_z\tau}}\right]\right) d\tau \quad (1)$$

where c is the concentration at time t [d], c_0 is the initial concentration, x, y, z are the distance coordinates [m], v is the groundwater velocity [m/d], D_x, D_y, D_z are the dispersion coefficients in x, y, z directions [m^2/d], τ is the integration variable with respect to t [d], k is the first-order reaction rate [d^{-1}], W is the

source width [m], and H is the source height [m]. Equation 1 was numerically integrated using the adaptive Lobatto quadrature function in Matlab. Groundwater velocity was assumed to be 0.24 m/d for both upper and lower zones, and the simulation period, t, was assumed to be 5000 d for both upper and lower zones. The simulation time was determined based on the stable concentrations of each chlorinated ethene species obtained from a time-series test which indicated that 5000 d was sufficient to simulate a steady-state condition at 1 km away from the source for the both calibrated upper and lower models.

7.4.2 Reactive transport model

A series of sequential reductive dechlorination steps of chlorinated ethenes is incorporated as follows:

$$\frac{\partial c_i}{\partial t} - D_x \frac{\partial^2 c_i}{\partial x^2} - D_y \frac{\partial^2 c_i}{\partial y^2} - D_z \frac{\partial^2 c_i}{\partial z^2} + v \frac{\partial c_i}{\partial x} = k_{i-1} c_{i-1} - k_i c_i \qquad (2)$$
$$\forall i = 1,2,...,n,$$

where i is the species index. By introducing a set of auxiliary variables as proposed by Sun *et al* (Sun *et al.* 1999), and substituting the variables for c and c_0 into Equation 1, an analytical expression for each indexed species can be obtained. The auxiliary variables, a_i, are defined as:

$$a_i = c_i + \sum_{j=1}^{i-1} \prod_{l=j}^{i-1} \frac{k_l}{k_l - k_i} c_j \qquad (3)$$
$$\forall i = 2,3,...,n,$$

where j and l are the species indexes of precedent species. As an example, cDCE can be denoted by an index i whereas TCE as j and PCE as l. Equation 3 for the case of cDCE is as follows.

$$a_{cDCE} = c_{cDCE} + \left(\frac{k_{PCE}}{k_{PCE} - k_{cDCE}} \right) \left(\frac{k_{TCE}}{k_{TCE} - k_{cDCE}} \right) c_{PCE} + \left(\frac{k_{TCE}}{k_{TCE} - k_{cDCE}} \right) c_{TCE} \qquad (4)$$

As noted in the original work (Sun *et al.* 1999), a_{i0} is applied instead of c_0, and k_i instead of k in Equation 1; thus, there are four parallel expressions to describe the sequential reductive dechlorination of PCE to ethene in a reactive model. After solving the a_i, c_i can be determined from a recursive substitution process based on Equation 3.

7.4.3 Isotope model

In order to simulate carbon isotope fractionations during reductive dechlorination, two subspecies representing the light and heavy isotopologues were simulated for each chlorinated ethene. The two subspecies differ in their reaction rates according to the isotope enrichment factor of a compound:

$$\varepsilon = (\alpha - 1) \times 1000$$
$$\alpha = \frac{k_L}{k_H} \qquad (5)$$

where ε is the isotope enrichment factor [‰], α is the isotope fractionation factor which is the ratio between k_H, the reaction rate for the heavy isotopologue and k_L, the rate for the light isotopologue. The reported average values from laboratory studies were regarded as the representative isotope enrichment factors: -5.2‰, -8.5‰, -17.8‰, and -23.2‰ for PCE, TCE, DCE and VC respectively (van Breukelen *et al.* 2005).

7.5 MODEL IMPLEMENTATION

7.5.1 Model domains

Due to the presence of two distinctive redox zones as a function of depth, two zones were assigned different model domains as shown schematically in Tables 1. The upper model domain extends from the source (located at B5-3) to approximately 350 m from the source. The size of the source was delineated by the field observation to be approximately 20 m in width and 1.75 m in depth. The observed concentration and isotope ratio of PCE from B5-3 were used directly as the source composition. Although less chlorinated ethenes are present at the source, they were not simulated. The lower zone starts from 750 m away from the source (B28-1, considered as the 'source zone' for the lower zone) to 1810 m at the well B64. In order to develop a stand-alone model for the lower zone, it was necessary to characterize the size of the lower 'source' zone. The lower source zone consists of a mixture of all chlorinated ethene species; thus, the observed concentrations and isotope ratios of chlorinated ethenes from B28-1 were directly used as the source composition.

7.5.2 Flow and transport model calibration

As analytical solutions assume homogeneous composition of the aquifer, which is not the case for the field scenario, model calibrations focused on the data obtained along the 'core' of the plume to better represent the homogeneity of the medium (Tables 1). Flow and transport parameters were calibrated to the tracer concentrations (summed concentrations of chlorinated ethenes) along the plume core. For the calibration of the upper zone model, the summed concentrations from B5-3, B11-3, B16 and B23-3 were used. For the lower zone, only three points along the plume core (B28-1, B34-3 and B47-1) satisfied the assumption of stable combined isotope ratios to serve as a quasi-conservative tracer. Calibrated parameters were also used to simulate other observation points away from the plume core to evaluate the general trend of simulated plumes and to illustrate the level of deviation from observations caused by assuming a homogeneous medium.

A tracer was simulated according to Equation 1 holding the reaction rate at 0. The core of the plume was assigned the coordinate $z = 0$ in Equation 1, and other wells had z coordinates relative to the depth of the plume core at each location. All wells used in this study were aligned to the plume centerline ($y = 0$ in Equation 1). For the upper zone transport model, three parameters, longitudinal dispersivity denoted as α_x

($D_x = v \times \alpha_x$), the ratio between longitudinal to transversal dispersivities α_y/α_x ($D_y = v \times \alpha_y$) and the ratio between longitudinal to vertical dispersivities α_z/α_x ($D_z = v \times \alpha_z$), were calibrated in order. For the lower zone, the same dispersivity values (α_x, α_y/α_x, and α_z/α_x) as the upper zone were used assuming that the hydraulic properties of porous media do not change significantly between the two zones. Since the approximate size of the lower 'source' zone (W and H) could not be estimated from the field data, W and H were calibrated to the tracer data in the lower zone. Calibration was performed in a trial-and-error approach by minimizing the least-squares as:

$$error = \sum \left(\frac{c_{simulated} - c_{observed}}{c_{observed}} \right)^2 \quad (6)$$

Since multiple parameters needed to be calibrated, the calibrated values would not be the unique solution. In order to avoid a unrealistically estimated α_x value, empirical expressions between the flow distance and α_x such as $\alpha_x \approx 0.1 \times L$ where L is the flow distance (Wiedemeier *et al.* 1997; Charbeneau 2000) and $\alpha_x \approx c \times (L)^m$ where c is a characteristic parameter for a geological medium (0.85 or 0.063 for unconsolidated sediments in the order of reliability) and m is the scaling exponent (0.81 or 0.94 in the respective order (Schulze-Makuch 2005)) were regarded as reference. Given the flow distance of 2 km, these expressions provided the α_x values of 200, 40, and 80 m in the order of mention.

7.5.3 Quantification of transformation rates

Reactive-isotope models with the calibrated flow and transport parameters were used to quantify the transformation rates of chlorinated ethenes. The quantification process resembled the above-mentioned 'trial-and-error' calibration process in which a transformation rate was iteratively changed until it best reproduced the observed contaminant behaviors along the plume. Reactive-isotope simulations for the lower zone included the plume front since the hydraulic properties are not expected to change significantly from the downgradient. Despite the absence of ethene at the site, the reductive dechlorination of VC was assumed to take place in the lower zone because VC carbon isotope ratios strongly increased over distance (Figure 2B). Further reductive dechlorination of VC in the lower zone seems to contradict the assumption that all carbon is conserved within the chlorinated ethenes. However, the majority of the plume had VC concentrations less than 1% of its precursor cDCE, suggesting that further VC transformation did not significantly influence the combined carbon isotope ratios except at the plume front where VC starts to predominate.

Two quantification approaches were carried out for comparison. The first approach involved with the fitting of the reactive-isotope model to the observed carbon isotope data, and the second to the observed concentrations data to evaluate the practical situation where isotope data were not available. Due to the simultaneous formation and transformation of intermediate species, the transformation rates were

quantified in the order of a greater number of chlorine atoms according to Equation 5. For the PCE transformation rate in the lower zone, the isotope ratio at B34-3 was assumed to be in the range of –5‰ to 10‰ (based on the isotopic shift for TCE at the same location) since the calibration process requires at least two observation points (B28-1 as the lower 'source' and B34-3).

7.5.4 Parameter sensitivity analyses

The use of analytical solutions allows evaluation of a wider range of parameter values and different scenarios. In order to characterize the degree of uncertainties associated with the flow and transport parameters, several series of sensitivity analyses were performed. In order to evaluate the possible uncertainties with the estimated groundwater flow velocity (0.24 m/d based on a pumping test), the flow and transport model for the upper zone was calibrated for the three dispersion parameters (α_x, α_y/α_x, and α_z/α_x) under different flow velocities (0.1 to 1.0 m/d). In addition, assuming the employed best-fit dispersion parameters in this study, the estimated transformation rate of each chlorinated ethene was evaluated under the same range of flow velocities for the lower zone. The sensitivity of groundwater velocity to the estimated transformation rates was quantified for both isotope- and concentration-based calibration methods. Furthermore, the effect of different source dimension for the lower zone was evaluated. First, using the flow and transport model, the best-fit value for *H* was obtained under different values of *W* (20 to 90 m). Then, for each pair of *H* and *W*, the reactive-isotope model for the lower zone was employed to estimate the best-fit transformation rates for individual chlorinated ethene species. The sensitivity of source dimension to the estimated transformation rates was quantified for both calibration methods.

7.6 RESULTS AND DISCUSSION

7.6.1 Transport model

Calibrated transport parameters are listed in Table 2. The best-fit α_x value from the calibration is 100 m, and the α_y/α_x and α_z/α_x ratios are both 0.01, indicating an isotropic dispersion in *y* and *z* directions. For the source dimension in the lower zone, the best-fit values are 60 m in width and 30 m in height under the calibrated dispersivity values.

Table 2 Calibrated transport parameters in Equation 1

Zone	W [m]	H [m]	α_x [m]	α_y/α_x	α_z/α_x
Upper	20	1.75	**100**	**0.01**	**0.01**
Lower	**60**	**30**	100	0.01	0.01

* Values in bold represents the calibrated parameters

Simulated tracer concentrations are compared with the observed concentrations as shown in Figures 3. Both upper and lower models are capable of reproducing the tracer concentrations along the plume core, suggesting the reliability of calibrated parameters based on the tracer concentrations along the plume core. On the contrary, the concentrations from the observation points away from the plume core are, in general, overestimated except at the source area in the upper zone and two observation points in the lower zone. The general overestimation of the tracer concentrations implies the inherent difficulty with simulating a 3D heterogeneous plume with analytical solutions, which assume a homogeneous aquifer medium. In addition, it is possible that the exact location of the plume core could not be correctly captured due to the limited number of observation depths at each location. Moreover, the geometry of the source is assumed to be a rectangle according to Equation 1, but the actual source geometry in heterogeneous subsurface environments is more complex, which would also affect the observed concentration values. However, based on the good agreement between the simulated and observed tracer concentrations along the plume core, 3D analytical solutions can effectively be used to derive flow and transport parameters based on the tracer data and to simulate the tracer behavior at least along the plume core.

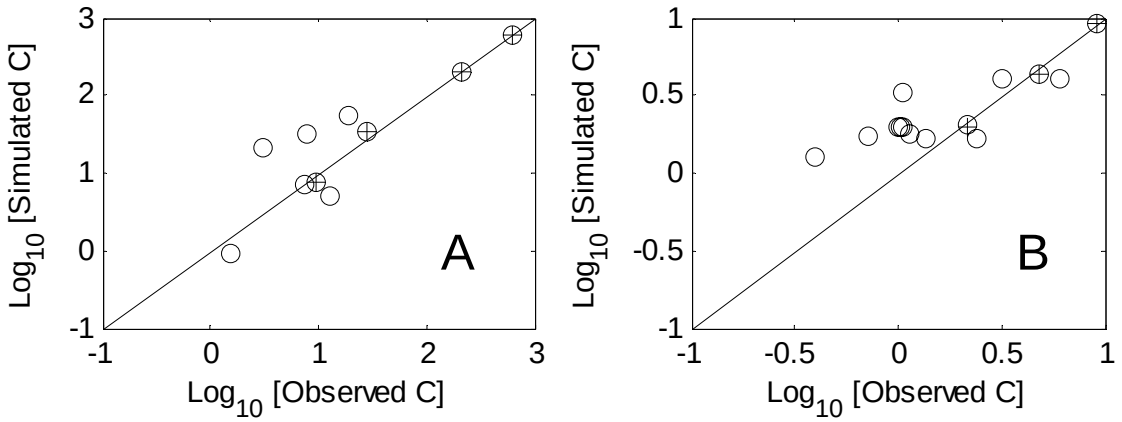

Figure 3 Observed vs. simulated values for the pooled contaminant concentrations. A: upper zone, B: lower zone. The points along the core of the plume are indicated as a cross in a circle.

7.6.2 Reactive-isotope models

Based on the calibrated flow and transport parameters from Table 2, reactive-isotope models are developed to quantify the transformation rates of chlorinated ethenes. Two quantification methods (isotope- and concentration-based) are performed and compared for the upper and the lower zones. In the upper zone, only PCE follows isotope fractionation over distance; thus, only the transformation rate of PCE can be quantified. On the other hand, all chlorinated ethenes demonstrate isotope fractionations over distance in the lower zone; hence, the transformation rates of all chlorinated ethenes can be quantified. The quantified first-order transformation rates for the upper and lower zones are summarized in Table 3.

Comparison of the first-order PCE transformation rates between the upper (0.15 $year^{-1}$) and the lower (8.03 $year^{-1}$) zones reveals that the PCE reductive dechlorination in the lower zone is faster by a factor of four. The faster rate of PCE transformation rate is anticipated based on the different redox conditions since the absence of a competing electron acceptor (nitrate) in the lower zone can enhance the rate and the progress of reductive dechlorination.

Figures 4 compare the simulated isotope ratios and concentrations of PCE with the observed values for the upper zone. The quantification method based on isotope data can reproduce the PCE isotope behavior over distance along the plume core, but the deviation from the observed isotope ratios increased further away from the plume core, and in general the model yields rather uniform isotope ratios regardless of observation depths (Figure 4 A-1). On the other hand, the concentration-based method is not able to properly simulate the PCE isotope ratios (Figure 4 B-1). In terms of PCE concentrations, both quantification methods result in good agreement between the simulated and the observed PCE concentrations along the plume core (Figures 4 A-2 and B-2) despite the fact that the PCE transformation rates vary by more than a factor of four. Regardless of the quantification method, the concentration deviation from the observation is inherent from the original flow and transport model for the observation points away from the plume core.

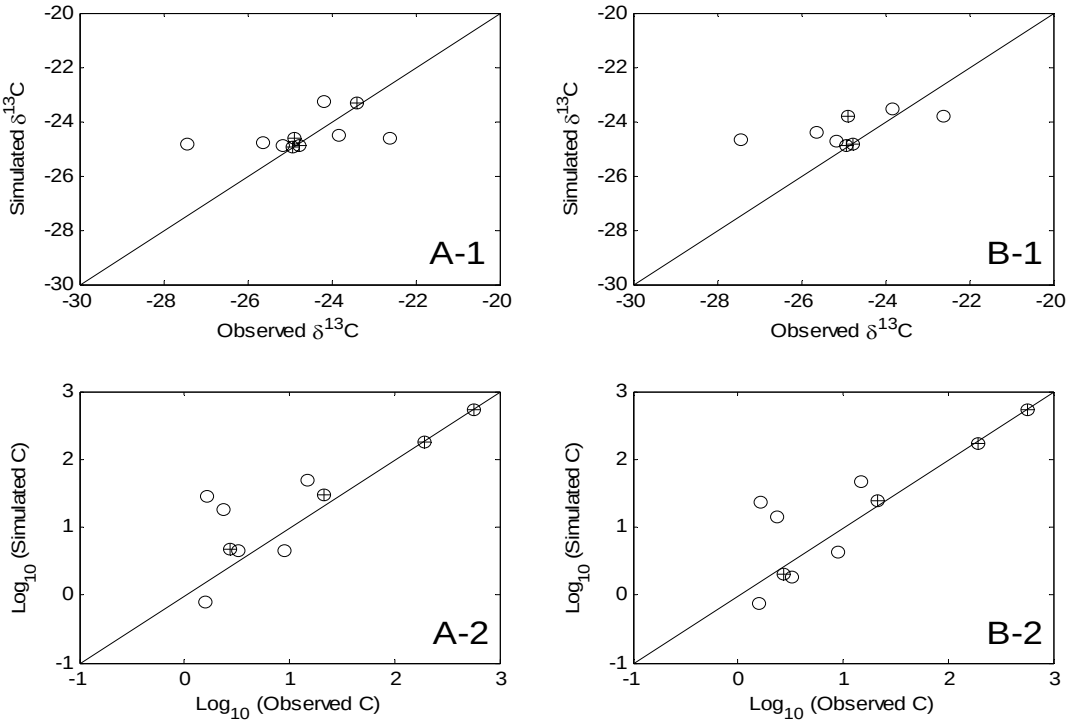

Figure 4 Observed vs. simulated carbon isotope ratios and concentrations for PCE in the upper zone. The points along the core of the plume are indicated as a cross in a circle. Series A: Isotope-based quantification approach, series B: Concentration-based quantification approach.

Figures 5 illustrate the results from the lower zone models. As shown in Table 3, two quantification methods yield similar transformation rates of PCE and TCE. Consequently, the isotope ratios and concentrations of PCE and TCE are similar.

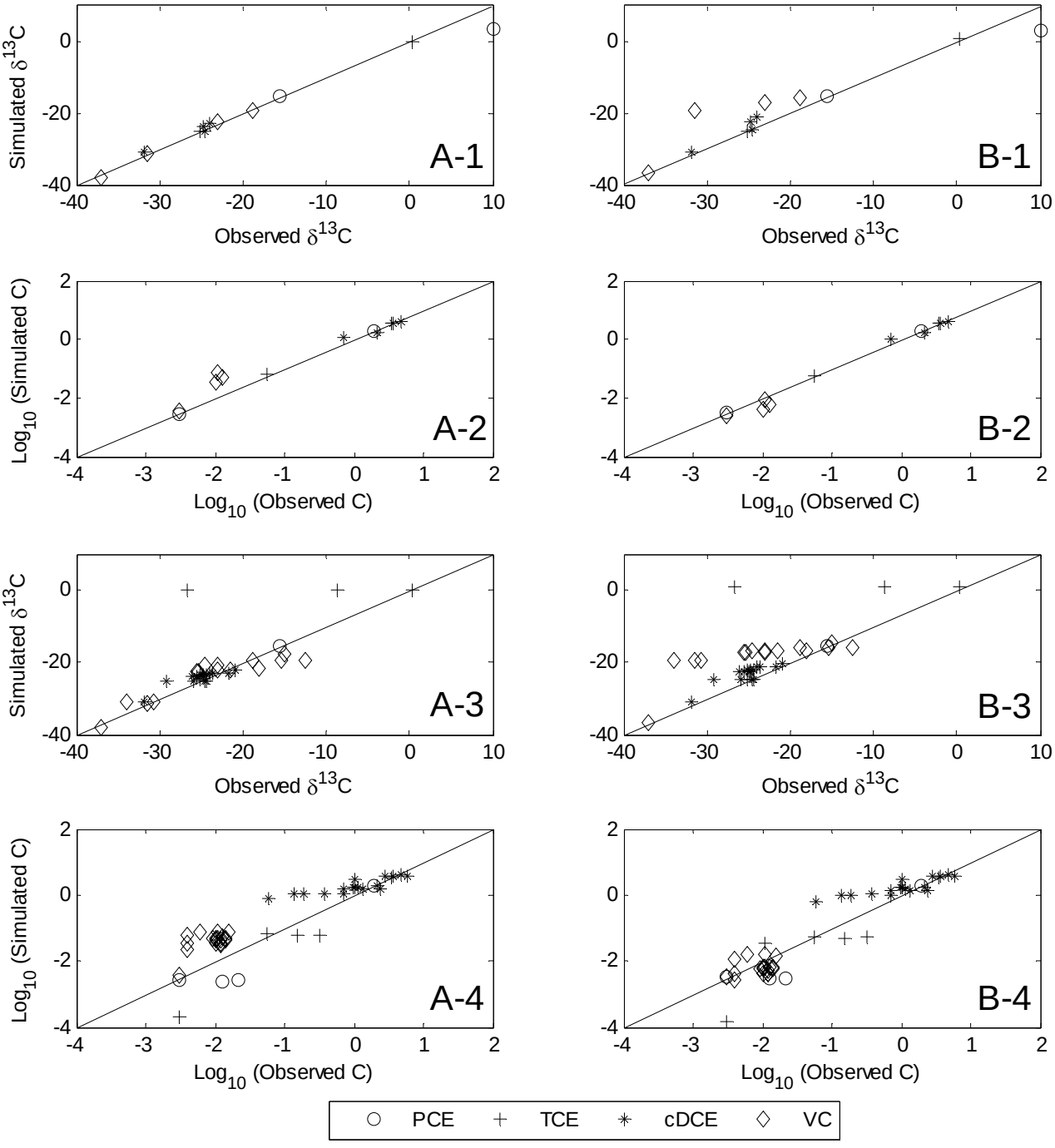

Figure 5 Observed vs. simulated carbon isotope ratios and concentrations for PCE, TCE and DCE for the plume core (A-1, 2 and B-1, 2) and all data points (A-3, 4 and B-3, 4) in the lower zone. Series A: Isotope-based calibration approach, series B: Concentration-based calibration approach.

Along the core of the plume, the isotope-based quantification method reproduced the isotope ratios of all chlorinated ethenes (Figure 5 A-1). Although the concentrations of PCE, TCE and cDCE are well reproduced, the VC concentrations are overestimated (Figure 5 A-2). Reciprocally, the concentration-based quantification reproduced the concentrations of all chlorinated ethenes and the isotope ratios of PCE, TCE and cDCE but not the VC isotope ratios (Figures 5 B-1 and B-2). With respect to the simulation of observation points away from the plume core, both quantification methods could not simulate the variations in depth-dependent isotope ratios and concentrations, consistently with the upper zone models. It implies the limit with simulating a 3D plume with analytical solutions and that the lower zone probably consists of several different flow path lines and the assumption that the source could be characterized by a single source composition is not valid for simulating observation wells located away from the plume core. Different flow paths would have different residence times of water, the concentrations and isotope ratios would also vary because of the difference in *t* of the Equation 1. Such variations can not be modeled with an analytical solution as the solution assumes a homogeneous medium.

Table 3 Quantified first-order transformation rates [year^{-1}]

Zone	Method	PCE	TCE	cDCE	VC
Upper	δ^{13}C-based	0.15	-	-	-
	conc-based	0.62	-	-	-
Lower	δ^{13}C-based	8.03	4.38	0.02	0.73
	conc-based	7.67	4.75	0.06	17.16

For the quantification of transformation rates in the lower zone, both methods result in decreasing transformation rates in the order of reductive dechlorination except for VC. This pattern corresponds to other field studies where the VC transformation rate is somewhat similar to in the range with those of PCE and TCE while the rate for cDCE is much smaller (Wiedemeier *et al.* 1997). The similar transformation rates are obtained for PCE and TCE probably because the rate quantification of these compounds involves with only two data points and they are accompanied by sharp concentration decreases and strong isotope fractionation within the distance of 250 m. On the other hand, the transformation rates of intermediates, cDCE and VC, vary between the two quantification methods as in the upper zone with PCE. Although the rates for PCE in the upper zone and cDCE in the lower zone remain in the same order of magnitude, those of VC in the lower zone are significantly different between the two quantification methods. The unrealistically high transformation rate obtained for VC from the concentration-based quantification method may suggest that it is particularly misleading when the observed concentrations are very low. The obtained transformation rates are all in the range of field-estimated values (Wiedemeier *et al.* 1997), numerically calibrated value (Clement *et al.* 2000) and analytically calibrated values with BIOCHLOR (Lu *et al.* 2006) in the literature.

7.6.3 Parameter sensitivity analyses

The evaluation of the effect of groundwater flow velocity on the calibrated dispersivity parameters (α_x, α_y/α_x, and α_z/α_x) for the upper zone model reveals that the dispersivity parameters are not affected by the groundwater flow velocity as far as the plume core along the plume centerline is concerned. The study on the effect of dispersion (α_x and α_y) on the first-order degradation rates suggests that increasing α_x by a factor of ten can causes the rate to increase two folds and increasing α_y by ten folds generally decreases the rate on average by 35% under the investigated conditions (Stenback2004). Although the groundwater velocity does not affect the quantification of dispersion parameters along the plume core, it is expected to give rise to a significant variation in terms of rate quantification as it affects the residence time of contaminants. Figures 6 A and B show the effect of groundwater velocity on estimated transformation rates for the isotope-based (A) and concentration-based (B) quantification methods. As expected, increasing the groundwater velocity results in increasing transformation rates for all chlorinated ethenes. In general, the increase in velocity from 0.1 to 1.0 m/d is accompanied by ten-fold increase in transformation rates for both quantification methods since the residence time of contaminants is shortened by a factor of ten. In addition there is no significant difference among simulated chlorinated ethenes nor between the two methods.

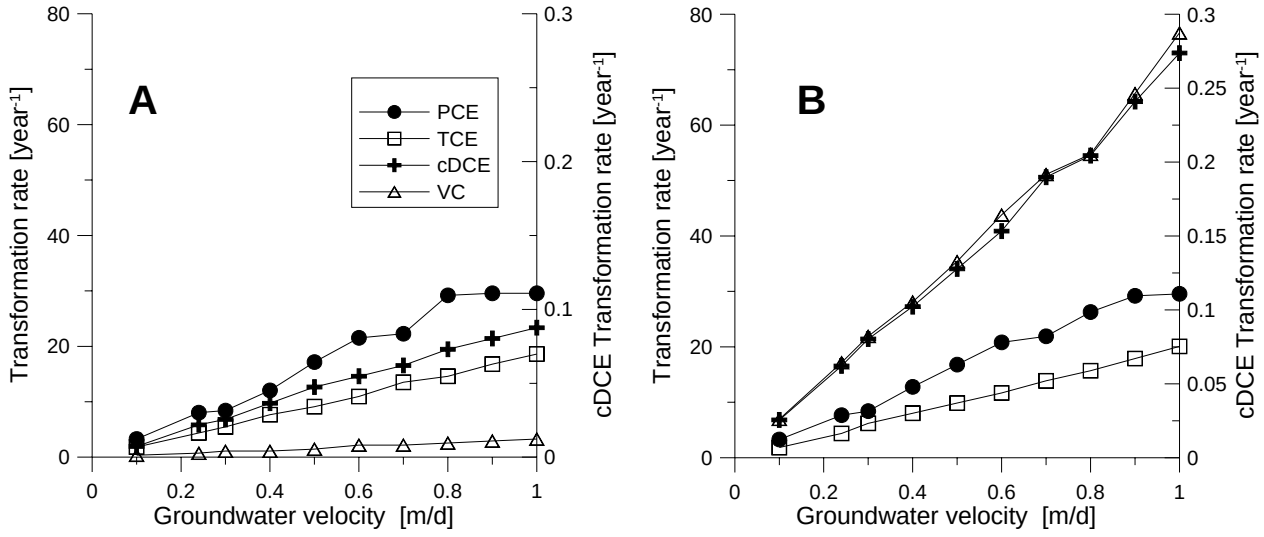

Figure 6 Effect of groundwater velocity on quantified transformation rates. A: isotope-based quantification method. B: concentration-based quantification method.

In order to investigate the effect of source width (W) on transformation rates, the corresponding source height (H) needs to be determined from the flow and transport model. Best-fit H values all reproduced the tracer concentrations in the lower zone. For the range of W evaluated (20 to 90 m with the increment of 10 m), the corresponding H values are determined to be 90, 70, 50, 45, 30, 30, 30 and 25 m in the order of

increasing *W*. The sensitivity analysis for the effect of source dimension on transformation rates is shown in Figures 7 A (isotope-based method) and B (concentration-based method).

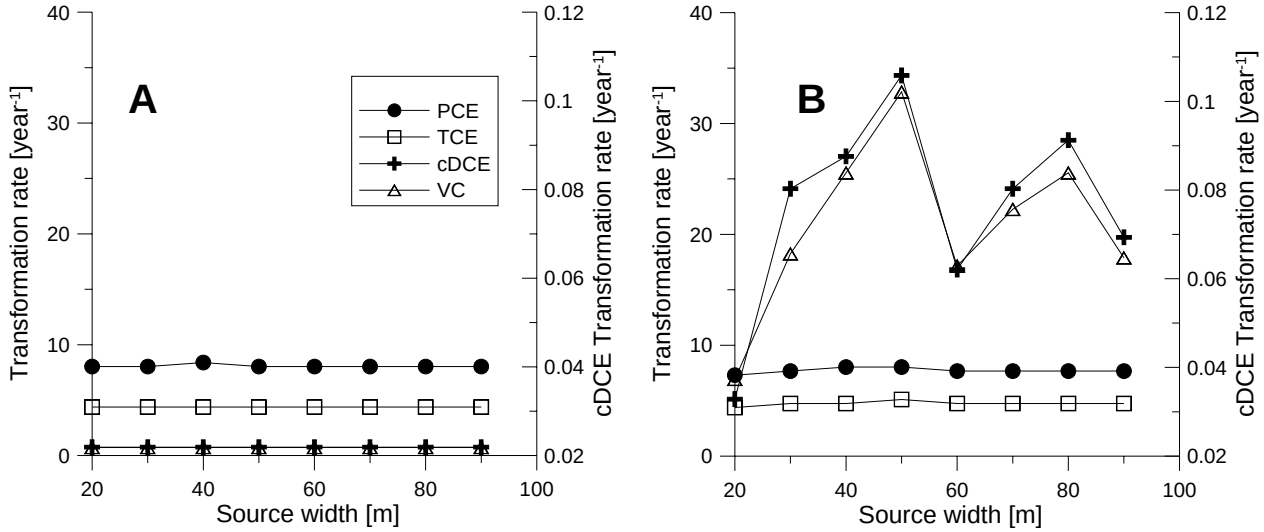

Figure 7 Effect of source dimension on quantified transformation rates. A: isotope-based quantification method. B: concentration-based quantification method.

The results demonstrate that the source dimension in the lower zone had virtually no influence on the quantified transformation rates based on the isotope-based method. On the other hand, the concentration-based method shows a significant variation in the transformation rates of cDCE and VC and they are consistently greater than the rates estimated from the isotope-based method. The observed variations in transformation rates of cDCE and VC indicate that the source dimension affects the rate quantification with the concentration-based method although the estimated rates still fall with in a narrow range of four. Therefore, from the sensitivity analyses, the results clearly show that the groundwater velocity is the key factor to estimate a reliable transformation rate and that the isotope-based quantification method is more stable than the concentration-based method when the source dimension is not well defined.

7.6.4 Comparison of different methods to estimate a reaction rate

Centerline-concentration and the Rayleigh-based isotope methods to estimate the field reaction rates were carried out for comparison. For chlorinated ethenes, these methods are applicable only for the parent compound and intermediates once the precursor compounds are completely transformed. The centerline-concentration method is based on the interpolation of log-linear plot of field concentrations over distance (Buscheck and Alcantar 1995). The empirical expression follows as:

$$k = \frac{v_c}{4\alpha_x}\left\{\left[1 + 2\alpha_x\left(\frac{\eta}{v_x}\right)\right]^2 - 1\right\} \qquad (6)$$

where v_c is the retarded contaminant velocity, v_x is the seepage velocity, η/v_x is the negative slope of a line formed by log-linear plot of contaminant concentration versus distance along the center of the plume as shown in Figure 8. For the present case, v_c was 0.24 m/d, α_x was 100 m, and η/v_x ratios were 0.00139 and 0.0052 for PCE and cDCE, respectively. While the method only takes into account longitudinal dispersion it provides a quick estimate on the *in situ* reaction rate. Reaction rates can also be estimated from the field isotope data based on the relationship depicted by the Rayleigh equation as follows (Hunkeler *et al.* 2002; Morrill *et al.* 2005):

$$k = \frac{\frac{1000}{\varepsilon} \cdot \ln\left(\frac{R}{R_0}\right)}{t} \qquad (7)$$

where R is the isotope ratio at time t, R_0 is the initial isotope ratio, and t is the travel time generally estimated from the average groundwater velocity and the distance traveled. For the present study, PCE in the upper zone and cDCE in the lower zone where PCE and TCE are completely transformed would be the cases where the log-linear-based and the Rayleigh-type estimations of reaction rates can apply. Table 4 compares the estimated reaction rates for PCE in the upper zone and DCE in the lower zone.

Table 4 Comparison of transformation rates

	PCE		cDCE	
	k [yr^{-1}]	$t_{1/2}$ [yr]	k [yr^{-1}]	$t_{1/2}$ [yr]
Buscheck and Alcantar (1995)	2.92	0.24	0.69	1.00
Rayleigh-type	0.07	9.50	0.03	21.10
Present study (isotope approach)	0.15	4.75	0.02	31.65
Present study (concentration approach)	0.62	1.12	0.06	11.17

As expected, the log-linear plot method yields the highest transformation rates for both PCE and cDCE as it neglects the transversal and vertical dispersion effects. The Rayleigh-type estimation of the reaction rate and the isotope-based method from this study result in reaction rates in the similar range for both PCE and cDCE, suggesting the robustness and consistency of the use of field isotope data to estimate reaction rates.

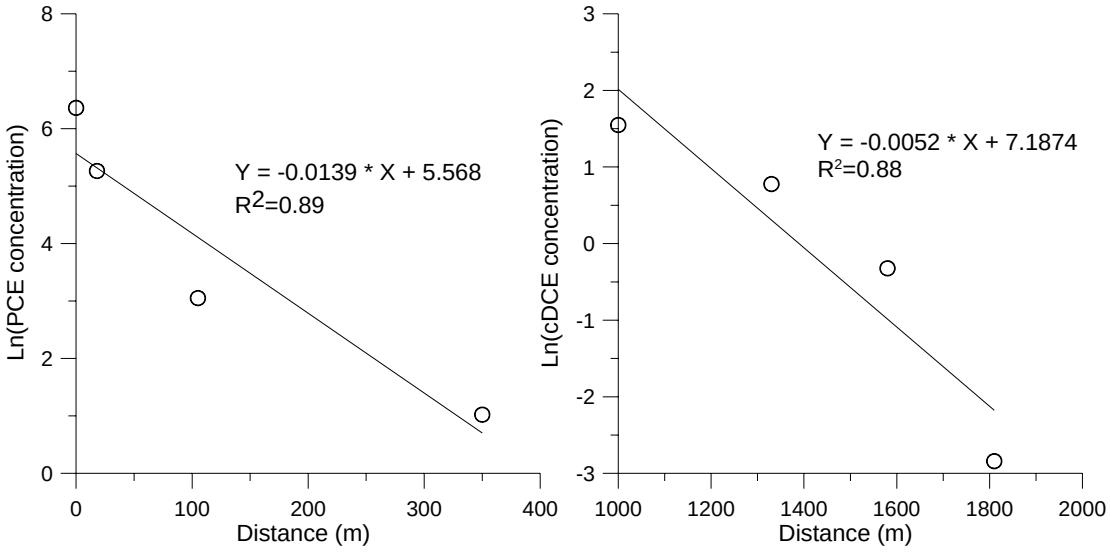

Figure 8 Log-linear plots of PCE and cDCE concentrations vs. distance

In addition to the above-mentioned estimation methods, 1D numerical simulation of isotope behaviors during reductive dechlorination can estimate the transformation rates of individual chlorinated ethenes (van Breukelen *et al.* 2005). The same procedures as described in the original work except for the use of numerical parameter estimation (van Breukelen *et al.* 2005) were carried out to simulate the isotope behavior along the plume core in the lower zone to estimate the transformation rates. The best-fit values for the transformation rates are presented in Table 5, and Figure 7 shows the fitted model performance with respect to the observed carbon isotope ratios of chlorinated ethenes. The transformation rates from the 1D numerical approach were smaller than those of the 3D analytical approach except for cDCE and VC the lower zone.

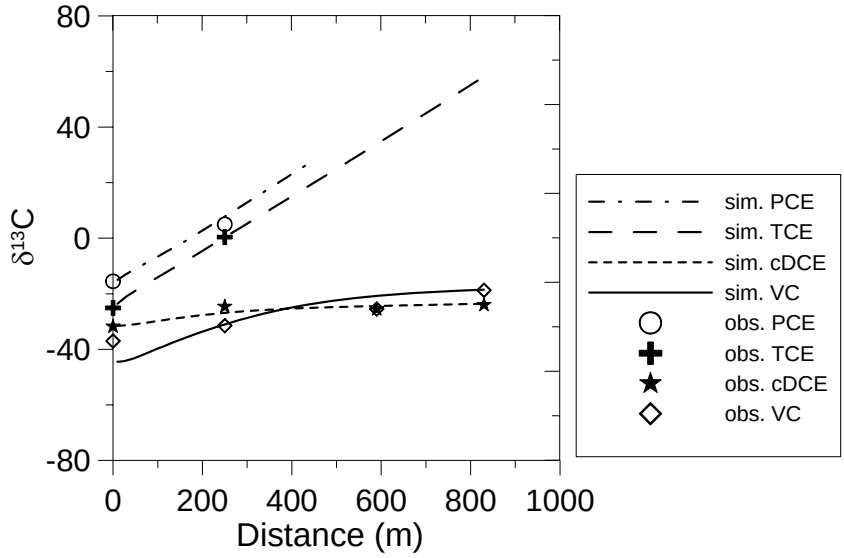

Figure 9 Results from a 1D numerical model

Table 5 Calibrated first-order reaction rates [year^{-1}]

	approach	PCE	TCE	DCE	VC
upper	3D analytical	0.15	-	-	-
	1D numerical	0.04	-	-	-
lower	3D analytical	8.03	4.38	0.02	0.73
	1D numerical	1.83	1.10	0.04	1.10

7.7 SUMMARY AND IMPLICATIONS

The study demonstrated that the summed concentrations of chlorinated ethenes (and ethene if present) can effectively be used as quasi-conservative tracer concentrations as long as reductive dechlorination of chlorinated ethenes is the only transformation process. A 3D analytical transport model was used to calibrate the transport parameters (dispersivities and the size of the source zone) to the tracer concentrations. Based on the calibrated transport model, the reactive-isotope models were simulated to quantify the transformation rates of chlorinated ethenes during *in situ* reductive dechlorination. The quantification was achieved by iteratively changing the transformation rate of preceding chlorinated ethene species to best reproduce the observed behavior. The rate quantification based on field isotope and concentration observations were carried out for comparison. The results suggest concentration-based quantification method tends to yield greater transformation rates than the isotope-based method especially when the contaminant concentrations are low. However, the difference between the two methods is relatively small by the factor of four, suggesting that once effective flow and transport parameters are derived from the simulating a tracer, relatively stable transformation rates can be obtained regardless of the method employed. Therefore, at chlorinated-ethene contaminated sites which are suspected to carry out reductive dechlorination as the only transformation process (often with characteristic cDCE accumulation), the same approach of using the summed concentrations as a tracer can significantly improve the reliability of rate estimation, and it is possible to estimate the transformation rates even without the isotope data. Parameter sensitivity analyses revealed that the variation in groundwater velocity is directly reflected to the quantified transformation rate; thus, it plays a significant role in quantifying the rate. The source dimension does not affect the isotope-based rate quantification method as long as the observation points are along the plume core aligned to the plume centerline.

Chapter 8

Conclusions, Implications and Outlook

The natural attenuation of chlorinated ethenes is particularly difficult to demonstrate due to the limitation imposed to the classical investigation methods. Chlorinated ethenes undergo sequential reductive dechlorination under anoxic conditions; hence, the presence of less chlorinated transformation intermediates indicates the transformation of more chlorinated parent compounds. However, the transformation intermediates can be degraded by other pathways such as aerobic and anaerobic oxidation and abiotic reduction, which impedes the use of a mass-balance approach to demonstrate the contaminant mass reduction over migration distance. In addition, the detection of metabolites from other pathways to identify the occurrence of such degradation pathways would not be feasible due to their ubiquitous presence in subsurface environments. Nevertheless, it is important to clearly identify the fate of reductive dechlorination intermediates in order to assess the feasibility and the efficacy of natural attenuation of chlorinated ethenes. This thesis explored the possibilities and limits of the use of compound-specific stable isotope analysis to document and to quantify the progress of *in situ* reductive dechlorination of chlorinated ethenes. The thesis focused particularly on the identification of the fate of reductive dechlorination intermediates such as *cis*-dichloroethene (cDCE) and vinyl chloride (VC) because the fate of these compounds determine the feasibility of natural attenuation at a chlorinated-ethene contaminated site. In addition, factors influencing the occurrence of complete reductive dechlorination of chlorinated ethenes (hydrological, geochemical, and microbial) were investigated.

8.1 Conclusions

8.1.1 Assessment of natural attenuation of chlorinated ethenes

Field investigations at Angus and Rødekro sites confirm that carbon isotope analysis is a reliable tool to identify whether an intermediate compound of sequential reductive dechlorination of chlorinated ethenes is accumulating or further degrading under extremely dynamic hydrological and geochemical conditions (Angus site) and even when the transformation rates are very slow as indicated by the presence of a long plume (Rødekro site). The method is based on the principle that the carbon isotope signature of an accumulating intermediate progressively approaches that of the original parent compound because all carbons in the ethene backbone are preserved during the course of reductive dechlorination. Based on this approach, it was demonstrated at the Angus site that at some locations ethene is the final product while at other locations it is further reduced to ethane as indicated by the carbon isotope ratio of ethene which was greater than the original tetrachloroethene (PCE). At the Rødekro site, cDCE mostly accumulates except

at the plume front where the isotope ratio of cDCE becomes greater than that of the source PCE. The carbon isotope ratio of cDCE remains fairly constant over the approximately 1-km-long mid-section of the plume, suggesting cDCE accumulation although cDCE concentrations decrease sharply. Hence, the approach can also assist in determining that a compound is not further degrading and that the observed concentration decrease is due to the effect of dispersion, which would suggest that active remediation efforts is necessary. This approach, however, requires *a priori* knowledge of the source carbon isotope ratio. If the source carbon isotope ratio is not known or in case of mixed sources, it may be possible to estimate the source carbon isotope ratio by calculating the carbon isotope mass balance among all chlorinated ethene species near the source zone. Furthermore, it has to be taken into account that under non-steady conditions, sorption can indirectly affect the isotope ratios of intermediate products (van Breukelen *et al.* 2005).

Carbon isotope analysis of chlorinated ethenes can also indicate the occurrence of alternative degradation pathways such as oxidative degradation, further reduction to ethane and to methane, and chemical reduction. The approach is based on the fact that the total carbon isotope ratios of chlorinated ethenes and ethene remain constant as long as reductive dechlorination is the only active transformation pathway. Alternative degradation pathways are accompanied by the loss of carbons from the pool of chlorinated ethenes and ethene; hence, the total carbon isotope ratios will deviate from the source ratio. At the Rødekro site, the total carbon isotope ratios at the plume front become greater than the source ratio, suggesting the possibility of either anaerobic oxidation of cDCE or complete reductive dechlorination despite the absence of ethene and ethane at detectable levels. This approach only indicates the possibility of alternative pathway and cannot identify the responsible reaction pathway. Therefore, carbon isotope analysis alone cannot identify the responsible degradation pathway because of the effect of dispersion which in itself decreases the contaminant concentration, hence, hinders the estimation of a pathway- and compound-specific isotope enrichment factor.

The dual isotope analysis is a promising tool to identify the on-going degradation pathway at field scales (Zwank *et al.* 2005). It is because the approach does not depend on the contaminant concentrations. The laboratory study demonstrated that the ratio between the observed carbon and chlorine isotope fractionations is different for reductive dechlorination and aerobic oxidation; hence, the approach was employed at the Rødekro site. It determined that cDCE is further transformed by reductive dechlorination since significant chlorine isotope fractionation was observed while oxidative reactions are not expected to give rise to such a significant chlorine isotope fractionation. However, the observed ratio between carbon and chlorine isotope fractionations at Rødekro site is greater than the ratio obtained from the laboratory study, which would require further investigations.

8.1.2 Quantification of natural attenuation

The interpretation of field isotope data based on the Rayleigh isotope fractionation model has been proposed to estimate the extent of degradation and the first-order degradation rate in previous studies (Richnow *et al.* 2003; Morrill *et al.* 2005). However, the model is based on an assumption of a well-mixed and closed system where mass balance is maintained, which contradicts the subsurface system. Hence, it is expected that the Rayleigh-type estimated values deviate from the true values. Therefore, the degree of deviations for the estimation of the extent of degradation and the degradation rate was systematically quantified. In general, the Rayleigh-type quantification of the extent of degradation and the degradation rate underestimates the true values by up to 40% under typical flow conditions at contaminated aquifers. The magnitude of underestimation increases with the increasing dominance of dispersion over advection in flow conditions. However, the estimation uncertainty associated with the Rayleigh-type quantification of the degradation rate is significantly lower than field concentration-based methods which can overestimate the rate by up to orders of magnitude because concentration-based methods are affected by the unknown effect of dispersion and the assumption associated with the alignment of sampling wells along the plume centerline. In addition, with the knowledge of local flow conditions at a site, the degree of underestimation can be corrected based on the systematic type-curves presented in the thesis. Although the study was based on a 2D analytical solution, a numerical study to integrate the effect of physical and geochemical heterogeneities on the degree of underestimation should be feasible using the same approach.

Due to the simultaneous degradation and transformation of reaction intermediates during reductive dechlorination of chlorinated ethenes, the Rayleigh-type quantification method does not apply to estimate the degradation rates of transformation intermediates. Therefore, a set of three-dimentional analytical solutions was employed to estimate the reductive dechlorination rate at the Rødekro site. The isotope approach confirmed that the only active degradation pathway is reductive dechlorination, which implies that the summed molar concentrations of all chlorinated ethenes and ethene can be considered as a quasi-conservative tracer to calibrate the flow and transport models. After the calibration of flow and transport model based on the tracer data at the Rødekro site, the estimated dechlorination rates based on the concentration data of individual chlorinated ethene species are greater than the rates estimated based on the carbon isotope data especially for cDCE and VC by up to one order of magnitude due probably to the unknown effect of dispersion. Although the concentrations of cDCE and VC are relatively low, carbon isotope ratios of cDCE and VC progressively increase due to their large isotope enrichment factors. Hence, carbon isotope analysis can depict even a small change in their isotope ratios, and consequently the quantification method based on the isotope data is capable of estimating even a very low transformation rate.

8.1.3 Limiting step during reductive dechlorination

The interpretation of field carbon isotope data at the Angus and Rødekro sites demonstrate the occurrence of cDCE accumulation, but the field isotope data do not indicate the occurrence of VC accumulation but support the active degradation of VC instead. Hence, these two field investigations suggest that the limiting transformation step during reductive dechlorination at these sites is the dechlorination of cDCE to VC, and that the reductive dechlorination of VC to ethene is not as limiting as previously expected. The thermodynamic considerations (Heimann and Jakobsen 2006) also agree with the field observations that the reductive dechlorination of cDCE and VC can occur almost concomitantly.

8.1.4 Factors influencing the progress of reductive dechlorination

Carbon isotope analysis provides clear documentation of the progress of reductive dechlorination at Angus and Rødekro sites, which facilitates the comparison of different field parameters in terms of their influence on the progress of reductive dechlorination. In general, the progress of reductive dechlorination is controlled by the availability of electron donor species (generally H_2), the presence of competing electron acceptors (redox conditions) and the presence of appropriate microorganisms such as *Dehalococcoides* (Bradley 2000). Although the concentrations of H_2 were not analyzed, the presence of sedimentary organic matter (SOM) is associated with H_2 availability as the elevated level of SOM increases the possibility of the occurrence of fermentation which yields H_2 as a result. At the Angus site, investigated locations with relatively high SOM levels are accompanied by the complete reductive dechlorination of chlorinated ethenes and the further reduction of ethene to ethane.

In terms of the redox conditions, locations with elevated SOM levels where ethane is present are under methanogenic conditions at the Angus site. Under sulfate-reducing conditions both cDCE accumulation and complete reductive dechlorination to ethene are possible as observed at Angus site. The different fate of cDCE under the same redox condition is probably due to the fact that the two locations have different flow conditions. Under relatively fast flow conditions, cDCE accumulation was observed due to the insufficient residence time of the interstitial water. In contrast, complete reductive dechlorination took place under extremely slow flow conditions which lead to a long residence time of the water. Therefore, given a sufficiently long residence time, complete reductive dechlorination can take place under sulfate-reducing conditions even when the SOM as a carbon source to produce H_2 are relatively low. The identification of redox conditions at a chlorinated-ethene contaminated site is helpful for speculating the possible progress of reductive dechlorination; however, the occurrence of complete reductive dechlorination is driven by a complex interaction between geochemical and hydrological conditions which are difficult to foresee. Hence, the geochemical parameters alone can not conclusively provide the evidence for the progress of reductive dechlorination at field scales. Assessing the progress of

reductive dechlorination of chlorinated ethenes requires investigations of other parameters such as stable isotope ratios of individual species.

At the Angus site, the presence of *Dehalococcoides* in the streambed sediment was investigated for the extracted DNA and RNA with the taxon-specific PCR primers. Locations with elevated SOM levels and the presence of ethane contain variable levels *Dehalococcoides* whereas the location under sulfate-reducing condition with the presence of ethene dose not. Therefore, the absence of *Dehalococcoides* based on the PCR analysis should not be considered as the evidence for the inability of the site to undergo complete reductive dechlorination of chlorinated ethenes especially because of the constrains from the detection limit.

8.2 PRACTICAL IMPLICATIONS

The robustness of the isotope approach was demonstrated at very different hydrological and geochemical settings at the Angus and Rødekro sites. In addition, the quantification of the extent of degradation and the degradation rate is not strongly affected by the plume geometry. The isotope approach is particularly valuable for the cDCE-accumulating site to determine the possibility of alternative degradation pathways of cDCE by calculating the combined carbon isotope ratios of all chlorinated ethenes present at a site. With isotope approach, the quantification of a trace level of cDCE transformation is possible as demonstrated at Rødekro site where other concentration-based quantification methods would misleadingly overestimate the cDCE transformation rate due to the unknown effect of dispersion.

One of the locations at the Angus site where *Dehalococcoides* is detected has elevated concentrations of ethane but do not contain chlorinated ethenes or ethene. Therefore, due to the possibility of the further reduction of ethene to ethane under strongly reducing conditions, the analysis of ethane should be included in the assessment of reductive dechlorination of chlorinated ethenes.

At a cDCE-accumulating site with low VC concentrations, the dechlorination rate of VC can be greater than that of cDCE as estimated at the Rødekro site. However, the very low cDCE dechlorination already indicates that the process takes place only at redox micro-environments where conditions favor cDCE dechlorination to VC. As the two field investigations suggest that the reductive dechlorination of cDCE and VC occurs almost simultaneously, such redox micro-environments would also allow VC dechlorination to ethene and further to ethane. At cDCE-accumulating site, the cDCE rate estimation is based on the bulk cDCE while the VC rate estimation is based only on the processes at micro-environments. Therefore, the greater VC dechlorination rate estimated at such sites does not translate into a general statement that the dechlorination of VC is faster than that of cDCE.

In addition to the use of the isotope approach to assess the progress of natural attenuation, the approach is also applicable for the follow-up monitoring of active remediation measures such as

biostimulation (Song *et al.* 2002), bioaugmentation, chemical oxidation (Hunkeler *et al.* 2003) and the use of reactive barriers (Dayan *et al.* 1999; Schüth *et al.* 2003). The isotope approach relies on the transformation of the contaminant; hence, the approach is not relevant for remediation measures which do not involve with the transformation. As compound-specific isotope analysis is an investigation tool which can document and quantify the degradation of organic contaminants, the same principles apply for its use in assessing the performance of active remediation measures. For the active source treatment, the monitoring of the source isotope ratio over time can suggest whether the treatment is effective or not. With respect to plume remediation, it is important to measure the isotope ratios before the start of a remediation measure. However, the quantification of the extent of degradation and the degradation rate may be complicated particularly for chlorinated ethenes due to the possibility of a mixed isotope signature caused by a newly produced daughter product with light isotope ratios.

The quantification of dechlorination rates based on the use of summed chlorinated-ethene concentrations as a quasi-conservative tracer is also relevant for the chlorinated-ethene contaminated sites where field isotope data are not available but the possibility of alternative degradation pathways is excluded by other investigation methods. The presence of intrinsic tracer data significantly improves the estimated flow and transport parameters, and consequently the estimated dechlorination rates.

8.3 OUTLOOK

Further investigation is necessary for the application of dual isotope approach for sequential reductive dechlorination. The ratio between carbon and chlorine isotope enrichment factors from the laboratory studies was quite similar to the theoretical estimate; however, the ratio obtained from the Rødekro site was larger than the theoretical estimate. It may be caused by the difference in the chlorine isotope ratios of cDCE. The laboratory study demonstrated substantial chlorine isotope fractionation during the reductive dechlorination of cDCE, which suggest that the preceding dechlorination steps (from PCE to cDCE via TCE) also involve chlorine isotope fractionation. As a result, cDCE present at the Rødekro site is expected to be more enriched in ^{37}Cl than the commercially manufactured cDCE used in the laboratory study, and the difference in the starting chlorine isotope ratios may influence the observed isotope effect.

Anaerobic oxidation of VC and cDCE is reported, but the corresponding enrichment factors are not yet known. Although a similar mechanism involving the initial epoxidation step is generally assumed, it needs to be clarified and the magnitude of carbon and chlorine isotope effects needs to be identified to increase the knowledge of isotope fractionation patterns of chlorinated ethenes.

With respect to the quantification of reaction rates based on the field isotope data, the effect of physical heterogeneity was assessed by the various degree of dispersion. The study illustrated the general underestimation trend; however, the approach was based on an analytical solution which assumes a

homogeneous medium. Therefore, more vigorous numerical studies to incorporate a series of generated heterogeneous media would further clarify the level of uncertainties associated with the isotope approach in subsurface environments, particularly for the case in which a preferential flow path is present.

References:

Abe, Y. and D. Hunkeler (2006). "Does the Rayleigh equation apply to evaluate field isotope data in contaminant hydrology?" Environmental Science and Technology **40**(5): 1588-1596.

Aelion, C. M. (1996). "Impact of aquifer sediment grain size on petroleum hydrocarbon distribution and biodegradation." Journal of Contaminant Hydrology **22**: 109-121.

Albrechtsen, H. J., B. L. Bjerg, L. Ludvigsen, K. Rügge and T. H. Christensen (1999). "An anaerobic field injection experiment in a landfill leachate plume, Grindsted, Denmark 2. Deduction of anaerobic (methanogenic, sulfate- and Fe(III)-reducing) redox conditions." Water Resources Research **35**(4): 1247-1256.

Allan, J. D. (1995). Stream Ecology: Structure and function of running waters. Dordrecht, The Netherlands, Kluwer Academic Publishers.

Anderson, M. P. (2005). "Heat as a ground water tracer." Ground Water **43**(6): 951-968.

Appelo, C. A. J. and D. Postma (2005). Geochemistry, groundwater and pollution. Leiden, The Netherlands, A.A. Balkema Publishers.

Aziz, C. E., C. J. Newell, J. R. Gonzales, P. E. Haas, T. P. Clement and Y. Sun (2000). BIOCHLOR natural attenuation decision support system: User's manual version 1.1. Washington DC, U.S. EPA Office of Research and Development.

Bagley, D. M. and J. M. Gossett (1990). "Tetrachloroethene transformation to trichloroethene and cis-1,2-dichloroethene by sulfate-reducing enrichment cultures." Applied and Environmental Microbiology **56**(8): 2511-2561.

Barth, J. A. C., G. F. Slater, C. Schüth, M. Bill, A. Downey, M. J. Larkin and R. M. Kalin (2002). "Carbon isotope fractionation during aerobic biodegradation of trichloroethene by *Burkholderia cepacia* G4: a tool to map degradation mechanisms." Applied and Environmental Microbiology **68**(4): 1728-1734.

Bass, D. H., N. A. Hastings and R. A. Brown (2000). "Performance of air sparging systems: a review of case studies." Journal of Hazardous Materials **72**: 101-119.

Bedient, P. B., H. S. Rifai and C. J. Newell (1999). Ground Water Contamination Transport and Remediation. NJ, Prentice-Hall PTR.

Behar, F., V. Beaumont and H. L. D. Penteado (2001). "Rock-Eval 6 technology: Performances and developments." Oil and Gas Science Technology **56**: 111-134.

Beller, H. R. (2000). "Metabolic indicators for detecting in situ anaerobic alkylbenzene degradation." Biodegradation **11**(2-3): 125-139.

Beyer, C., C. Chen, J. Gronewold, O. Kolditz and S. Bauer (2007). "Determination of first-order degradation rate constants from monitoring networks." Ground Water **45**: Online Early Article.

Bloom, Y., R. Aravena, D. Hunkeler, E. Edwards and S. K. Frape (2000). "Carbon isotope fractionation during microbial dechlorination of trichloroethene, *cis*-1,2-dichloroethene, and vinyl chloride: Implications for assessment of natural attenuation." Environmental Science and Technology **34**(13): 2768-2772.

Böckelmann, A., T. Ptak and G. Teutsch (2001). "An analytical quantification of mass fluxes and natural attenuation rate constants at a former gasworks site." Journal of Contaminant Hydrology **53**: 429-453.

Böckelmann, A., D. Zamfirescu, T. Ptak, P. Grathwohl and G. Teutsch (2003). "Quantification of mass fluxes and natural attenuation rates at an industrial site with a limited monitoring network: a case study." Journal of Contaminant Hydrology **60**: 97-121.

Boopathy, R. and R. Peters (2001). "Enhanced biotransformation of trichloroethylene under mixed electron acceptor conditions." Current Microbiology **42**: 134-138.

Borden, R. C., R. A. Daniel, L. E. LeBrun IV and C. W. Davis (1997). "Intrinsic biodegradation of MTBE and BTEX in a gasoline-contaminated aquifer." Water Resources Research **33**(5): 1105-1115.

Bourg, A. C. M. and C. Bertin (1993). "Biogeochemical processes during the infiltration of river water into an alluvial aquifer." Environmental Science and Technology **27**(4): 661-666.

Bradley, P., J. Landmeyer and R. Dinocola (1998). "Anaerobic oxidation of [1,2-^{14}C] dichloroethene under Mn(IV)-reducing conditions." Applied Environmental Microbiology **64**: 1560-1562.

Bradley, P. M. (2000). "Microbial degradation of chloroethenes in groundwater systems." Hydrogeology Journal **8**: 104-111.

Bradley, P. M. (2003). "History and ecology of chloroethene biodegradation: A review." Bioremediation Journal **7**(2): 81-109.

Bradley, P. M. and F. H. Chapelle (1996). "Anaerobic mineralization of vinyl chloride in Fe(III)-reducing aquifer sediments." Environmental Science and Technology **30**: 2084-2086.

Bradley, P. M. and F. H. Chapelle (1997). "Kinetics of DCE and VC mineralization under methanogenic and Fe(III)-reducing conditions." Environmental Science and Technology **31**(9): 2692-2696.

Bradley, P. M. and F. H. Chapelle (1998). "Effect of contaminant concentration on aerobic microbial mineralization of DCE and VC in stream-bed sediments." Environmental Science and Technology **32**(5): 553-557.

Bradley, P. M. and F. H. Chapelle (1998). "Microbial mineralization of VC and DCE under different terminal electron accepting conditions." Anaerobe **4**: 81-87.

Bradley, P. M. and F. H. Chapelle (1999). "Methane as a product of chloroethene biodegradation under methanogenic conditions." Environmental Science and Technology **33**: 653-656.

Bradley, P. M. and F. H. Chapelle (2000). "Acetogenic microbial degradation of vinyl chloride." Environmental Science and Technology **34**: 2761-2763.

Bradley, P. M. and F. H. Chapelle (2000). "Aerobic microbial mineralization of dichloroethene as sole carbon substrate." Environmental Science and Technology **34**: 221-223.

Bradley, P. M., F. H. Chapelle and D. R. Lovley (1998). "Humic acids as electron acceptors for anaerobic microbial oxidation of vinyl chloride and dichloroethene." Applied and Environmental Microbiology **64**(8): 3102-3105.

Bradley, P. M., F. H. Chapelle and J. T. Wilson (1998). "Field and laboratory evidence for intrinsic biodegradation of vinyl chloride contamination in a Fe(III)-reducing aquifer." Journal of Contaminant Hydrology **31**: 111-127.

Brauner, J. S. and M. A. Widdowson (2001). "Numerical simulation of a natural attenuation experiment with a petroleum hydrocarbon NAPL source." Ground Water **39**(6): 939-952.

Bundesamt für Umwelt (2004). Wald und Landschaft/Bundesamt für Wasser und Geologie (Hrsg.) NAQUA - Grundwasserqualität in der Schweiz 2002/2003. Bern**:** 204.

Buscheck, T. E. and C. M. Alcantar (1995). Regression techniques and analytical solutions to demonstrate intrinsic bioremediation. Proceedings of the 1995 Battelle International Conference on In Situ and On site Bioremediation, Columbus, OH, USA, Battelle Press.

Butler, E. C. and K. F. Hayas (1999). "Kinetics of the transformation of trichloroethylene and tetrachloroethylene by iron sulfide." Environmental Science and Technology **33**: 2021-2027.

Chapelle, F. H., P. M. Bradley, D. R. Lovley and D. A. Vroblesky (1996). "Measuring rates of biodegradation in a contaminated aquifer using field and laboratory methods." Ground Water **34**(4): 691-698.

Chapman, S. W., B. L. Parker, J. A. Cherry, R. Aravena and D. Hunkeler (2007). "Groundwater-surface water interaction and its role on TCE groundwater plume attenuation." Journal of Contaminant Hydrology **91**: 203-232.

Charbeneau, R. J. (2000). Groundwater Hydraulics and Pollutant Transport. Upper Saddle River, NJ, Prentice-Hall, Inc.

Chartrand, M. M. G., A. Waller, T. E. Mattes, M. Elsner, G. Lacrampe-Couloume, J. M. Gossett, E. A. Edwards and B. Scherwood Lollar (2005). "Carbon isotopic fractionation during aerobic vinyl chloride degradation." Environmental Science and Technology **39**: 1064-1070.

Christensen, T. H., P. L. Bjerg, S. A. Banwart, R. Jakobsen, G. Heron and H. J. Albrechtsen (2000). "Characterization of redox conditions in groundwater contaminant plumes." Journal of Contaminant Hydrology **45**: 165-241.

Christensen, T. H., P. Kjeldsen, P. L. Bjerg, D. L. Jensen, J. B. Christensen, A. Baun, H. J. Albrechtsen and G. Heron (2001). "Biogeochemistry of landfill leachate plumes." Applied Geochemistry **16**: 659-718.

Chu, K., S. Mahendra, D. L. Song, M. E. Conrad and L. Alvares-Cohen (2004). "Stable carbon isotope fractionation during aerobic biodegradation of chlorinated ethenes." Environmental Science and Technology **38**: 3126-3130.

Clark, I. D. and P. Fritz (1997). Environmental isotopes in hydrogeology. Boca Raton, Florida, USA, Lewis Publishers.

Clement, T. P., C. D. Johnson, Y. Sun, G. M. Klecka and C. Bartlett (2000). "Natural attenuation of chlorinated ethene compounds: model development and field-scale application at the Dover site." Journal of Contaminant Hydrology **42**: 113-140.

Coleman, N. V., T. E. Mattes, J. M. Gossett and J. C. Spain (2002). "Biodegradation of *cis*-dichloroethene as the sole carbon source by a β-Proteobacterium." Applied and Environmental Microbiology **68**(8): 2726-2730.

Coleman, N. V., T. E. Mattes, J. M. Gossett and J. C. Spain (2002). "Phylogenetic and kinetic diversity of aerobic vinyl chloride-assimilating bacteria from contaminated sites." Applied and Environmental Microbiology **68**(12): 6162-6171.

Coleman, N. V. and J. C. Spain (2003). "Distribution of the coenzyme M pathway of epoxide metabolism among ethene- and vinyl chloride-degrading *Mycobacterium* strains." Applied and Environmental Microbiology **69**(10): 6041-6046.

Coleman, N. V. and J. C. Spain (2003). "Epoxyalkane:coenzyme M tansferase in the ethene and vinyl chloride biodegradation pathways of *Mycobacterium* Strain JS60." Journal of Bacteriology **185**(18): 5536-5545.

Conant, B. J. (2004). "Delineating and quantifying ground water discharge zones using streambed temperatures." Ground Water **42**(2): 243-257.

Conant, B. J., J. A. Cherry and R. W. Gillhan (2004). "A PCE groundwater plume discharging to a river: influence of the streambed and near-river zone on contaminant distributions." Journal of Contaminant Hydrology **73**: 249-279.

Cornaton, F. (2004). Deterministic models of groundwater age, life expectancy & transit time distributions in advective-dispersive systems (Ph.D thesis), University of Neuchâtel, Switzerland.

Cozzarelli, I. M., B. A. Bekins, M. J. Baedecker, G. R. Aiken, R. P. Eganhouse and M. E. Tuccillo (2001). "Progression of natural attenuation processes at a crude-oil spill site: I. Geochemical evolution of the plume." Journal of Contaminant Hydrology **53**: 369-385.

Cupples, A. M., A. M. Spormann and P. L. McCarty (2003). "Growth of a *Dehalococcoides*-like microorganism on vinyl chloride and *cis*-dichloroethene as electron acceptors as determined by competitive PCR." Applied and Environmental Microbiology **69**(2): 953-959.

Cvetkovic, V. and G. Dagan (1994). "Transport of kinetically sorbing solute by steady random velocity in heterogeneous porous formations." Journal of Fluid Mechanics **265**: 189-215.

Dagan, G. (1988). "Time-dependent macrodispersion for solute transport in anisotropic heterogeneous aquifers." Water Resources Research **24**(13): 2031-2046.

Dagan, G. (1989). Flow and transport in porous formations, Springer-Verlag Heidelberg Berlin, New York.

Davis, J. W. and C. L. Carpenter (1990). "Aerobic biodegradation of vinyl chloride in groundwater samples." Applied and Environmental Microbiology **56**: 3870-3880.

Dayan, H., T. A. Abrajano Jr, N. C. Sturchio and L. Winsor (1999). "Carbon isotopic fractionation during reductive dehalogenation of chlorinated ethenes by metallic iron." Organic Geochemistry **30**: 755-763.

de Bruin, W. P., M. J. J. Kotterman, M. A. Posthumus, G. Schraa and A. J. B. Zehnder (1992). "Complete biological reductive transformation of tetrachloroethene to ethane." Applied and Environmental Microbiology **58**(6): 1996-2000.

DiStefano, T. D., J. M. Gossett and S. H. Zinder (1991). "Reductive dechlorination of high concentrations of tetrachloroethene to ethene by an anaerobic enrichment culture in the absence of methanogenesis." Applied and Environmental Microbiology **57**(8): 2287-2292.

Domenico, P. A. (1987). "An analytical model for multidimensional transport of a decaying contaminant species." Journal of Hydrology **91**: 49-58.

Domenico, P. A. and G. A. Robbins (1984). "A dispersion scale effect in model calibration and field tracer experiments." Journal of Hydrology **70**: 123-132.

Duhamel, M. and E. Edwards (2006). "Microbial composition of chlorinated ethene-degrading cultures dominated by *Dehalococcoides*." FEMS Microbiology Ecology **58**(3): 538-549.

Einarson, M. D. and D. M. Mackay (2001). "Predicting impacts of groundwater contamination-A new framework for prioritizing environmental site cleanups considers the interaction of contaminant plumes with water supply wells." Environmental Science and Technology **35**: 66A-73A.

Elshahed, M. S., L. M. Gieg, M. J. Mcinerney and J. M. Suflita (2001). "Signature metabolites attesting to the in situ attenuation of alkylbenzenes in anaerobic environments." Environmental Science and Technology **35**: 682-689.

Elsner, M., L. Zwank, D. Hunkeler and R. P. Schwarzenbach (2005). "A new concept linking observable stable isotope fractionation to transformation pathways of organic pollutants." Environnemental Science and Technology **39**(18): 6896-6916.

Epspitalié, J., G. Deroo and F. Marquis (1985). "La pyrolyse Rock-Eval et ses applications." Revue de l'Institut Français du Pétrole **40**(563-579).

Fennell, D. E., A. B. Carroll, J. M. Gossett and S. H. Zinder (2001). "Assessment of indigenous reductive dechlorinating potential at a TCE-contaminated site using microcosms, polymerase chain reaction analysis, and site data." Environmental Science and Technology **35**: 1830-1839.

Finkel, M., R. Liedl and G. Teutsch (1998). "Modelling surfactant influenced PAH migration." Physical, Chemical & Earth Sciences **23**(2): 245-250.

Fleckenstein, J. H., R. G. Niswonger and G. E. Fogg (2006). "River-aquifer interactions, geologic heterogeneity and low-flow management." Ground Water.

Flynn, S. J., F. E. Loffler and J. M. Tiedje (2000). "Microbial community changes associated with a shift from reductive dechlorination of PCE to reductive dechlorination of *cis*-DCE and VC." Environmental Science and Technology **34**(1056-1061).

Fox, B. G., J. G. Borneman, L. P. Wackett and J. D. Lipscomb (1990). "Haloalkene oxidation by the soluble methane monooxygenase from *Methylosinus trichosporium* OB3b: mechanistic and environmental implications." Biochemistry **29**(6419-6427).

Freedman, D. L. and J. M. Gossett (1989). "Biological reductive dechlorination of tetrachloroethylene and trichloroethylene to ethylene under methanogenic conditions." Applied and Environmental Microbiology **55**(9): 2144-2151.

Friis, A. K., H. J. Albrechtsen, E. Cox and B. L. Bjerg (2006). "The need for bioaugmentation after thermal treatment of a TCE-contaminated aquifer: Laboratory experiments." Journal of Contaminant Hydrology **88**: 235-248.

Garabedian, S. P., D. R. LeBlanc, L. W. Gelhar and M. A. Celia (1991). "Large-scale natural gradient tracer test in sand and gravel, Cape Cod, Massachusetts, 2, Analysis of spatial moments for a nonreactive tracer." Water Resources Research **27**(5): 911-924.

Gelhar, L. W., C. Welty and K. R. Rehfeldt (1992). "A critical review of data on field-scale dispersion in aquifers." Water Resources Research **28**: 1955-1974.

Gentry, T. J., C. Rensing and I. L. Pepper (2004). "New approaches for bioaugmentation as a remediation technology." Critical Reviews in Environmental Science and Technology **34**(5): 447-494.

Glod, G., U. Brodmann, C. Holliger and R. Schwarzenbach (1997). "Cobalamin-mediated reduction of *cis*- and *trans*-dichloroethene, 1,1-dichloroethene, and vinyl chloride in homogeneous aqueous solution: Reaction kinetics and mechanistic considerations." Environmental Science and Technology **31**: 3154-3160.

Griebler, C., M. Safinowski, A. Vieth, H. H. Richnow and R. U. Meckenstock (2004). "Combined application of stable carbon isotope analysis and specific metabolites determination for assessing in site degradation of aromatic hydrocarbons in a tar oil-contaminated aquifer." Environmental Science and Technology **38**: 617-631.

Griebler, C., M. Safinowski, A. Vieth, H. H. Richnow and R. U. Meckenstock (2004). "Combined application of stable carbon isotope analysis and specific metabolites determination for assessing In site degradation of aromatic hydrocarbons in a tar oil-contaminated aquifer." Environmental Science and Technology **38**: 617-631.

Guilbeault, M. A., B. L. Parker and J. A. Cherry (2005). "Mass and flux distributions from DNAPL zones in sandy aquifers." Ground Water **43**(1): 70-86.

Guyonnet, D. and C. Neville (2004). "Dimensionless analysis of two analytical solutions for 3-D solute transport in groundwater." Journal of Contaminant Hydrology **75**: 141-153.

Hadim, A., F. F. Shah and G. P. Korfiatis (1993). "Laboratory studies of steam tripping of NAPL-contaminated soils." Journal of Soil Contamination **2**: 37-58.

Hamby, D. M. (1996). "Site remediation techniques supporting environmental restoration activities - a review." The Science of the Total Environment **191**: 203-224.

Harkness, M., A. A. Bracco, M. J. Brennan, K. A. Deweerd and J. L. Spivach (1999). "Use of bioaugmentation to stimulate complete reductive dechlorination of trichloroethene in Dover soil columns." Environmental Science and Technology **33**(7): 1100-1109.

Harrington, R. R., S. R. Poulson, J. I. Drever, P. J. S. Colberg and E. F. Kelly (1999). "Carbon isotope systematics of monoaromatic hydrocarbons: vaporization and adsorption experiments." Organic Geochemistry **30**(8A): 765-775.

Hartmans, S. and J. A. M. de Bont (1992). "Aerobic vinyl chloride metabolism in *Mycobacterium aurum* L1." Applied and Environmental Microbiology **58**: 1220-1226.

Hartmans, S., deBont. JAM., J. Tramper and K. Luyben (1985). "Bacterial degradation of vinyl chloride." Biotechnology Letters **7**: 383-388.

Hartmans, S., A. Kaptein, J. Tramper and J. A. M. de Bont (1992). "Characterization of a *Mycobacterium* sp. and a *Xanthobacter* sp. for the removal of vinyl chloride and 1,2-dichloroethane from waste gases." Applied Microbiology and Biotechnology **37**: 796-801.

Haston, Z. C. and P. L. McCarty (1999). "Chlorinated ethene half-velocity coefficients (K_s) for reductive dehalogenation." Environmental Science and Technology **33**(2): 223-226.

He, J., K. M. Ritalahti, M. R. Aiello and F. E. Loffler (2003). "Complete detoxification of vinyl chloride by an anaerobic enrichment culture and identification of the reductively dechlorinating population as a *Dehalococcoides* species." Applied and Environmental Microbiology **69**(2): 996-1003.

Hedeselskabet (2005). Sonjeriyllands Amt. Tidligere renseri, Clip Rens, Fladhojvej 1, Rødekro. Kortlaegning af forureningsspredning**:** 697.

Heimann, A. C. and R. Jakobsen (2006). "Experimental evidence for a lack of thermodynamic control on hydrogen concentrations during anaerobic degradation of chlorinated ethenes." Environmental Science and Technology **40**(11): 3501-3507.

Hendrickson, E. R., J. Payne, R. M. Young, M. G. Starr, P. M.P., S. Fahnestock, D. E. Ellis and R. C. Ebersole (2002). "Molecular analysis of Dehalococcoides 16S ribosomal DNA from chloroethene-contaminated sites throughout North America and Europe." Applied and Environmental Microbiology **68**(2): 485-495.

Heraty, L. J., M. E. Fuller, L. Huang, T. A. Abrajano Jr and N. C. Sturchio (1999). "Isotope fractionation of carbon and chlorine by microbial degradation of dichloromethane." Organic Geochemistry **30**: 793-799.

Herfort, M. and T. Ptak (2002). "Multitracer-Versuch im kontaminierten Grundwasser des Testfeldes Sud." Grundwasser(1): 31-40.

Heron, G., S. Carroll and S. G. Nielsen (2005). "Full-scale removal of DNAPL constituents using steam-enhanced extraction and electrical resistance heating." Ground Water Monitoring and Remediation **25**(4): 92-107.

Hess, K. M., S. H. Wolf and M. A. Celia (1992). "Large-scale natural gradient tracer test in sand and gravel, Cape Cod, Massachusetts 3. Hydraulic conductivity variability and calculated macrodispersivities." Water Resources Research **28**(8): 2011-2027.

Hirschorn, S. K., M. J. Dinglasan, M. Elsner, S. A. Mancini, G. Lacrampe-Couloume, E. A. Edwards and B. Sherwood Lollar (2004). "Pathway dependent isotopic fractionation during aerobic biodegradation of 1,2-dichloroethane." Environmental Science and Technology **38**: 4775-4781.

Hoelen, T. P. and M. Reinhard (2004). "Complete biological dehalogenation of chlorinated ethylenes in sulfate containing groundwater." Biodegradation **15**: 395-403.

Holliger, C., G. Schraa, A. J. M. Stams and A. J. B. Zehnder (1993). "A highly purified enrichment culture couples the reductive dechlorination of tetrachloroethne to growth." Applied and Environmental Microbiology **59**: 2991-2997.

Holliger, C., G. Wohlfarth and G. Diekert (1999). "Reductive dechlorination in the energy metabolism of anaerobic bacteria." FEMS Microbiology Reviews **22**: 383-398.

Hopkins, G. D. and P. L. McCarty (1995). "Field-evaluation of in-situ aerobic cometabolism of trichloroethylene and 3 dichloroethylene isomers using phenol and toluene as the primary substrates." Environmental Science and Technology **29**(6): 1628-1637.

Hunkeler, D., N. Andersen, R. Aravena, S. M. Bernasconi and B. J. Butler (2001). "Hydrogen and carbon isotope fractionation during aerobic biodegradation of benzene." Environmental Science and Technology **35**: 3462-3467.

Hunkeler, D. and R. Aravena (2000). "Evidence of substantial carbon isotope fractionation among substrate, inorganic carbon, and biomass during aerobic mineralization of 1,2-dichloroethane by *Xanthobacter autotrophicus*." Applied and Environmental Microbiology **66**(11): 4870-4876.

Hunkeler, D., R. Aravena and B. J. Butler (1999). "Monitoring microbial dechlorination of tetrachloroethene (PCE) in groundwater using compound-specific stable carbon isotope ratios: Microcosm and field studies." Environmental Science and Technology **33**: 2733-2738.

Hunkeler, D., R. Aravena and E. Cox (2002). "Carbon isotopes as a tool to evaluate the origin and fate of vinyl chloride: Laboratory experiments and modeling of isotope evolution." Environmental Science and Technology **36**: 3378-3384.

Hunkeler, D., N. Chollet, X. Pittet, R. Aravena, J. A. Cherry and B. L. Parker (2004). "Effect of source variability and transport processes on carbon isotope ratios of TCE and PCE in two sandy aquifers." Journal of Contaminant Hydrology **74**: 265-282.

Hutzler, N. J., B. E. Murphy and J. S. Gierke (1991). "State of technology review - Soil vapor extraction systems." Journal of Hazardous Materials **26**(3): 336-229.

Istok, J. D., M. D. Humphrey, M. H. Schroth and M. R. Hyman (1997). "Single-well, "push-pull" test for in situ determination of microbial activities." Ground Water **35**(4): 619-631.

Jawitz, J. W., R. K. Sillan, M. D. Annable, P. S. C. Rao and K. Warner (2000). "In situ alcohol flushing of a DNAPL source zone at a dry cleaner site." Environmental Science and Technology **34**: 3722-3729.

Johnson, R. L., P. C. Johnson, D. B. McWhorter, R. E. Hinchee and I. Goodman (1993). "An overview of in situ air sparging." Ground Water Monitoring and Remediation **13**(4): 127-135.

Kao, C. M. and Y. S. Wang (2001). "Field investigation of the natural attenuation and intrinsic biodegradation rates at an underground storage tank site." Environmental Geology **40**(4-5): 622-631.

Khan, F. I., T. Husain and R. Hejazi (2004). "An overview and analysis of site remediation technologies." Journal of Environmental Management **71**: 95-122.

Kjeldsen, P. (1993). "Groundwater pollution source characterization of an old landfill." Journal of Hydrology **142**: 349-371.

Klier, N. J., R. J. West and P. A. Donberg (1999). "Aerobic biodegradation of dichloroethylenes in surface and subsurface soils." Chemosphere **38**(5): 1175-1188.

Koene-Cottaar, F. H. M. and G. Schraa (1998). "Anaerobic reduction of ethene to ethane in an enrichment culture." FEMS Microbiology Ecology **25**: 251-256.

Kolhatkar, R., T. Kuder, P. Philip, J. Allen and J. T. Wilson (2002). "Use of compound-specific stable carbon isotope analyses to demonstrate anaerobic biodegradation of MTBE in groundwater at a gasoline release site." Environmental Science and Technology **36**(23): 5139-5146.

Komatsu, T., K. Momonoi, T. Matsuo and K. Hanaki (1994). "Biotransformation of *cis*-1,2-dichloroetheylene to ethylene and ethane under anaerobic conditions." Water Science and Technology **30**(7): 75-84.

Kopinke, F. D., A. Georgi, M. Voskamp and H. H. Richnow (2005). "Carbon isotope fractionation of organic contaminants due to retardation on humic substances: Implications for natural attenuation studies in aquifers." Environmental Science and Technology **39**(16): 6052-6062.

Kuder, T., J. T. Wilson, P. Kaiser, R. Kolhatkar, P. Philp and J. Allen (2005). "Enrichment of stable carbon and hydrogen isotopes during anaerobic biodegradation of MTBE: Microcosm and field evidence." Environmental Science and Technology **39**(1): 213-220.

LeBlanc, D. R., S. P. Garabedian, K. M. Hess, L. W. Gelhar, R. D. Quadri, K. G. Stollenwerk and W. W. Wood (1991). "Large-scale natural gradient tracer test in sand and gravel, Cape Cod, Massachusetts, 1, Experimental design and observed tracer movement." Water Resources Research **27**(5): 895-910.

Lee, W. and B. Batchelor (2002). "Abiotic reductive dechlorination of chlorinated ethylenes by iron-bearing soil minerals. 1. Pyrite and Magnetite." Environmental Science and Technology **36**: 5147-5154.

Lee, W. and B. Batchelor (2004). "Abiotic reductive dechlorination of chlorinated ethylenes by iron-bearing phyllosilicates." Chemosphere **56**: 999-1009.

Lenda, A. and A. Zuber (1970). Tracer dispersion in groundwater experiments. Symposium on the use of isotopes in Hydrology, Vienna, I.A.E.A.

Lewandowicz, A., J. Rudzinski, L. Tronstad, M. Widersten, P. Ryberg, O. Matsson and P. Paneth (2001). "Chlorine kinetic isotope effects on the haloalkane dehalogenase reaction." Journal of American Chemistry Society **123**: 4550-4555.

Ling, M. and H. S. Rifai (2007). "Modeling natural attenuation with source control at a chlorinated solvents dry cleaner site." Ground Water Monitoring and Remediation **27**(1): 108-121.

Little, C. D., A. V. Palumbo, S. E. Herbes, M. E. Lidstrom, R. L. Tyndall and P. J. Gilmer (1988). "Trichloroethylene biodegradation by a methane-oxidizing bacterium." Applied and Environmental Microbiology **54**(4): 951-956.

Loffler, F. E., K. M. Rithlahti and J. M. Tiedje (1997). "Dechlorination of chloroethenes is inhibited by 2-bromoethanesulfonate in the absence of methanogens." Applied and Environmental Microbiology **1997**(12): 4982-4985.

Loffler, F. E., Q. Sun, J. Li and J. M. Tiedje (2000). "16S rRNA gene-based detection of tetrachloroethene (PCE)-dechlorinating *Desulfuromonas* and *Dehalococcoides* species." Applied and Environmental Microbiology **66**: 1369-1374.

Lorah, M. M. and L. D. Olsen (1999). "Natural attenuation of chlorinated volatile organic compounds in a freshwater tidal wetland: Field evidence of anaerobic biodegradation." Water Resources Research **35**(12): 3811-3827.

Lu, G., T. Prabhakar Clement, C. Zheng and T. H. Wiedemeier (1999). "Natural attenuation of BTEX compounds: Model development and field-scale application." Ground Water **37**(5): 707-717.

Lu, X., J. T. Wilson and D. H. Kampbell (2006). "Relationship between *Dehalococcoides* DNA in ground water and rates of reductive dechlorination at field scale." Water Research **40**: 3131-3140.

Lunn, M., R. J. Lunn and R. Mackay (1996). "Determining analytic solutions of multiple species contaminant transport with sorption and decay." Journal of Hydrology **180**: 195-210.

Mackay, D. M. and J. A. Cherry (1989). "Groundwater contamination: pump-and-treat remediation." Environmental Science and Technology **26**(6): 630-636.

Magnuson, J. K., R. V. Stern, J. M. Gossett, S. H. Zinder and D. R. Burris (1998). "Reductive dechlorination of tetrachloroethene to ethene by a two-component enzyme pathway." Applied and Environmental Microbiology **64**(4): 1270-1275.

Mancini, S. A., G. Lacrampe-Couloume, H. Jonker, B. M. van Breukelen, J. Groen, F. Volkering and B. Sherwood Lollar (2002). "Hydrogen isotopic enrichment: An indicator of biodegradation at a petroleum hydrocarbon contaminated field site." Environmental Science and Technology **36**(11): 2464-2470.

Mancini, S. A., A. C. Ulrich, G. Lacrampe-Couloume, B. Sleep, E. A. Edwards and B. Sherwood Lollar (2003). "Carbon and hydrogen isotopic fractionation during anaerobic biodegradation of benzene." Applied and Environmental Microbiology **69**(1): 191-198.

Maymo-Gatell, X., T. Anguish and S. H. Zinder (1999). "Reductive dechlorination of chlorinated ethenes and 1,2-dichloroethane by "*Dehalococcoides ethenogenes*" 195." Applied and Environmental Microbiology **65**(7): 3108-3113.

Maymo-Gatell, X., Y. T. Chien, J. M. Gossett and S. H. Zinder (1997). "Isolation of a bacterium that reductively dechlorinates tetrachloroethene to ethene." Science **276**: 1568-1571.

Maymo-Gatell, X., V. Tandoi, J. M. Gossett and S. H. Zinder (1995). "Characterization of an H_2-utilizing enrichment culture that reductively dechlorinates tetrachloroethene to vinyl chloride and ethene in the absence of methanogenesis and acetogenesis." Applied and Environmental Microbiology **61**: 3928-3933.

McCray, J. E. (2000). "Mathematical modeling of air sparging for subsurface remediation: state of the art." Journal of Hazardous Materials **72**: 237-263.

McGuire, T. M., J. M. McDade and C. J. Newell (2006). "Performance of DNAPL source depletion technologies at 59 chlorinated solvent-impacted sites." Ground Water Monitoring and Remediation **26**(1): 73-84.

Meckenstock, R. U., B. Morasch, C. Griebler and H. H. Richnow (2004). "Stable isotope fractionation analysis as a tool to monitor biodegradation in contaminated aquifers." Journal of Contaminant Hydrology **75**: 215-255.

Meckenstock, R. U., B. Morasch, M. Kastner, A. Vieth and H. H. Richnow (2002). "Assessment of bacterial degradation of aromatic hydrocarbons in the environment by analysis of stable carbon isotope fractionation." Water, Air, and Soil Pollution: Focus **2**: 141-152.

Meckenstock, R. U., B. Morasch, R. Warthmann, B. Schink, E. Annweiler, W. Michaelis and H. H. Richnow (1999). "$^{13}C/^{12}C$ stable isotope fractionation of aromatic hydrocarbons during microbial degradation." Environmental Microbiology **1**(5): 409-414.

Moran, M. J., J. S. Zogorski and P. J. Squillace (2007). "Chlorinated solvents in groundwater of the United States." Environmental Science and Technology **41**: 71-81.

Morasch, B., H. H. Richnow, B. Schink, A. Vieth and R. U. Mechenstock (2002). "Carbon and hydrogen stable isotope fractionation during aerobic bacterial degradation of aromatic hydrocarbons." Applied and Environmental Microbiology **68**(10): 5191-5194.

Morasch, B., H. H. Richnow, A. Vieth, B. Schink and R. U. Meckenstock (2004). "Stable isotope fractionation caused by glycyl radical enzymes during bacterial degradation of aromatic compounds." Applied and Environmental Microbiology **70**(5): 2935-2940.

Morrice, J. A., H. M. Valett, C. N. Dahm and M. E. Campana (1997). "Alluvial characteristics of groundwater-surface water exchange and hydrological retention in headwater streams." Hydrological Processes **11**: 253-267.

Morrill, P. L., G. Lacrampe-Couloume, G. F. Slater, B. Sleep, E. A. Edwards, M. L. McMaster, D. W. Major and B. Sherwood Lollar (2005). "Quantifying chlorinated ethene degradation during reductive dechlorination at Kelly AFB using stable carbon isotopes." Journal of Contaminant Hydrology **76**: 279-293.

Müller, J. A., B. M. Rosner, G. von Abendroth, G. Meshulam-Simon, P. L. McCarty and A. M. Spormann (2004). "Molecular identification of the catabolic vinyl chloride reductase from *Dehalococcoides* sp. strain VS and its environmental distribution." Applied and Environmental Microbiology **70**(8): 4880-4888.

Nelson, M. J. K., S. O. Montgomery, W. R. Mahaffey and P. H. Pritchard (1987). "Biodegradation of trichloroethylene and involvement of an aromatic biodegradative pathway." Applied and Environmental Microbiology **53**: 949-954.

Newell, C. J., R. K. McLeod and J. Gonzales (1996). BIOSCREEN Natural Attenuation Decision Support System. Washington DC, U.S. EPA Office of Research and Development.

Nijenhuis, I., J. Andert, K. Beck, M. Kastner, G. Diekert and H. H. Richnow (2005). "Stable Isotope Fractionation of tetrachloroethene during reductive dechlorination by *Sulfurospirillum multivorans* and *Desulfitobacterium* sp. strain PCE-S and abiotic reactions with cyanocobalamin." Applied and Environmental Microbiology **71**(7): 3413-3419.

Northrop, D. B. (1977). Determining the absolute magnitude of hydrogen isotope effects. Isotope effects on enzyme-catalyzed reactions. W. W. Cleland, M. H. O'Leary and D. D. Northrop. Baltimore, USA, University Park Press.

Oldenhuis, R., L. J. M. R. Vink, D. B. Janssen and B. Withold (1989). "Degradation of chlorinated aliphatic hydrocarbons by *Methlosinus trichosporium* OB3b expressing soluble methane monooxygenase." Applied and Environmental Microbiology **55**: 2819-2826.

Ovreas, L., L. Forney, F. L. Daae and V. Torsvik (1997). "Distribution of bacterioplankton in meromictic Lake Saelenvannet, as determined by denaturing gradient gel electrophoresis of PCR-amplified gene fragments coding for 16S rRNA." Applied and Environmental Microbiology **63**: 3367-3373.

Pankow, A. and J. A. Cherry (1996). Dense chlorinated solvents and other DNAPLs in groundwater. Waterloo, Canada, Waterloo Press.

Pavlostathis, S. G. and P. Zhuang (1993). "Reductive dechlorination of chloroalkenes in microcosms developed with a field contaminated soil." Chemosphere **27**(4): 585-595.

Pennell, K. D., M. Jin, L. M. Abriola and G. A. Pope (1994). "Surfactant-enhanced remediation of soil columns contaminated by residual tetrachloroethylene." Journal of Contaminant Hydrology **16**: 35-53.

Peter, A., A. Steinbach, R. Liedl, T. Ptak, W. Michaelis and G. Teutsch (2004). "Assessing microbial degradation of *o*-xylene at field-scale from the reduction in mass flow rate combined with compound-specific isotope analyses." Journal of Contaminant Hydrology **71**: 127-154.

Pittet, X. (2001). Use of stable carbon isotopes to identify multiple sources and biodegradation of tetrachloroethene in a sandy aquifer in Angus, Canada. Neuchâtel, Switzerland, Centre d'hydrogéologie, Université de Neuchâtel.

Postma, D., C. Boesen, H. Kristiansen and F. Larsen (1991). "Nitrate reduction in an unconfined sandy aquifer: Water chemistry, reduction processes, and geochemical modeling." Water Resources Research **27**(8): 2027-2045.

Postma, D. and B. S. Brockenhuus-Schack (1987). "Diagenesis of iron in proglacial sand deposits of late- and post-Weichselian age." Journal of Sedimentary Petrology **57**(6): 1040-1053.

Rajaram, H. and L. W. Gelhar (1995). "Plume-scale dependent dispersion in aquifers with a wide range of scales of heterogeneity." Water Resources Research **31**(10): 2469-2482.

Rasche, M. E., R. E. Hicks, M. R. Hyman and D. J. Arp (1990). "Biodegradation of halogenated hydrocarbon fumigants by nitrifying bacteria." Applied and Environmental Microbiology **56**: 2568-2571.

Rasche, M. E., M. R. Hyman and D. J. Arp (1990). "Oxidation of monohalogenated ethanes and *n*-chlorinated alkanes by whole cells of *Nitrosomonas europaea*." Journal of Bacteriology **172**(5368-5373).

Reitzel, L. A. (2005). Quantification of Natural Attenuation using Analytical-Chemical Tools. Environment & Resources, Technical University of Denmark. Ph.D dissertation.

Richardson, J. R. and J. W. Nicklow (2002). "*In situ* permeable reactive barriers for groundwater contamination." Soil and Sediment Contamination **11**(2): 241-268.

Richnow, H. H., E. Annweiler, W. Michaelis and R. U. Meckenstock (2003). "Microbial in situ degradation of aromatic hydrocarbons in a contaminated aquifer monitored by carbon isotope fractionation." Journal of Contaminant Hydrology **65**: 101-120.

Richnow, H. H., R. U. Meckenstock, L. A. Reitzel, A. Baun, A. Ledin and T. H. Christensen (2003). "In situ biodegradation determined by carbon isotope fractionation of aromatic hydrocarbons in an anaerobic landfill leachate plume (Vejen, Denmark)." Journal of Contaminant Hydrology **64**: 59-72.

Rügge, K., B. L. Bjerg, J. K. Pedersen, H. Mosbæk and T. H. Christensen (1999). "An anaerobic field injection experiment in a landfill leachate plume, Grindsted, Denmark 1. Experimental setup, tracer movement, and fate of aromatic and chlorinated compounds." Water Resources Research **35**(4): 1231-1246.

Rügner, H., M. Finkel, A. Kaschl and M. Bittens (2006). "Application of monitored natural attenuation in contaminated land management - A review and recommended approach for Europe." Environmental Science and Policy **9**: 568-576.

Sager, B. (1982). "Dispersion in three dimensions: approximate analytical solutions." ASCE, Journal of Hydraulics Division **108 (HY1)**: 47-62.

Salanitro, J. P., P. C. Johnson, G. E. Spinnler, P. M. Maner, H. L. Wisniewski and C. Bruce (2000). "Field scale demonstration of enhanced MTBE bioremediation through aquifer bioaugmentation and oxygenation." Environmental Science and Technology **34**(19): 4152-4162.

Schafer, W. (2001). "Predicting natural attenuation of xylene in groundwater using a numerical model." Journal of Contaminant Hydrology **52**(1-4): 57-83.

Schippers, A. and B. B. Jørgensen (2001). "Oxidation of pyrite and iron sulfide by manganese dioxide in marine sediments." Geochimica et Cosmochimica Acta **65**(6): 915-922.

Schippers, A. and B. B. Jørgensen (2002). "Biogeochemistry of pyrite and iron sulfide oxidation in marine sediments." Geochimica et Cosmochimica Acta **66**(1): 58-92.

Schnarr, M., C. Truax, G. Farquhar, E. Hood, T. Gonullu and B. Stickney (1998). "Laboratory and controlled field experiments using potassium permanganate to remediate trichloroethylene and perchloroethylene DNAPLS in porous media." Journal of Contaminant Hydrology **29**: 205-224.

Schulze-Makuch, D. (2005). "Longitudinal dispersivity data and implications for scaling behavior." Ground Water **43**(3): 443-456.

Schüth, C., H. Taubald, N. Balano and K. Maciejczyk (2003). "Carbon and hydrogen isotope effects during sorption of organic contaminants on carbonaceous materials." Journal of Contaminant Hydrology **64**: 269-281.

Schwarzenbach, R., W. Giger, E. Hoehn and J. K. Schnelder (1983). "Behavior of organic compounds during infiltration of river water to groundwater. Field studies." Environmental Science and Technology **17**(8): 472-479.

Schwarzenbach, R., P. Gschwend and D. Imboden (2003). Environmental organic chemistry. New York, USA, John Wiley & Sons.

Sherwood Lollar, B., G. F. Slater, J. Ahad, B. Sleep, J. Spivach, M. Brennan and P. MacKenzie (1999). "Contrasting carbon isotope fractionation during biodegradation of trichlorothylene and toluene: Implications for intrinsic bioremediation." Organic Geochemistry **30**: 813-820.

Sherwood Lollar, B., G. F. Slater, B. Sleep, M. Witt, G. M. Klecka, M. Harkness and J. Spivack (2001). "Stable carbon isotope evidence for intrinsic bioremediation of tetrachloroethene and trichlorothene at Area 6, Dover Air Force Base." Environmental Science and Technology **35**(2): 261-269.

Shouakar-Stash, O., R. J. Drimmie, M. Zhang and S. K. Frape (2006). "Compound-specific chlorine isotope ratios of TCE, PCE and DCE isomers by direct injection using CF-IRMS." Applied Geochemistry **21**: 766-781.

Slater, G. F., J. M. E. Ahad, B. Scherwood Lollar, R. Allen-King and B. Sleep (2000). "Carbon isotope effects resulting from equilibrium sorption of dissolved VOCs." Analytical Chemistry **72**(5669-5672).

Slater, G. F., B. Sherwood Lollar, B. Sleep and E. A. Edwards (2001). "Variability in carbon isotope fractionation during biodegradation of chlorinated ethenes: Implications for field applications." Environmental Science and Technology **35**: 901-907.

Soga, K., J. W. E. Page and T. H. Illangasekare (2004). "A review of NAPL source zone remediation efficiency and the mass flux approach." Journal of Hazardous Materials **110**: 13-27.

Song, D. L., M. E. Conrad, K. S. Sorenson and L. Alvarez-Cohen (2002). "Stable carbon isotope fractionation during enhanced in situ bioremediation of trichloroethene." Environmental Science and Technology **36**: 2262-2268.

Song, D. L., M. E. Conrad, K. S. Sorenson and L. Alverez-Cohen (2002). "Stable carbon isotope fractionation during enhanced in situ bioremediation of trichloroethene." Environmental Science and Technology **36**: 2262-2268.

Squillace, P. J., M. J. Moran, W. W. Lapham, C. V. Price, R. M. Clawges and J. S. Zogorski (1999). "Volatile organic compounds in untreated ambient groundwater of the United States, 1985-1995." Environmental Science and Technology **33**(23): 4176-4187.

Srinivasan, V., T. P. Clement and K. K. Lee (2007). "Domenico Solution-Is it valid?" Ground Water **45**(2): 136-146.

Stehmeiner, L. G., M. M. Francis, T. R. Jack, E. Diegor, L. Winsor and T. A. Abrajano Jr (1999). "Field and in vitro evidence for in-situ bioremediation using compound-specific $^{13}C/^{12}C$ ratio monitoring." Organic Geochemistry **30**: 821-833.

Steinbach, A., R. Seifert, E. Annweiler and W. Michaelis (2004). "Hydrogen and carbon isotope fractionation during anaerobic biodegradation of aromatic hydrocarbons-A field study." Environmental Science and Technology **38**(2): 609-616.

Stenback, G. A., S. Kee Ong, S. W. Rogers and B. H. Kjartanson (2004). "Impact of transverse and longitudinal dispersion on first-order degradation rate constant estimation." Journal of Contaminant Hydrology **73**: 3-14.

Sturchio, N. C., J. K. Bohlke, A. D. Beloso, S. H. Streger, L. J. Heraty and P. B. Hatzinger (2007). "Oxygen and chlorine isotope fractionation during perchlorate biodegradation: Laboratory results and implications for forensics and natural attenuation studies." Environmental Science and Technology(2796-2802).

Sturchio, N. C., J. L. Clausen, L. J. Heraty, L. Huang, B. D. Holt and T. A. Abrajano Jr (1998). "Chlorine isotope investigation of natural attenuation of trichloroethene in an aerobic aquifer." Environmental Science and Technology **32**(20): 3037-3042.

Sun, Y., J. N. Petersen and T. P. Clement (1999). "Analytical solutions for multiple species reactive transport in multiple dimensions." Journal of Contaminant Hydrology **35**: 429-440.

Thornton, S. F., D. N. Lerner and S. A. Banwart (2001). "Assessing the natural attenuation of organic contaminants in aquifers using plume-scale electron and carbon balances: model development with analysis of uncertainty and parameter sensitivity." Journal of Contaminant Hydrology **53**: 199-232.

Tong, W. and Y. Rong (2002). "Estimation of methyl *tert*-butyl ether plume length using the Domenico analytical model." Environmental Forensics **3**: 81-87.

Tsien, H. C., G. A. Brussaue, R. S. Hanson and L. P. Wackett (1989). "Biodegradation of trichloroethylene by *Methylosinus trichosporium* OB3b." Applied and Environmental Microbiology **55**: 3155-3161.

USEPA (1991). Superfund NPL Characterization Project: National Results., Environmental Protection Agency, Office of Emergency and Remedial Response.

USEPA (2003). 2001 Toxics Release Inventory Public Data Release Report: 260-R-03-001, Office of Environmental Information: Washington DC.

van Breukelen, B. M., D. Hunkeler and F. Volkering (2005). "Quantification of sequential chlorinated ethene degradation by use of a reactive transport model incorporating isotope fractionation." Environmental Science and Technology **39**(11): 4189-4197.

van Genuchten, M., T. (1985). "Convective-dispersive transport of solutes involved in sequential first-order decay reactions." Computational Geosciences **11**(2): 129-147.

van Hylckama Vlieg, J. E. T., W. de Koning and D. B. Janssen (1996). "Transformation kinetics of chlorinated ethenes by *Methylosinus trichosporium* OB3b and detection of unstable epoxides by on-line gas chromatography." Applied and Environmental Microbiology **62**: 3304-3312.

van Hylckama Vlieg, J. E. T., K. Kingma, A. J. van den Wijngaard and D. B. Janssen (1998). "A glutathione *S*-transferase with activity towards *cis*-dichloroepoxyethane is involved in isoprene utilization by *Rhodococcus* sp. strain AD45." Applied and Environmental Microbiology **64**: 2800-2805.

Vannelli, T., M. Logan, D. M. Arciero and A. B. Hooper (1990). "Degradation of halogenated aliphatic compounds by the ammonia-oxidizing bacterium *Nitrosomonas europaea*." Applied and Environmental Microbiology **56**: 1169-1171.

Verce, M. F., R. L. Ulrich and D. L. Freedman (2000). "Characterization of an isolate that uses vinyl chloride as a growth substrate under aerobic conditions." Applied and Environmental Microbiology **66**(8): 3535-3542.

Verce, M. F., R. L. Ulrich and D. L. Freedman (2001). "Transition from cometabolic to growth-linked biodegrdtaion of vinyl chloride by a *Pseudomonas* sp. isolated on ethene." Environmental Science and Technology **35**(21): 4242-4251.

Vieth, A., J. Müller, G. Strauch, M. Kästner, M. Gehre, R. U. Meckenstock and H. H. Richnow (2003). "In-situ biodegradation of tetrachloroethene and trichloroethene in contaminated aquifers monitored by stable isotope fractionation." Isotopes Environmental and Health Studies **39**(2).

Vogel, T. M., C. S. Criddle and P. L. McCarty (1987). "Transformation of halogenated aliphatic compounds." Environmental Science and Technology **21**(8): 722-736.

Vogel, T. M. and P. L. McCarty (1985). " Biotransformation of tetrachloroethylene to trichloroethylene, dichloroethylene, vinyl chloride, and carbon dioxide under methanogenic conditions." Applied and Environmental Microbiology **49**(5): 1080-1083.

Vogel, T. M. and P. L. McCarty (1985). "Biotransformation of tetrachloroethylene to trichloroethylene, dichloroethylene, vinyl chloride, and carbon dioxide under methanogenic conditions." Applied and Environmental Microbiology **49**(5): 1080-1083.

Vroblesky, D. A., L. C. Rhodes, J. F. Robertson and J. A. Harrigan (1996). "Locating VOC contamination in a fractured-rock aquifer at the ground-water/surface-water interface using passive vapor collectors." Ground Water **34**(2): 223-230.

Wackett, L. P. and D. T. Gibson (1988). "Degradation of trichloroethylene by toluene dioxygenase in whole-cell studies with *Pseudomonas putida* F1." Applied and Environmental Microbiology **54**: 1703-1708.

Weber, W. J. J. and F. A. DiGiano (1996). Process dynamics in environmental systems. N.Y., John Wiley & Sons, Inc.

West, M. R., B. H. Kueper and M. J. Ungs (2007). "On the use and error of approximation in the Domenico (1987) solution." Ground Water **45**(2): 126-135.

Wexler, E. J. (1992). Analytical solutions for one-, two, and three-dimensional solute transport in groundwater systems with uniform flow, Techniques of Water Resources Investigations of the United States Geological Survey.

Wiedemeier, T. H., H. S. Rifai, C. J. Newell and J. T. Wilson (1997). Natural Attenuation of Fuels and Chlorinated Solvents in the Subsurface. New York, John Wiley & Sons, Inc.

Williams, G. M., I. Harrison, C. A. Carlick and O. Crowley (2003). "Changes in enantiomeric fraction as evidence of natural attenuation of mecoprop in a limestone aquifer." Journal of Contaminant Hydrology **64**(3-4): 253-267.

Witt, M. E., G. M. Klecka, E. J. Lutz, T. A. Ei, N. R. Grosso and F. H. Chapelle (2002). "Natural attenuation of chlorinated solvents at Area 6, Dover Air Force Base: groundwater biogeochemistry." Journal of Contaminant Hydrology **57**: 61-80.

Woessner, W. W. (2000). "Stream and fluvial plain ground water interactions: Rescaling hydrogelogic thought." Ground Water **38**(3): 423-429.

Yang, Y. and P. L. McCarty (1998). "Competition for hydrogen within a chlorinated solvent dehalogenating anaerobic mixed cultures." Environmental Science and Technology **32**(22): 3591-3597.

Yaws, C. L. (1999). Chemical properties handbook. New York City, McGraw-Hill.

Zhang, Y.-K. and R. C. Heathcote (2003). "An improved method for estimation of biodegradation rate with field data." Ground Water Monitoring and Remediation **23**(3): 112-116.

Zhou, M. and R. D. Rhue (2000). "Screening commercial surfactants suitable for remediating DNAPL source zones by solubilization." Environmental Science and Technology **34**: 1985-1990.

Zipper, C., M. J. F. Sater, S. B. Haderlein, M. Gruhl and H. P. E. Kohler (1998). "Changes in the enantiomeric ratio of (R)- to (S)-mecoprop indicate in situ biodegradation of this chiral herbicide in a polluted aquifer." Environmental Science and Technology **32**(14): 2070-2076.

Zwank, L., M. Berg, M. Elsner, T. C. Schmidt, R. Schwarzenbach and S. B. Haderlein (2005). "New evaluation scheme for two-dimensional isotope analysis to decipher biodegradation processes: Application to groundwater contamination by MTBE." Environmental Science and Technology **39**(4): 1018-1029.

Zwank, L., M. Berg, M. Elsner, T. C. Schmidt, R. P. Schwarzenbach and S. B. Haderlein (2005). "New evaluation scheme for two-dimensional isotope analysis to decipher biodegradation processes: Application to groundwater contamination by MTBE." Environmental Science and Technology **39**: 1018-1029.

Appendix A

Effect of molecule size on carbon isotope fractionation during biodegradation of chlorinated alkanes by *Xanthobacter autotrophicus* GJ10

Yumiko Abe, Jakob Zopfi and Daniel Hunkeler
Submitted to Isotopes in Environmental and Health Studies

Abstract

The effect of the number of carbon and chlorine atoms on carbon isotope fractionation during haloalkanes dechlorination by *Xanthobacter autotrophicus* GJ10 was studied with C2-C4 chlorinated alkanes using pure culture and cell-free extract experiments. The magnitude of carbon isotope fractionation quantified by the Rayleigh equation decreased with increasing carbon number. The decrease can be explained by an increasing probability that the heavy isotope is located at a non-reactive position for increasing molecule size. The isotope data were corrected for the number of carbons as well as the number of reactive sites to obtain reactive-site-specific values denoted as apparent kinetic isotope effect (AKIE). Even after the correction, the obtained AKIE values varied. Cell-free extract experiments were carried out to evaluate the effect of transport across the cell membrane on the observed variability in the AKIE values, and revealed that the variability still persisted. The study demonstrates that even after differences related to the carbon number and structure of the molecule are taken into account, there still remain differences in AKIE values even for compounds that are degraded by the same pure culture and an identical reaction mechanism.

A.1 INTRODUCTION

Stable isotope fractionation analysis is used increasingly to assess *in situ* biodegradation of organic compounds in contaminated subsurface environments (Hunkeler *et al.* 1999; Sherwood Lollar and Slater 2001; Song *et al.* 2002; Vieth *et al.* 2003). The quantitative evaluation of isotope data requires reliable values for isotope fractionation factors. There are a number of laboratory studies that determined isotope fractionation factors for the degradation of different organic compounds such as chlorinated ethenes (Hunkeler *et al.* 1999; Bloom *et al.* 2000; Slater *et al.* 2001; Hunkeler *et al.* 2002; Chu *et al.* 2004; Chartrand *et al.* 2005), methyl tert-butyl ether (Hunkeler *et al.* 2001; Gray *et al.* 2002; Kuder *et al.* 2005) and monoaromatic hydrocarabons (Meckenstock *et al.* 1999; Stehmeier *et al.* 1999; Hunkeler *et al.* 2001; Morasch *et al.* 2001; Morasch *et al.* 2002; Mancini *et al.* 2003; Morasch *et al.* 2004). The concentration and isotope data are usually evaluated using the Rayleigh distillation equation (Mariotti *et al.* 1981). The resulting isotope fractionation factors are denoted as *bulk* isotope fractionation factors since they are based on the average isotope ratio of the whole molecule. For enzyme studies, the observed isotope fractionation is the result of a *kinetic isotope effect* (KIE) during the first irreversible transformation step (O'Leary 1977). The isotope effect associated with this step is usually referred to as *intrinsic isotope effect* (Northrop 1977) where the enzymatic reaction rate for the light isotope is faster than that of the heavy isotope. In general, the observed bulk isotope effect is smaller than the intrinsic isotope effect for several reasons. First, the heavy isotopes may not be located at the reactive position; thus, the molecule, even if a heavy isotope is present, may react at the same rate as molecules without a heavy isotope (Elsner *et al.* 2005)]. Second, if the catalytic step is fast compared to the preceding binding steps, the intrinsic isotope effect will be partly masked (Northrop 1977). The relative velocity of reactive to binding steps is often expressed as the *commitment to catalysis* which corresponds to the ratio between the rate of the catalytic step to the rate of substrate-enzyme dissociation step (Northrop 1977). The larger the commitment to catalysis, the smaller is the observed isotope fractionation. Third, as in the binding steps on the enzymatic level, the rate-limiting transport of a substrate to an enzyme can lower the observed isotope effect as previously shown for reductive dehalogenation of PCE (Nijenhuis *et al.* 2005). Finally for a given reaction mechanism acting on different substrates, the intrinsic isotope effect may vary due to the differences in the structure of the transition state (Huskey 1991), leading to variable degrees of observed isotope fractionation even if all other factors are identical.

The main objective of this study was to evaluate experimentally how bulk isotope fractionation factors are related to the carbon number and molecular structure (number of reactive sites). It is expected that an increase in the carbon number influences the bulk isotope fractionation primarily in two ways: By lowering the probability that the heavy isotope is in the reactive position, and possibly by slowing down

the transfer through the cell membrane to the enzyme due to its increased bulkiness. Previous studies investigated the effect of carbon number on isotope fractionation during biodegradation of aromatic compounds by different microorganisms that all make use of the same initial transformation reaction (Morasch *et al.* 2004). Even after correction for carbon numbers, the isotope effect expressed in terms of isotope enrichment factors varied by a factor of nine, which may be due to differences in the properties of the enzyme of different organisms. In contrast to this study, we investigated the variation of isotope fractionation of different compounds degraded by the same pure culture. Haloalkane degradation by *Xanthobacter autothrophicus* GJ10, which had been characterized in detail in previous studies (Janssen *et al.* 1985; Keuning *et al.* 1985; van den Wijngaard *et al.* 1993; Verschueren *et al.* 1993; Schanstra *et al.* 1996; Lightstone *et al.* 1998), was chosen as a model system for two reasons. First, transformation of haloalkane by *Xanthobacter autotrophicus* GJ10 is associated with a substantial carbon isotope effect as previously shown for the degradation of 1,2-dichloroethane (1,2-DCA) (Hunkeler and Aravena 2000). Thus, even if the isotope effect decreases with increasing carbon chain length, it should still be possible to measure the perhaps subtle difference in the isotope effect with a relatively high precision. Second, the haloalkane dehalogenase responsible for the initial transformation step is known to degrade haloalkanes of variable size with one or two reactive positions by hydrolytic dehalogenation using an identical S_N2 mechanism (Janssen *et al.* 1985; van den Wijngaard *et al.* 1993); hence, it allows direct comparison of the isotope effect on the degradation of haloalkanes with different numbers of carbon atoms and reactive sites.

The studies involved experiments with the pure culture and corresponding cell-free extracts. Bulk isotope fractionation factors were determined using the classical Rayleigh equation and varied as a function of molecular size and structure evaluated. To gain additional insight into the origin of observed variations, the obtained isotope data were corrected for the dilution due to non-reactive positions and multiple reactive sites to obtain the bond-specific *apparent kinetic isotope effect* (AKIE) using a procedure recently proposed by Elsner et al. (2005). The results of pure culture and cell-free extract studies were compared to evaluate the influence of transport across the cell membrane on the observed variation in isotope effects.

A.2 MATERIALS AND METHODS

A.2.1 Bacterial growth conditions

Xanthobacter autotrophicus GJ10 was obtained from D.B. Janssen (Department of Biochemistry, University of Groningen, Groningen, the Netherlands). The growth medium was prepared as described in Hunkeler and Aravena (2000). Cultures were grown in 250-mL glass bottles, which contained 180mL of medium and were capped with Mininert-Valves (Vici Precision Sampling, Baton Rouge, LA.). Growth was monitored by measuring the decreasing substrate concentrations and the optical density at 570 nm.

A.2.2 Culture experiments

Four haloalkanes, 1,2-DCA (≥99.5% purity, $\delta^{13}C_0$ = -28.50±0.12‰, with uncertainty corresponding to the standard deviation of five replicate measurements), 1-chloropropane (CP) (≥99.5% purity, $\delta^{13}C_0$ = -33.70 ± 0.15‰), 1,3-dichloropropane (DCP) (≥98% purity, $\delta^{13}C_0$ = -19.36 ± 0.18‰) and 1-chlorobutane (CB) (≥99.5% purity, $\delta^{13}C_0$ = -26.80 ± 0.14‰) were obtained from Fluka, Switzerland, and used for degradation experiments. Initial isotope ratios were determined after dissolution of the compound in growth medium as described below in analytical methods. Cultures were incubated at 24°C under continuous shaking, and they were kept upside down to prevent the leakage of gas phase through the valve. Cultures used for experiments always received the same haloalkane and transferred three times to the fresh medium prior to the experiment. All experiments were carried out in triplicate for each haloalkane. For concentration and $\delta^{13}C$ analyses of substrates, aqueous samples were taken and preserved with NaN_3 (final concentration of 1% weight to weight). In general, concentrations and isotope ratios were monitored until the concentration had decreased by more than 3 orders of magnitude.

A.2.3 Preparation of cell-free extracts

Cells of 1 L of exponentially-growing *X. autotrophicus* GJ10 culture were harvested by centrifugation (10 min at 10,000 x g), washed once with 10mM Tris sulfate buffer (pH 7.5), centrifuged again, and resuspended in the same buffer as described in Janssen *et al.* (Janssen *et al.* 1985). Ultrasonic disruption (Branson Sonifier 450) of the cells was performed in a pulse manner of 30 s duration (1 pulse per s) in an ice-water bath until the cell lysis was visually confirmed by microscopy. Cell-free extracts were finally obtained after centrifugation at 45,000 x g for 30 min in the supernatant phase.

Protein content of cell-free extracts was determined by the micro-biurette method (Goa 1953).

A.2.4 Cell-free extract experiments

The cell-free extract was added until a final protein concentration of 0.3 mg/mL into 50 mM Tris sulfate buffer containing 0.5 mM of substrate in a 120mL glass bottle with a Teflon cap. The experiments were performed at 24°C in bottles without headspace and under constant magnetic stirring. Immediately after the cell-free extracts were introduced into the buffer, samples were withdrawn by a sterile syringe and analyzed for the initial concentration and $\delta^{13}C_0$ as described below. During the experiments, samples for concentrations and $\delta^{13}C$ were taken and measured immediately.

A.2.5 Analytical methods

Aqueous concentrations and carbon isotope ratios were measured using a Thermo Finnigan Trace gas chromatograph (GC) coupled to a Thermo Finnigan Delta Plus XP isotope-ratio mass spectrometer (IRMS) via a combustion interface set to 940°C (Thermo Finnigan, Bremen, Germany). The GC was equipped with a DB-5 column (30m x 0.32 mm) and a Tekmar Velocity Purge and Trap system (Tekmar Dohrmann). Samples from both pure culture and cell-free extract studies were diluted with deionized

water to a final volume of 20 mL. Samples were purged for 10 min and the compounds were retained on a VOCARB trap at room temperature. Compounds were desorbed for 3 min at 245°C, condensed in a cryogenic unit at -100°C, and injected splitless into the GC-C-IRMS system. The GC oven temperature program was 70°C for 2 min, 15°C/min to 220°C, and 220°C for 4 min. Based on repeated measurements of 4 external standards, the standard uncertainty of the concentration was estimated to be 7%. Aqueous concentrations were determined based on the calibration curve with four standards. Carbon isotope ratios are reported in the δ-notation:

$$\delta^{13}C = (\frac{R}{R_{std}} - 1) \cdot 1000 \quad ‰ \tag{1}$$

where R and R_{std} are the carbon isotope ratios of the sample and the VPDB standard, respectively.

A.2.6 Calculations

Isotope fractionation during the biodegradation of haloalkanes was quantified using the Rayleigh equation to yield bulk isotope enrichment factors (Mariotti *et al.* 1981; Clark and Fritz 1997) as follows:

$$\ln(\frac{R}{R_0})_{bulk} = \ln \frac{\left(1000 + \delta^{13}C\right)}{\left(1000 + \delta^{13}C_0\right)} = \frac{\varepsilon_{bulk}}{1000} \cdot \ln f \tag{2}$$

where R is the isotope ratio ($^{13}C/^{12}C$), R_o the initial isotope ratio, $\delta^{13}C$ the measured isotope ratio, $\delta^{13}C_o$ the measured initial isotope ratio, ε_{bulk} the bulk isotope enrichment factor for the whole molecule, and f the fraction of substrate remaining. The isotope enrichment factors were quantified by least square linear regression according to equation 2 without forcing the regression through the origin (Scott *et al.* 2004)]. The bulk isotope enrichment factor is related to the bulk isotope fractionation factor (α_{bulk}) by

$$\varepsilon_{bulk} = (\alpha_{bulk} - 1) \cdot 1000 \tag{3}$$

The bond-specific AKIE was calculated using the following two equations (Elsner *et al.* 2005)]:

$$ln(\frac{R}{R_0})_{rp} = ln \frac{\left[1000 + \delta^{13}C_0 + \frac{n}{x}\left(\Delta\delta^{13}C\right)\right]}{\left(1000 + \delta^{13}C_0\right)} = \frac{\varepsilon_{rp}}{1000} \cdot ln\, f \tag{4}$$

$$AKIE = \left(\frac{^{L}k}{^{H}k}\right)_{app} = \frac{1}{\alpha_{rp}} = \frac{1}{z \cdot \varepsilon_{rp} / 1000 + 1} \tag{5}$$

where n is the number of carbons par molecule, x is the number of reactive sites per molecule, $\Delta\delta^{13}C$ is the difference between the actual $\delta^{13}C$ and $\delta^{13}C_0$, ε_{rp} is the isotopic enrichment factor for a specific reactive site, α_{rp} the corresponding isotope fractionation factor, z the number of identical reactive site undergoing intramolecular competition, ^{L}k and ^{H}k are the reaction rates for light and heavy isotopes in the reacting bond, respectively. Equation 4 corrects for the presence of heavy isotopes at non-reactive position while equation 5 accounts for multiple reactive sites as present in chlorinated alkanes with two chlorine atoms.

A.3. RESULTS AND DISCUSSION

A.3.1 Pure culture studies

In the pure culture studies, *X. autotrophicus* GJ10 degraded 1,2-DCA, 1,3-DCP, CP, and CB as expected based on previous studies (Janssen *et al.* 1985). The $\delta^{13}C$ value of 1,2-DCA shifted from -28‰ to 250‰, corresponding to approximately six orders of magnitude decrease in concentration. The other haloalkanes also demonstrated significant increases in $\delta^{13}C$. Using the Rayleigh equation (equation 2), the bulk isotope fractionation factors were calculated (Figure 1 A shows representative experimental results for each compound). The reported variance among triplicate experiments was calculated based on the variance of regression from each experiment according to the method proposed by Scott *et al* (2004). The inverse value of α_{bulk} is reported (Table 1) in order to facilitate the comparison with AKIE values (see below). In general, the magnitude of isotope fractionation decreased with increasing number of carbon atoms as expected. For 1,2-DCA, $1/\alpha_{bulk}$ (1.030) corresponded well to the value observed in a previous study (1.032, (Hunkeler and Aravena 2000)). For the C3 compounds, double-chlorinated DCP showed slightly larger $1/\alpha_{bulk}$ than the single-chlorinated CP.

Table 1. Bulk isotope effect for pure culture studies with *Xanthobacter autotrophicus* GJ 10. The isotope effect is expressed as $1/\alpha_{bulk}$ to facilitate comparison with AKIE values.

	n	No. of C	No. of Cl	$1/\alpha_{bulk}$	variance
1,2-DCA	3	2	2	1.0295	0.0003
CP	3	3	1	1.0172	0.0004
1,3-DCP	3	3	2	1.0203	0.0001
CB	3	4	1	1.0149	0.0002

In order to compare the magnitude of isotope effects independent of molecule structure and size, AKIE values for all experiments were calculated using equations 4 and 5 (Figure 1B and Table 2). The comparison between Figures 1 A and B suggests that after the corrections for molecular structure and size, the differences in the slopes (or the isotope enrichment factors) became less obvious even though these two plots originated from the same four sets of experimental results. The calculated AKIE values based on pure culture studies lie in a rather narrow range between 1.0477 and 1.0616, corresponding to the typical KIE of S_N2 reactions (1.03-1.09 (Shiner and Wilgis 1992)). In previous studies with different aromatic compounds transformed by the same reaction mechanism but different organisms, a larger variability of AKIE values between 1.0035 and 1.0273 was observed (Morasch *et al.* 2004). The higher variability might be due to differences in the enzymes, hence, the differences in the commitment to catalysis between different organisms.

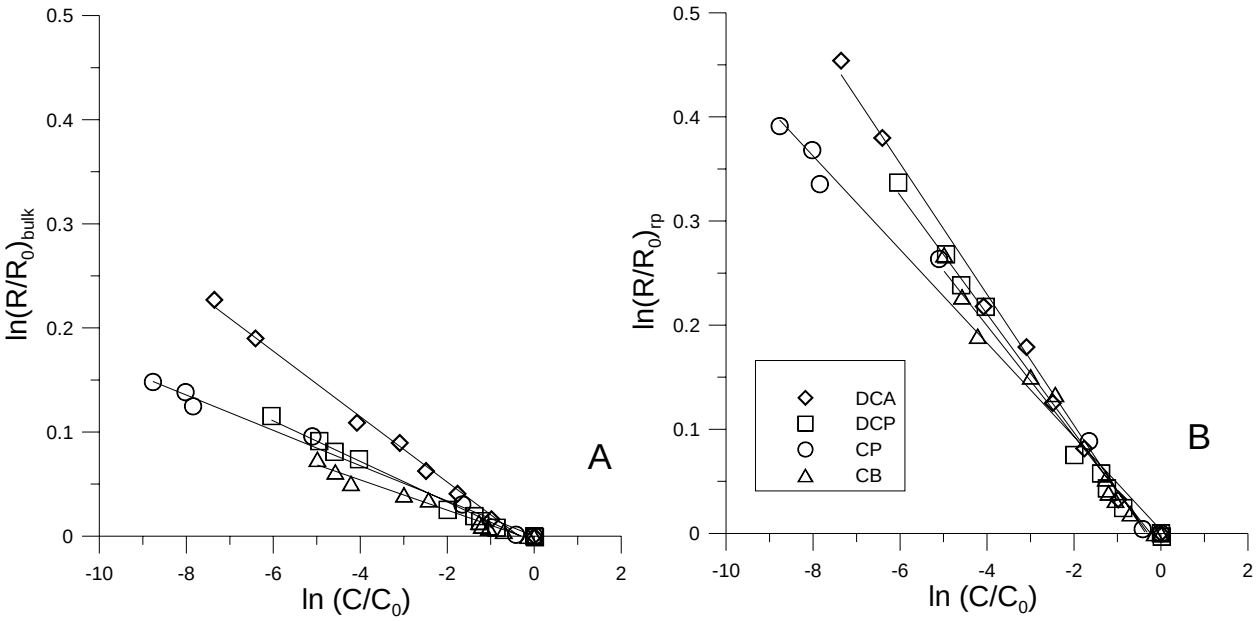

Figure 1 A: Rayleigh plots for pure culture experiments, B: Rayleigh plots after the corrections from Equations 2 to 4 for pure culture experiments.

Although the AKIE values observed in this study were in a quite narrow range, a single factor analysis of variance among the pure culture studies demonstrated that there was a statistically significant difference in the AKIE values for different substrates (two-tail *P*-value of 0.014). In general, haloalkanes with two chlorine atoms had larger AKIE values than those with one chlorine atom. According to paired *t*-tests, AKIE values could be grouped for double chlorinated and single chlorinated haloalkanes (two-tail *P*-values of 0.86 and 0.07 for double and single chlorinated haloalkanes at 95% confidence interval, respectively, and *P*-value of 0.01 between lumped single and double chlorinated haloalkanes).

Table 2. AKIE values from pure culture, AKIE cell-free extract experiments and P-value for pairwise t-test between pure culture and cell-free extract AKIE values.

	Pure culture experiments			Cell-free extract experiments			*P*-value
	n	average	variance	n	average	variance	
1,2-DCA	3	1.0608	0.0003	3	1.0597	0.0003	0.85
CP	3	1.0477	0.0011	2	1.0454	0.0014	0.80
1,3-DCP	3	1.0616	0.0002	3	1.0621	0.0002	0.94
CB	3	1.0555	0.0008	3	1.0527	0.0007	0.42

The observed variations in the magnitude of AKIE values for pure cultures could have several reasons: Slow transfer of the substrate to the enzyme could partly mask the isotope effect, commitment to catalysis could be variable for different substrates, or the location of the transition state along the reaction coordinate could vary for the different substrates leading to different intrinsic KIE. By disrupting the cell membrane to expose the cytoplasmic enzyme, haloalkane dehalogenase, the substrates do not need to

permeate through the membrane before transformation takes place. Therefore, the cell-free extract experiments could reveal the effect of substrate transport on the isotope effect. A previous study on reductive dehalogenation had observed an increase in observed isotope fractionation for cell-free extracts compared to whole cell experiments (Nijenhuis *et al.* 2005).

A.3.2 Cell-free extract studies

In the cell-free extract studies, transformation of all substrates was observed as in the pure culture studies. Triplicate experiments yielded reproducible AKIE values, reflected by the range of variances which corresponded to the pure culture studies (Table 2). Comparing pure culture and cell-free extract experiments for each compound using paired *t*-tests (*P*-values shown in table 2) revealed that there was no statistically significant difference for each pair. This observation suggested that substrate transport across the cell membrane is fast compared to substrate transformation in the cell for all the substrates. Such a conclusions was previously drawn for 1,2-DCA by comparing the kinetics of the haloalkane dehalogenase with the velocity of compound degradation in continuous cultures (Janssen *et al.* 1985; van den Wijngaard *et al.* 1993). Hence the observed difference in AKIE was caused by another factor such as differences in commitment to catalysis and/or differences in the intrinsic KIE for different substrates.

An alternative explanation for the variability of the AKIE values could be an uneven distribution of ^{13}C in the starting substrate due to isotope fractionation during the production of chlorinated hydrocarbons. To evaluate this possibility, theoretical calculations were made, varying the difference in $\delta^{13}C$ between chlorinated and non-chlorinated carbon atoms of the haloalkanes until the AKIE of the compounds could be reproduced. The actual isotope effect associated with the reactive step was assumed to be equal for all compounds corresponding to that observed for 1,2-DCA. Because it is symmetric with the same probability of having a heavy carbon isotope for both carbons, 1,2-DCA cannot be affected by an uneven isotope distribution. The obtained $\delta^{13}C$ values for chlorinated and non-chlorinated carbons were -252‰ / 76‰, -109‰ / 2.5‰, and 81‰ / -219‰ for CP, CB, and DCP, respectively and the difference is much larger than anticipated. Furthermore, even if chlorination leads to isotope fractionation, it would be expected that the non-chlorinated carbon retain an isotope ratio typical for biomass which is not the case for the calculated values. Hence, while an uneven distribution may contribute to the observed difference in AKIE, it cannot explain it alone.

In summary, the study demonstrates that even for compounds that are degraded by the same initial transformation step and the same pure culture, some variability in AKIE remains after corrections for carbon numbers and reactive positions are made. For the case of *X. autotrophicus* GJ10, the effect of substrate transport through cell membrane did not give rise to the observed discrepancy in the AKIE values. Comparison with other studies indicates that if different cultures are involved, the variability further increases. Hence, it is necessarily to evaluate the degree of isotope fractionation for each substrate

and each culture separately and the variability of isotope fractionation factors has to be taken into account when quantifying biodegradation at the field scale.

A.4 References:

Bloom, Y., R. Aravena, D. Hunkeler, E. Edwards and S. K. Frape (2000). "Carbon isotope fractionation during microbial dechlorination of trichloroethene, cis-1,2-dichloroethene and vinyl chloride: implication for assessment of natural attenuation." Environmental Science and Technology **34**: 2768-2772.

Chartrand, M. M. G., A. Waller, T. E. Mattes, M. Elsner, G. Lacrampe-Couloume, J. M. Gossett, E. A. Edwards and B. Sherwood Lollar (2005). "Carbon isotopic fractionation during aerobic vinyl chloride degradation." Environmental Science and Technology **39**(1064-1070).

Chu, K.-H., S. Mahendra, D. L. Song, M. E. Conrad and L. Alveres-Cohen (2004). "Stable carbon isotope fractionation during aerobic biodegradation of chlorinated ethenes." Enviromental Science and Technology **38**(3126-3130).

Clark, I. D. and P. Fritz (1997). Environmental isotopes in hydrogeology. Boca Raton, Florida, USA, Lewis Publishers.

Elsner, M., L. Zwank, D. Hunkeler and R. P. Schwarzenbach (2005). "A new concept to link observed stable isotope fractionation to degradation pathways of organic groundwater contaminants." Environmental Science and Technology **39**: 6896-6916.

Goa, J. (1953). "A micro-biuret method for protein determination: determination of total protein in cerebrospinal fluid." Journal of Clinical Laboratory Investigation **5**: 218-222.

Gray, J. R., G. Lacrampe-Couloume, D. Gandhi, K. M. Scow, R. D. Wilson, D. M. Mackay and B. Sherwood Lollar (2002). "Carbon and hydrogen isotopic fractionation during biodegradation of methyl tert-butyl ether." Environmental Science and Technology **36**: 1931-1938.

Hunkeler, D., N. Andersen, R. Aravena, S. M. Bernasconi and B. J. Butler (2001). "Hydrogen and carbon isotope fractionation during aerobic biodegradation of benzene." Environmental Science and Technology **35**: 3462-3467.

Hunkeler, D. and R. Aravena (2000). "Evidence of substantial carbon isotope fractionation between substrate, inorganic carbon, and biomass during aerobic mineralization of 1,2-dichloroethene by Xanthobacter autotrophicus." Applied and Environmental Microbiology **66**(11): 4870-4876.

Hunkeler, D., R. Aravena and B. J. Butler (1999). "Monitoring microbial dechlorination of tetrachloroethene (PCE) using compound-specific carbon isotope ratios: Microcosms and field experiments." Environmental Science and Technology **33**(16): 2733-2738.

Hunkeler, D., R. Aravena and E. Cox (2002). "Carbon isotopes as a tool to evaluate the origin and fate of vinyl chloride: Laboratory experiments and modeling of isotope evolution." Environmental Science and Technology **36**: 3378-3384.

Hunkeler, D., B. J. Butler, R. Aravena and J. F. Barker (2001). "Monitoring biodegradation of methyl tert-butyl ether (MTBE) using compound-specific carbon isotope analysis." Environmental Science and Technology **35**: 676-681.

Huskey, W. P. (1991). Origin and interpretation of heavy-isotope effects. Enzyme mechanism from isotope effects. P. F. Cook. Boca Raton, FL, USA, CRC Press**:** 37-72.

Janssen, D. B., A. Scheper, L. Dijkhuizen and B. Witholt (1985). "*Xanthobacter autotrophicus* GJ10." Applied and Environmental Microbiology **49**(3): 673-677.

Keuning, S., D. B. Janssen and B. Witholt (1985). "*Xanthobacter autotrophicus* GJ10." Journal of Bacteriology **163**(2): 635-639.

Kuder, T., J. T. Wilson, P. Kaiser, R. Kolhatkar, P. Philp and J. Allen (2005). "Enrichment of stable carbon and hydrogen isotopes during anaerobic biodegradation of MTBE: Microcosm and field evidence." Environmental Science and Technology **39**: 213-220.

Lightstone, F. C., Y. J. Zheng and T. Bruice (1998). "$_N$2 displacement of Cl^- from 1,2-Dichloroethane of the active site of *Xanthobacter autotrophicus* haloalkane dehalogenase." Journal of American Chemical Society **120**(23): 5611-5621.

Mancini, S. A., A. C. Ulrich, G. Lacrampe-Couloume, B. Sleep, E. A. Edwards and B. Sherwood Lollar (2003). "Carbon and hydrogen isotopic fractionation during anaerobic biodegradation of benzene." Applied and Environmental Microbiology **69**(1): 191-198.

Mariotti, A., J. C. Germon, P. Hubert, P. Kaiser, T. Letolle, A. Tardieux and P. Tardieux (1981). "Experimental determination of nitrogen kinetic isotope fractionation: some principles; illustration for the denitrification and nitrification processes." Plant and Soil **62**: 413-430.

Meckenstock, R. U., B. Morasch, R. Warthmann, B. Schink, E. Annweiler, W. Michaelis and H. H. Richnow (1999). "$^{13}C/^{12}C$ isotope fractionation of aromatic hydrocarbons during microbial degradation." Environmental Microbiology **1**(5): 409-414.

Morasch, B., H. H. Richnow, B. Schink and R. U. Meckenstock (2001). "Stable hydrogen and carbon isotope fractionation during microbial toluene degradation: mechanistic and environmental aspects." Applied and Environmental Microbiology **67**(10): 4842-4849.

Morasch, B., H. H. Richnow, B. Schink, A. Vieth and R. U. Mechenstock (2002). "Carbon and hydrogen stable isotope fractionation during aerobic bacterial degradation of aromatic hydrocarbons." Applied and Environmental Microbiology **68**(10): 5191-5194.

Morasch, B., H. H. Richnow, A. Vieth, B. Schink and R. U. Mechenstock (2004). "Stable isotope fractionation caused by glycyl radical enzymes during bacterial degradation of aromatic compounds." Applied and Environmental Microbiology **70**(5): 2935-2940.

Nijenhuis, I., J. Andert, K. Beck, M. Kästner, G. Diekert and H. H. Richnow (2005). "*Sulfurospirillum multivorans* and *Desulfitobacterium sp.* strain PCE-S and abiotic reactions with cyanocobalamin." Applied and Environmental Microbiology **71**(7): 3413-3419.

Northrop, D. B. (1977). Determining the absolute magnitude of hydrogen isotope effects. Isotope effects on enzyme-catalyzed reactions. W. W. Cleland, M. H. O'Leary and D. D. Northrop. Baltimore, USA, University Park Press.

O'Leary, M. H. (1977). Studies of enzyme reaction mechansims by means of heavy-atom isotope effects. Isotope effects on enzyme-catalyzed reactions. W. W. Cleland, M. H. O'Leary and D. B. Northrop. Baltimore, USA, University Park Press.

Schanstra, J. P., J. Kingma and D. B. Janssen (1996). "Specificity and kinetics of haloalkane dehalogenase." Journal of biological chemistry **271**(25): 14747-14753.

Scott, K. M., X. Lu, C. M. Cavanaugh and J. S. Liu (2004). "Optimal methods for estimating kinetic isotope effects from different forms of the Rayleigh distillation equation." Geochimica and Cosmochimica Acta **68**: 433-442.

Sherwood Lollar, B. and G. F. Slater (2001). "Stable carbon isotope evidence for intrinsic bioremediation of tetrachloroethene and trichloroethene at area 6, Dover Air Force Base." Environmental Science and Technology.

Shiner, V. J. and F. P. Wilgis (1992). Heavy atom isotope rate effects in solvolytic nucleophilic reactions at saturated carbons. Isotopes in organic chemistry, Vol.8: Heavy isotope effects. E. Buncel and W. H. Saunders. New York, Elsevier.

Slater, G. F., B. Sherwood Lollar, B. Sleep and E. Edwards (2001). "Variability in carbon isotopic fractionation during biodegradation of chlorinated ethenes: implications for field applications." Environmental Science and Technology **35**: 901-907.

Song, D. L., M. E. Conrad, K. S. Sorenson and L. Alvarez-Cohen (2002). "Stable carbon isotope fractionation during enhanced in situ bioremediation of trichloroethene." Environmental Science and Technology **36**(10): 2262-2268.

Stehmeier, L. G., M. Francis, T. R. Jack, E. Diegor, L. Winsor and T. A. Abrajano (1999). "$^{13}C/^{12}C$ ratio monitoring." Organic Geochemistry **30**(8a): 821-833.

van den Wijngaard, A. J., R. D. Wind and D. B. Janssen (1993). "Kinetics of bacterial growth on chlorinated aliphatic compounds." Applied and Environmental Microbiology **59**(7): 2041-2048.

Verschueren, K. H. G., F. Sejee, H. Rozeboom, K. H. Kalk and B. W. Dijkstra (1993). "Crystallographic analysis of the catalytic mechanism of haloalkane dehalogenase." Nature **363**: 693-698.

Vieth, A., J. Müller, G. Strauch, M. Kästner, M. Gehre, R. U. Meckenstock and H. H. Richnow (2003). "In-situ biodegradation of tetrachloroethene and trichloroethene in contaminated aquifers monitored by stable isotope fractionation." Isotopes Environmental and Health Studies **39**(2).

Appendix B

Supporting Information
Does the Rayleigh equation apply to evaluate field isotope data in contaminant hydrogeology?

Yumiko Abe and Daniel Hunkeler[*]
Centre for Hydrogeology, University of Neuchâtel, Switzerland
[*] corresponding author: Centre for Hydrogeology, University of Neuchâtel,
Rue Emile Argand 11, CH-2007 Neuchâtel, Switzerland,
Tel. ++ 41 32 718 25 60, Fax ++ 41 32 718 26 03,
e-mail: Daniel.Hunkeler@unine.ch

B1. TEXT

The following table summarizes the typical plume geometry found in the literature. These values were referred to our study to estimate the typical *G* values (the ratio of half-width to the length of the plume).

Table S1. Reported BTEX plume dimensions and groundwater velocities

w [m]	plume length, x_R [m]	G $\frac{x_R}{(w/2)}$	v [m/d]	Ref.
107	503	9.4	1.34	*(Wiedemeier et al. 1997)*
30	213	14.2	0.22	*(Wiedemeier et al. 1997)*
152	351	4.6	0.04	*(Wiedemeier et al. 1997)*
21	110	10.5	0.01	*(Wiedemeier et al. 1997)*
43	219	10.2	0.39	*(Wiedemeier et al. 1997)*
9	96	21.3	0.08	*(Wiedemeier et al. 1997)*
9	128	28.4	0.06	*(Wiedemeier et al. 1997)*
91	914	20.1	0.13	*(Wiedemeier et al. 1997)*
18	192	21.3	0.01	*(Wiedemeier et al. 1997)*
120	280	4.7	2.00	*(Wiedemeier et al. 1997)*
25	120	9.6	0.05	*(Stehmeier et al. 1999)*
27	100	7.4	0.09	*(Cozzarelli et al. 2001)*

The following graph shows the effect of dispersion on the C/C_0 presentation. When the effect of dispersion is neglected (C/C_0 in the graph), the resultant concentration is approximately twice as high as the concentration obtained after extracting the effect of dispersion ($C/C_{dispersion}$) at X_D of 1. Experiments where the concentrations were corrected by using the dilution factor derived from a non-reactive compound as a tracer, $C/C_{dispersion}$ can be obtained although most field isotope studies do not include such correction scheme in their concentration determination.

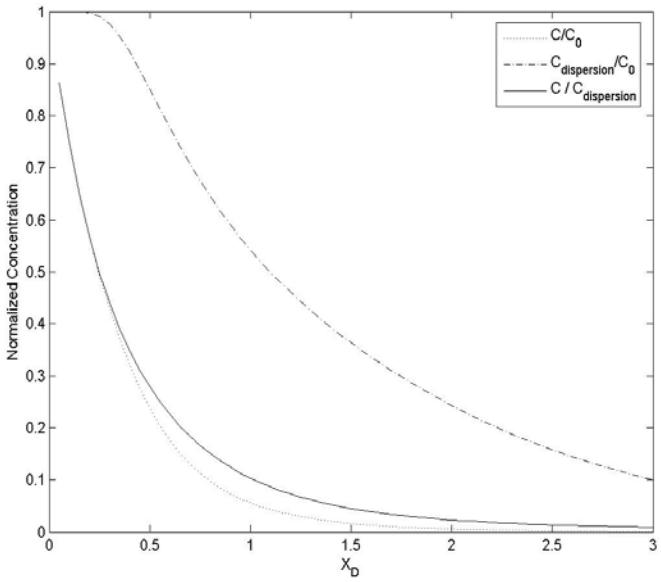

Figure S1. Effect of dispersion on calculating normalized concentrations (*Pe*=10, *Da*=3, and *G*=10)

The following type curve illustrates the systematic effect on estimating the fraction remaining. As in the estimation of the extent of biodegradation, lower *Pe* values are affected more from the systematic effect due to physical heterogeneity. Notice that the systematic effect increases with increasing Damköhler values unlike the systematic effect on the extent of biodegradation (Figure 3 in Chapter 2).

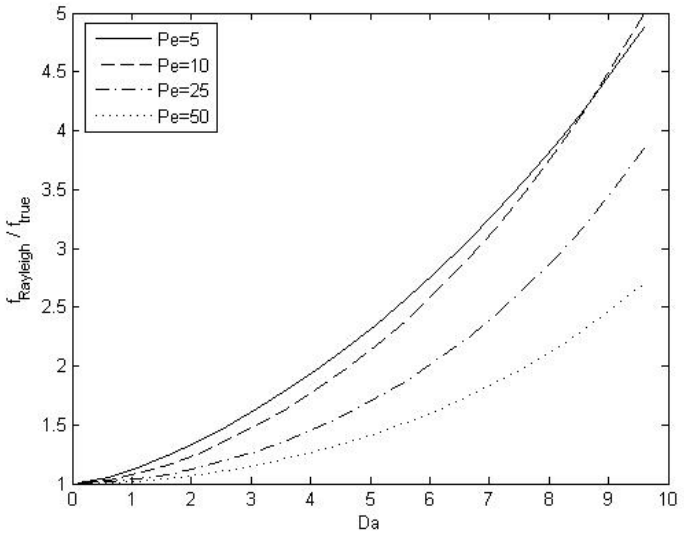

Figure S2. Type curve for the systematic effect associated with estimating the fraction remaining

The following set of break through curves (BTC) shows the effect of simulated chemical heterogeneity. Chemical heterogeneity was considered by varying *Da* as a function of *T* in the linear equation (see legend for the exact equations). As shown in the graph, higher levels of chemical heterogeneity (*Da* changing

more rapidly with *T*) yield lower peak height, and greater level of tailing. Note that the area under the BTC was held constant for all cases.

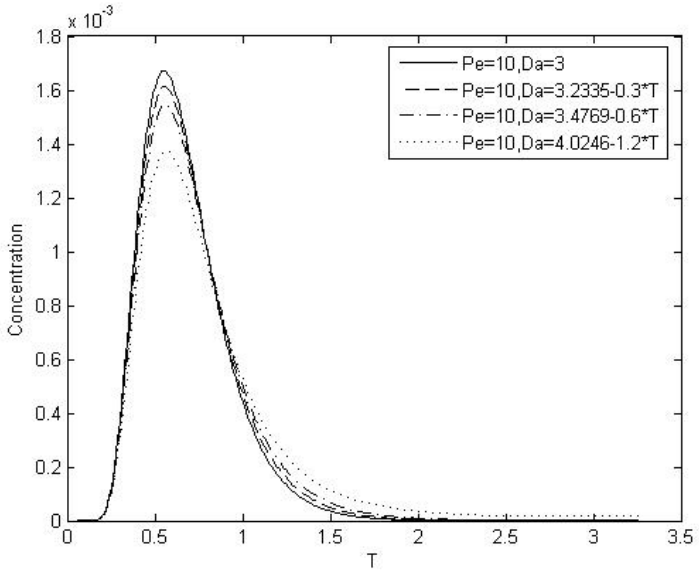

Figure S3. Effect of linearly decreasing Damkohler Values

B.2 References:

Cozzarelli, I. M., B. A. Bekins, M. J. Baedecker, G. R. Aiken, R. P. Eganhouse and M. E. Tuccillo (2001). "Progression of natural attenuation processes at a crude-oil spill site: I. Geochemical evolution of the plume." Journal of Contaminant Hydrology **53**: 369-385.

Stehmeier, L. G., M. M. Francis, T. R. Jack, E. Diegor, L. Winsor and T. A. Abrajano Jr (1999). "Field and in vitro evidence for in-situ bioremediation using compound-specific $^{13}C/^{12}C$ ratio monitoring." Organic Geochemistry **30**: 821-833.

Wiedemeier, T. H., H. S. Rifai, C. J. Newell and J. T. Wilson (1997). Natural Attenuation of Fuels and Chlorinated Solvents in the Subsurface. New York, John Wiley & Sons, Inc.